UNIVERSITÀ DELLA CALABRIA

UNIVERSITA' DELLA CALABRIA

Dipartimento di Farmacia e Scienze della Salute e della Nutrizione

Dottorato di Ricerca in

Medicina Traslazionale

XXXIV CICLO

DESIGN AND DEVELOPMENT OF NEW FUNCTIONAL MATERIALS FOR PHARMACEUTICAL AND BIOMEDICAL PURPOSES

Settore Scientifico Disciplinare CHIM-09

Coordinatore: Ch.mo Prof. Sebastiano Andò

Firma SEBASTIANO ANDO' 18.02.2022 11:31:33 GMT+00:00

Supervisore/Tutor: Prof.ssa Sonia Trombino

Firma Trombino Sonia 09.02.2022 09:23:38 GMT+00:00

Dottoranda: Dott.ssa Federica Curcio

Firma FEDERICA CURCIO 09.02.2022 09:20:23 GMT+00:00

Author's e-mail: federica.curcio@unical.it

Author's address:
Department of Pharmacy, Health and Nutritional Sciences
University of Calabria
Edificio Polifunzionale
87036 Arcavacata di Rende, Cosenza, Italy.

ph: + 39 0984 493296
cell: +39 342 0182673

To my daughter

Sprout of life in my womb and
little flower of May.

To my husband

Together we make plans for this life of ours,
which has many faults and sometimes goes uphill.
But with two, the effort becomes circumstance.
I love you.

Table of contents

Preface

General Introduction, Aims and Organization of this Thesis

1. General Introduction

Over the last 10 years, developments in nanotechnology have led to the identification, design and manufacture of new systems and nano-materials useful in various fields, including medicine, cosmetics, nutraceuticals, food industry and tissue engineering [1]. By exploiting characteristics such as controlled size, long-term stability, drug entrapment, sustained release and low toxicity, it is possible to design devices using starting substrates such as natural polymers (chitosan, hyaluronic acid), proteins (gelatine), fatty acids (linolenic acid) and plant-derived substances (glycerine, resveratrol, naringenin).

These substrates can be functionalised with therapeutic molecules to obtain *"drug delivery systems"* [2]. These colloidal and multifunctional structures are capable of selectively and quantitatively transporting a drug to its site of action, regardless of the compartment and method of administration [3]. Examples of *drug delivery systems* are solid lipid nanoparticles, metal nanoparticles, nanospheres, hydrogels, polymersomes, and membranes [4].

The transport of substances by means of these carriers can be passive in nature or expressed through self-delivery mechanisms. This means that, if the substances are incorporated in the internal cavity of the structure, they undergo an immediate passive release (by diffusion between compartments); on the contrary, if they are directly conjugated to the nanostructure materials, they will dissociate from the carrier only following induced changes (chemical reaction or *stimuli* responsive) in the acceptor compartment, thus decreeing a slow release at the specific site [5].

Nanoparticle-based formulations exploit the principle that a high surface area/volume ratio often leads to a significant increase in pharmacological activity [6,7]. Furthemore, they can be used to deliver therapeutic agents with different chemical and physical properties to the specific site, releasing them in a controlled and targeted manner while protecting them from premature degradation. These carriers are also widely used in the food sector [8,9]. They can increase the shelf life of various types of food, and also are used as delivery

systems to transport food additives into products without disturbing their basic morphology, improve the texture and appearance of food, and have an effect on shelf life [10-12].

However, the nanoparticles can have some limitations, including their low ability to incorporate a considerable amount of water-soluble substances. For this reason, in the last years technological progress has made possible to identify new type of *drug delivery systems* capable of containing larger quantities of hydrophilic molecules [13]. These structures are called polymersomes and are considered an evolution of existing nanotechnologies as they are able to facilitate the encapsulation process by dissolving or dispersing the substances with the blocks of copolymers used and promoting their release through a concentration gradient (passive diffusion) between the membrane and the external environment [14].

Furthemore the advent of synthetic and/or natural polymers with bioactive properties such as antimicrobial, immunomodulatory, cell proliferative and angiogenic has made possible to develop, in recent years, not only nanoparticles and polymersomes, but also structures capable of creating microenvironments conducive to the process of tissue healing or restoration [15]. These structures, known as scaffolds, are mainly used in tissue engineering where it is necessary to mimic the functions of damaged organs and tissues and activate their regeneration [16].

However, it has been observed that substances such as polysaccharides or proteins are also capable of performing these functions, although they are characterized by rapid degradation and low mechanical resistance, which is being remedied by encapsulation in hydrogels.

In this respect, the nanotechnology is considered a very versatile and constantly evolving field of science, which has give drug delivery systems an attractive strategy for the encapsulation and tran sport of various bioactive substances.

2. Aims of this thesis

The present thesis was realized in the Pharmaceutical Techonology group, in the Department of Pharmacy, Health and Nutritionals Sciences (University of Calabria) and it based on the design and development of new functional materials for pharmaceutical and biomedical purposes.

3. Organization of this thesis

The present thesis consisted of three self-contained sections. The first sction, titled “Micro- and nano-materials based drug delivery systems” and consisted of four self-explained parts. In the first one, gels containing SLNs based on an ester of the naringenin and linolenic acid, useful as cyclosporin A release system, were prepared and studied. The obtained results indicate that these gels could be useful in the treatment of dermatological diseas such as psoriasis.

The second part was dedicated to the application of the SLNs in the treatment of infectious diseases since they are difficult to treat by common pharmaceutical formulations.

The aim of third part was to investigate the different applications of copper-based nanoparticles in numerous fields, specifying the mechanisms of action in response to a differents *stimuli*.

The fourth part focused the attention on the importance of micro- and nano-technology in the food and nutritional sector and, in particular, provides an overview of these materials used for the administration of nutritional constituents essential to maintain and improve the health state.

The second section titled “Cross-linked systems for drug delivery” is divided into other four parts. In particular the first ones regard a review in which were discuss recent advances on the design of chemical and physical HA-based hydrogels and their application for biomedical purposes. More attention was given to these materials for targeted therapy of cancer and osteoarthritis. The second part concerns the preparation and characterization of nanospheres based on the antioxidants resveratrol and epigallocatechin gallate, useful for site-specific release of resveratrol to breast cancer cells. All the obtained results suggest that these platforms, thanks to their release profile, biocompatibility, antioxidant and antitumor activity, could be a suitable approach for breast cancer treatment and prevention.

In the third part were described the preparation and characterization of a hydrogel based on gelatin and glycerine, useful for site-specific release of benzydamine, an antiinflammatory drug, able to attenuate the inflammatory process typical of the vaginal infection. In particular, the swelling tests and release studies support the hypothesis that the hydrogel could be potentially usefuò for the site-specif release of benzydamine in the vaginal mucosa.

The last part of the second section is based on the treats of hydrogels based on polysaccharides and proteins and their applications in the field of tissue engineering.

The third section opens with a work focused on the most employed natural and synthetic biomaterials in cardiac regeneration, paying particular attention to the contribution of Italian research groups in this field. In particular, the fabrication techniques, and the status of the clinical trials were described. Many studies dealt with the evaluation of cardiac scaffolds and patches as cell delivering systems, promoting stem cell proliferation and differentiation and could be useul in the treatment of injuries derived from myocardial infarction.

In the second part of this sections was described research on the design, preparation and characterization of membranes based on cyclosporine A (CsA) and chitosan carboxylate (CC) useful as an implantable subcutaneous medical device for a prolonged therapeutic effect in the treatment of breast cancer. The obtained data show both complete dispersion of CsA within the polymer membrane and a high reduction in tumour cell proliferation, conducted *in vitro* on MDA-MB-231 cell lines.

The last part describes a new class of nanocarriers called polymersomes as an attractive strategies for the release of drugs, correlated to a series of internal biological *stimuli* (pH, redox potential, glucose concentration) and external physical ones (temperature, light, ultrasound), which induce significant changes in the structure of the same polymersomes with consequent destruction of the membrane and release of the encapsulated substance.

REFERENCES

1. Sindhwani, S.; Chan, W.C. Nanotechnology for modern medicine: Next step towards clinical translation. *J. Intern. Med.* 2021.
2. Sumaira A.; Sara I.; Hijab F.; Wajiha F.; Christophe H.; Bilal H.A.; Iram A. Emerging Applications of Nanotechnology in Healthcare Systems: Grand Challenges and Perspectives. *Pharmaceuticals.* 2021, 14, 707.
3. Khan, A.U.; Khan, M.; Cho, M.H.; Khan, M.M. Selected nanotechnologies and nanostructures for drug delivery, nano medicine and cure. *Bioprocess Biosyst. Eng.* 2020, 43, 1339–1357.
4. Minakshi P.; Upendra P. L.; Basanti B.; Ikbal S.; Manimegalai J.; Koushlesh R.; Rekha R.; Sunil K.; Sheefali M.; Sandip K.K.; Hafiz M.N.I.; Kuldeep D.; Jyoti M.; Gaya P. Nanotherapeutics: An insight into healthcare and multi-dimensional applications in medical sector of the modern world., *Biomedicine & Pharmacotherapy*, 97, 1521–1537, 2018.
5. Serjay S.; Nyet K. Nanotechnology and its use in imaging and drug delivery (Review). Wong. Biomedical Reports, 2021.
6. Wanisa A. Review of Therapeutic Applications of Nanotechnology in Medicine Field and its Side Effects. *Journal Of Chemical Reviews, 2019, 243-251.*
7. Wiwanitkit, V. Biodegradable Nanoparticles for Drug Delivery and Targeting. *Surf. Modif. Nanopart.Target. Drug Deliv.* 2019, 167–181.
8. Rizvi, S.A.; Saleh, A.M. Applications of nanoparticle systems in drug delivery technology. *Saudi Pharm. J.* 2018, *26*, 64–70.
9. Khan, I.; Saeed, K.; Khan, I. Nanoparticles: Properties, applications and toxicities. *Arab. J. Chem.* 2019, *12*, 908–931
10. Chaudhry, Q.; Watkins, R.; Castle, L. Nanotechnologies in Food: What, Why and How? In: *Nanotechnologies in Food*. Chaudhry, Q.; Castle, L.; Watkins, R.; Royal Society of Chemistry: Washington, USA, 2017, 1-19.
11. Fursik, O.; Strashynskiy, I.; Pasichniy, V.; Marynin A. Some aspects of using the nanotechnology in food industry. *Ukrainian J. Food Sci.*, 2019, *7*, 298–306

12. Jones D.; Caballero, S.; Davidov-Pardo, G. Bioavailability of nanotechnology-based bioactives and nutraceuticals. *Adv Food Nutr Res*. 2019, 88, 235-273.
13. Jung Seok L.; Jan F. Polymersomes for drug delivery: Design, formation and characterization, *Journal of Controlled Release*. 161, 2012, 473–483.
14. Xiao-ying Z.; Pei-ying Z. Polymersomes in Nanomedicine - A Review, *Current Nanoscience*, 2017, 13, 124-129.
15. Brown, B.N.; Badylak, S.F. Extracellular matrix as an inductive scaffold for functional tissue reconstruction. *Transl. Res.* 2014, *163*, 268–285.
16. Huawei Q.; Hongya F.; Zhenyu H.; Yang S. Biomaterials for bone tissue engineering scaffolds: a review. *RSC Adv*., 2019, 9, 26252-26262.

Italian Abstract:

Negli ultimi anni la tecnologia farmaceutica attraverso lo sviluppo di "*drug delivery systems"* ha rivolto l'attenzione alla possibilità di modulare, migliorare e potenziare le caratteristiche di sostanze biologicamente attive. Tutto ciò è possibile con la realizzazione di *drug delivery systems* che hanno lo scopo di fornire la quantità terapeutica di farmaco in un sito specifico dell'organismo in modo da raggiungere una data concentrazione terapeutica e un succesivo steady state per tutto il periodo di trattamento necessario. La modulazione del rilascio può essere ottenuta anche mediante "*devices*" costituiti da materiali polimerici biodegradabili che vengono impiantati nell'organismo e che sono in grado di rilasciare le sostanze per periodi di tempo molto lunghi.

Pertanto, lo scopo del presente lavoro di tesi è stato quello di indagare, progettare, realizzare e caratterizzare, attraverso l'utilizzo di sostanze polimeriche, proteine e acidi grassi, carriers innovativi in grado di incapsulare e veicolare sostanze attive con caratteristiche chimico-fisiche differenti. Sono stati presi in considerazione anche materiali polimerici con elevata biocompatibilità e biodegradabilità (chitosano, acido ialuronico), in grado di fungere da strutture (scaffold e membrane polimeriche) capaci di stimlare la rigenerazione cellulare e tissutale nell'ambito dell'ingegneria biomedicale. Studi *in vitro* hanno permesso di verificare la capacità di rilascio, le proprietà farmacologiche e la risposta agli stimoli di drug delivery systems, portando alla conclusione che tuttavia è necessario effettuare ulteriori valutazioni *in vivo* che permetteranno di confermare l'applicazione clinica e l'eventuale produzione su larga scala.

SECTION 1

MICRO-AND NANO-MATERIALS BASED DRUG DELIVERY SYSTEMS

Part A: Solid Lipidic Nanoparticles Based on Naringenin and Linolenic Acid Viscosified with Biocompatible Polymers for The Transport and Release of Cyclosporine.

Part B: Solid Lipid Nanoparticles: An Interesting Strategy for Antibiotics Administration.

Part C: Copper nanoparticles based stimuli-responsive approaches.

Part D: Nano- and Micro-Technologies Applied to Food Nutritional Ingredients.

PART A

Solid Lipidic Nanoparticles Based on Naringenin and Linolenic Acid Viscosified with Biocompatible Polymers for The Transport and Release of Cyclosporine A

1. Introduction

This work aimed to design, prepare and study gels containing SLNs, based on an ester of the naringenin and linolenic acid, useful as cyclosporin A release system (Figure 1) [1–2].

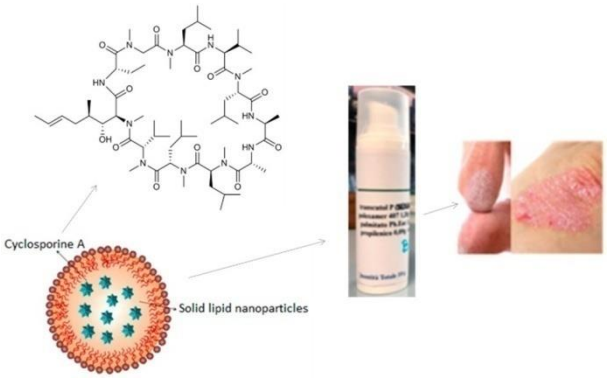

Figure 1. Schematic design of cyclosporin A-loaded SLN formulation

2. Materials and Method

The ester was characterized by FT-IR and ^{1}H-NMR and the SLNs by Dynamic Light Scattering and Scanning Electronic Microscopy (Figure 2). Their capacity to inhibit the lipid peroxidation induced by a free radical generator, has been examined in rat liver microsomal membranes and compared to that of the free ester and various prepared gels, containing the empty lipid nanoparticles. All the materials were able to preserve the antioxidant capacity of the precursor (Figure 3) [3].

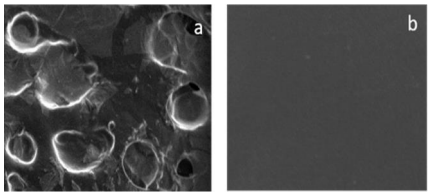

Figure 2. Photomicrography of empty SLN (Mag = 100 X) (**a**) and of gel based on HA and Poloxamer 407 containing empty SLN (Mag = 1.00 K X) (**b**).

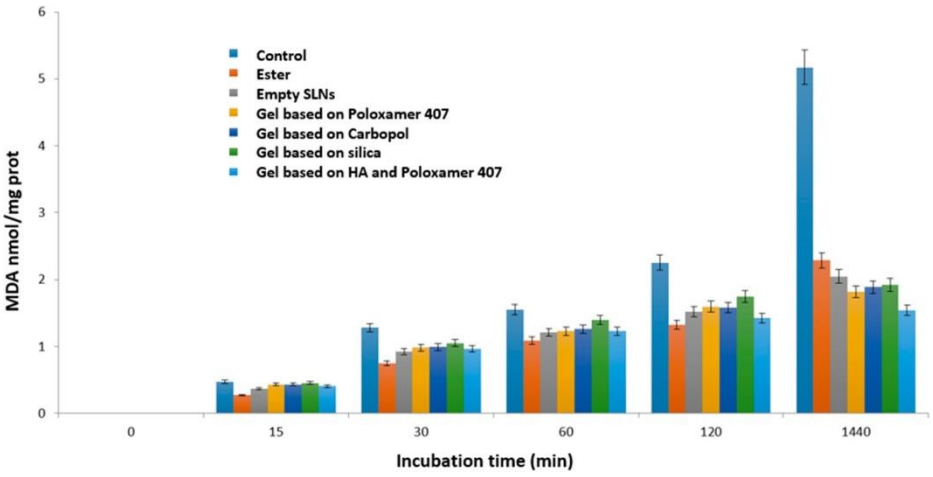

Figure 3. Inhibition of lipid peroxidation induced by *tert*-BOOH over 24 h.

3. Results and Conclusion

In particular, the major activity was exhibited by the free ester, the empty SLNs and the HA (hyaluronic acid)-based gel and Poloxamer 407 containing the empty SLNs [4]. This last result is due to the presence of the HA which also exerts an antioxidant action. However, even the other gels, despite being made up of non-antioxidant substances, show that they can preserve the microsomal membranes from lipid peroxidation due to the empty SLNs they contain.

Nanoparticles have been shown also to possess excellent encapsulation efficiency, stability and size suitable for topical administration. This hypothesis was supported by the results obtained with the transdermal release studies, performed using Franz cells, which revealed that in the case in which the SLN are incorporated in gels containing promoters of absorption, such as Poloxamer 407 and Carbopol, the gels release a maximum of 5% of the loaded drug in contrast to free SLNs and colloidal silica gels. To validate this hypothesis

and evaluate the amount of cyclosporin A released in the stratum corneum and in the epidermis-dermis layer, the tape stripping method was used (Figure 4). The obtained data revealed that the amount of drug released by the colloidal silica-based gel was negligible in the stratum corneum (SC) and equal to 23% in the epidermis-dermis layer over 24 h. In contrast, the gel containing Poloxamer 407 at concentrations of 1.28% released about 79% of the drug over the 10 h in the SC and 15% in the epidermis-dermis layer. When the polymer changes, i.e., using Carbopol at 0.1%, the drug was more retained inside the gel than observed with the Poloxamer 407. In particular, the percentage of cyclosporin A released within 24 h was equal to 36% in the SC and 28% in the epidermis-dermis layer.

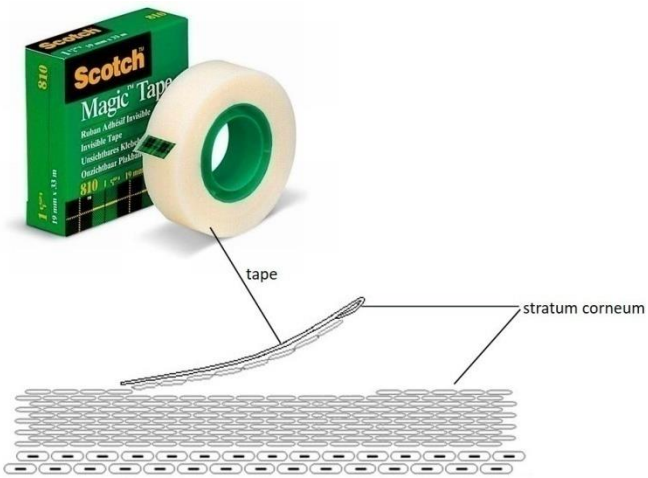

Figure 4. Tape stripping method.

Furthermore, with the increase in the concentration of Poloxamer 407 in the gel, obtained using in addition also HA, the viscosity and strength of the gel increase, and the drug was more retained inside the matrix, but the release can be conditioned by the presence of ethanol which increase the permeation of cyclosporin A by virtue of its solubility in this solvent. The obtained data following the release of cyclosporin A from the HA-based gel and Poloxamer 407 revealed that the drug was present in the SC at 15% and in the epidermis-dermis layer at 12% after 10 h. Then, the amount of the polymer, cross-linker and drug, as well as the amount and type of absorption promoter can influence drug release from gel formulations in the topical administration of cyclosporin A in the treatment of psoriasis skin lesions, ensuring an adequate concentration of the drug at the skin level and

a simultaneous reduction in the systemic absorption of cyclosporine. Furthermore, they could reduce the inflammation affecting the skin and the dermis in the presence of psoriasis [5], as shown by the inhibitory capacity that both empty and full SLN exhibit against nitroxide (Figure 5).

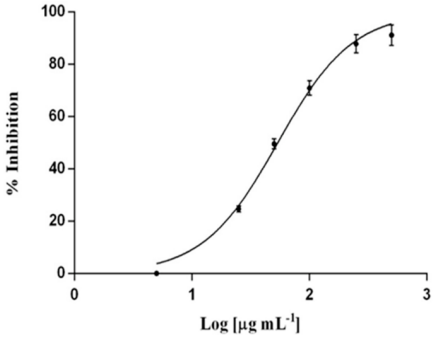

Figure 5. Inhibition of nitroxide production

References

Trombino S.; Servidio C.; Curcio F.; Iemma F.; Cassano R. Solid lipidic nanoparticles based on naringenin and linolenic acid viscosified with biocompatible polymers for the transport and release of Cyclosporine A. In: Steering the Clinical Translation of Delivery Systems for Drugs and Health Products, Ed. Pignatello R. and Matricardi P. *Pharmaceutics* 2020, 12, 350.

1. Gaggeri, R.; Rossi, D.; Christodoulou, M.S.; Passarella, D.; Leoni, F.; Azzolina, O.; Collina, S. Chiral Flavanones from Amygdalus lycioidesSpach: Structural Elucidation and Identification of TNFalpha Inhibitors by Bioactivity-guided Fractionation. Molecules 2012, 17, 1665–1674. *Pharmaceutics* 2020, 12, 350 47 of 49

2. Esposito, M.; Diluvio, L.; Nisticò, S.; Chimenti, S. Cyclosporin-A in the treatment of psoriasis. *Trends in Medicine* 2003, 3, 57–65.

3. Mayser, P.; Grimm, H.; Grimminger, F. n-3 fatty acid in psoriasis. *Br. J. Nutr.* 2002, 87, S77–S82.

4. Trombino, S.; Russo, R.; Mellace, S.; Verano, G.P.; Laganà, A.S.; Martucci, F.; Cassano, R. Solid lipid nanoparticles made of trehalose monooleate for cyclosporin-A topic release. *J. Drug Deliv. Sci. Technol.* 2019, 49, 563–569.

5. Huang, G.; Huang, H. Application of hyaluronic acid as carriers in drug delivery. *Drug Deliv.* 2018, 25, 766–772.

6. Monguilhott Dalmarco, E.; Frode, T.S.; Medeiros, Y.S. Additional evidence of acute anti-inflammatory effects of cyclosporin A in a murine model of pleurisy. *Transplant Immuno.* 2004, 12, 151–157.

PART B

Solid Lipid Nanoparticles: An Interesting Strategy for Antibiotics Administration

Abstract

In the last years, nanoparticle systems have assumed considerable importance as drug delivery carriers also in the treatment of bacterial infections, thanks to their different advantages such as more efficacy, and site-specific release than conventional treatments. Among them solid lipid nanoparticles (SLNs), a class of colloidal carriers consisting of a lipid matrix dispersed in an aqueous phase, represent a valid therapeutic option for a local or systemic delivery of numerous drugs. Their small size (50-1000μm), the ability to overcome cellular barriers, the interaction with a target site and the possibility to control the release of drug, make these carriers excellent systems also for antibiotics delivery. In addition, compared to conventional methods, SLNs can also promote antibiotics solubility in the physiological fluids, prolong their lifetime, reduce frequency of doses administration, minimize systemic side effects, and increase patient compliance. Furthermore, the solid lipid core favours the encapsulation, conjugation and adsorption of a hydrophobic drugs. This doesn't exclude, regardless of the chemical nature of the substances that make up the SLNs matrix, the possibility of including also hydrophilic drugs, proteins and other macromolecules stabilizing and protecting them from degradation.

The present chapter has the aims to describe the advantages of using SLNs in the treatment of infectious diseases, that affect various organs and located in areas of the body which are difficult to treat by common pharmaceutical formulations or caused by microorganism's resistant to the action of antibiotics.

Keywords: solid lipid nanoparticles, bacterial infections, antibiotics, drug delivery

1. Introduction

The World Health Organization (WHO) has labelled bacterial infections as one of the leading causes of death in healthcare. In fact, some bacterial strains, generally responsible for easily treatable bacterial infections, have developed a resistance against many antibiotics already on the market, thus increasing a series of therapeutic failures with a consequent increase in national health spending and hospital stays (Valappil 2018; Lakshminarayanan2018). With the advent of nanotechnology, the therapeutic treatment of bacterial infections has undergone a significant change, mainly dictated by the use of innovative carriers such as solid lipid nanoparticles (SLNs) (Shirure2019; Gao 2014). Thanks to their chemical-physical properties (size, structure, surface, hydrophilicity), and to the advantages offered in terms of release, these nanoparticles represent a valid therapeutic option to conveyantibiotics to areas of the bodydifficult to reach by common pharmaceutical forms (Gordillo-Galeano2018; Wang2017). In particular, SLNs guarantee the prolonged release of drugs by increasing its therapeutic efficiency, minimizing systemic side effects and lowering the frequency of administration. They also improve the bioavailability of the antibiotics, the solubility in biological fluids and are useful carriersfor combined synergistic therapies (Ranghar 2014). The site-specific release is strongly influenced by the surrounding microenvironment and the structural characteristics of the particles (Gao2014; Shimanovich and Gedanken 2016). Specifically, it is influenced by stimuli, external and internal to the cell (change in pH, temperature, enzymatic inactivation, etc.), and the distribution of the active ingredient in nanoparticle formulations that can be homogeneous, internal to the lipid core (core-shell structure) or superficial (outer-shell structure) (Zazo 2016; Abed and Couvreur 2014; Gaspar and Almeida 2019). Compared to conventional drug forms, the use of SLNs could improve the therapeutic index of already existing antibiotics, and of those under development by enhancing their antimicrobial action through direct contact of nanoparticles with bacteria or by diffusion of the active ingredients in the target site (Abed and Couvreur 2014). Since nanoparticles are carriers capable of penetrating within the various cell compartments, once absorbed, they are internalized and tend to accumulate in outbreaks of an infection through recognition and transport by phagocytic cells (Valappil 2018; Xie 2014; Polo 2017). The antibacterial effect is exerted through the rupture of the bacterial membrane, activation of ROS (inserire nome per intero), penetration of the microorganism's cell membrane and interaction with bacterial DNA and

proteins (Wang2017; Canaparo2019). Cephalosporins, aminiglycosides, macrolides, fluoroquinolones, and rifampicins are the antibiotics most carried in SLNs even at an intracellular level (Xie 2014). The therapeutic potential of these drugsis closely related to the route of administration used. In fact, intravenous administration allows the SLNs toconvey antibiotics mainly at the hepatic and splenic level, thanks tothe rich vascularization of these organs; the oral routeis effective in the treatment of intestinal tract infections; the pulmonary administration allows the treatment of serious respiratory infections and the topical ones favours the treatment of skin and ophthalmic infections that are difficult to treat snellire frase (Xie 2014).The purpose of this chapter is to describe the advantages offered by SLNs in the treatment of bacterial infections supported by bacterial strains resistant to common antibiotics, and located in districts which are difficult to treat.

2. Cephalosporins

Cephalosporins are antiobitics belonging to the broad-spectrum beta-lactam class. Structurally they are constituted by a beta-lactamic ring fused with a dihydrothiazine ring containing six sulfur atoms and a cephalic nucleus (Craig and Andes 2015) (Figure 1).

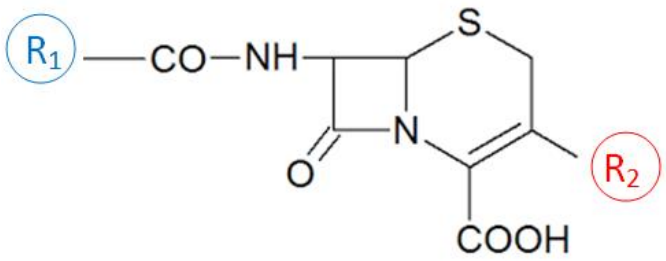

Figure 1. Cephalosporin chemical structure.

Theyare classified according to their spectrum of action and chemical structure. Therefore, there are first-generation cephalosporins active only against Gram-positive bacteria (streptococcus and staphylococcus), the second-generation isactive only against Gram-negative bacteria (*Haemophilus influenzae, Enterobacter aerogenes*), the third-generation isactive against both Gram-positive and Gram-negative bacteria, and the fourth and fifth-

generation broad-spectrum cephalosporins active on methicillin-resistant strains and Gram-negative bacilli (*P. aeruginosa*) (Chaudhry2019; Nath2020;Zaffiri 2012).

These antibioticsact by inhibiting the synthesis of peptidoglycan, one of the main components involved in bacterial cell membrane synthesis. Without the protection offered by the membrane, the bacterium is susceptible to the surrounding environment and is certain to die (Shahbaz2017; ZAffiri 2012; Shaikh2015). Cephalosporins have a time-dependent efficacy proportional to the drug concentration reached at the target site over a given period of time that is maintained above the minimal inhibitory concentration (MIC) (Ozcengiz and Demain 2013; Corallo and Zaidi 2016). Since, they are very hydrophilic, they reach fatty tissues and the more lipophilic targets with more difficulty, so they may need carriers in the treatment of certain infections. In this regard, Kumar et al. RealizedSLNs as carriers for the delivery of ceftriaxone, a third-generation cephalosporin used in the treatment of infectious diseases such as myocarditis, skin infections, meningitis, urinary tract infections, etc. (Wang2017; Corallo and Zaidi 2016). In particular, ceftriaxone has been encapsulated within SLNs (CL-SLNPs) with15-20 nm size, consisting of a lipid matrix based on lecithin and cholesterol. The studies carried out in this work showed that this cephalosporin, encapsulated in a percentage equal to 77.19%, was released by CL-SLNPs within 24h exerting a remarkable antibacterial action on microorganisms such as Bacillus polymyxa, Bacillus cereus, Pseudomonas aeruginosa and Enterobacter aerogenes (Kumar2016). SLNs also showed a significant efficacy in the treatment of infections related to biofilm formation by bacteria. An example was reportedby Singh et al., that obtained SLNs encapsulating cefuroxime axethyl, a second-generation broad-spectrum cephalosporin, by solvent emulsification technique. These SLNs consistedof a lipid matrix based on stearic acid and binary lipids containing tristearin (Singha 2014). The *in vitro* tests, carried outthrough the disc diffusion method, revealed an accentuated antibacterial activity on *S. aureus* cultures, with MIC lower than those shown by a pure solution ofthe free drug. This is probably due to the ability of SLNs to penetrate more easily into cells, releasing the cefuroxime axethyl and destroying bacteria more effectively. Also, in this case the release of cephalosporin was time dependent with a percentage of 95.5% after 12 h (Singha 2014). Some cephalosporins, orally administered, are found in the form of pro-drug and undergo a conversion into metabolites active only in the liver. One example is cefpodoxime proxethyl, that after oral administration is converted to cefpodoxime, a third-generation cephalosporin

used in the treatment of severe respiratory and urinary tract infections. This substance showed a lower solubility in gastric fluids and for this reason itsbioavailability after oral administration was less than 50% (Singh2015). To overcome this problem Shah et al. have thought to deliver the cefpodoxime proxethyl through solid lipidic nanoparticles based on coconut oil. Studies on the zeta potential of these SLNs showed an improvement in the dispersion mechanism of the drug when it was encapsulated in a lipid matrix (Shah 2017).

3. Fluoroquinolones

Fluoroquinolones are antibiotics belonging to the family of quinolones that are used in the treatment of urinary, respiratory, skin, soft tissue, sexually transmitted diseases, tuberculosis, and pyelonephritis (Ezelarab2018). They consist of a complex chemical structure in which is present the quinolonic nucleus, derived from nalidixic acid, and a fluorine atom in position 6 (Zhanel2002). The pharmacological activity of these drugs is closely related to the presence of substitutes in positions 1,5,7 and 8 (Owens and Paul 2005) (Figure 2).

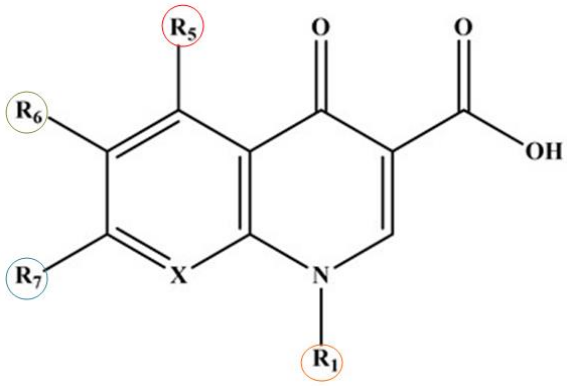

Figure 2. Quinolone chimical structure.

The antibacterial spectrum of fluoroquinolones and their pharmacokinetic profile vary according to their structure. In particular , first generation fluoroquinolones are active against Gram-negative bacteria, the second generation (ciprofloxacin, norfloxacin, enoxacin, pefloxacin) is active against Gram-negative, Gram-positive and *P. aeruginosa bacteria* the third generation (levofloxacin, temafloxacin, etc.) is active against Gram-negative, Gram-positive, and anaerobic, and fourth generation fluorochinolones (prulifloxacin, trovafloxacin,

alatrofloxacin, delafloxacin etc.) is active against *Streptococcus pneumoniae* and *Enterobacteriaceae*, atypical and anaerobic bacteria with a long serum half-life (Ezelarab2018; Owens and Paul 2005).

The antibacterial action of these drugs is expressed through a mechanism of inhibition of replication and transcription of bacterial DNA that is reflected in the inactivation of topoisomerase IV (Zhanel2002). The disadvantages in the use of fluoroquinolones such as the resistance developed by some bacterial strains against them, their toxicityon different body districts of the body and the inability to reach specific target sites, have allowed researchers to turn their attention to nanotechnology as a new option for the topical and systemic administration of these drugs (Le-Deygen2017; Furneri and Fuochi 2017). In particular, the focus was on the use of SLNs, which not only act as carriers but also as green systems highly biocompatible with human tissue (Islan2016). In this regard, Islanet al. have developed myristyl myristate SLNs, through the ultrasonification method, in which have encapsulated levofloxacin in the presence of the mucolytic enzyme DNase. The aim of this work was the realization of systems useful in the treatment of respiratory infections and in particular cystic fibrosis. *In vitro* release studies have shown that the obtained SLNs, with a size equal to 200 nm, were able to release a percentage of levofloxacin equal to 80% after 4 hours of administration. Further tests have demonstrated that the presence of the mucolytic enzyme Dnase did not affect the stability of nanoparticles but increased the antibacterial efficiency of levofloxacin by reducing mucus viscosity in the lungs (Islan2016). On the other hand, Baiget al. have studied the antibacterial action of levofloxacin encapsulated in stearic acid nanoparticles in the treatment of conjunctivitis. Through *in vitro* studies they exhibited that the drug was released from the carrier by 84% in 12 h with a peak 4 hours after administration due to the lipophilic characteristics of the carrier. This was also confirmed by *ex vivo* corneal permeation studies, which showed a cumulative curve of the drug at corneal level 4 h after administration without causing toxic effects to the mucosa (Baig2016). Corneal infections are not only very annoying but also difficult to treat from a topical point of view because the high tear secretion rapidly eliminates the drug, reducing its bioavailability and having to resort to repeated administration (Reimondez-Troitiño2015). Using the SLNs it is possible to overcome these limitations, as the drug tends to be released gradually and remaining in the affected site for a longer period, especially if the SLNs also contain mucus adhesive substances that

increase their bioadhesion. With the aim of increasing the retention and bioavailability of the ofloxacin at the corneal level, Eid et al. developed SLNs encapsulating this antibiotic based on chitosan and polyethylene glycol (PEG). Specifically, permeation studies have shown that the effect of PEG on the action of SLNs was closely related to the percentage of lipid substances used. A lipid-to-pharmaceutical ratio of 17:1 implied a percentage of antibiotic permeation at corneal level greater than 71% in the absence of PEG, greater than 65% in the presence of PEG. In addition, *in vitro* studies showed a 63% of ofloxacin release from SLNs compared to the free drug (Eid2019). The use of chitosan, to increase the stability, adhesion, and antimicrobial potential of SLNs, and ofloxacin, as a bactericidal agent, has recently been taken up by Rodenak-Kladniewet al. They realized, by homogenization and ultrasonification, SLNs based on a lipid matrix in which chitosan and eugenol were incorporated individually and then together. Subsequently, ofloxacin, was loaded to the SLNs. Release tests on all samples showed a peak after 2h and a sustained drug release after 22h. Antimicrobial evaluation activity was conducted through the determination of MIC and revealed a significant antimicrobial efficacy of the nanoformulations against *P. aeruginosa* and *S. Aureus* (Figure 3) (Rodenak-Kladniew2019). *In vivo* tests have shown a possible application of these SLNs in pulmonary infections through inhaled administration. The presence of a lipid coating, such as stearic acid, increased the drug solubility in the external phase, as demonstrated by Shazly (Shazly 2017). In fact, ciprofloxacin has been encapsulated in stearic acid-based SLNs (CIPSTE-SLNs) potentially useful in the treatment of those infections in which it is necessary to administer several doses at regular intervals. With these nanoparticles Shazly hypothesized a reduction in terms of antibiotic administration, and release studies have revealed that the spread of the drug from lipid matrices was sustained up to 12 hours. In addition, the small size and the presence of stearic acid in the SLNs matrix improved their entry into bacterial cells, thus exerting a greater antibacterial action compared to the one expressed by free ciprofloxacin (Shazly 2017).

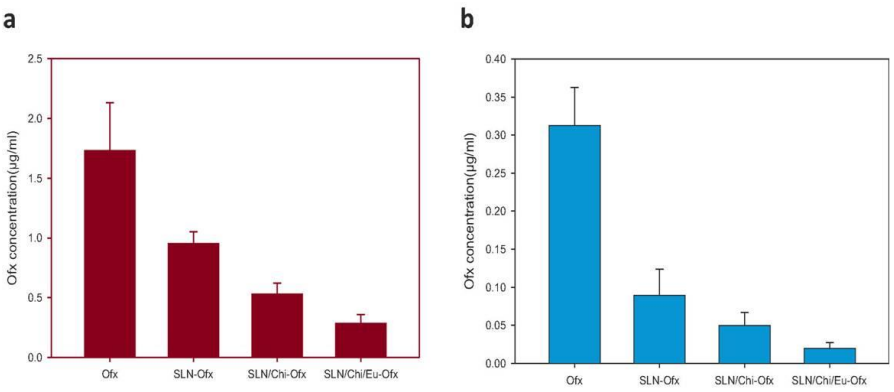

Figure 3. Determination of minimum inhibitory concentration of ofloxacin and ofloxacin-loaded SLNs against *P. aeruginosa* (a) and *S. aureus* (b).
(Adapted with slightly modifications from ref. Rodenak-Kladniew2019).

Generally, in the manufacture of conventional pharmaceutical forms, ciprofloxacin is used as a hydrochloride salt, but cannot be used in the manufacture of vector lipid systems. For this reason, Pignatelloet al. in order to effectively ensure the encapsulation of the antibiotic as a commercial salt in nano-particle systems, have developed SLNs based on ciprofloxacin hydrochloride with the addition of triethylamine (fat-soluble base) which would ensure the in situ conversion of the drug into the free form. Furthermore, with the aim of improving physical stability and interaction with bacterial cell membranes, cationic lipidic didecyldimethylammonium bromide was added to the SLNs. Antimicrobial studies have revealed that these systems could perform a bactericidal action, with a superimposable MIC respect to solutions of free drug was present, against E. *coli, P. aeruginosa, S. aureus, E. faecalis* (Pignatello2018). Encapsulating a fluoroquinolone within nanoparticles may be possible an intracellular drug delivery. Such studies have been conducted by Xieet al. who hypothesized the production of docosanoic acid solid lipid nanoparticles for the intracellular treatment of Salmonella-associated infections. The results obtained showed an inhibition of 99.97%, exerted by enrofloxacin, at minimal concentrations, against Salmonella after 48 h, at intracellular level (Xie2017). Therefore, these SLNs could be optimal carriers for intracellular drug delivery.

4. Macrolides

Macrolides are considered inhibitors of protein synthesis because they exert their antibacterial action through the bond that establishes with the 50S ribosomal subunit, thus inhibitingthe protein synthesis of the bacterium (Dinos 2017). From the chemical point of view, they are made up of a macrocyclic lactonic ring of variable sizes depending on the carbon atoms that make it up (12 or 16) to which one or more deoxy sugars are bound (Zhanel2001). There are four different generations of macrolides classified according to the number of carbon atoms present on the lactonic ring. Macrolides with 12 carbon atoms such as methimycin are very unstable natural derivatives, those with 14 carbon atoms such as erythromycin are very unstable antibiotics under acidic conditions, with poor bioavailability and reduced pharmacokinetics, 15 carbon atoms such as azithromycin and clarithromycin are more stable macrolides under acidic conditions and with good bioavailability, and 16 carbon atoms such as roxithromycin are considered very broad-spectrum macrolides (Sunazuka2003). The spectrum of action of such antibiotics covers microorganisms such as *Streptococcus, Diplococcus, Neisseria gonorrhea, Haemophilus influenzae, Bordetella pertusis, Neisseria meningitis* and*Miycoplasma* (Dinos 2017) (Figure 4) responsible for numerous infections including respiratory ones (Guillot2011).

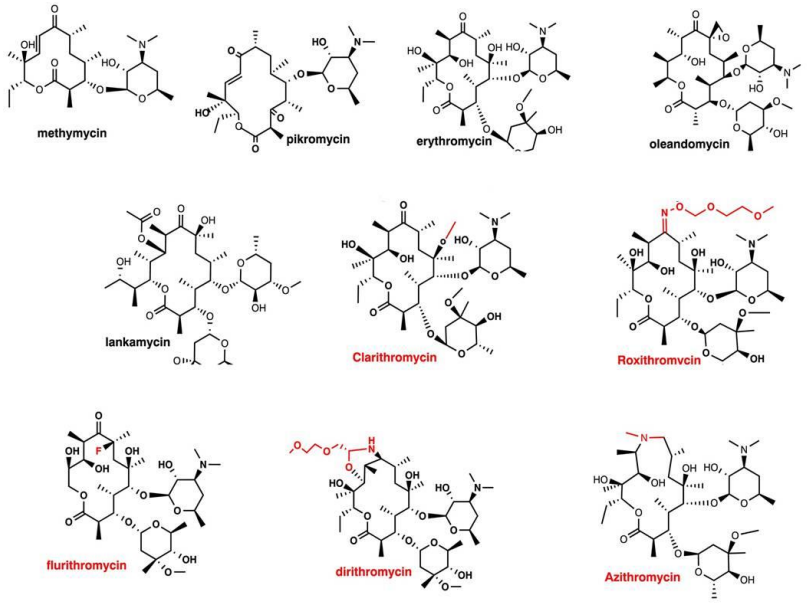

Figure 4. Macrolids chimical structure and their classification according to the number of carbon atoms present on the lactonic ring.
(Adapted with slightly modifications from ref. Dinos 2017).

The chemical-physical instability of some macrolides, including erythromycin, considerably limits the use of these antibiotics in the treatment of gastric infections, as the extremely acidic conditions in this district reduce their activity. The SLNs were usedto overcome this limit since the outer shell of the SLNs can offer protection to the drug from the degradation caused by gastric juices. An example was given by the work of Tran et al. whose aim was to produce stable acidic nanoparticles in which erythromycin has been encapsulated. *In vitro* studies, in fact, have shown a relevant efficacy of erythromycin against *Helicobacter Pylori,* the agent responsible of the gastric ulcers'formation. Specifically, the small size of the nanoparticles (243 nm), the presence of mucoadhesive substances in the lipid coating and the high encapsulation efficiency allowed researchers to obtain satisfactory results in terms of release, gastric mucosa penetration, efficacy, stability and antibacterial action of the drug in acidic environments colonized by *H. pylori* (Le Tuyet2017). The low bioavailability (36%) and the reduced solubility in biological fluids of some macrolides often prevent their use. In this regard, Bhattacharyya and Reddy, realized solid lipidic nanoparticles based on stearic acid as carriers of azithromycin dihydrate, a macrolide antibiotic with poor bioavailability and

solubility in physiological fluids but with a high bactericidal power. *In vitro* release studies carried out on different formulations of the same SLNs have shown a lower release of the drug when encapsulated in lipid matrices made in a 2:1 ratio between stearic acid and surfactant. Conversely, the presence of reduced amounts of stearic acid and surfactant in a 1:1 ratio allowed to show a better release than the nanoparticle drug. In addition, stability studies performed on these formulations, in phosphate buffer, have shown a stability in terms of chemistry and content of the active ingredient (98% drug) at 40±2°C up to 90 days (Bhattacharyya and Priyanka 2019). Often the type of lipid used for the realization of nanoparticles can influence positively or negatively the drug release properties, particle size and encapsulation efficiency. In this regard, Öztürket al. have developed clarithromycin based SLNs for oral administration, using different lipid matrices based on glyceryl behenate, tripalmitin and stearic acid for its delivery. These studies carried out showed that the encapsulation efficiency of clarithromycin in the different formulations obtained was between 63-89% and that the release of the drug from SLNs showed a peak after 6 h with a constant trend for the following 48h, all closely related indirectly to the length of the carbon chain of lipids. This means that the release takes place according to the size of the particles which in turn, together with the internal content of the drug, are directly affected by the growth of the carbon chain of lipids. The antibacterial activity of the formulations tested against *Staphylococcus aureus* showed inhibition halos due to the bactericidal action of clarithromycin (Öztürka2019). It is therefore evident that lipid characteristics can affect several parameters of nanoparticles but rarely induce toxicity at the tissue level.

5. Aminoglycoside

They are a class of antibiotics that act against microorganisms such as *Acinetobacter, Citrobacter, Enterobacter, E. coli, Klebsiella, Proteus, Providencia, Pseudomonas, Salmonella, Serratia, Shigella, Staphylococci* and *M. tuberculosis* (Krause2020; Takahashi and Igarashi 2018). The mechanism of action of aminoglycosides involves inhibition of the 30S subunit and 16S subunit of ribosomal RNA as shown in Figure 5 (Poulikakos and Falagas 2013) and is closely related to the chemical structure of the antibiotic.

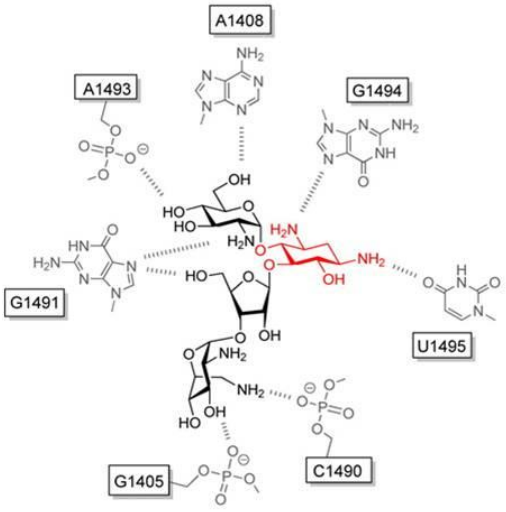

Figure 5. Mechanism of aminoglycoside interaction with 16S subunit of ribosomal RNA. (Adapted with slightly modifications from ref. Poulikakos and Falagas 2013).

The latter, in fact, consisting of an inositol derivative bound to an amino sugar as shown in Figure 6, has several hydroxyl groups and two amino acids that are the main elements of connection with the 30S subunit of the ribosome (Forgea and Schacht2000; Becker and Cooper 2013).

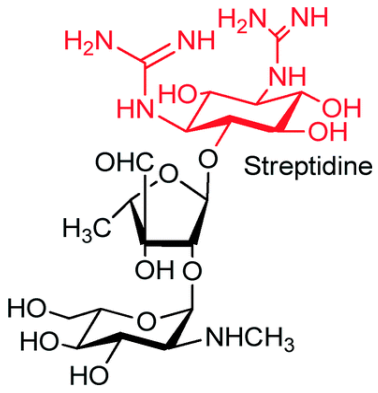

Figure 6. Streptomicyn chemical structure.

Aminoglycosides are classified according to their origin: natural (streptomycin, kanamycin, tobramycin, gentamicin, paranomycin, sisomycin) and semi-synthetic (amikacin, dibekacin, netilmycin, isepamycin). Some aminoglycosides of natural origin are commonly topically

administered in the treatment of ears, eyes, and skin infections, others are administered as aerosols for the treatment of lung infections and intranasally in the treatment of central nervous system infections. Those of semisynthetic origin are administered intravenously or intramuscularlyin the treatment of more serious infections such as tuberculosis, abdominal, urinary and sepsis (Takahashi and Igarashi 2018). From a pharmacokinetic and pharmacodynamic point of view, aminoglycosides are drugs that have a poor body distribution, as they cannot overcome all biological barriers in the body. Moreover, they induce nephrotoxicity and are therefore administered in a single daily dose (Forgea and Schacht2000). The possibility of delivering these antibiotics through nanotechnological carriers such as SLNs could improve pharmacokinetic parameters (bioavailability, release), distribution in tissues, frequency of administration and their toxicity (Poulikakos and Falagas 2013). For example, at ocular level, topical administration of aminoglycosides ensures effective pharmacological action only in the anterior portion of the eye where, however, poor corneal retention and the presence of aqueous humor further reduce the absorbed amount (Battaglia 2016). On the other hand, in the posterior segment, the poor permeation of drugs, especially hydrophobic ones, through the retinal barrier and within the vitreous humour prevents their administration by topical administration due to the poor pharmacological activity manifested. The lipid component of SLNs, however, unlike conventional pharmaceutical forms, is able to interact with the lipid layer of the tear film, increasing the drug time residence in the conjunctival sac and its absorption at both the anterior and posterior segment (Farid2017; Sánchez-López2016). In this regard, Chetoniet al. have realized SLNs based on stearic acid in which tobramycin, an aminoglycoside of natural origin, complexed with hexadecylphosphate, has been encapsulated for possible topical administration at pre-corneal and retinal level. Morphological analyses using Transmission electron microscope (TEM) and Fourier Transform Infrared Spectroscopy (FT-IR) showed a complete dispersion of tobramycin in the lipid matrix of nanoparticles without obvious electrostatic interactions with stearic acid (Chetoni 2016). *In vitro* release studies have also confirmed the massive presence of the drug within the lipid core due to the absence of an initial burst release effect typical of the presence of the drug on SLNs surface. This could mean that carriers are able to promote the slow release of the antibiotic in biological fluids as also revealed by *in vivo* tests carried out on rabbit eye tissues. Specifically, obtained the results confirmed that the drug

released amount by SLNs after topical administration was five times higher than that released by commercial drops and standard solution with free tobramycin. In addition, the release of the antibiotic to the mucous membrane of the eye remained constant up to 3h after administration, showing high concentrations of the antibiotic in both the aqueous and vitreous humours. Similar results were also obtained after intravenous administration in the rabbit, as shown in Figure 7, where a peak drug concentration was evident one hour after administration at retinal level.

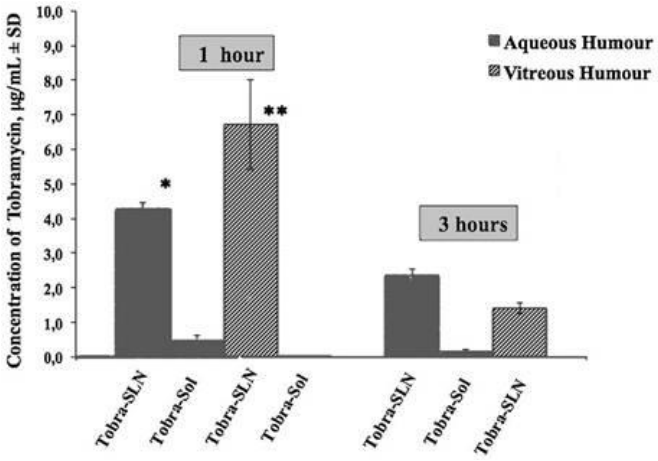

Figure 7. *In vivo* studies of tobramycin loaded SLNs and tobramycin solution release to the humor vitreo and humor acqueo of the rabbit eye after 1h and 3h after intravenous administration. (Adapted with slightly modifications from ref. Chetoni 2016).

In addition, antibacterial studies on SLNs have shown an antibacterial action exerted by tobramycin encapsulated in them, on *Pseudomonas aeruginosa* cultures (Chetoni 2016). These nanocarriers may be useful not only in the treatment of eye infections, but also in the treatment of lung infections caused by *Pseudomonas aeruginosa*, especially in patients with cystic fibrosis. However, the inhalation of tobramycin is not sufficient to ensure a high concentration of the drug at the target site because there is poor mucus penetration with rapid mucus elimination and the need of multiple administrations (Kamal and Debonnett 2017). Patients with cystic fibrosis are subject to accumulation of significant amounts of mucus in the lungs, therefore it is necessary to use carriers capable of penetrating in the mucus, releasing the drug and prolonging its retention (Klinger-Strobel2015). Moreno-Sastreet al. have developed and characterized tobramycin-based SLNs for the treatment of cystic fibrosis patients. In

particular, *in in vitro* release studies these nanoparticles showed a drug release of 80% after the first 24 h, while at the end of the study, after 92 h, there was a prolonged release of 100% encapsulated tobramycin. Moreover, thanks to the addition of specific dyes during the production phase of SLNs, it was possible to observe the effect of the drug on cell growth and mucus penetration by means of cell viability and artificial mucus penetration studies.The obtained results have shown that no formulation induces toxicity on *A549* and *H441* cell lines and that the presence of mucolytic agents such as carboximethylcysteine increases the penetration of nanoparticles (73%) through artificial mucus (Figure 8) promoting the release of tobramycin. Antimicrobial studies, on the other hand, have shown antibacterial activity of aminoglycoside on Pseudomonas aeruginosa cultures at a concentration of 0.5 mg/ml (Moreno-Sastre2016).

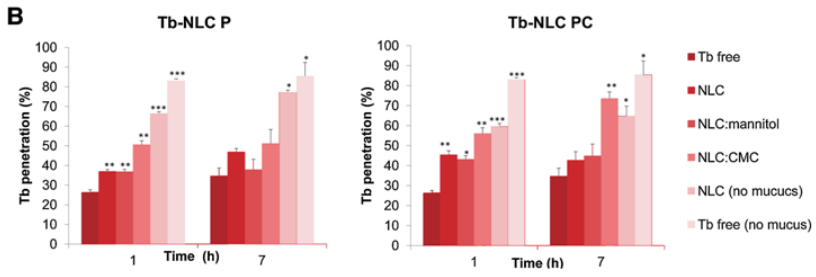

Figure 8. Study of mucus penetration of Tobramycin-loaded NLCs.
(Adapted with slightly modifications from Moreno-Sastre2016).

Aminoglycosides, such as streptomycin, are antibiotics of choice in the treatment of *M. tuberculosis* infections, a bacterium capable of replicating within the alveolar macrophages by killing them and spreading the infection to the lungs. A drug capable of inhibiting the replication of these microorganisms is streptomycin (Manu and Rogozea 2016), which is also useful in the treatment of cerebral tuberculosis, an extrapulmonary disease characterized by a migration in the blood, of tubercular bacilli of pulmonary origin capable of reaching the brain and infecting the subpial or subependimal region of the brain and the spinal cord. This is the origin of tubercular meningitis, tubercolar abscesses, intracranial tuberculosis and tuberculosis encephalopathies (Bosaeed and Alothman 2017). As reported by Kumar *et al.*, intranasal

administration of streptomycin encapsulated in SLNs may be a viable option for the treatment of cerebral tuberculosis as these carriers may be able to cross cell membranes in the brain and release the drug directly into the affected site. The small size of these SLNs (140 nm) could facilitate the transport of streptomycin through the nasal mucosa so that it penetrates brain tissue via the bloodstream. *In vitro* release studies on streptomycin nanoparticles have shown a 100% release of streptomycin after 24 h after administration while in vivo gamma scintigraphy release studies have shown a slow and controlled renal excretion of these drugs as renal radioactivity after 1 h after administration was negligible. For this reason, they could be carriers useful for the delivery of streptomycin to the brain (Kumar2014).

6. Rifamycins

Rifamycins represent a class of broad-spectrum antibiotics used in the treatment of numerous infections caused by Gram-positive and Gram-negative bacteria and microorganisms such as *M. tuberculosis* (Floss and Yu 2005). They possess a heterocyclic structure containing a naphthoquinone nucleus crossed by an aliphatic chain as shown in Figure 9 (YulugBurak2014).

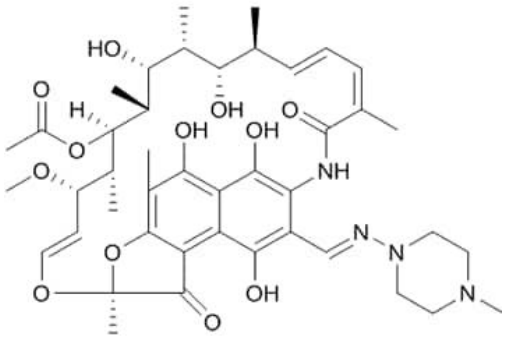

Figure 9. Rifamycin heterocyclic chemical structure.

The four hydroxyl groups and naphthalene rings, which form hydrogen bonds with the amino acid residues of RNA, are responsible for the interaction between antibiotic and microorganism. In fact, the mechanism of action by which the rifamycins inhibit bacterial activity consists in the inhibition of "RNA polymerase DNA" dependent through the binding with the beta subunit (Floss and Yu 2005). There are different types of rifamycins, the most

widely used, especially in the treatment of tuberculosis (TB) and tuberculosis meningitis is rifampicin, a lipophilic drug able to cross the blood-brain barrier with extreme ease (Sekaggya-Wiltshire and Dooley 2019). However, as with many antibiotics, rifampicin has pharmacokinetic parameters, including poor bioavailability, short half-life, and hepatotoxicity, which reduce its use (Abulfathi2019). In the last ten years, however, rifampicin has evolved in the treatment of tuberculosis, as several studies have shown that the use of high doses of this antibiotic reduces the duration of treatment without the need for repeated administration, and without increasing relapses or causing side effects (Grobbelaara2019). The improvement of pharmacokinetic parameters could improve the effectiveness of the therapy and increase patient compliance. Therefore, drug transport systems that protect drugs from early degradation and promote their prolonged release may be useful. In this regard, a few nanoparticulated carriers have been developed, including SLNs capable of delivering rifampicin directly to the target site, improving its bioavailability and transport. As reported in Chokshiet al. rifampicin encapsulated in SLNs through microemulsion has shown some stability and resistance under gastric-like conditions, because such formulations could be administered orally, increasing the bioavailability of the drug. In addition, *in vitro* studies have shown that the rifampicin contained in SLNs would undergo a biphasic pH dependent release as it would result in an initial burst phase that would tend to stabilize after about 120h after administration, thus promoting a prolonged drug release of 90% (Chokshi2018). Of the SLNs made for the treatment of tuberculosis and specifically to be deposited on the alveolar epithelium and subsequently absorbed by the infected macrophages, it is important to know the interactions with the surfactant that covers the pulmonary alveoli. In fact, when nanoparticles administered in the form of dry dust by inhalation reach the lung alveoli, the first component they encounter in the form of a monolayer or oligolamellar layer is the lung surfactant. The presence of a lipidic corona layer around the SLNs, could modulate the cellular internalization of antitubercular drugs as demonstrated by the study conducted by Marettiet al. on solid lipidic nanoparticles loaded with rifampicin (Maretti 2019). Specifically, SLNs functionalized with a mannosilate surfactant of synthetic origin were treated during *in vitro* tests with Curosurf, a commercial substitute for the natural lung surfactant, and with simulated lung fluids (SLF). The obtained data showed that the rifampicin release from mannosylated SLNs, in contact with the simulated lung fluids, was gradual and approximately 40% after 3h

after inhalation. Conversely, the release obtained from SLNs in contact with Curosurf was 20-25% lower than that of mannosylated SLNs. This could mean that the presence of a functionalizing agent inside the lipid component, as in the case of mannosylated SLNs, was able to generate a more solid layer of lipidic corona capable of increasing the retention of the drug inside it, preventing the superficial diffusion at surfactant level and ensuring an intramacrophagic internalization of 100% after 0.5h and 45% after 3h as shown in Figure 10.

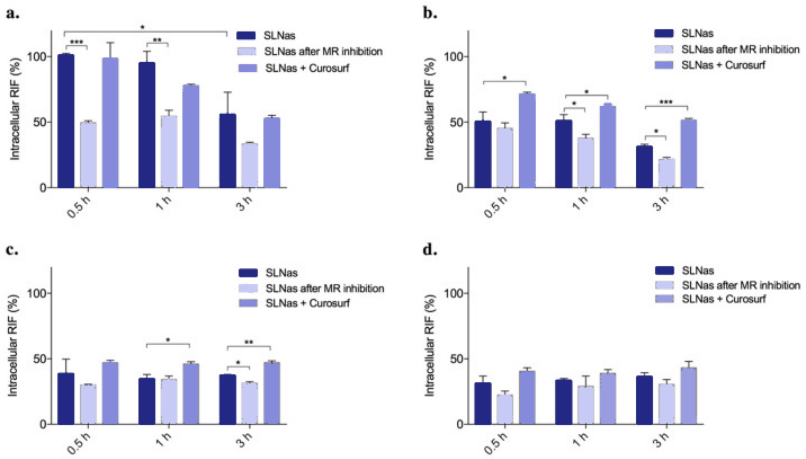

Figure 10. Studies of intramacrophagic internalization of rifampycin mannosylated SLNs after 0.5h and 3h administration.
(Adapted with slightly modifications from ref. Maretti 2019).

Once it enters the macrophage, the lipid carrier could undergo a phagocytosis process that would lead to the degradation of lipid materials and to the intracellular loss of rifampicin, which would thus exert antibacterial activity against *M. tubercolosis* (Maretti 2019). Literature ata have shown that some patients suffering from tuberculosis are not very susceptible to the action of rifampicin and for this reason it was necessary, over time, to replace it with a more powerful rifamycin such as rifabutin (Whitfield2018). The administration of this antibiotic with the use of SLNs, as demonstrated by the studies of Gaspar et al. could not only have an effective action in the treatment of M. tuberculosis infections, but also ensure reduced cytotoxicity on the lung cell lines used. In addition, studies of intracellular uptake through fluorescence have shown an increased internalization of SLNs in macrophagic cells 24 hours after incubation. This means that in the case of tuberculosis, the use of these rifabutin-laden nanoparticles would allow the drug to be localized in the macrophages for a period that would

ensure that the antibacterial activity would be carried out (Gaspara2016). AlsoNirbhavaneet al. realized SLNs based on glyceryl monostearate for the delivery of rifabutin (RFB-SLN) in animal models. Specifically, the pharmacokinetics and biodistribution of these nanoformulations in mice after single oral administration were studied. The obtained results from the *in vitro* studies showed that the drug, encapsulated at 60% in the lipid matrix of SLNs, remained stable under acidic conditions up to 48 h, thus demonstrating a good bioavailability probably due to the direct absorption of nanoparticles through the gastrointestinal tract into the systemic circulation. Furthemore, *in vivo* studies have shown that after a single oral administration, RFB-SLN was able to be distributed in all organs of the reticuloendothelial system (lungs, liver, and spleen) for up to seven days. The amount of drug found in one of the tissues mentioned above was well above the MIC level (0.125 μ g/ml), especially in those tissues more prone to infection with microorganisms, i.e., alveolar macrophages and liver macrophages (Nirbhavane2017).

7. Conclusion

Many antimicrobial drugs are characterized by several limitations, including low water solubility, narrow activity spectrum, rapid degradation, poor bioavailability, and reduced tolerability. In addition, the effectiveness of conventional antibiotic therapy is hampered by the difficulty of reaching many target tissues and crossing several biological barriers. The advent of nanotechnology has significantly revolutionized the use of antibiotics, in fact, solid lipid nanoparticles (SLNs) with their small size and chemical-physical properties, are able to increase the biological availability of many drugs making them more susceptible to entry into cells or tissues than common pharmaceutical forms. SLNs are also able to improve the quality of antibiotic treatment through a reduction in side effects, frequency of administration and an extension of the drug's residence time. From a pharmacokinetic point of view, such nanoformulationsare able to control the uniform distribution of drug by exerting a sustained and controlled release capable of improving cellular internalization. Several studies reported in this chapter have shown a reassuring efficacy in the use of SLNs for the delivery of antibiotics in the treatment of numerous infections. Specifically, it has been seen that these carriers are able to transport drugs into tissues that are difficult to reach, including the blood-brain barrier and the inside of macrophages, bringing numerous novelties in the approach to diseases such

as encephalic and pulmonary tuberculosis. In addition, some SLNs have also proved to be useful in the treatment of infections localized in tissues difficulty accessible by common pharmaceutical forms. For this reason, it is possible to declare that the development of these nanoformulations has modified the systems of administration of antibiotics making them much more effective in the management of bacterial infections.

References

Cassano Roberta, Curcio Federica and Trombino Sonia. Solid Lipid Nanoparticles: An Interesting Strategy for Antibiotics Administration. In: Lipid Nanoparticles: Advances in Research and Applications, Ed. Sabine Ziegler, Chapter 2. *Nova publisher 2020*.

1. Abed, Nadia and Patrick Couvreur. 2014. "Nanocarriers for antibiotics: A promising solution to treat intracellular bacterial infections" *International Journal of Antimicrobial Agents* 43:485-496.
2. Abulfathi, Ahmed Aliyu, Eric H. Decloedt, Elin M. Svensson, Andreas H. Diacon, Peter Donald, Helmuth Reuter. 2019. "Clinical Pharmacokinetics and Pharmacodynamics of Rifampicin in Human Tuberculosis" *Clinical Pharmacokinetics and Pharmacodynamics of Rifampicin in Human* TB 58:9:1103-1129.
3. Baig, Mirza Salman, Abdul Ahad, Mohammed Aslam, Syed Sarim Imam, Mohd Aqi and Asgar Ali. 2016. "Application of Box–Behnken design for preparation of levofloxacin-loaded stearic acid solid lipid nanoparticles for ocular delivery: Optimization, in vitro release, ocular tolerance, and antibacterial activity." *International Journal of BiologicalMacromolecules* 85:258-270.
4. Battaglia, Luigi, Loredana Serpe, Federica Foglietta, Elisabetta Muntoni, Marina Gallarate, Ana Del Pozo Rodriguezand Maria Angeles Solinis. 2016. "Application of lipid nanoparticles to ocular drug delivery." *Expert opinion on drug delivery*.
5. Becker, Bernd and Matthew A. Cooper. 2013. "Aminoglycoside Antibiotics in the 21st Century." *ACS Chemical Biology*8:105-115.
6. Bhattacharyya, Sayani andPriyanka Reddy. 2019. "Effect of surfactant on azithromycin dihydrate loaded stearic acid solid lipid nanoparticles. " *Turkish Journal ofPharmaceuticalSciences*16:4:425-31.
7. Bosaeed, Mohammad A. and Adel Alothman. 2017."Pathogenesis of Tuberculosis of the Nervous System." In *Tuberculosis of the Central Nervous System Pathogenesis, Imaging, and Management*. Edited by Mehmet Turgut, Ali Akhaddar, Ahmet T. Turgut, Ravindra K. Garg. Chapter 3. Springer.
8. Canaparo, Roberto, Federica Foglietta, Francesca Giuntini, Carlo Della Pepa, Franco Dosio and Loredana Serpe. 2019. "Recent developments in antibacterial therapy: focus

on stimuli-responsive drug-delivery systems and therapeutic nanoparticles." *Molecules 24*:1991.

9. Chaudhry, Saira B., Michael P. Veve and Jamie L. Wagner. 2019. "Cephalosporins: a focus on side chains and lactam cross-reactivity." *Pharmacy* 7:103.
10. Chetoni, Patrizia, Susi Burgalassi, Daniela Monti, Silvia Tampucci, Vivian Tullio, Anna Maria Cuffini Elisabetta Muntoni, Rita Spagnolo, Gian Paolo Zara and Roberta Cavalli. 2016. "Solid lipid nanoparticles as promising tool for intraocular tobramycin delivery: Pharmacokinetic studies on rabbits." *European Journal of Pharmaceutics and Biopharmaceutics* 109:214-223.
11. Chokshi, Nimitt V., Hiren N. Khatri and Mayur M. Patel.2018. "Formulation, Optimization and Characterization of Rifampicin Loaded Solid Lipid Nanoparticles for the Treatment of Tuberculosis*." Drug Development and Industrial Pharmacy* 44:12:1975-1989.
12. Combrink, Keith D., Andrea Ramirez Ramos, Stephanie Spring, Sebastian Schmidl, Kira Elizondo, Petronilo Morin, Bryant De Jesus and Florian P. Maurer. 2019. "Rifamycin derivatives active against pathogenic rapidly-growing mycobacteria." *Bioorganic & Medicinal Chemistry Letters* 29:2112–2115.
13. Corallo, Carmela and Syed Tabish R. Zaidi. 2016. "Cephalosporins." In *Drug Dosing in Obesity.* Edited byS.T.R. Zaidi and J.A. Roberts. Chapter 3. Switzerland: Springer International Publishing.
14. Craig, William A. and David R. Andes. 2015. "Cephalosporins." In *Basic Principles in the Diagnosis and Management of Infectious Diseases*. Edited by Mandell, Douglas, and Bennett's. Chapter 21. Elsevier.
15. Dinos, George P. 2017. "The macrolide antibiotic renaissance." *British Journal of Pharmacology*174: 2967-2983.
16. Eid, Hussein M., Mohammed H. Elkomy, Shahira F. El Menshawe and Heba F. Salem. 2019. "Development, optimization, and in vitro/in vivo characterization of enhanced lipid nanoparticles for ocular delivery of ofloxacin: the influence of pegylation and chitosan coating." *AAPS PharmSciTech* 20:183.

17. Ezelarab, Hend A., Samar H. Abbas, Heba A., Hassan and Gamal El-Din A. Abuo-Rahma. 2018. “Recent updates of fluoroquinolones as antibacterial agents.” *Arch Pharm Chem Life Sci* 351.
18. Farid, Ragwa M., Noha S. El-Salamouni, Amal H. El-Kamel and Safaa S. El-Gamal. 2017. “Lipid-based nanocarriers for ocular drug delivery.” In *Nanostructures for Drug Delivery*. Edited by Ecaterina Andronescu and Alexandru Mihai Grumezescu, chapter 16:495-522.
19. Floss, Heinz G. and Tin-Wein Yu. 2005. “Rifamycins: mode of action, resistance, and biosynthesis.” *Chemical Reviews*.105:621-632.
20. Forgea, Andrew and Jochen Schacht.2000. “Aminoglycoside Antibiotics.” *AudiolNeurootol* 5:3-22.
21. Furneri, Pio Maria and Virginia Fuochi.2017.“Lipid-based nanosized delivery systems for fluoroquinolones: a review.” *Current Pharmaceutical Design*23:43.
22. Gao, Weiwei, SorachaThamphiwatana, PavimolAngsantikul, and Liangfang Zhang. 2014. “Nanoparticles approaches against bacterial infections.” Wiley Periodicals 6.
23. Gaspar, Diana P. and António J. Almeida. 2019. “Surface-functionalized lipid nanoparticles for site-specifc drug delivery.” In *Surface Modifcation of Nanoparticles for Targeted Drug Delivery.* Edited by Pathak, Y. V. Chapter 4.
24. Gaspara, Diana P. Vasco Fariaa, Lídia M.D. Gonçalvesa, Pablo Taboadac, Carmen Remuñán-Lópezb, António J. Almeida. 2016. “Rifabutin-loaded solid lipid nanoparticles for inhaled antitubercular therapy: Physicochemical and in vitro studies.” *International Journal of Pharmaceutics* 497:199-209.
25. Gordillo-Galeano, Aldemar, and Claudia Elizabeth Mora –Huertas. 2018. “Solid lipid nanoparticles and nanostructured lipid carriers: A review emphasizing on particle structure and drug release.” *European Journal of Pharmaceutics and Biopharmaceutics* 133: 285-308.
26. Grobbelaara, Melanie, Gail E. Louwb, Samantha L. Sampsona, Paul D. van Heldena, Peter R. Donaldc and Robin M. Warren. 2019. “Evolution of rifampicin treatment for tuberculosis Infection.” *Genetics and Evolution* 74:103937.

27. Guillot, Loïc, Olivier Tabary, Nadia Nathan, Harriet Corvol and Annick Clement. 2011. "Macrolides: New therapeutic perspectives in lung diseases." *The International Journal of Biochemistry & Cell Biology* 43:1241-1246.
28. Hussain, Sazid, JinmyoungJoo, Jinyoung Kang, Byungj Kim, Gary B. Braun, Zhi-Gang She, Dokyoung Kim, Aman P. Mann, TarmoMölder, TambetTeesalu, Santina Carnazza, Salvatore Guglielmino, Michael J. Sailor and ErkkiRuoslahti. 2018."Antibiotic-loaded nanoparticles targeted to the site of infection enhance antibacterial efficacy." *Nature Biomedical Engineering* 2:95-103.
29. Islan, Germán A., Pablo Cortez Tornello, Gustavo A. Abraham, Nelson Duran and Guillermo R. Castro. 2016. "Smart lipid nanoparticles containing levofloxacin and DNase for lung delivery. Design and characterization." *Colloids and Surfaces B: Biointerfaces* 143:168–176.
30. Kamal, Hamed and Laurie Debonnett. 2017. "Tobramycin inhalation powder for the treatment of pulmonary *Pseudomonas aeruginosa* infection in patients with cystic fibrosis: a review based on clinical evidence." *Therapeutic Advances inRespiratoryDisease*. 11:5:193-209.
31. Klinger-Strobel, Mareike, Christian Lautenschläger, Dagmar Fischer, Jochen G Mainz, Tony Bruns, Lorena Tuchscherr, Mathias W Pletz&OliwiaMakarewicz. 2015. "Aspects of pulmonary drug delivery strategies for infections in cystic fibrosis where do we stand?" *Expert Opinion Drug Delivery* 12:8:1351-1374.
32. Krause, Kevin M., Alisa W. Serio, Timothy R. Kane and Lynn E. Connolly. 2020. "Aminoglycosides: An Overview." In *Cold Spring Harbor Laboratory Press*. Edited by Lynn L. Silver and Karen Bush.
33. Kumar, Manoj, VanditaKakkar, Anil Kumar Mishra, Krishna Chuttani, Indu Pal Kaur. 2014. "Intranasal delivery of streptomycin sulfate (STRS) loaded solid lipid nanoparticles to brain and blood." *International Journal of Pharmaceutics* 461: 223-233.
34. Kumar, Sandeep, Gaurav Bhanjana, Arvind Kumar, Kapila Taneja, Neeraj Dilbaghi and Ki-Hyun Kim. 2016."Synthesis and optimization of ceftriaxone-loaded solid lipid nanocarriers." *Chemistry and physics of lipids* 200:126-132.

35. Lakshminarayanan, Rajamani, Enyi Ye, David James Young, Zibiao Li andXian Jun Loh. 2018. “Recent advances in the development of antimicrobial nanoparticles for combating resistant “pathogens.” *Advanced Healthcare Materials* 7.
36. Le-Deygen, Irina M., Anna A. Skuredina and Elena V. Kudryashova, 2017. “Drug delivery systems for fluoroquinolones: new prospects in tuberculosis treatment.” *Russian journal of bioorganic chemistry* 43:5.
37. Le Tuyet, Chau Tran, Claire Gueutin, Ghislaine Frebourg, Christophe Burucoa and Vincent Faivre. 2017. “Erythromycin encapsulation in nanoemulsion-based delivery systems for treatment of Helicobacter pylori infection: Protection and synergy.” *Biochemical and Biophysical Research Communications* 493:146-151.
38. Manu and Rogozea. 2016. “Streptomycin for Pulmonary Tuberculosis.” *American Journal of Therapeutics* 23:653-654.
39. Maretti, Eleonora, Cecilia Rustichelli, Magdalena Lassinantti Gualtieri, Luca Costantino, Cristina Siligardi, Paola Miselli, Francesca Buttini, Monica Montecchi, Eliana Leo, Eleonora Truzzi and Valentina Iannuccelli. 2019. “The Impact of Lipid Corona on Rifampicin Intramacrophagic Transport Using Inhaled Solid Lipid Nanoparticles Surface-Decorated with a Mannosylated Surfactant.” *Pharmaceutics* 11:50.
40. Moreno-Sastre, María, Marta Pastor, Amaia Esquisabel, Eulàlia Sans, Miguel Viñas, Aarne Fleischer, Esther Palomino, Daniel Bachiller and José Luis Pedraz. 2016. “Pulmonary delivery of tobramycin-loaded nanostructured lipid carriers for Pseudomonas aeruginosa infections associated with cystic fibrosis.” *International Journal of Pharmaceutics* 498:263-273.
41. Nath, Aiswarya P., Arul Balasubramanian and Kothai Ramalingam. 2020. “Cephalosporins: An imperative antibiotic over the generations”. *International Journal of Research in Pharmaceutical Sciences*11:623-629.
42. Nirbhavane, Pradip, Nalini Vemuri, Neeraj Kumar, and Gopal Krishan Khuller. 2017. “Lipid nanocarrier-mediated drug delivery system to enhance the oral bioavailability of rifabutin.” *AAPS PharmSciTech* 18:3.
43. Owens, Robert C., and G. Paul. 2005. “Ambrose antimicrobial safety: focus on fluoroquinolones.” *Clinical Infectious Diseases* 41:144-57.

44. Ozcengiz, Gulay and Arnold L. Demain. 2013. “Recent advances in thebiosynthesis of penicillins, cephalosporins and clavams and its regulation.” *Biotechnology Advances* 31:287-311.
45. Öztürka, A. Alper, Abdurrahman Aygülb and BehiyeŞenel. 2019. “Influence of glyceryl behenate, tripalmitin and stearic acid on the properties of clarithromycin incorporated solid lipid nanoparticles (SLNs): Formulation, characterization, antibacterial activity and cytotoxicity.” *Journal of Drug Delivery Science and Technology*.
46. Pham, Thu D. M., Zyta M. Ziora and Mark A. T. Blaskovich. 2019.“Quinolone antibiotics”. *Medicinal Chemistry Communications* 10:1719.
47. Pignatello, Rosario, Leonardi, Antonio, Fuochi, Virginia, Petronio, Giulio, Greco, Antonio S., Furneri, Pio Maria. 2018. “A method for efficient loading of ciprofloxacin hydrochloride in cationic solid lipid nanoparticles: formulation and microbiological evaluation.” *Nanomaterials*8:304.
48. Polo, Ester, Manuel Collado, BeatrizPelaz and Pablo Del Pino. 2017. “advances toward more efficient targeted delivery of nanoparticles in vivo: understanding interactions between nanoparticles and cells.” *American Chemical Society.* 11:3:2397-2402.
49. Poulikakos, Panagiotis and Matthew E. Falagas. 2013. “Aminoglycoside therapy in infectious diseases.” *Expert Opinion Pharmacotheraphy*14:12.
50. Ranghar, Shweta, ParulSirohi, Pritam Verma and Vishnu Agarwal. 2014.“Nanoparticle-based drug delivery systems: promising approaches against infections.” *Brazilian Archives of Biology and Technology*57:2: 209-222.
51. Reimondez-Troitiño, Sonia, NemethCsaba, Maria J. Alonso and Martinez dela Fuente.2015. “Nanotherapies for the treatment of ocular diseases.” *EuropeanJournal of Pharmaceutics and Biopaharmaceutics*. 95:279-293.
52. Rodenak-Kladniew, Boris, Sebastian Scioli Montoto, Maria Laura Sbaraglini, Miriam Di Ianni, Eric M. Ruiz, Alan TaleviVeronica A., Alvarez, Nelson Durán, Gustavo R. Castro and Gazi A. Islan. 2019. “Hybrid Ofloxacin/eugenol co-loaded solid lipid nanoparticles with enhanced and targetable antimicrobial properties.” *International Journal of Pharmaceutics* 569:8575.

53. Sánchez-López, Elsa., Marta Espina, Slavomira Doktorovova, Eliana B. Souto, M.L. García. 2016."Lipid nanoparticles (SLN, NLC): Overcoming the anatomical and physiological barriers of the eye-Part II-Ocular drug-loaded lipid nanoparticles." *European Journal of Pharmaceutics and Biopharmaceutics* 1-12.
54. Sekaggya-Wiltshire, Christineand Kelly E. Dooley. 2019. "Pharmacokinetic and pharmacodynamic considerations of rifamycin antibiotics for the treatment of tuberculosis". *Expert opinion on drug metabolism & toxicology* 15:8:615-618.
55. Shahbaz, Kiran. 2017. "Cephalosporins: pharmacology and chemistry." *Pharmaceutical and Biological Evaluations*.4.6:234-238.
56. Shah, Dushyant, DollyGupta and Yamini Shah. 2017."Effect of lipid and surfactant concentration on cefpodoximeproxetil solid lipid nanoparticle." *European journal of biomedicaland pharmaceutical sciences* 4.
57. Shaikh, Sibhghatulla, Jamale Fatima, Shazi Shakil, Syed Mohd, Danish Rizvi and Mohammad Amjad Kamal. 2015."Antibiotic resistance and extended spectrum beta-lactamases: Types, epidemiology and treatment." *Saudi Journal of Biological Sciences* 22:90-101.
58. Shazly, Gamal A. 2017. "Ciprofloxacin controlled-solid lipid nanoparticles: characterization, in vitro release, and antibacterial activity assessment." *BioMed Research International* 9.
59. Shimanovich and AhoronGedanken. 2016. "Nanotechnology solutions to restore antibiotic activity". *Journal of Materials Chemistry B.* 4:824.
60. Shirure, Parikshit Dhanu, MahewashAsadulla Pathan, Priyanka Ramesh Surwase and Manjusha Shivkumar Kareppa**.** 2019. "A review on solid lipid nanoparticles: as a promisingapproach for targeted drug delivery system." *World journal of pharmacy and pharmaceutical sciences*8:3.
61. Singha, Bhupender, Parameswara Rao Vuddandaa, M.R. Vijayakumar, VinodKumarb, Preeti S. Saxenab and Sanjay Singha. 2014 "Cefuroxime axetil loaded solid lipid nanoparticles for enhancedactivity against S. aureus biofilm." *Colloids and Surfaces B: Biointerfaces* 121:92-98.
62. Singh, Chandra Kala, Vishnu Tiwari, Ravi Shankar, Chandra Prakash Mishra, Sarvesh Jain, Sandeep Jain and Sandhya Jaiswal. 2015. "A short review on oral fast dissolving

film containing cefpodoxime proxetil nanoparticle." *World journal of pharmacy and pharmaceutical sciences* 5.

63. Sunazuka, Toshiaki, SadafumiOmura, Shigeo Iwasaki and Satoshi Mura. 2003. "Chemical modification of macrolides." In *Macrolide Antibiotics (Second Edition) Chemistry, Biology and Practice*. Edited by Satoshi Ōmura, Chapter 399-180. USA:Elsevier.
64. Takahashi, Yoshiaki and Masayuki Igarashi. 2018. "Destination of aminoglycoside antibiotics in the post-antibiotic era." *The Journal of Antibiotics* 71: 4-14.
65. Valappil, Sabeel Padinhara. 2018. "Nanosystems and antibacterial applications." In *Drug Delivery Nanosystems for Biomedical Applications,* edited by Chandra P. Sharma. Chapter 5. Amsterdam: Elsevier.
66. Wang, Linlin, Chen Hu andLongquan Shao. 2017. "The antimicrobial activity of nanoparticles: present situation and prospects for the future." *International Journal of Nanomedicine* 12.
67. Whitfield, Michael G., Robin M. Warren, Vanessa Mathys, Lesley Scott, Elise De Vos, Wendy Stevens, Elizabeth M. Streicher, Guido Groenen, Frederick A. Sirgel and Annelies Van Rie. 2018. "The potential use of rifabutin for treatment of patients diagnosed with rifampicin-resistant tuberculosis." *Journal of Antimicrobial Chemotherapy*. 73: 2667-2674.
68. Xie, Shuyu, Yanfei Tao, Yuanhu Pan, Wei Qu, Guyue Cheng, Lingli Huang, Dongmei Chen, Xu Wang, Zhenli Liu andZonghui Yuan. 2014. "Biodegradable nanoparticles for intracellular delivery of antimicrobial agents." *Journal of Controlled Release* 187:101-117.
69. Xie, Shuyu, Fei Yang, Yanfei Tao, Dongmei Chen, Wei Qu, Lingli Huang, Zhenli Liu, Yuanhu Pan and Zonghui Yuan. 2017. "Enhanced intracellular delivery and antibacterial efficacy of enrofloxacin-loaded docosanoic acid solid lipid nanoparticles against intracellular *Salmonella". Scientific reports* 7:41104.
70. YulugBurak, LütfüHanoglu, ErtugrulKilic and Wolf RüdigerSchabitz. 2014. "Rifampicin: An antibiotic with brain protective function." *Brain Research Bulletin* 1-6.

71. Zaidi, Sahar, Lama Misba and Asad U. Khan. 2017. “Nano-therapeutics: A revolution in infection control in post antibiotic era.” *Nanomedicine: Nanotechnology, Biology, and Medicine* 13:2281-2301.
72. Zaffiri, Lorenzo, Jared Gardne and Luis H. Toledo-Pereyra.2012. “History of antibiotics. from salvarsan to cephalosporins.” *Journal of Investigative Surgery.* 25:67-77.
73. Zazo, Hinojal, Clara I. Colino and José M. Lanao. 2016.“Current applications of nanoparticles in infectious diseases.” *Journal of Controlled Release* 224:86-102.
74. Zhanel, George G., Maria Dueck, Daryl J. Hoban, Lavern M. Vercaigne, John M. Embil, Alfred S. Gin and James A. Karlowsky. 2001. “Review of macrolides and ketolides focus on respiratory tract infections.” *Drugs* 61:4:443-498.
75. Zhanel, George G., Kelly Ennis, Lavern Vercaigne, Andrew Walkty, Alfred S. Gin, John Embil, Heather Smith and Daryl J. Hoban. 2002.“A critical review of the fluoroquinolones focus on respiratory tract infections”. *Drugs* 62:13-59.

PART C

Copper nanoparticles based stimuli-responsive approaches

Abstract

Copper nanoparticles are small particles (1-100 nm) with ultraviolet visible sensitivity, electrical, catalytic, thermal, and antibacterial properties depending on their high volume/surface ratio. These nanoparticles are synthesized by physical, chemical, and biological methods, which however lead to the formation of highly toxic by-products. In this regard, most of the copper nanoparticles studied in the biomedical field are obtained using green tecniques. In recent years, studies on these nanocarriers have focused on their ability to respond to internal or external stimuli such as pH, temperature, enzymatic reactions, redox reactions, glucose concentration, light, magnetic fields, etc. This has enabled the design, manufacture and testing of copper-based nanoparticles drug delivery systems. It has been observed that after stimulus-induced activation, such carriers would be able to release targeted anticancer drugs to destabilize the growth of tumor cells; they could act as screening agents for haemoglobinopathies and would be very useful for exerting antithrombotic activity or for imaging applications.

The aim of this chapter is to investigate the different applications of copper-based nanoparticles in biomedicine, nanomedicine, and diagnostics, specifying the mechanisms of action in response to a stimulus.

Keywords: copper, nanoparticles, preparation, chemical, physical, biological, stimuli-responsive, biomedical.

1. Introduction

Nanotechnologies currently have a wide range of applications ranging from electronics to the chemical industry and above all to biotechnology [1]. Nanotechnology refers to the design, characterization, production and use of materials, structures, devices, and control systems of nanometric dimensions ranging from 1 to 100 nm. The size of nanoparticles (NPs) constituent molecules and biological systems and their chemical, physical, electrical, and biological properties can be exploited in the biomedical field [2]. As for the application of nanotechnologies in the pharmaceutical field, this aims above all at creating new drug transport systems capable of improving their pharmacokinetics and in some cases their efficacy or safety. NPs have a surface to volume ratio that is several orders of magnitude higher than larger particles. Therefore, they can be used as Drug Delivery Systems (DDS) by delivering a large variety of drugs to target tissues, where they are released once the carrier degrades [3]. The NPs can be coated on the surface with "bio-recognizable" substances that improve their biocompatibility or selectivity of action on biological targets. In addition to being used as DDS, NPs are also used in diagnostic imaging, particularly in oncology and regenerative medicine [3]. In diagnostic imaging a contrast agent containing NPs characterized by a certain behavior during magnetic resonance, for example, can offer more detailed, reliable, and precise images of tumor formations, than can a traditional contrast agent. Again, in oncology, the smaller size of the NPs would allow a better focus of the radiative therapies [4]. Furthermore, depending on their size, NPs can overcome different barriers as well as to penetrate different biological structures. In fact, if they are smaller than 40 nm, they can enter the nucleus [5]. On the other hand, if they are smaller than 35 nm, they can also penetrate the blood brain barrier (BBE) [6]. Some research is underway on the possible exploitation of nanotechnologies also in the development of implantable devices for dosing drugs for chronic diseases such as diabetes or for controlling body temperature [7]. In surgery, nanotechnologies are 60 being studied to develop better healing and suturing techniques [8]. NPs can be extensively divided into two groups organic including carbon NPs and inorganic ones that consist of magnetic NPs [9]. There is a developing enthusiasm for inorganic NPs, like gold, silver, and copper, as they give main material properties for functional compliance. Copper nanoparticles (Cu-NPs) are high conductive and can be synthesized both physical, chemical, biological and hybrid techniques [10]. The synthesis of Cu-NPs through conventional

chemical and physical methods results in toxic derivatives that are biologically harmful and then cannot be used in biomedical fields [11]. To overcome these drawbacks, recently, increased interest has been given to green synthesis using plants and micro-organisms that do not produce toxic waste products during the production process [12]. Much work has been done regarding the synthesis and stability of Cu-NPs and a huge number of these have been successively developed with both therapeutic and diagnostic purposes for various diseases, such as cancer, diabetes, inflammation, cardiovascular, and neurodegenerative diseases. In this regard, many recent literatures, focused on Cu-NPs as effective drug carriers'system sensitive to environment and physiological processes, is available (Figure 1). The aim of this chapter is to describe and critically analyse the main results obtained in this field.

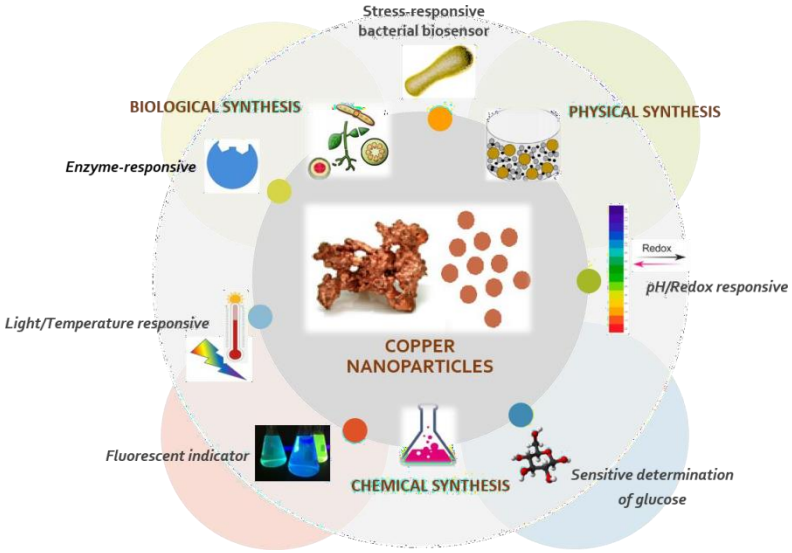

Figure 1: Stimuli-sensitive Cu-NPs

2. Methods for the synthesis of Cu-NPs

The preparation of Cu-NPs is problematic because exists the possibility of oxidation of copper, when exposed to air, and of agglomeration of the particles following surface oxidation. With the aim to inhibit oxidation, these particles are realized in an inert gas atmosphere [13]. Nevertheless, it has been reported that oxidation could occur following exposure to air also after preserving the particles in an inert atmosphere [13]. This

phenomenon could be prevented by means of the nanoparticles coating with carbon or silicon or using toluene, tridecylamine, and dodecanethiol as reaction solvents, and borohydride and lauric acid as reducing and protective agents, respectively [11]. Oxidation can be inhibited also by using protective polymers such as polyethylene glycols (PEG) and polyacrylic acid (PAA) or surfactants like sodium dodecyl benzene sulfonate, sodium dodecyl sulfate [10].

The synthesis of Cu-NPs through chemical methods includes microemulsion/colloid, reduction, electrochemical, photochemical, and thermal procedures [11, 12]. Physical strategies for synthesis of NPs involve pulse laser ablation/deposition, mechanical/ball milling, and Pulsed Wire Discharge methods (PWD) [11, 12]. The biological synthesis of Cu-NPs utilizes plants, such as inactivated tissue plant, extracts and living plant, enzymes, and microorganism such as bacteria and fungi. Biological synthesis is preferred because using this method it is easier to control the nanoparticles size and distribution (Figure 2). In addition, contrary to chemical and physical methods there is not toxic effect on the environment [11, 12].

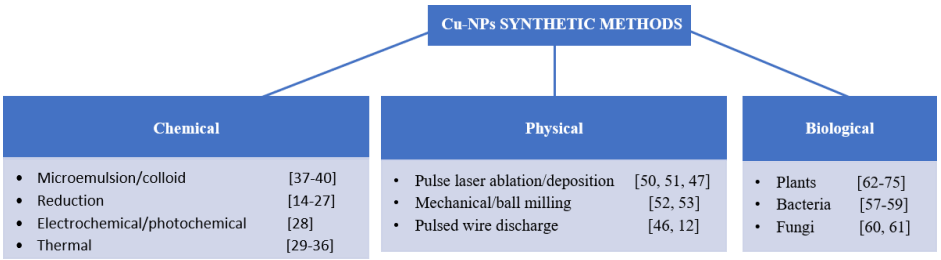

Figure 2: Synthesis of Cu-NPs by various methods

2.1 Chemical synthesis

Chatterjee et al. synthesized stable copper nanoparticles with a diameter of 50-60 using CuCl2 waste in the presence of the stabilizer like gelatin and hydrazine as reducing agent [14]. Cu-NPs can be synthesized in methanol by mixing graphite and copper acetate monohydrate [15] and in sodium dodecyl sulfate (SDS) solution by reducing the copper salt along with hydrazine [16]. Colloidal Cu-NPs can be synthesized in water by using hydrazine hydrate as reducing agent, copper sulphate as copper precursor, and gum acacia as capping agent [17]. Highly pure, monodisperse and antioxidant Cu-NPs can be synthesized by using copper hydroxide, L-ascorbic acid, and PEG-2000 respectively as precursor, reducing, and protector agents [12]. Gotoh et al. reported about the production of Cu/PAA composite films using long-chain PAA (MW 150,000) [18]. Nanocrystals obtained using Cu reduction by sodium borohydride, with a particles size of 14 nm, were described by Procek et al. [19]. Ostaeva et al. produced Cu-NPs with a diameter of ~10 nm reducing Cu2+ in poly (acrylic acid) - pluronic blends solution [20]. Cu-NPs can be synthesized, in an inert atmosphere also using hydrazine by reducing Cu (II) acetate [12]. Cu-NPs of 3-10 nm size can be synthesized from copper hydrazine carboxylate (CHC) both by thermal reduction process and sonochemical process [21-23]. Mandal et al. reported about Cu-NPs production from mixture of surfactant aerosolOT (AOT), a strong reducing agents like NaBH4, copper sulphate and water exhibiting property like high electrical conductivity [24]. Photoreducing a solution of copper acetate film of Cu-NPs deposited over a substrate coated with titanium dioxide (TiO2) were obtained [25]. Memoni et al. described fluorescence Cu-NPs that can be synthesized at low cost by a simple method which employs ascorbic acid as a reducing and protective agent [26]. Mixed nanoparticles consisting of multiple metals were realized by means of reducing agents like Carica papaya leaf aqueous extracts and silver nitrate and Cu (NO3)2. The mixture was heated, and the conditions were optimized to yield small bimetallic Ag-Cu-NPs [27]. Nanopowders were obtained and these could be recovered from the flame top by using glass fibes filters [23]. The copper nanoparticles in an aqueous phase can be produced in a size-controlled manner by sono-electrochemical method by using poly(N-vinylpyrrolidone) (PVP) as a stabilizer [28]. Fine powder of nanoparticles backed by alumina can be synthesized using aerogel protocol and 1,2-hexadecandiol Cu (II) solution containing oleylamine and oleic acid as capping agents

[29]. Antifungal nanoparticles having low dispersity and good stability were obtained starting from Cu

(II) acetylacetonate and a surfactant [30]. Also, hydrothermal synthesis was adopted to synthesize Cu-NPs from supercritical water and a very little quantity of formaldehyde [31]. Using deionized water, copper sulfate pentahydrate and nitric acid graphene encapsulated Cu-NPs were synthesized through Kraft lignin synthesis [32]. Realizing the hydrothermal process in a pressure and temperature-controlled container, like an autoclave, it was possible to obtain Cu-NPs of 3.5-40 nm [33-35]. Chen et al. applied hydrothermal method to synthesize copper nanoparticles with different sizes by using as surfactant the sodium dodecyl benzenesulfonate (SDBS) to stabilize and control the shape and size of the nanoparticles [36]. Microemulsion and reverse micelles method have been used as a chemical method to produce Cu-NPs in which two immiscible liquids, such as water-in-oil, become a thermodynamically stable dispersion with the aid of a surfactant [37-40]. By using reverse micelles method Salzemann et al. synthesized nanoparticles of copper with size of 3-13 nm [41] and Kaminskiene et al. obtained Cu colloidal solution with a size of 70-80 nm [42]. Microwaves were an additional method of obtaining copper nanoparticles. Zhu et al. synthesized Cu-NPs of 10 nm diameter by using copper sulfate as a precursor and sodium hypophosphite as a reducing agent in ethylene glycol under microwave irradiation [43]. The photochemical method has also proved effective in obtaining Cu-NPs with various size in the presence of poly(N-vinylpyrrolidone) (PVP) as the stabilizer [44, 45]. Even the electricity has been employed as a controlling force to produce copper nanoparticles starting from an electrolytic solution of copper salt and sulfuric acid [46, 47].

2.2 Physical synthesis

The production of Cu-NPs in the presence of surfactants and polymers is influenced by several factors like the pH and concentration of the metal ion, surfactant, and polymer. To overcome these limitations, highly pure copper nanoparticles can be produced through alternative methods to the synthetic ones such as gamma radiolysis [48]. It is possible to produce them also in an argon gas atmosphere by the method of wire-explosion [49]. Muraia et al. showed that organic materials coated Cu-NPs could be successfully synthesized through Pulsed Wire Discharge (PWD) method that is industrially rarely used due to its high cost [46, 12].

Colloidal nanoparticles could be obtained by the Pulse Laser Ablation/Deposition method [50, 51]. This process takes place in the presence of some inert gases and under vacuum [47]. An inexpensive method enabling copper nanoparticles large-scale production is represented by Mechanical/Ball Milling [52]. The quality of the final product depends on different factors like the type of mill, milling speed, temperature, time, atmosphere, and container [53].

2.3 Biological synthesis

Biological synthesis of metal nanoparticles is preferred to chemical one since it has no toxic impact on the environment. In addition, it is easier to control the nanoparticles size compared to other methods. [54, 55].

3. Microorganisms, fungi, and plants

Ramanathan et al. [56] and Varshney et al. [57] synthesized Cu-NPs using bacteria such as Morganella and Pseudomonas stutzeri. They produced particles in the range of 8-15 nm [57] and 50-150 nm [58], respectively. Cu-NPs showed potent antibacterial activity against Escherichia coli and Salmonella typhi bacteria, and radical scavenging activity have been developed using aqueous leaves extract of Cassia occidentalis and an ecofriendly and green method [59]. Few papers have reported the preparation of Cu-NPs using fungi. Pavani et al. used Aspergillus species of fungus for the synthesis of Cu nanoparticles [60]. Honary et al. have used Penicillium vaksmanii, Penicillium aurantiogriseum, and Penicillium citrinum, segregated from soil, for the synthesis of copper nanoparticles [61].

Copper nanoparticles can be synthesized by microwave assisted one-pot method by using hydrazine as reducing agent and the Psidiumguajava leaf extract as stabilizer. However, due to the lack of adequate nanoparticles form these are not effective in the in vivo drugs delivery [62]. Cu-NPs could be synthesized also by isolating the actinomycetes from the seaweeds [63].

Bali et al. realized copper nanoparticles in different plants such as Helianthus annus (Sunflower), Brassica juncea (Indian mustard), and Medicago sative (Alfa alfa) [64]. Lee et al. used the reducing magnolia leaf extract for the synthesis of Cu-NPs in the range of 40-100 nm [65]. Valodkar et al. obtained copper particles from a plant with medicinal properties

(Euphorbia nivulia) [66]. In addition, Subhankari and Nayak produced copper nanoparticles by using both Ginger (Zinngiber officinalis), and cloves (Syzygium aromaticum) [67, 68]. Plant extracts such as Terminalia arjuna bark have been used for Cu-NPs synthesis in the range size of 23 nm [69]. Magnolia leaf extract [70], Artabotrys odoratissimus (Nag Champa) [71], and Datura metel leaf extract have been also used as a reducing agent for the synthesis of copper nanoparticles [72]. Potato starch has been reported as a stabilizing agent for copper nanoparticles in the presence of L-ascorbic acid as the antioxidant and NaOH as a catalyst [73].

Cu-NPs exhibiting superior antioxidant, antibacterial, antidiabetic, and anti- inflammatory activities were synthesized from the extract of M. pinnata flower [74] and using intra generic edible medicinal plants of Rosaceae family [75].

4. Stimuli-responsive copper nanoparticles

The external or internal stimuli, like pH, enzyme, thermal, magnetic, and electronic field, ultrasound, and light, could influence the nanocarriers behaviour inside the biological systems and facilitate their ingress in a specific compartment ensuring a controlled release, intracellular drug delivery, favouring therapy and imaging [76]. In this section the application of stimuli-responsive Cu-NPs will be discussed.

Nanoparticles type	Ref.
Sensitive ability for glucose	[77, 78, 79, 80]
Redox/pH responsive nanoparticles	[81, 82, 83]
Cu-NPs toxicity based on a stress-responsive bacterial biosensor array	[84, 85, 86, 87, 88, 89, 90, 91]
Fluorescent and enzyme-responsive particles	[92, 93, 94, 95, 96, 97]

Table 1: Cu nanoparticles behaviour

4.1 Sensitive ability for glucose

A reproducible and stable biosensor glucose sensitive based on Cu-NPs anchored on laser-induced graphene (LIG) was successfully developed by a substrate-assisted electroless deposition (SAED) technique. This sensor is an attractive candidate as implantable non-enzymatic glucose diagnostic device [77]. A glucose sensor based on Cu-NPs/flexible graphite sheet self-supporting enzyme-free were prepared by the hydrothermal method. The sensor possesses excellent anti-interference properties against dopamine, uric acid, sodium chloride, acetaminophenol, and ascorbic acid. In addition, this sensor and has good [78]. Yang et al. realized a nanocomposite with high surface area and conductive with rough morphology based on phytic acid (PA) doped with poly(3,4-ethylenedioxy-thiophene) (PEDOT) was realized. The loading with copper nanoparticles (Cu-NPs) onto the rugged surfaces of nanocomposite furnished a platform useful as glucose sensor [79]. pH-Responsive luminescent materials were fabricated by dispersing copper nanoclusters (Cu-NCs) into alginate solution, together with calcium carbonate (CaCO3) nanoparticles. This material is potentially applicable in the development of a chemical sensor for glucose by integrating its pH-responsive properties with the ability to produce H+ in the reaction of glucose oxidase (GOx) with glucose [80].

4.2 Effect of redox/pH responsive copper nanoparticles

Rezaei et al. realized a sensor displaying good selectivity for H2O2 detection in the presence of common interferences such as ascorbic acid. They used copper nanoparticles to decorate functionalized-multiwall carbon nanotubes and to obtain a nanocomposite employable for amperometric peroxide recognition [81].

The addition of Cu-NPs in the diet reduces protein oxidation and nitration as well as DNA oxidation and methylation. Lowering the level of Cu in the diet increases the DNA methylation and oxidation of proteins [82].

A highly selective system towards glucose oxidation based on Cu nanoparticles (CuNPs)/polyaniline (PANI)/graphene nanocomposite was also fabricated. This system was also highly sensitive as a non-enzymatic glucose sensor [83].

4.3 Cu-NPs toxicity based on a stress-responsive bacterial biosensor array

Cu-NPs toxicity was analyzed by Li et al. [84] using a stress-respective bacterial biosensor array. Nanoparticles induced various damages in the bacterial cells, such as oxidative stress, DNA/protein/ damage, and membrane damage.

Yadav et al. also designed and prepared Cu-NPs with antibacterial activities against strain of E. coli, Staphylococcus aureus and Pseudomonas aeruginosa. The Cu-NPs has been found to generate reactive oxygen species (ROS) causing cell death.

It is probable that Cu-NPs are oxidized to form Cu ions when interacting with the cell membrane due to the higher O2 concentration of the cell membrane than the cell media. The toxicity was also due to the nanoparticles size. More precisely, the major toxicity was obtained with smaller particles [85, 86]. Wang et al. used albumin as a reducing agent to obtain pH-sensitive Cu-NPs which can encapsulate histone deacetylase (HDAC) inhibitor vorinostat and furnish a carrier useful for synergistic chromatin remodelling and chemodynamic therapy [87].

Copper nanoparticles also exhibit a strong ability to inhibit in addition to pathogenic bacteria such as B. Subtilis too fungi (Issatchenkia orientalis), and viruses [88-90]. Interesting are the coatings based on copper nanoparticles that prevent the accumulation and spread of viruses and bacteria on portable devices such as tablets and mobile phones [91].

4.4 Fluorescent and enzyme-responsive Cu-NPs

DNA-templated Cu-NPs are developed as a novel fluorescent indicator for actin assays and digestion of deoxyribonuclease I (DNase I) [92]. Actin is a globular protein whose highest presence occurs in the cells of muscle tissue.

Qing et al. developed an analytical method to monitor the enzymes ligase and polynucleotide kinase (PNK) that are involved in DNA repair pathways. They proposed a new strategy for label-free monitoring PNK and ligase activity by using dumbbell- shaped DNA templated Cu-NPs [93].

DNA-Cu-NPs are employed also as fluorescent indicators to detect the hydroxylamine (HA), a potent reducing agent, and an important intermediate or raw material in pharmaceutical processes, known as a nitric oxide (NO) donor, and an inhibitor for the release of insulin [94].

Cu-NPs were also reported for micro-RNA sensors. Rotaru et al. developed a sensor based on random double-stranded DNA- templated/Cu-NPs (dsDNA–Cu-NPs) [95]. Xu et al. prepared

poly(thymine)-templated Cu-NPs and used dsDNA–Cu-NPs as the model to produce the RCR-mediated concatemeric Cu-NPs strategy [96]. Concatemeric dsDNA-templated copper nanoparticles strategy with improved sensitivity and stability based on rolling circle replication and its application in micro-RNA detection [97].

5. Applications of Cu-NPs for wound healing and cancer

Wounds often become a proliferation site for various microorganisms that can infiltrate the inside of the body resulting in an expansion of the infection. Therefore, for wound healing it becomes necessary to resort to the use of antibacterial materials. In this regard, copper nanoparticles are used as antibacterial and anti-inflammatory materials. Copper causes angiogenesis at the wound site, improves immunity against
various microorganisms by stimulating the production of interleukin 2 (IL-2), moderates oxidative damage in tissues and activates remodeling by integrin expression and stabilization of fibrinogen and up-regulation of copper-dependent enzymes such as lysyl oxidase. For this reason, copper has also been used to arrest severe phosphorus burns. Tiwari et al. showed that copper nanoparticles can enhance cell proliferation and increase cell migration from the scar within 24 hours. Furthermore, copper nanoparticles have been shown to be highly anti-inflammatory compared to copper as such by suppressing the expression of the COX2 enzyme [98-103]. Tao et al. prepared antibacterial Cu-NPs-embedded hydrogels composed of methacrylate-modified gelatin (Gel-MA) and N, N-bis(acryloyl)- cystamine (BACA) chelated with copper nanoparticles useful for skin tissue regeneration. In vitro antimicrobial experiments revealed that this material exhibited antibacterial efficacy against both Gram-positive and Gram-negative bacteria [104].

Wound dressing made of copper nanoparticles (Cu NPs) loaded bacterial cellulose (BC) membranes were fabricated by He et al. using in situ chemical reduction method. Membranes showed efficient long-term antibacterial activity against S. aureus and E. coli [105]. Sun et al. investigated the fluorescent self-assembled tripeptide glycyl-L- histidyl-L-lysine (GHK)-Cu nanoparticles (GHK-Cu-NPs) abilities to improve wound healing, accelerate anti-inflammatory activity, and repair DNA damage. The obtained results showed that the fabricated functional polypeptidic nanomaterial could be applied in drug delivery, tissue engineering, and cosmetic fields [106].

Cu-NPs could be used also for anticancer therapeutic applications including drug delivery, cancer imaging, and image-guided therapy [107]. Cu-NPs possess moderate cytotoxic behaviour to PC3 and HeLa human cell lines and a low cytotoxicity [107].

Copper NPs prepared using plants such as Nerium oleander, and Magnolia Kobus, showed activity against cell proliferation. The in vitro cytotoxic potential of increasing nanoparticles concentrations on the human HepG2 cancer cell line indicated a good cellular toxicity [108].

Microwave-assisted Cu-NPs, obtained using P. cineraria leaf extracts, were active against human MCF-7 cancer cell line [109]. Copper NPs prepared utilizing the Quisqualis indica Linn floral extract exhibit cytotoxic activity towards B16F10 melanoma cells. The peptide-coated copper nanoparticles in the latex of the therapeutic plant species Euphorbia nivulia [110] showed antiproliferative activity in human A549 lung cancer cells confirming the ability of copper NPs to induce structural damage to the cellular environment, mitochondrial dysfunction, and oxidative stress [110].

6. Conclusion

In this chapter, the methods for synthesis of copper nanoparticles were assesses. Literature data have shown that the particles properties, like size, morphology, stability, depend on experimental conditions. Chemical and physical methods require the use of toxic substances or are expensive. On the contrary, biological methods are not expensive and result eco-friendly. Nanoparticles could be used in the development of novel therapeutic approaches against several diseases including cancer, inflammation, bacterial infection, as well as in the diagnostic field. Copper nanoparticles can be successfully employed also for the detection of specific target, like ions, proteins, and glucose. Furthermore, investigated nanoparticles, due to their unique optical properties such as great luminescence, represent a novel fluorescent material for sensing and bioimaging application.

References

R. Cassano, F. Curcio, M.L. Di Gioia and S. Trombino. Copper nanoparticles based stimuli-responsive approaches. In: Stimuli-Responsive Nanocarriers: Recent Advances in Tailor-Made Therapeutics, Eds. Virendra Gajbhiye. Elsevier, 2021

1. A. P. Dowling, Development of nanotechnologies, Nano today 7 (12) (2004) 30-35. DOI: 10.1016/S1369-7021(04)00628-5.

2. I. Khan, K. Saeed, I. Khan. Nanoparticles: Properties, applications, and toxicities, Arabian Journal of Chemistry 12 (2019) 908-931. DOI: 10.1016/j.arabjc.2017.05.011.

3. A. Z. Wilczewska, K. Niemirowicz, K. H. Markiewic, H. Car, Nanoparticles as drug delivery systems, Pharmacological Reports 64 (2012) 1020-1037. DOI: 10.1016/s1734-1140(12)70901-5.

4. G. S. Rama Raju, L. Benton, E. Pavitra, J. Yu, Multifunctional nanoparticles: recent progress in cancer therapeutics, Chemical Communication 51 (2015) 13248-13259. DOI: 10.1039/c5cc04643b.

5. M. Wu, H. Guo, L. Liu, Y. Liu, L. Xie, Size-dependent cellular uptake and localization profiles of silver nanoparticles, International Journal of Nanomedicine 14 (2019) 4247-4259. DOI: 10.2147/IJN.S201107.

6. M. Sajid, M. Ilyas, C, Basheer, M. Tariq, M. Daud, N. Baig, F. Shehzad, Impact of nanoparticles on human and environment: review of toxicity factors, exposures, control strategies, and future prospects, Environmental Science and Pollution Research 22 (2015) 4122–4143. DOI: 10.1007/s11356-014-3994-1.

7. A. K. Mitra, K. Cholkar, A. Mandal, Emerging Nanotechnologies for Diagnostics, Drug Delivery and Medical Devices Micro and Nano Technologies (2017) 249-290. ISBN: 9780323429979.

8. N. Mariappan, Recent Trends in Nanotechnology Applications in Surgical Specialties and Orthopedic Surgery, Biomedical & Pharmacology Journal 12 (2019) 1095-1127. DOI: https://dx.doi.org/10.13005/bpj/1739.

9. L. Li, Y. Guan, H. Xiong, T. Deng, Q. Ji, Z. Xu, Y. Kang, J. Pang, Fundamentals and applications of nanoparticles for ultrasound-based imaging and therapy, Nano Select 1 (2020) 263-284. doi.org/10.1002/nano.202000035

10. A. Tamilvanan, K. Balamurugan, K. Ponappa, B. Madhan Kumar. Copper Nanoparticles: Synthetic Strategies, Properties and Multifunctional Application, International Journal of Nanoscience 13 (2014) 1430001-1430023. DOI: 10.1142/S0219581X14300016

11. B. Khodashenas, H. R. Ghorbani, Synthesis of copper nanoparticles: An overview of the various methods, Korean Journal of Chemical Engineering 31 (2014) 1105-1109. DOI: 10.1007/s11814-014-0127-y.

12. K. V. Radha., K. Gayathri, Synthesis, Characterization and application of Copper Nano-Particles: A Review, International Journal of Engineering Research & Technology 8 (2019) 412-421. ISSN: 2278-0181.

13. T. M. Dung Dang, T. T. Tuyet Le, E. Fribourg-Blanc, M. C. Dang, The influence of solvents and surfactants on the preparation of copper nanoparticles by a chemical reduction method, Advances in Natural Sciences: Nanoscience and Nanotechnology 2 (2011) 025004-025011. DOI: 10.1088/2043-6262/2/1/015009.

14. A. K. Chatterjee, R. K. Sarkar, A. P. Chattopadhyay, P. Aich, R. Chakraborty, T. Basu, A simple robust method for synthesis of metallic copper nanoparticles of highantibacterial potency against E. coli, Nanotechnology. 23 (2012) 085103-085114. DOI: 10.1088/0957-4484/23/8/085103.

15. M. D. Halluin, T. Mabit, N. Fairley, V. Fernandez, M. B. Gawande, E. Crognec, F. X. Felpin, Graphite-supported ultra-small copper nanoparticles – Preparation, characterization and catalysis applications, Carbon. 93 (2015) 974-983.

16. C. Dong, H. Cai, X. Zhang, C. Cao, Synthesis and characterization of monodisperse copper nanoparticles using gum acacia, Physica and Low-dimensional Systems and Nanostructures 57 (2014) 12–20. DOI: 10.1016/j.physe.2013.10.025.

17. Y. Zhang, P. Zhu, G. Li, T. Zhao, X. Fu, R. Sun, F. Zhou, C. P.Wong, Facile Preparation of Monodisperse, Impurity-Free, and Antioxidation Copper Nanoparticles on a Large Scale for Application in ConductiveInk, ACS Applied Materials & Interfaces 6 (2014) 560-567. DOI: 10.1021/am404620y.

18. Y. Gotoh, R. Igarashi, Y. Ohkoshi, M. Nagura, K. Akamatsu, S. Deki, Preparation and structure of copper nanoparticle/poly(acrylic acid) composite films, Journal of Material Chemistry 10 (2020) 2548-2552. DOI: 10.1039/B003899G.

19. R. Prucek, L. Kvítek, A. Panáček, L. Vančurová, J. Soukupová, D Jančík, R. Zbořil, Polyacrylate-assisted synthesis of stable copper nanoparticles and copper (I) oxide nanocubes with high catalytic efficiency, Journal of Materials Chemistry 19 (2009) 8463-8469. DOI: 10.1039/B913561H.

20. G. Y. Ostaeva, E. D. Selishcheva, V. D. Pautov, I. M. Papisov, Pseudotemplate synthesis of copper nanoparticles in solutions of poly(acrylic acid)-pluronic blends, Polymer Science Series B 50 (2008) 147-149. DOI: 10.1134/S1560090408050102.

21. N. A. Dhas, C. P. Raj, A. Gedanken, Synthesis, Characterization and Properties of Metallic Copper Nanoparticles, Chemical Materials. 10, (1998), 1446. doi.org/10.1021/cm9708269.

22. S. Ikeda, K. Akamatsu, H. Nawafune, T. Nishino, S. Deki, Formation and Growth of Copper Nanoparticles from Ion-Doped Precursor Polyimide Layers, The Journal of Physical Chemistry B 108 (2004) 15599-15607. DOI: 10.1021/jp0478559.

23. E. K. Athanassiou, R. N. Grass, W. J. Stark, Large-scale production of carbon-coated copper nanoparticles for sensor applications, Nanotechnology. 17, (2006), 1668. doi: 10.1088/0957-4484/17/6/022.

24. S. Mandal, S. De, Copper nanoparticles in AOT “revisited”-direct micelles versus reverse micelles, Materials Chemistry and Physical 183 (2016) 410-421. DOI: 10.1016/j.matchemphys.2016.08.046.

25. M. Miyagawa, M. Yonemura, H. Tanaka, Lustrous copper nanoparticle film: Photodeposition with high quantum yield and electric conductivity, Chemical Physic Letters A. (2016), 665, 95. doi.org/10.1016/j.cplett.2016.10.057.

26. S. Momeni, R. Ahmadi, A. Safavi, I. Nabipour, Blue-emitting copper nanoparticles as a fluorescent probe for detection of cyanideions, Talanta 175 (2017) 514-521. DOI: 10.1016/j.talanta.2017.07.056.

27. T. M. S. Rosbero, D. H. Camacho, Green preparation and characterization of tentacle-like silver/copper nanoparticles for catalytic degradation of toxic chlorpyrifos in water, J. Environ. Chem. Eng. 5 (2017) 2524-2532. DOI: 10.1016/j.jece.2017.05.009.

28. I. Haas, S. Shanmugam, A. Gedanken, Pulsed Sono-electrochemical Synthesis of Size-Controlled Copper Nanoparticles Stabilized by Poly(N-vinylpyrrolidone), Journal of Physical Chemistry B 110 (2006) 16947-16952. DOI: 0.1021/jp064216k.

29. D. Mott, J. Galkowski, L. Wang, J. Luo, C. J. Zhing, Synthesis of Size-Controlled and Shaped Copper Nanoparticles, Langmuir, 23 (2007) 5740-5745. DOI: 10.1021/la0635092.

30. Y. Wei, S. Chen, B. Kowalczyk, S. Huda, T. P. Gray, B. A. Grzybowski, Synthesis of Stable, Low-Dispersity Copper Nanoparticles and Nanorods and Their Antifungal and Catalytic Properties, Journal of Physical Chemistry C 114 (2010) 15612-15616. DOI: 10.1021/jp1055683.

31. L. Zhou, S. Wang, H. Ma, S. Ma, D. Xu, Y., Guo, Size-controlled synthesis of copper nanoparticles in supercritical water, Chemical Engineering Research and Design 98 (2015) 36-43. DOI: 10.1016/j.cherd.2015.04.004.

32. W. Leng, H. M. Barnes, Q. Yan, Z. Cai, J. Zhang, Low temperature synthesis of graphene-encapsulated copper nanoparticles from kraft lignin, Materials Letters 185 (2016) 131-134. DOI: 10.1016/j.matlet.2016.08.122.

33. S. H. Yu, Hydrothermal/solvothermal processing of advanced ceramic materials, Journal of the Ceramic Society of Japan 109 (2001) S65-S75. DOI: 10.2109/jcersj.109.1269_S65.

34. M. Rajamathi, R. Seshadri, Oxide and chalcogenide nanoparticles from hydrothermal/solvothermal reactions, Current Opinion in Solid State and Material Science, 6 (2002) 337-345. DOI: 10.1016/S1359-0286(02)00029-3.

35. V. Baco-Carles, L. Datas and P. h. Tailhades, International Scholarly Research Network ISRN Nanotechnology 10 (2011) 1-7. DOI: 10.5402/2011/29594.

36. H. Chen, J. H. Lee, Y. H. Kim, D. W. Shin, S. C. Park, X. Meng, J. B. Yoo, Metallic Copper Nanostructures Synthesized by a Facile Hydrothermal Method, Journal of Nanoscience and Nanotechnology 10 (2010) 629-636. DOI: 10.1166/jnn.2010.1739.

37. L. Chen, D. Zhang, H. Zhou and H. Wan, The use of CTAB to control the size of copper nanoparticles and the concentration of alkylthiols on their surfaces, Materials Science and Engineering 415 (2006) 156-161. DOI: 10.1016/j.msea.2005.09.060.

38. S. Kapoor, R. Joshi, T. Mukherjee, Influence of I− anions on the formation and stabilization of copper nanoparticles, Chemical Physics Letters 354 (2002) 443-448. DOI: 10.1016/S0009-2614(02)00159-8.

39. A. M. L. Jackelen, M. Jungbaur and G. N. Glavee, Nanoscale materials synthesis. 1. Solvent effects on hydridoborate reduction of copper ions, Langmuir 15 (1999) 2322-2326. DOI: 10.1021/la9807311.

40. N. Dadgostar, S. Ferdous and D. E. Henneke, Colloidal synthesis of copper nanoparticles in a two-phase liquid–liquid system, Materials Letters 64 (2010) 45-48. DOI: 10.1016/j.matlet.2009.09.067.

41. C. Salzemann, I. Lisiecki, A. Brioude, J. Urban and M. P. Pileni, Collections of Copper Nanocrystals Characterized by Different Sizes and Shapes: Optical Response of These Nanoobjects Journal Physic and Chemistry B 108 (2004) 13242-13248. doi.org/10.1021/jp048491n.

42. Z. Kaminskiene, I. Prosycevas, J. Stonkute and A. Guobiene, Evaluation of Optical Properties of Ag, Cu, and Co Nanoparticles Synthesized in Organic Medium, Acta Physica Polonica A 123 (2013) 111-114. DOI:10.12693/APhysPolA.123.111.

43. H. T. Zhu, C. Y. Zhang and Y. S. Yin, J. Cryst. Rapid synthesis of copper nanoparticles by sodium hypophosphite reduction in ethylene glycol under microwave irradiation, Growth 270 (2004) 722-728. doi.org/10.1016/j.jcrysgro.2004.07.008.

44. S. Tatasov, A. Kolubaev, S. Belyaev, M. Lerner, F. Tepper, Study of friction reduction by nanocopper additives to motor oil, Wear 252 (2002) 63-69. doi.org/10.1016/S0043-1648(01)00860-2.

45. S. Giuffrida, L. L. Costanzo, G. Ventimiglia and C. Bongiorno, Photochemical synthesis of copper nanoparticles incorporated in poly(vinyl pyrrolidone), Journal of Nanoparticle Research 10 (2008) 1183-1192. DOI 10.1007/s11051-007-9343-2.

46. U. Asim, N. Shahid and R. Naveed, Selection of a Suitable Method for the Synthesis of Copper Nanoparticles, World Scientific Publishing Company 7 (2012) 1230005-1230023. DOI: 10.1142/S1793292012300058.

47. M. Raja, J. Subha, F. Binti Ali and S. H. Ryu, Synthesis of Copper Nanoparticles by Electroreduction Process, Materials and Manufacturing Processes 23 (2008) 782-785. DOI: 10.1080/10426910802382080.

48. S. S. Joshi, S. F. Patil, V. Iyer, S. Mahumuni, Radiation induced synthesis and characterization of copper nanoparticles, Nanostructured Materials 10 (1998) 1135-1144. DOI: 10.1016/S0965-9773(98)00153-6.

49. P. K. Dash, Y. Balto, Generation of Nano-copper Particles through Wire Explosion Method and its Characterization, Research Journal of Nanoscience and Nanotechnololy 1 (2011) 25-33. DOI: 10.3923/rjnn.2011.25.33.

50. V. Amendola, M. Meneghetti, Laser ablation synthesis in solution and size manipulation of noble metal nanoparticles, Physical Chemistry Chemical Physic. 11 (2009) 3805-3821. DOI: 10.1039/b900654k.

51. V. Amendola, S. Polizzi, M. Meneghetti, Laser Ablation Synthesis of Gold Nanoparticles in Organic Solvents, The Journal of Physical Chemistry B 110 (2006) 7232-7237. DOI: 10.1021/jp060509252.

52. C. Suryanarayana, Mechanical Alloying and Milling, Progress in Material Science 46 (2001) 1-184. DOI: 10.1016/S0079-6425(99)00010-9.

53. J. S. Benjamin, New Materials by Mechanical Alloying Techniques, Eds. E. Arzt and L. Schultz, (1989) 3-18. ISBN 3-88355-133-3.

54. R. Varshney, S. Bhadauria and M. S. Gaur, A Review: Biological synthesis of silver and copper nanoparticles, Nano Biomedicine and Engineering 4 (2012) 99-106. DOI: 10.5101/nbe.v4i2.p 99-106.

55. V. Bansal, D. Rautaray, A. Bharde, K. Ahire, A. Sanyal, A. Ahmad and M. Sastry, Fungus-mediated biosynthesis of silica and titania particles, Journal of Material Chemistry, 15 (2005) 2583-2589. DOI: 10.1039/B503008K.

56. R. Ramanathan, S. K. Bhargava, V. Bansal, Biological synthesis of Copper/Copper Oxide nanoparticles, In Rose Amal (Ed.) Chemeca Conference. Engineering A Better World, Australia, pp. 1-8 (2011).

57. R. Varshney, S. Bhadauria, M.S. Gaur and R. Pasricha, Copper Nanoparticles Synthesis from Electroplating Industry Effluent, Nano Biomedical Engineering 3 (2011) 115-119. DOI: 10.5101/nbe.v3i2.p 115-119.

58. R. Varshney, S. Bhadauria, M. S. Gaur, R. Pasricha. Characterization of copper nanoparticles synthesized by a novel microbiological method. JOM 62 (2010), 102- 104. DOI: 10.1007/s11837-010-0171-y.

59. M. Gondwal, G. J. Pant, Synthesis and Catalytic and Biological Activities of Silver and Copper Nanoparticles Using Cassia occidentalis, International Journal of Biomaterials 2018 (2018) 1-10. DOI: 10.1155/2018/6735426.

60. K. Mallikarjuna, G. Narasimha, G. R. Dillip, B. Praveen, B. Shreedhar, C. Sree Lakshami, B. V. S. Reddy, B. Deva Prasad Raju, Green synthesis of silver nanoparticles using ocimum leaf extract and their characterization, Digest Journal of Nanomaterials and Biostructures 6 (2011) 181-186. DOI: 10.1007/s13562-019-00522-2.

61. S. Honary, H. Barabadi, E. Gharaei-Fathabad, and F. Naghibi, Green synthesis of copperoxidenanoparticlesusing Penicillium aurantiogriseum, Penicillium citrinum and Penicillium waksmanii, Digest Journal of Nanomaterials and Biostructures 7 (2012) 999–1005. DOI: 10.9734/jalsi/2020/v23i730172.

62. N. Sreeju, A. Rufus, D. Philip, Microwave-assisted rapid synthesis of copper nanoparticles with exceptional stability and their multifaceted applications, Journal of Molecular Liquids 221 (2016) 1008-1021. DOI: 10.1016/j.molliq.2016.06.080.

63. M. I. Nabila, K. Kannabiran, Biosynthesis, characterization and antibacterial activity of copper oxide nanoparticles (CuO NPs) from actinomycetes, Biocatalysis and Agricultural Biotechnology 15 (2018) 56-62. DOI: 10.1016/j.bcab.2018.05.011.

64. R. Bali, N. Razak, A. Lumb, A. T. Harris, The synthesis of metallic nanoparticles inside live plants, IEEE Xplore (2006) 224-227. DOI: 10.1109/ICONN.2006.340592.

65. H. J. Lee, G. Lee, N. R. Jang, J. H. Yun, J. Y. Song, B. S. Kim, Biological synthesis of copper nanoparticles using plant extract, Nanotechonoly 1 (2011) 371-374. DOI: 10.1016/j.inoche.2019.04.023.

66. M. Valodkar, R. N. Jadeja, M. C. Thounaojam, R. V. Devkar, S. Thakore, Biocompatible synthesis of peptide capped copper nanoparticles and their biological effect on tumor cells, Material Chemistry and Physic 128 (2011) 83-89. DOI: 10.1016/j.matchemphys.2011.02.039.

67. I. Subhankari, P. L. Nayak, Antimicrobial Activity of Copper Nanoparticles Synthesised by Ginger (Zingiber officinale) Extract, World Journal of Nano Science & Technology, 2 (2013) 10-13. DOI: 10.5829/idosi.wjnst.2013.2.1.21133.

68. I. Subhankari, P. L. Nayak, Antimicrobial Activity of Copper Nanoparticles Synthesised by Ginger (Zingiber officinale) Extract, World Journal of Nano Science & Technology 2 (2013) 10-13. DOI: 10.5829/idosi.wjnst.2013.2.1.21134.

69. S. Yallappa, J. Manjanna, M. A. Sindhe, N. D. Satyanarayan, S. N. Pramod, K. Nagaraja. Microwave assisted rapid synthesis and biological evaluation of stable copper

nanoparticles using T. arjunabark extract. Spectrochimica Acta Part A: Molecular and Biomolecular Spectroscopy 110 (2013) 108–115. DOI: 10.1016/j.saa.2013.03.005.

70. H. Lee, G. Lee, N. Jang, J. Yun, J. Song, B. Kim, Biological synthesis of copper nanoparticles using plante extract, Nanotechnology 1 (201) 371–374. DOI: 10.1002/jctb.4052

71. U. Kathad, H. P. Gajera, Synthesis of copper nanoparticles by two different methods and size comparison, International Journal of Pharma and Bio Sciences 5 (2014) 533–540.

72. P. Parikh, D. Zala, B. A. Makwana. Biosynthesis of copper nanoparticles and their antimicrobial activity. OALib 1 (2014) 1–15. DOI: 10.1080/00032719.2016.1172081.

73. Y. Suresh, S. Annapurna, G. Bhikshamma, A. K. Singh. Characterization of green synthesized copper nanoparticles: A novel approach. InternationaI Conference on Advanced Nanomaterials & Emerging Engineering 13 (2013) 63–67. DOI: 10.1109/ICANMEET.2013.6609236.

74. M. Thiruvengadam, I.M. Chung, T. Gomathi, M. A. Ansari, V. G. Khanna, V. Babu, G. Rajakumar, Synthesis, characterization and pharmacological potential of green synthesized copper nanoparticles, Bioprocess and Biosystems Engineering 42 (2019) 1769–1777. DOI: 10.1007/s00449-019-02173-y.

75. S. Khatak, H. Abhilasha, D.K. Malik, Biological synthesis of copper nanoparticles using intra generic edible medicinal plants of Rosaceae family, International Journal of Chemical Studies 7 (2019) 753-756. ISSN: 2349–8528.

76. P. Mi, Stimuli-responsive nanocarriers for drug delivery, tumor imaging, therapy and theranostics, Theranostics 10 (2020) 4557-4588. DOI: 10.7150/thno.38069.

77. Y. Zhang, N. Li, Y. Xiang, D. Wang, P. Zhang, Y. Wang, S. Lu, R. Xu, J. Zhao, A flexible non-enzymatic glucose sensor based on copper nanoparticles anchored on laser-induced Carbon 156 (2020) 506-513. DOI: 10.1016/j.carbon.2019.10.006.

78. J. Li, J. Tang, L. Wei, S. He, L. Ma, W. Shen, F. Kang, Z. Huang, Preparation and performance of electrochemical glucose sensors based on copper nanoparticles loaded on flexible graphite sheet, Carbon Research 35 (2020) 410-419. DOI: 10.1016/S1872-5805(20)60498-X.

79. L. Yang, H. Wang, H. Lü, N. Hui, Phytic acid doped poly(3,4-ethylenedioxythiophene) modified with copper nanoparticles for enzymeless amperometric sensing of glucose, Microchimica Acta 187 (2020) 49-56. DOI: 10.1007/s00604-019-3988-2.

80. S. Gou, Y. Shi, P. Li, H. Wang, T. Li, X. Zhuang, W. Li, Z. Wang, Stimuli-Responsive Luminescent Copper Nanoclusters in Alginate 2 and Their Sensing Ability for Glucose, ACS Applied Materials Interfaces 11 (2019) 6561–6567. DOI: 10.1021/acsami.8b20835.

81. B. Rezaei, N. Askarpour, M. Ghiaci, F. Niyazian, A. A. Ensafi, Synthesis of Functionalized MWCNTs Decorated with Copper Nanoparticles and Its Application as a Sensitive Sensor for Amperometric Detection of H2O2, (2015), 27, 6 2015 1457-146. doi.org/10.1002/elan.201400612.

82. K. Ognik, E. Cholewińska, J. Juśkiewicz, Z. Zduńczyk, K. Tutaj, R. Szlązak, The effect of copper nanoparticles and copper (II) salt on redox reactions and epigenetic changes in a rat model, Journal of Animal Physiology and Animal Nutrition 103 (2019) 675-686. DOI: 10.1111/jpn.13025.

83. W. Zheng, L. Hu, Y. S. Lee, K. Wong, Copper nanoparticles/polyaniline/graphene composite as a highly sensitive electrochemical glucose sensor, Journal of Electroanalytical Chemistry 781 (2016) 155-160. DOI: 10.1016/j.jelechem.2016.08.004.

84. Y. Zhang, N. Li, Y. Xiang, D. Wang, P. Zhang, Y. Wang, S. Lu, R. Xu, J. Zhao, A flexible non-enzymatic glucose sensor based on copper nanoparticles anchored on laser-induced graphene, Carbon 156 (2020) 506-513. DOI: 10.1016/j.carbon.2019.10.006.

85. L. Yadav, R.M. Tripathi, R. Prasad, R.N. Pudake, J. Mittal, Antibacterial Activity of Cu Nanoparticles against E. coli, Staphylococcus aureus and Pseudomonas aeruginosa, Nano Biomed Eng 9 (2017) 9-14. DOI: 10.5101/nbe.v9i1.p9-14.

86. S. Mallick, S. Sharma, M. Banerjee, et al., Iodine stabilized Cu nanoparticle chitosan composite for antibacterial applications. ACS Applied Materials&Interfaces, (2012), 41 313-1323. DOI: 10.1021/am201586w.

87. L Wang, Z Zhang, Y Ding, J Wu, Y Hu, A. Yuan, Novel copper-based and pH-sensitive nanomedicine for enhanced chemodynamic therapy, Chemical Communication 56(2020) 7753-7756. DOI: 10.1039/D0CC00165A.

88. A. P. Ingle, N. Duran, M. Rai, Bioactivity, mechanism of action, and cytotoxicity of copper-based nanoparticles: A review, Applied Microbiology and Biotechnology 98 (2014) 1001-1009. DOI 10.1007/s00253-013-5422-8.

89. L. Esteban-Tejeda, F. Malpartida, A. Esteban-Cubillo, C. Pecharromán, J. Moya, Antibacterial and antifungal activity of a soda-lime glass containing copper nanoparticles, Nanotechnology 20 (2009) 505701-500707 DOI: 10.1088/0957-4484/20/50/505701.

90. R. Lakshminarayanan, E. Ye, D.J. Young, Z. Li, X. Jun Loh, Recent Advances in the Development of Antimicrobial Nanoparticles for Combating Resistant, Advanced Healthcare Materials 7 (2018) 1701400-1701413. DOI: 10.1002/adhm.201701400.

91. https://themarketherald.com.au/nanoveu-asxnvu-applies-antiviral-anotechnology- to-smartphone-screen-protectors-2020-04-16/.

92. Q. Song, L. Yang, H. Chen, R. Zhang, N. Na, J Ouyang, A label-free fluorometric assay for actin detection based on enzyme-responsive DNA-templated copper nanoparticles, Talanta 174 (2017) 444-447. DOI: 10.1016/j.talanta.2017.06.031.

93. T. Qing, X. He, D. He, X. Ye, J. Shangguan, J. Liu, Dumbbell, B. Yuan, K. Wang, DNA-templated CuNPs as a nano-fluorescent probe for detection of enzymes involved in ligase-mediated DNA repair, Biosensors and Bioelectronics 94 (2017) 456-463. DOI: 10.1016/j.bios.2017.03.035.

94. Q. Song, C. Chen, W. Yu, L. Yang, K. Zhang, J. Zheng, X. Duab, H. Chen, In situ formation of DNA-templated copper nanoparticles as fluorescent indicator for hydroxylamine detection, RSC Adv. 9 (2019) 25976. DOI: 10.1039/C9RA04476K.

95. A. Rotaru, S. Dutta, E. Jentzsch, K. Gothelf and A. Mokhir, Selective dsDNA-Templated Formation of Copper Nanoparticles in Solution, Angew. Chem., Int. Ed., 49 (2010) 5665–5667. DOI: 10.1002/anie.200907256.

96. F. Xu, H. Shi, X. He, K. Wang, D. He, Q. Guo and J. Tang, Concatemeric dsDNA-templated copper nanoparticles strategy with improved sensitivity and stability based on rolling circle replication and its application in microRNA detection, Analitical Chemistry 86 (2014) 6976–6982. DOI:10.1021/ac500955r.

97. Y.H. Wang, L.L. He, K.J. Huang, Y.X. Chen, S.Y. Wang, Z.H. Liu, D. Li, Recent advances in nanomaterial-based electrochemical and optical sensing platforms for microRNA assays, Analyst 144(2019) 2849-2866. DOI: 10.1039/C9AN00081J.

98. F. Xu, H. Shi, X. He, K. Wang, D. He, Q. Guo, Z. Qing, L. Yan, X. Ye, D. Li, J. Tang, Concatemeric dsDNA-Templated Copper Nanoparticles Strategy with Improved Sensitivity

and Stability Based on Rolling Circle Replication and Its Application in MicroRNA Detection. Analitycal Chemistry 86 (2014) 6976–6982.

99. Y. Qiao, F. Ma, C. Liu, B. Zhou, Q. L. Wei, W. L. Li, D. N. Zhong, Y. Y. Li, M. Zhou, Near-Infrared Laser-Excited Nanoparticles To Eradicate Multidrug-Resistant Bacteria and Promote Wound Healing ACS Appl. Mater. Interfaces 10 (2017) 193–206. DOI: 10.1021/acsami.7b15251.

100. X. Li, S. M. Robinson, A. Gupta, K. Saha, Z. Jiang, D. F. Moyano, A. Sahar, M. A. Riley, V. M. Rotello, Functional Gold Nanoparticles as Potent Antimicrobial Agents against Multi-Drug-Resistant Bacteria, ACS Nano 8 (2014) 10682–10686. DOI: 10.1021/nn5042625.

101. M. E. Villanueva, A. M. Diez, J. A. Gonza´lez, C. J. Pe´rez, M. Orrego, L. Piehl, S. Teves and G. J. Copello, Antimicrobial Activity of Starch Hydrogel Incorporated with Copper Nanoparticles, ACS Appl. Mater. Interfaces 8 (2016) 16280–16288. DOI: 10.1021/acsami.6b02955.

102. J. Qiu, W. D. Wei, Surface Plasmon-Mediated Photothermal Chemistry, Journal Physical Chemistry 118 (2014) 20735–20749. DOI: 10.1021/jp5042553

103. S. C. Zhao, L. Li, H. Wang, Y. D. Zhang, X. G. Cheng, N. Zhou, M. N. Rahaman, Z. T. Liu, W. H. Huang, C. Q. Zhang, Wound dressings composed of copper-doped borate bioactive glass microfibers stimulate angiogenesis and heal full-thickness skin defects in a rodent model, Biomaterials 53 (2015) 379–391. DOI:10.1016/j.biomaterials.2015.02.112.

104. B. Tao, C. Lin, Y. Deng, Z. Yuan, X. Shen, M. Chen, Y. He, Z. Peng, Y. Hu, K. Cai, Copper-nanoparticle-embedded hydrogel for killing bacteria and promoting wound healing with photothermal therapy, Journal Materials Chemistry B 7 (2019) 2534-2548. DOI: 10.1039/C8TB03272F.

105. W He, X Huang, Y Zheng, Y Sun, Y Xie, Y. Wang 1, L. Yue, In situ synthesis of bacterial cellulose/copper nanoparticles composite membranes with long-term antibacterial property, Journal Biomaterial Science Polymer Edition 29 (2018) 2137-2153. DOI: 10.1080/09205063.2018.1528518.

106. L. Sun, A. Li, Y. Hu, Y. Li, L. Shang, L. Zhang, Self-Assembled Fluorescent and Antibacterial GHK-Cu Nanoparticles for Wound Healing Applications, Particle and Particle System Characterization 36 (2019) 1800420. DOI: 10.1002/ppsc.201800420.

107. E.G. Halevas, A.A. Pantazaki, Copper Nanoparticles as Therapeutic Anticancer Agents, Nanomedicine Nanotechnology Journal 2 (2018) 119-140. ISSN: 2329-9053

108. Y. Tauran, A. Brioude, A.W. Coleman, M. Rhimi, B. Kim, Molecular recognition by gold, silver and copper nanoparticles. World Journal of Biologycal Chemistry 4 (2013) 35-63. DOI: 10.4331/wjbc.v4.i3.35.

109. I.M. Chung, A. Abdul Rahuman, Green synthesis of copper nanoparticles using Eclipta prostrata leaves extract and their antioxidant and cytotoxic activities, Experimental and Therapeutic Medicine 14 (2017) 18-24. DOI: 10.3892/etm.2017.4466.

110. R. Mukhopadhyay, J. Kazi, M.C. Debnath, Synthesis and characterization of copper nanoparticles stabilized with Quisqualis indica extract: Evaluation of its cytotoxicity and apoptosis in B16F10 melanoma cells, Biomedicine and Pharmacotherapy 97 (2018) 1373-1385. DOI: 10.1016/j.biopha.2017.10.167.

PART D

Nano- and Micro-Technologies Applied to Food Nutritional Ingredients

Abstract

New technologies are currently investigated to improve the quality of foods by enhanc- ing their nutritional value, freshness, safety, and shelf-life, as well as by improving their tastes, fla- vors and textures. Moreover, new technological approaches are being explored, in this field, to ad- dress nutritional and metabolism-related diseases (*i.e.*, obesity, diabetes, cardiovascular diseases), to improve targeted nutrition, in particular for specific lifestyles and elderly population, and to maintain the sustainability of food production. A number of new processes and materials, derived from micro- and nano-technology, have been used to provide answers to many of these needs and offer the possibility to control and manipulate properties of foods and their ingredients at the molec- ular level. The present review focuses on the importance of micro- and nano-technology in the food and nutritional sector and, in particular, provides an overview of the micro- and nano-mate- rials used for the administration of nutritional constituents essential to maintain and improve health, as well as to prevent the development and complications of diseases.

Keywords: delivery, micro-technology, nanotechnology, nutrients, nutrition-related diseases, food applications, risk assess-ment.

1. Introduction

Over the past few decades, the evolution of a number of new scientific disciplines and technologies has allowed the development of new approaches to providing our body with nutritional agents in a safer and more efficient way. Nan- otechnology is mainly involved because it represents a broad interdisciplinary area, encompassing the study, produc- tion, processing and application of materials with one or more dimensions in the order of 100 nanometres (nm). This nanoscale approach may affect nutrient safety, efficiency, bioavailability, and nutritional properties and has allowed the molecular synthesis of new products and ingredients [1, 2]. Nanotechnology may be useful for developing new func- tional materials, micro- and nano-scale processing and the design of methods and instrumentation in food production. The application of nanotechnology in the food sector has emerged only recently. Still, they are predicted to grow rapidly in the coming years, and many of the world's largest food companies are actively exploring the potential of nan- otechnology, for its use in food production [3]. Particularly, a lot of attention was given to the nanotechnology applied to artificial food ingredients, such as food additives, that are in- tentionally added directly or indirectly to food [4]. This is very interesting since the additives are essential for preserv- ing the qualities and characteristics of food that consumers demand for keeping food safe, nutritious, and appetizing from farm to fork. In fact, foods are subject to many enviro-nmental variables, such as temperature fluctuations, oxida- tion, and exposure to microbes, which can change their origi-nal composition.

Nanotechnology has the potential to affect some aspects of food production, including the encapsula- tion of ingredients in delivery systems able to carry, protect, and deliver functional them to their specific site of action[5]. A variety of processes are being used in order to control and manipulate properties of food ingredients and additives at the molecular level, including nano-emulsions, surfactant micelles, emulsion bilayers and reverse micelles [6] (Fig. 1). An example of nanostructured ingredients of foods, de- veloped with the aim of improving their taste, texture, consis- tency and/or increasing nutritional efficiency, are employed for the production of low-fat nanostructured mayonnaise, spreads and ice creams. These foods containing nanostruc- tured ingredients appear to be as "creamy" as their full-fat al- ternatives but offer a healthier option to the consumers [7]. A second example is the microencapsulation of omega-3 fatty acids rich tuna

fish oil, which has been broadly used to mask the taste and smell ingredient when added to bread for health purposes [8]. A variety of other microencapsulated food ingredients and additives are available for use in several food products, and a recent and very interesting trend in the health food area is the microencapsulation of live probiot- ic microbes to promote healthy gut function [9, 10]. A number of nutraceuticals and nutritional supplements containing nano-ingredients and additives (*i.e.* vitamins, an- timicrobials, and antioxidants, *etc*.) are currently available. Virtually all these products claim enhanced absorption and bioavailability of nano-sized ingredients in the body [11].

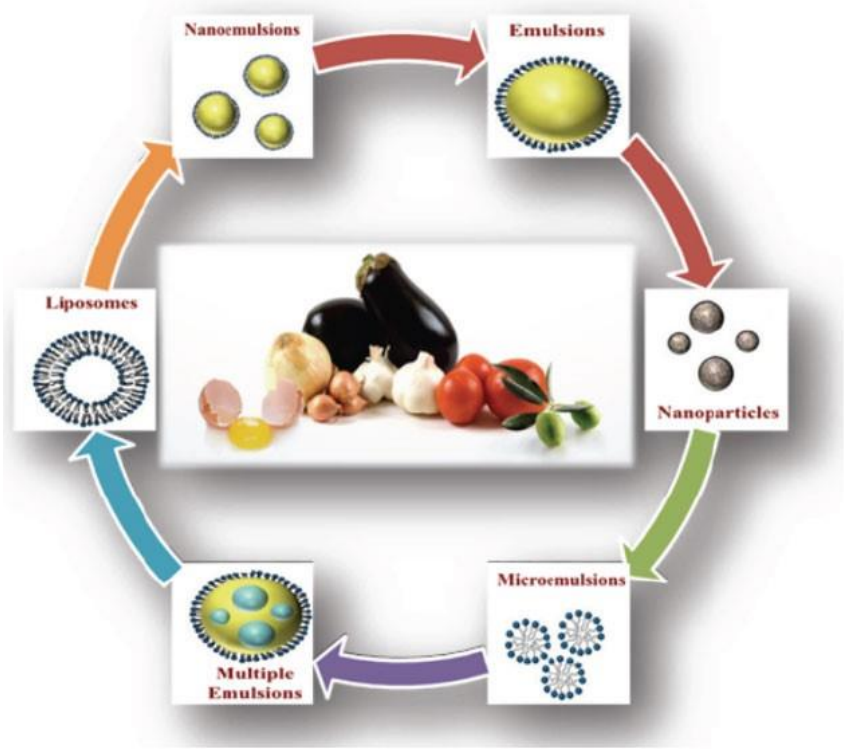

Fig. (1). Nanotechnologies applied in the food sector. (*A higher resolution / colour version of this figure is available in the electronic copy ofthe article*).

Examples of these nanostructured materials include different Nanoceuticals, Nano Calcium/Magnesium, and nano-seleni- um-enriched Nanotea [12]. In the following paragraphs, an overview of the most used nanotechnology-based delivery systems in the food andnutritional area will be provided.

2. APPLICATION OF NANOTECHNOLOGY-BASED DELIVERY SYSTEMS FOR FOOD AND NUTRITION

2.1 Microcarriers

The term microcarrier refers to particle with a diameter of 1-1000 μm. In these broad categories are included spherical microparticles and microcapsules, which possess a core that may be solid, liquid, or even gas, and that is surrounded by a different material [14]. Microspheres are, in the strict sense, empty spherical particles. However, the terms micro- capsules and microspheres are often used indifferently. In ad- dition, some related terms are alternatively used, such as "microbeads" and "beads". Spherical particles are mainly em- ployed for their large size and rigid morphology [15]. Fig. (**2**) is a representation of the possible ingredients encapsula- tion in microsphere and microcapsules.

2.2 Microcapsules

Micro-encapsulation is a process in which small parti- cles or droplets are surrounded by a coating to give small capsules with many useful properties. In general, microcap- sules are used to incorporate food ingredients, enzymes, drugs, cells or other materials on a micrometric scale [16]. The use of microencapsulated food additives is already well established. In particular, microencapsulation has been used to mask the odor of turmeric extract used as a nutrient sup- plement or natural colorant for food products. In particular, Laokuldilok *et al.* [8] reported that microcapsules prepared by a binary blend of wall materials, *i.e.* brown rice flour and beta-cyclodextrin (β-CD), are useful to obtain a highly effi- cient curcuminoid encapsulation with very low volatile re- lease and reduced smell. Moreover, microcapsules obtained using maltodextrin (MD) as coating agent were used [17] to encapsulate and protect the powerful antioxidant phenolic compounds contained in the waste product of olive oil pro- duction (olive pomace) [18]. The CD encapsulation im- proved the antioxidant activity of the olive pomace-derived phenolic extracts. Another interesting CD application is the stabilization of betalains, water-soluble pigments obtained from the purple fruit of the cactus *Opuntia ficus-indica*, through microencapsulation using the spray drying tech- nique [19]. The betalains are also known for their health-pro- moting and wellbeing effect [20] mainly through their an-

tioxidant ability [21, 22]. In the study of Otalora *et al.* [17], these pigments were encapsulated by using maltodextrin (MD), alone or in combination with mucilage (MD-CM) from Cactus cladodes. The microcapsules obtained were of spherical and uniform size. Moreover, MD-CM allowed to reduce microcapsule moisture content and to increase encap- sulation efficiency. Microencapsulation has also been proven to be one of the most efficient methods for maintain-ing the viability and stability of probiotics. Since probiotics are known to induce a number of health benefits, much ef- fort has been expended by the food industry, pharmaceuti- cals, nutraceuticals, and cosmetics in protecting them by the use of new encapsulation methods [23]. Encapsulation may be particularly useful in protecting probiotics during food processing and storage and in the extreme conditions of the human gastrointestinal system. Instead, the encapsulation of probiotics within a physical barrier may protect these living cells against adverse environmental conditions and improve their survival [24].

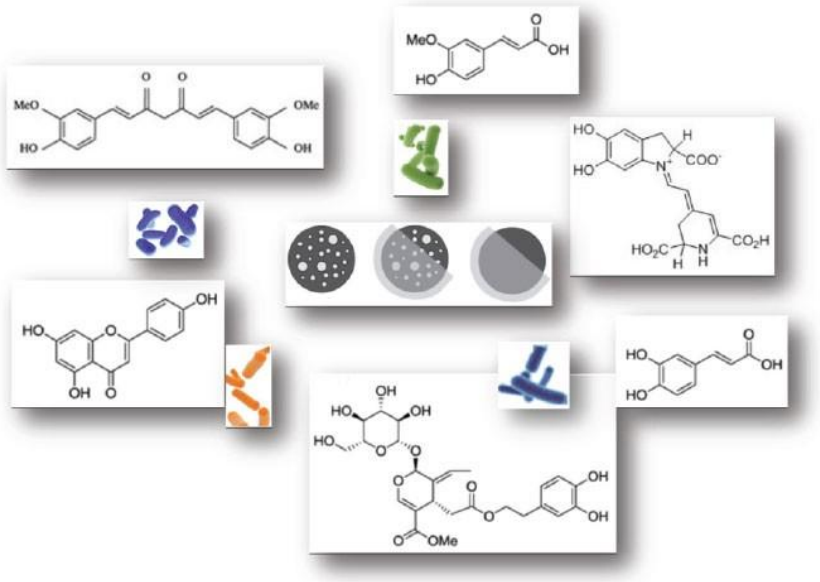

Fig. (2). Microcapsules and microspheres useful for food ingredient release. (*A higher resolution / colour version of this figure is available in the electronic copy of the article*).

2.3 Cyclodextrins

Cyclodextrins (CDs) are water-soluble fibers with a ring-shaped approved as food additives in various countries. From a molecular point of view, they are oligosaccharides having six(α-CD), seven (β-CD), and eight (γ-CD) glucose units bound by α-1.4 linkages that are produced from starch by enzymatic conversion [25]. Their structure creates a cyclic molecule having a hydrophilic surface and a hydro- phobic internal cavity, where they can embrace other com- pounds with hydrophobic properties. Thanks to this capacity, CDs represent optimal candidates to encapsulate ingredi- ents [26]. Moreover, they are considered useful for protecting active substances from environmental hazards and thus increasing their bioavailability. Similarly, to the microcap- sules, CDs have the property of covering nasty smells of some ingredients. Furthermore, CDs have been successfully used as emulsifying agents. Remarkably, several reports have recently demonstrated that α-CD dietary supplementation can ameliorate the blood lipid profile, either by binding to and reducing the intestinal absorption of triglycerides [27] or by dissolving cholesterol crystals [28, 29], which were able to induce complement activation, and thus phagocytosis and ROS production by inflammatory cells. Altogether, these phenomena are considered as critical steps in atherosclerosis development. Therefore, α-CD seems particularly apt to be used as a food additive for the prevention of metabolic and cardiovascular diseases. A variety of foods, such as salad dressings, mayonnaise, dessert creams or margarine, contain both water and oil phases that can be mixed only with the addition of an emulsifier. α-CD has been recently used for the preparation of oil-in-water emulsions due to its emulsifying properties. In this kind of micro-formulation, the hydrophobic fatty acids occupy the interior part of the ring-shaped α-CD molecule which stabilizes the interfaces of the otherwise immiscible oil and water phases of the emulsion [29].

This approach represents considerable progress, since the commonly used animal-based emulsifiers, such as the mono- and di-glycerides of fatty acids, eggs yolk derived lecithin and proteins can be allergenic and are generally sensitive to heat and low pH values, which make their shelf life short. Moreover, they may contain large amounts of cholesterol. On the other hand, α- CDs are able to produce emulsions with varying degrees of viscosity, and being plant-derived, also suitable to be used in vegetarian diets.

2.4 Microparticles

The controlled release of bioactive compounds has repre- sented a significant challenge, not only for application in thepharmaceutical field, but, more recently, also for the food in

dustry [30-32]. One promising approach is the use of starch based microparticles since starch is particularly suitable for the encapsulation of food components, being nontoxic, edi- ble, abundant in nature, and easily achievable at very low costs. Starch-based microparticles have been usually pre- pared by the spray drying method [33]. However, this kind of microparticles dissolve very rapidly after oral ingestion, and this characteristic makes them not suitable for the con- trolled release of bioactive food components. To overcome this inconvenience, in pharmaceutical formulations, starch- based microparticles have been also prepared by water-in-oil (w/o) emulsification crosslinking methods [34,35]. This rep- resents an effective method to obtain water-insoluble micro- particles, where the release of included compound is modu- lated by crosslinking degree modifications [33]. However, the continuous phase in the w/o emulsification crosslinking method is represented by toxic organic solvents, that are un- suitable for food applications. In fact, they may leave noxious residues in food, and alter the chemical properties of the encapsulated bioactive compounds. An alternative method that allows avoiding the use of toxic organic sol- vents is the preparation of a water-in-water (w/w) emulsion where a water soluble polymer is emulsified with an aque- ous solution of poly-ethylene glycol (PEG) as the continu- ous phase [36, 37]. Then the polymer phase is crosslinked to obtain hydrogel microspheres. Recently, drug proteins have been enveloped in w/w emulsion microspheres using as a crosslinking agent trisodium trimetaphosphate (TSTP), a compound not showing adverse health effects. Such an ap- proach may also be useful for the encapsulation of nutrients. For instance, alginate-whey protein-based microspheres were constructed to encapsulate vitamins, such as riboflavin. This kind of formulation was found to be particularly suit- able to enhance riboflavin release and it was hypothesized that such an effect was ascribable to the small surface area/volume ratio and to the long diffusion path length ofthe microparticles [38]. Protein microparticles were also de- veloped by using the highly hydrophobic protein kafirin with the aim to encapsulate different bioactive polyphenols (catechin and sorghum condensed tannins). Various authors studied the antioxidant activity of these compounds in simu-lated gastric conditions, and observed that,

even though ka- firin microparticles were not able to completely avoid the time-dependent antioxidant activity reduction, they were pre-served from digestion [39].

3. Nanocarriers

Nanocarriers are structures characterized by a very small size comprised in the 1-100 nm range. They include nanopar- ticles, nanocapsules, nanoemulsions, nanodispersions, and micelles (Fig. **3**). These nanoformulations have been demon- strated to be useful to improve the chemical stability, absorp-tion and bioavailability of several nutrients and to specifical-ly deliver them to target tissues [13]. Currently, this is a dy- namic research field expected to grow in the next few years constantly. In the next paragraph, an overview of different kinds of nanoformulations that have been so far constructed for a more efficient delivery of food ingredients and nutri- ents will be done.

Fig. (3). Nanomaterials for food ingredient delivery. (*A higher reso- lution / colour version of this figure is available in the electronic copy of the article*).

3.1 Micelles

Micelles are aggregates of amphiphilic surfactants that arrange in a spherical shape in aqueous solutions and are characterized by diameters falling within a range of 5 to100 nm. The hydrophilic portion of the aggregate interacts with the adjacent solvent, and the hydrophobic portion represents the "core" of the micelle. This feature allows the micelles to entrap in their interior highly hydrophobic compounds and carry them through hydrophilic environments, such as the in- testinal lumen and blood circulation. In the nutritional area, these formulations are particularly suitable for the encapsula- tion of lipids, antioxidants and vitamins [40, 41]. In 2007 the Meridian Institute reported a new product (NovaSOL®) as a solution containing nanoparticles, which can be applied to add antioxidants into food and beverage. In this product, the nanoparticles called micelles carry antioxidants and can be used to introduce vitamins A, C, and E, α-lipoic acid, ß-carotene, curcumin, lutein, minerals and Q10 to food and beverages without changing substances. The NovaSOL® technology, which is based on "product micelles" with a di- ameter of around 30 nm, has been successfully applied to de- velop a variety of solubilizate. Other types of applications in- clude food additives, such as benzoic acid and citric acid [42]. Casein micelles may be useful as nano-vehiclesfor en- trapment, protection, and delivery of sensitive hydrophobic nutraceuticals within other food products [43]. The encapsu- lation of eugenol and carvacrol into nanometric surfactant micelles also resulted in enhanced antimicrobial activity [44], although the addition of micelle-encapsulated eugenol to milk resulted in being less or as inhibitory as unencapsu- lated eugenol [45]. Furthermore, limonene used to mask the unpleasant taste of some nutrients, but also as a dietary an- timicrobial and chemotherapeutic agent, is characterized by a low solubility and exhibits a bacteriostatic activity only if its concentration in the aqueous phase is increased, for exam- ple by favorable partitioning between the aqueous and a selected lipid phase, or by solubilization within appropriate sur-factant micelles [46].

3.2 Nanoemulsions

Nanoemulsions are colloidal particulate systems in the submicron size range, acting as carriers of drug molecules. Their size varies from 10 to 1000 nm. Nanoemulsions are produced by high-pressure value homogenizers or mi- crofluidizers [47]. Among the most

used nanoemulsions are: the oil in water (O/W) where the oil droplets are dispersed in the aqueous phase and the interphase is stabilized by emulsi- fiers; the multiple emulsions oil-in-water-in-oil (O/W/O) and water-in-oil-in-water (W/O/W), in which nanometer- size water droplets contained within large oil droplets are dis- persed within an aqueous phase (W/O/W); and the multilay- er emulsions which consist of oil droplets surrounded by nanometric size layers of different polyelectrolytes. Functio- nal food ingredients can be incorporated within the droplet, the interfacial region, or the continuous phase to reduce the chemical degradation process [48]. O/W nanoe- mulsions can encapsulate and deliver poorly water-soluble food antimicrobials, improving the physical stability of the active compound and increasing its active distribution in food matrices. About this, eugenol was incorporated in O/W nanoemulsion using sesame oil, Tween 80, and water. The nanoemulsion containing 0.003% eugenol was stable for more than one month and exhibited antibacterial activity against *Staphylococcus aureus* [49]. Terjung *et al.* devel- oped a nanoemulsion containing carvacrol and eugenol with triacylglyceride (Miglyol 812N) or Tween 80. Carvacrol emulsions with a mean oil droplet size of 3000 nm at a con- centration of 800 ppm completely inhibited *Listeriainnocua,* while for 80 nm emulsions, only a delay of growth was ob- served due to an increased sequestering of antimicrobials in emulsion interfaces and a decreased solubilization in excess Tween 80 micelles [50]. Carvacrol, limonene, and cin- namaldehyde were encapsulated in the sunflower oil-based nanoemulsions. The antimicrobial activity, measured against *Escherichia coli, Lactobacillus delbrueckii,* and *Saccharomyces cerevisiae,* was dependent on the compound concentration in the aqueous phase. Carvacrol emulsion com-pletely inactivate *E. coli, S. cerevisiae* and *L. delbrueckii* growth. Bacteriostatic action was promoted by emulsifiers, such as lecithin and pea proteins, that slightly solubilized the essential oil in the aqueous phase [51]. Basil oil (*Ocimumbasilicum*) containing 88% of estragole, encap- sulated in a nanoemulsion formulated with Tween 80 and water, showed antibacterial activity against *E. coli* even di- luted [52]. Nanoemulsion based on carnauba-shellac wax (C- SW) [53], encapsulating lemongrass oil (LO) decreased the total population of *E. coli* and *L. monocytogenes*. Also, the LO-alginate nanoemulsions demonstrated an antibacterial ef- fect against *E. coli*. Joe *et al.* developed a sunflower oil-sur- factin-based O/W nanoemulsion, where the synthetic surfac- tant was replaced by surfactin, a cyclic lipopeptide antibiotic biosurfactant produced by *B. subtilis* [54]. This nanoemul- sion

demonstrated high antibacterial activity against *S. Typhi*, *L. monocytogenes*, and *S. aureus*. When the sunflower oil-surfactin nanoemulsion was applied to food products such as raw chicken, apple juice, milk, and mixed vegetable, a reduction in the native cultivable bacterial and fungal popu- lations was observed. In addition, bovine lactoferrin, an iron-binding protein that strongly inhibits growth or kills iron-dependent pathogenic bacteria, was entrapped within W/O/W multiple nanoemulsions with lecithin and poloxam- ers by homogenization with the aim to increase its antibacte- rial activity [55]. Soybean oil-based nanoemulsion has shown bactericidal properties against Gram-positive bacteria [39] and fungistatic property [56]. Teixeira *et al.* prepared BCTP nanoemulsion (an O/W nanoemulsion of soybean oil and tri-n-butyl phosphate emulsified with Triton X-100) and showed that it could reduce *Listeria monocytogenes* cell number [57]. Nanoemulsions have also been reported to in- crease the bioavailability of antioxidants such as α -toco- pherol. In particular, literature data suggest that α-toco- pherol bioavailability was 10-fold more than that of the same vitamin contained in commercial gelatin capsules [58, 59]. α-Tocopherol, used alone or in combination with a stear- in-rich milk fraction for the preparation of oil-in-water sodi- um caseinate-stabilized nanoemulsions, was protected against degradation [60]. In other studies, it is evident that nanoemulsions could improve the stability and oral bioavail- ability of epigallocatechin gallate and curcumin [61]. Solid lipid nanoparticles (SLNs), formed by controlled crystalliza- tion of food nanoemulsions, could be useful for the transport and delivery of bioactives, such as lycopene and carotenoids [62]. The major advantages of solid lipid nanoparticles in- clude large-scale production without the use of organic sol- vents, high concentration of functional compounds in the sys- tem, long term stability, and the ability to be spray dried into powder form [63].

3.3 Nanospheres

Nanospheres can be defined as solid colloidal particles in which bioactive compounds are dissolved, entrapped, en- capsulated, chemically bound, or adsorbed to the polymer matrix. However, the central core can become solid-like depending on the copolymer composition, making it difficult to have a clear distinction between micelles and nanospheres [64]. Functional foods can be encapsulated in these nanospheres and released in response to specific envi- ronmental stimuli. In fact, the change of solution conditions could modify chemical-physical properties of these nano- spheres, including particles' porosity or

dissolution [65]. In this context, chitosan nanoparticles, loaded with jujube pulp and seed extracts, were prepared [66]. The stabilities of ju- jube pulp and seed extract, in terms of total phenolic content and antioxidant activity were effectively enhanced by na- noencapsulation. So, jujube pulp and seed extracts prepared using optimal conditions could be useful as a natural functio- nal food ingredient with antioxidant activity, and nanoencap- sulation can be used to improve the stability of jujube ex- tract [66]. Sanna *et al.* realized polymeric nanoparticles based on poly(ε-caprolactone) and alginate in which encap- sulated white tea extract [67]. Nanoparticles were prepared with the aim to obtain controlled release and to preserve the antioxidant activity of the polyphenols white tea extract. Re- sults confirmed that white tea extract retained its antioxidant activity and nanoparticles protected tea polyphenols from degradation, thus opening new perspectives for the exploita- tion of white tea extract-loaded nanoparticles for nutraceuti- cal applications [67].

3.4 Nanocapsules and Liposomes

Nanocapsules and polymersome are colloidal-sized, vesicular systems in which the bioactive compound is confined within a cavity surrounded by a polymer mem- brane or coating [68]. If the core is an oily liquid and the sur- rounding polymer a single layer, the vesicle is referred to as a nanocapsule; these systems have found utility in the deliv- ery of hydrophobic compounds. If the core of the vesicle is an aqueous phase and the surrounding coating is a polymer bilayer, the particle is referred to as a polymersome [69]. Th- ese vesicles are analogous to liposomes and find utility in the encapsulation and delivery of water-soluble compounds. Still, they differ from liposomes in that the external bilayer is composed of amphiphilic copolymers. Variation in compo- sition, molecular geometry, and relative monomer lengths re- sults in various physicochemical properties and morpholo- gies of the resulting nano-encapsulates [70]. Currently, a greater fundamental understanding of polymer-polymer and polymer-nutraceutical interactions at the molecular level and their impact on functional properties of the delivery systems is required to ensure the design of ideal nutraceutical carri- ers for use in the food industry. Liposomes can be used for the controlled delivery of functional ingredients, including enzymes, vitamins [71], and flavors in different food applica- tions [72]. Liposomes can encapsulate enzymes to increase the speed of cheese ripening [73] and vitamins to increase the nutritional quality of dairy products [74]. Lee and Martin reported that the degradation of retinol entrapped in lipo- somes was

decreased by the addition of vitamin E (α-toco- pherol) [75]. These studies shown that the use of liposomes could increase the protection of bioactivity of nutrients against degradation in food. In addition, a wide variety of nu- trients can be incorporated [76] in nanocapsules based on na-tural polymers such as albumin (protein), gelatin (protein), alginate (saccharide), collagen(protein), chitosan (saccharide), and the milk protein α-lactalbumin. These nanocapsules are particularly interesting because they are rel- atively easy to prepare and can form complexes with polysaccharides, lipids or other biopolymers. Also, the en- capsulation of essential oils at the nanoscale represents an available and efficient approach to increasing their antimicro-bial activities and physical stability and reducing the mass transfer resistances of the active molecules to the sites of ac- tion [77]. In this regard, Mohammadi *et al.* investigated the nanoencapsulation of Zatarian multiflora essential oil in chi- tosan nanoparticles to enhance antifungal activity and stability of the oils against one isolate of Botrytis cinerea *Pers.*, the causal agent of gray mould disease. The obtained data indicated that nanocapsules could enhance es- sential oil antifungal activities [78].

4. RISK ASSESSMENT

Though nanotechnology can potentially be helpful in all areas of food production and processing, a lot of techniques are too expensive or too impractical to implement on a com- mercial scale. Furthermore, in 2011, the European Food Safety Authority (EFSA) published a scientific opinion with the title "Guidance on the risk assessment of the application of nanoscience and nanotechnologies in the food and feed chain" [79]. The guidance is a practical approach to assess- ing potential risks when nanomaterials are applied in the food and feed chain. It builds upon the scientific opinion from 2009 [80]. EFSA concluded in both reports that "the risk assessment paradigm (hazard identification and hazard characterization followed by exposure assessment and risk characterization) is appropriate for these applications" of nanoscience and nanotechnologies in the food and feed chain. Therefore, the risk of an engineered nanomaterial will be determined by its chemical composition, physicochemi- cal properties, interactions with tissues, and potential expo- sure levels. EFSA states that there are currently uncertainties related to the identification, characterization and detection of engineered nanomaterial because of the lack of suitable and validated test methods. For these reasons, EFSA recom- mends that additional research

is needed to address the many current uncertainties and limitations. In general, EFSA supports the use of conventional risk assessment while ac- knowledging the limited knowledge on exposure to nano- food applications.

5. CONCLUSION

In the present review, a number of micro- and nano-tech- nologies based supplements, nutraceuticals and additives were analyzed. These technologies could be used to enhance food flavor and texture, to reduce fat content, or encapsulate nutrients. Functional ingredients such as drugs, vitamins, an-timicrobials, antioxidants, flavorings, colorants, and preser- vatives were characterized by a variety of different molecu- lar forms and chemical-physical properties, including polari-ty, molecular weight (low to high), and physical states (solid, liquid, gas). They have been often utilized directly in their pure form, but they are now increasingly incorporated into some forms of delivery systems to overcome their limits and optimize the properties. A wide variety of delivery sys- tems has been developed to encapsulate functional ingredi- ents, including simple solutions, association colloids, emul-sions, biopolymer matrices, and so on. Each type of delivery system has its specific advantages and disadvantages for the encapsulation, protection, and delivery of functional ingredi-ents, cost, regulatory status, ease of use, biodegradabilityand biocompatibility.

REFERENCES

Trombino S.; Curcio F.; Cassano R. Nano- and Micro-Technologies Applied to Food Nutritional Ingredients. *Current drug delivery*, 2021;18(6):670-678.

1. Blundell, J.E.; Thurlby, P.L. Experimental manipulations of eat- ing: advances in animal models for studying anorectic agents. *Pharmacol. Ther.*, 1987, *34*(3), 349-401. http://dx.doi.org/10.1016/0163-7258(87)90001-5 PMID: 3324113
2. Aguilera, J.M. Why food microstructure? *J. Food Eng.*, 2005, *67*, 3-11. http://dx.doi.org/10.1016/j.jfoodeng.2004.05.050
3. Singh, T.; Shukla, S.; Kumar, P.; Wahla, V.; Bajpai, V.K.; Rather, I.A. Application of Nanotechnology in Food Science: Perception and Overview. *Front. Microbiol.*, 2017, *8*, 1501. http://dx.doi.org/10.3389/fmicb.2017.01501 PMID: 28824605
4. Pressman, P.; Clemens, R.; Hayes, W.; Reddy, C. Food additive safety: A review of toxicologic and regulatory issues. *Toxicol. Res.*, 2017, *1*, 22.
5. He, X.; Deng, H.; Aker, W.G.; Hwang, H. Regulation and Safety of Nanotechnology in the Food and Agriculture Industry.*Food Ap- plications of Nanotechnology*; Molina, G., Inamuddin, Pelissari, F.M., Asiri, A.M. CRC Press: Florida, USA, 2020, 23, pp. 517-525.
6. Weiss, J.; Takhistov, P.; McClements, D.J. Functional Materials in Food Nanotechnology. *J. Food Sci.*, 2006, *719*, 107-116. http://dx.doi.org/10.1111/j.1750-3841.2006.00195.x
7. Chaudhry, Q.; Watkins, R.; Castle, L. Nanotechnologies in Food: What, Why and How? *Nanotechnologies in Food; Chaudhry, Q.; Castle, L.; Watkins, R*; Royal Society of Chemistry: Washington, USA, 2017, pp. 1-19. http://dx.doi.org/10.1039/9781782626879-00001
8. Laokuldilok, N.; Thakeow, P.; Kopermsub, P.; Utama-ang, N. Op- timisation of microencapsulation of turmeric extract for masking flavour. *Food Chem.*, 2016, *194*, 695-704. http://dx.doi.org/10.1016/j.foodchem.2015.07.150 PMID: 26471609
9. Zaeim, D.; Jamab, M.S.; Ghorani, B.; Kadkhodaee, R. WeilinLiu, W.; Tromp, R.H.

Microencapsulation of probiotics in multi-
-polysaccharide microcapsules by electro-hydrodynamic atomiza- tion and in corporation into ice-cream formulation. *Food Struc.*, 2020, *20*, 100147. http://dx.doi.org/10.1016/j.foostr.2020.100147

10. Yao, M.; Xie, J.; Du, H.; McClements, D.J.; Xiao, H.; Li, L. Progress in microencapsulation of probiotics: A review. *Food Sci Food Saf.*, 2020, *85*(2), 394-403. http://dx.doi.org/10.1111/1541-4337.12532
11. Fursik, O.; Strashynskiy, I.; Pasichniy, V.; Marynin, A. Some as- pects of using the nanotechnology in food industry. *Ukrainian J. Food Sci.*, 2019, *7*, 298-306. http://dx.doi.org/10.24263/2310-1008-2019-7-2-12
12. Santillán-Urquiza, E.; Ruiz-Espinosa, H.; Angulo-Molina, A.; Vélez Ruiz, J.F.; Méndez-Rojas, M.A. Applications of nanomate- rials in functional fortified dairy products: benefits and implica- tions for human health. *Nutrient Delivery; Grumezescu, A.M*; Aca- demic Press: London, UK, 2017, pp. 293-328. http://dx.doi.org/10.1016/B978-0-12-804304-2.00008-1
13. Jones, D.; Caballero, S.; Davidov-Pardo, G. Bioavailability of nan- otechnology-based bioactives and nutraceuticals. Adv. Food Nutr. Res., 2019, 88, 235-273. http://dx.doi.org/10.1016/bs.afnr.2019.02.014 PMID: 31151725
14. Zugic, A.; Tadic, V.; Savic, S. Nano- and Microcarriers as Drug Delivery Systems for Usnic Acid: Review of Literature. Pharma- ceutics, 2020, 12(2), 156. http://dx.doi.org/10.3390/pharmaceutics12020156 PMID: 32075296
15. Gutiérrez, T.J.; Álvarez, K. Biopolymers as microencapsulation materials in the food industry. Adv. Phys. Prop. Biop, 2017, 2, 296-322. http://dx.doi.org/10.2174/978168108544911701000 9
16. Paulo, F.; Santos, L. Design of experiments for microencapsula- tion applications: A review. Mater. Sci. Eng. C, 2017, 77, 1327-1340. http://dx.doi.org/10.1016/j.msec.2017.03.219 PMID: 28532010
17. Vitali Čepo, D.; Radić, K.; Jurmanović, S.; Jug, M. GrdićRa- jković, M.; Pedisić, S.; Moslavac, T.; Albahari, P. Valorization of Olive Pomace-Based Nutraceuticals as Antioxidants in Chemical. Molecules, 2018, 23, 8.http://dx.doi.org/10.3390/molecules23082070

18. Sánchez Moral, P.; Ruiz Méndez, M.V. Production of pomace olive oil. *Grasas Aceites,* 2006, *57*, 47-55. http://dx.doi.org/10.3989/gya.2006.v57.i1.21
19. Otálora, M.C.; Carriazo, J.G.; Iturriaga, L.; Nazareno, M.A.; Oso- rio, C. Microencapsulation of betalains obtained from cactus fruit (Opuntia ficus-indica) by spray drying using cactus cladode muci- lage and maltodextrin as encapsulating agents. *Food Chem.,* 2015, *187*, 174-181. http://dx.doi.org/10.1016/j.foodchem.2015.04.090 PMID: 25977013
20. Belhadj Slimen, I.; Najar, T.; Abderrabba, M. BelhadjSlimen. Chemical and Antioxidant Properties of Betalains. *J. Agric. Food Chem.,* 2017, *65*(4), 675-689. http://dx.doi.org/10.1021/acs.jafc.6b04208 PMID: 28098998
21. El-Mostafa, K.; El Kharrassi, Y.; Badreddine, A.; Andreoletti, P.; Vamecq, J.; El Kebbaj, M.S.; Latruffe, N.; Lizard, G.; Nasser, B.; Cherkaoui-Malki, M. Nopal cactus (Opuntia ficus-indica) as a source of bioactive compounds for nutrition, health and disease. *Molecules,* 2014, *19*(9), 14879-14901.http://dx.doi.org/10.3390/molecules190914879 PMID: 25232708
22. Osuna-Martínez, U.; Reyes-Esparza, J.; Rodríguez-Fragoso, L. Cactus (Opuntia ficus-indica): A review on its antioxidants proper- ties and potentialpharmacological use in chronic diseases. *Nat. Prod. Chem. Res.,* 2014, *2*, 153-160.
23. Šipailienė, A.; Petraitytė, S. Encapsulation of Probiotics: Proper Selection of the Probiotic Strain and the Influence of Encapsula- tion Technology and Materials on the Viability of Encapsulated Microorganisms. *Probiotics Antimicrob. Proteins,* 2018, *10*(1), 1-10. http://dx.doi.org/10.1007/s12602-017-9347-x PMID: 29124564
24. Vidhyalakshmi, R.; Bhakyaraj, R.S.; Subhasree, R. Encapsulation "The Future of Probiotics"-A Review. *Adv. Biol. Res. (Faisal-abad),* 2009, *3*, 96-103.
25. Tomasik, P.; Horton, D. Enzymatic conversions of starch. *Adv. Carbohydr. Chem. Biochem.,* 2012, *68*, 59-436. http://dx.doi.org/10.1016/B978-0-12-396523-3.00001-4 PMID: 23218124
26. Zipp, H. Cyclodextrins-novel solutions for the food industry. *Food Ingr. Brasil,* 2012, *22*, 56.
27. Artiss, J.D.; Brogan, K.; Brucal, M.; Moghaddam, M.; Jen, K.L. The effects of a new soluble dietary fiber on weight gain and se- lected blood parameters in rats.

Metabolism, 2006, *55*(2), 195-202.http://dx.doi.org/10.1016/j.metabol.2005.08.012 PMID: 16423626

28. Bessell, E.; Fuller, N.R.; Markovic, T.P.; Burk, J.; Picone, T.; Hendy, C.; Tan, M.M.C.; Caterson, I.D. Effects of alpha-cyclodex- trin on cholesterol control and Compound K on glycaemic control in people with pre-diabetes: Protocol for a Phase III randomized controlled trial. *Clin. Obes.*, 2019, *9*(4), e12324. http://dx.doi.org/10.1111/cob.12324 PMID: 31172667
29. Pilely, K.; Bakke, S.S.; Palarasah, Y.; Skjoedt, M.O.; Bartels, E.D.; Espevik, T.; Garred, P. Alpha-cyclodextrin inhibits choles- terol crystal-induced complement-mediated inflammation: A potential new compound for treatment of atherosclerosis. *Atheroscle- rosis*, 2019, *283*, 35-42. http://dx.doi.org/10.1016/j.atherosclerosis.2019.01.034 PMID: 30772772
30. Salles, C.; Tarrega, A.; Mielle, P.; Maratray, J.; Gorria, P.; Li- aboeuf, J.; Liodenot, J. *J. Food Eng.*, 2007, *82*(2), 189-198. http://dx.doi.org/10.1016/j.jfoodeng.2007.02.008
31. Soottitantawat, A.; Takayama, K.; Okamura, K.; Muranaka, D.; Yoshii, H.; Furuta, T.; Ohkawara, M.; Linko, P. *Innov. Food Sci. Emerg. Technol.*, 2005, *6*(2), 163-170. http://dx.doi.org/10.1016/j.ifset.2004.11.007
32. Malone, M.E. Appelqvist. I.A.M. Modulating Lipid Delivery in Food Emulsions. *J. Control. Release*, 2003, *90*(2), 227-241. http://dx.doi.org/10.1016/S0168-3659(03)00179-2 PMID: 12810305
33. Anand, U.; Ambarish, J. Fabrication of starch-based microparti- cles by an emulsification crosslinking method. *J. Chem. Pharm. Res.*, 2011, *3*, 839-845.
34. Mao, S.; Chen, J.; Wei, Z.; Liu, H.; Bi, D. Intranasal administra- tion of melatonin starch microspheres. *Int. J. Pharm.*, 2004, *272*(1-2), 37-43.http://dx.doi.org/10.1016/j.ijpharm.2003.11.028 PMID: 15019067
35. Atyabi, F.; Manoochehri, S.; Moghadam, S.H.; Dinarvand, R. Cross-linked starch microspheres: effect of cross-linking condi- tion on the microsphere characteristics. *Arch. Pharm. Res.*, 2006, *29*(12), 1179-1186.http://dx.doi.org/10.1007/BF02969311 PMID: 17225470

36. Franssen, O.; Hennink, W.E. A novel preparation method for poly- meric microparticles without the use of organic solvents. *Int. J. Pharm.*, 1998, *168*(1), 1-7.http://dx.doi.org/10.1016/S0378-5173(98)00071-4
37. Stenekes, R.J.H.; Franssen, O.; van Bommel, E.M.; Crommelin, D.J.; Hennink, W.E. The use of aqueous PEG/dextran phase sepa- ration for the preparation of dextran microspheres. *Int. J. Pharm.*, 1999, *183*(1), 29-32.http://dx.doi.org/10.1016/S0378-5173(99)00038-1 PMID: 10361149
38. Chen, L.; Subirade, M. Effect of preparation conditions on the nu- trient release properties of alginate-whey protein granular micro- spheres. *Eur. J. Pharm. Biopharm.*, 2007, *65*(3), 354-362.http://dx.doi.org/10.1016/j.ejpb.2006.10.012 PMID: 17150342
39. Taylor, J.; Taylor, J.R.N.; Belton, P.S.; Minnaar, A. Kafirin micro- particle encapsulation of catechin and sorghum condensed tan- nins. *J. Agric. Food Chem.*, 2009, *57*(16), 7523-7528.http://dx.doi.org/10.1021/jf901592q PMID: 19642673
40. Sun, X.; Bandara, N. Applications of reverse micelles technique in food science: A comprehensive review. *Trends Food Sci. Technol.*, 2019, *91*, 106-115.http://dx.doi.org/10.1016/j.tifs.2019.07.001
41. Chen, H.; Wooten, H.; Thompson, L.; Pan, K. Nanoparticles of ca- sein micelles for encapsulation of food ingredients. *Biopolymer Nanostructures for Food Encapsulation Purposes*; Jafari, S.M., Ed.; Academic Press: London, UK, 2019, pp. 39-68. http://dx.doi.org/10.1016/B978-0-12-815663-6.00002-1
42. Sozer, N.; Kokini, J.L. Nanotechnology and its applications in the food sector. *Trends Biotechnol.*, 2009, *27*(2), 82-89.http://dx.doi.org/10.1016/j.tibtech.2008.10.010 PMID: 19135747
43. Livney, Y.D.; Dalgleish, D.G. Casein micelles for nanoencapsula- tion of hydrophobic compounds. Europe PMC Patent CA2649788, 2019.
44. Gaysinsky, S.; Davidson, P.M.; Bruce, B.D.; Weiss, J. Growth in- hibition of Escherichia coli O157:H7 and Listeria monocytogenes by carvacrol and eugenol encapsulated in surfactant micelles. *J. Food Prot.*, 2005, *68*(12), 2559-2566. http://dx.doi.org/10.4315/0362-028X-68.12.2559 PMID: 16355826
45. Gaysinsky, S.; Taylor, T.M.; Davidson, P.M.; Bruce, B.D.; Weiss, J. Antimicrobial efficacy of eugenol microemulsions in milk against Listeria monocytogenes and

Escherichia coli O157:H7. *J. Food Prot.*, 2007, *70*(11), 2631-2637. http://dx.doi.org/10.4315/0362-028X-70.11.2631 PMID: 18044447

46. Donsì, F.; Annunziata, M.; Sessa, M.; Ferrari, G. Nanoencapsula tion of essential oils to enhance their antimicrobial activity in foods. Food Sci. Technol., 2011, 44, 1908-1914. http://dx.doi.org/10.1016/j.lwt.2011.03.003
47. Aswathanarayan, J.B.; Vittal, R.R. Nanoemulsions and Their Po- tential Applications in Food Industry. Front. Sustain. Food Syst., 2019, 19, 857-874. http://dx.doi.org/10.3389/fsufs.2019.00095
48. Ahsan, A.; Rezaul, M.; Shishir, I. Production, stability and applica- tion of micro- and nanoemulsion in food production and the food processing industry. Emulsions Nanotechnology in the Agri-Food Industry, 2016, 12, 405-442.
49. Hu, Q.; Gerhard, H.; Upadhyaya, I.; Venkitanarayanan, K.; Luo, Y. Antimicrobial eugenol nanoemulsion prepared by gum arabic and lecithin and evaluation of drying technologies. Int. J. Biol. Macromol., 2016, 87, 130-140. http://dx.doi.org/10.1016/j.ijbiomac.2016.02.051 PMID: 26902894
50. Terjung, N.; Löffler, M.; Gibis, M.; Hinrichs, J.; Weiss, J. Influ- ence of droplet size on the efficacy of oil-in-water emulsions load- ed with phenolic antimicrobials. Food Funct., 2012, 3(3), 290-301.http://dx.doi.org/10.1039/C2FO10198J PMID: 22183117
51. Donsì, F.; Annunziata, M.; Vincensi, M.; Ferrari, G. Design of na- noemulsion-based delivery systems of natural antimicrobials: ef- fect of the emulsifier. J. Biotechnol., 2012, 159(4), 342-350.PMID: 21763730
52. Ghosh, V.; Mukherjee, A.; Chandrasekaran, N. Ultrasonic emulsi- fication of food-grade nanoemulsion formulation and evaluation of its bactericidal activity. Ultrason. Sonochem., 2013, 20(1), 338-344.PMID: 22954686
53. Jo, W.; Song, H.; Song, N.; Lee, J.; Min, S.; Song, K. Quality and microbial safety of “Fuji” apples coated with carnauba ashellac wax containing lemongrass oil. Lebensm. Wiss. Technol., 2014, 55, 490-497.
54. Joe, M.M.; Bradeeba, K.; Parthasarathi, R. Development of sur- factin based nanoemulsion formulation fromselected cooking oils: evaluation for antimicrobial activity against selected food associat-ed microorganisms. J. Taiwan Inst. Chem. Eng., 2012, 43, 172-180.

55. Balcåo, V.; Costa, I.; Matos, C.; Moutinho, C.G.; Amorim, M.; Pintado, M.E.; Patrícia Almeida Gomes, A.P.; Vila, M.; Caldas Teixeira, J.A. Nanoencapsulation of bovine lactoferrin for food and biophamarceutical applications. Food Hydrocoll., 2013, 32, 425-431.http://dx.doi.org/10.1016/j.foodhyd.2013.02.004
56. Hamouda, T.; Myc, A.; Donovan, B.; Shih, A.Y.; Reuter, J.D.; Baker, J.R., Jr A novel surfactant nanoemulsion with a unique non-irritant topical antimicrobial activity against bacteria, en- veloped viruses and fungi. Microbiol. Res., 2001, 156(1), 1-7.http://dx.doi.org/10.1078/0944-5013-00069 PMID: 11372645
57. Teixeira, P.C.; Leite, G.M.; Domingues, R.J.; Silva, J.; Gibbs, P.A.; Ferreira, J.P. Antimicrobial effects of a microemulsion and a nanoemulsion on enteric and other pathogens and biofilms. Int. J. Food Microbiol., 2007, 118(1), 15-19. http://dx.doi.org/10.1016/j.ijfoodmicro.2007.05.008 PMID: 17610974
58. Gonnet, M.; Lethuaut, L.; Boury, F. New trends in encapsulation of liposoluble vitamins. J. Control. Release, 2010, 146(3), 276-290.http://dx.doi.org/10.1016/j.jconrel.2010.01.037 PMID: 20600399
59. Wajda, R.; Zirkel, J.; Schaffer, T. Increase of bioavailability of coenzyme Q(10) and vitamin E. J. Med. Food, 2007, 10(4), 731-734.http://dx.doi.org/10.1089/jmf.2006.254 PMID: 18158850
60. Relkin, P.; Yung, J.M.; Kalnin, D.; Ollivon, M. Structural be- haviour of lipid droplets in protein-stabilized nano-emulsions and stability of α-tocopherol. Food Biophys., 2008, 3, 163-168. http://dx.doi.org/10.1007/s11483-008-9064-9
61. Shtay, R.; Keppler, J.K.; Schrader, K.; Schwarz, K. Encapsulation of (—)-epigallocatechin-3-gallate (EGCG) in solid lipid nanoparti- cles for food applications. J. Food Eng., 2019, 244, 91-100. http://dx.doi.org/10.1016/j.jfoodeng.2018.09.008
62. da Silva Santos, V.; Badan Ribeiro, A.P.; Andrade Santana, M.H. Solid lipid nanoparticles as carriers for lipophilic compounds for applications in foods. Food Res. Int., 2019, 122, 610-626. http://dx.doi.org/10.1016/j.foodres.2019.01.032 PMID: 31229120
63. Ghanbarzadeh, B.; Keivani, F.; Mohammadi, M. Encapsulation of food ingredients by solid lipid nanoparticles (SLNs). Lipid-Based Nanostructures for Food Encapsulation

Purposes; Jafari, S.M., Ed.; Academic Press: London, UK, 2019, pp. 179-216. http://dx.doi.org/10.1016/B978-0-12-815673-5.00006-4

64. Guragain, S.; Bastakoti, B.P. Synthesis of Inorganic Hollow Nano- spheres and their Application in Drug in Delivery. J. Nepal Chem. Soc., 2018, 38.
65. Wang, Y. Y.; Gao, D., Zhou, D.; Li, Y., Wang, X.; He, P.; Zhang, Y., Multifunctional Ag/polymer composite nanospheres for drug delivery and cell imaging. J. Mater. Sci., 2020, 55, 13995-14007. http://dx.doi.org/10.1007/s10853-020-04912-z
66. Han, H.J.; Lee, J.S.; Park, S.A.; Ahn, J.B.; Lee, H.G. Extraction optimization and nanoencapsulation of jujube pulp and seed for en- hancing antioxidant activity. Colloids Surf. B Biointerfaces, 2015, 130, 93-100. http://dx.doi.org/10.1016/j.colsurfb.2015.03.050 PMID: 25911157
67. Sanna, V.; Lubinu, G.; Madau, P.; Pala, N.; Nurra, S.; Mariani, A.; Sechi, M. Polymeric nanoparticles encapsulating white tea ex- tract for nutraceutical application. J. Agric. Food Chem., 2015, 63(7), 2026-2032. http://dx.doi.org/10.1021/jf505850q PMID: 25599125
68. Granata, G.; Stracquadanio, S.; Leonardi, M.; Napoli, E.; Consoli, G.M.L.; Cafiso, V.; Stefani, S.; Geraci, C. Essential oils encapsu- lated in polymer-based nanocapsules as potential candidates for ap- plication in food preservation. Food Chem., 2018, 269, 286-292. http://dx.doi.org/10.1016/j.foodchem.2018.06.140 PMID: 30100436
69. Jhala, D.; Rather, H.; Vasita, R. Nano-delivery of Food-Derived Biomolecules: An Overview. Funct. Food Human Health, 2018, 447-470.
70. Letchford, K.; Burt, H. A review of the formation and classification of amphiphilic block copolymer nanoparticulate structures: bmicelles, nanospheres, nanocapsules and polymersomes. Eur. J. Pharm. Biopharm., 2007, 65(3), 259-269. http://dx.doi.org/10.1016/j.ejpb.2006.11.009 PMID: 17196803
71. Alavi, M.; Karimi, N.; Safaei, M. Application of Various Types of Liposomes in Drug Delivery Systems. Adv. Pharm. Bull., 2017,7(1), 3-9. http://dx.doi.org/10.15171/apb.2017.002 PMID: 28507932
72. Srinivasan, V.; Chavan, S.; Jain, U.; Tarwadi, K. Liposomes for Nanodelivery Systems in Food Products.Nanoscience for Sustainable Agriculture; Pudake, R.M., Chauhan,

N., Kole, C. Springer: Heidelberg, Germany, 2019, pp. 624-638.http://dx.doi.org/10.1007/978-3-319-97852-9_24

73. Emami, S.; Azadmard-Damirchi, S.; Hadi Peighambardoust, S.; Valizadeh, H.; Hesari, J. Liposomes as carrier vehicles for functio- nal compounds in food sector. J. Exp. Nanosci., 2016. http://dx.doi.org/10.1080/17458080.2016.1148273
74. Rovoli, M.; Pappas, I.; Lalas, S.; Gortzi, O.; Kontopidis, G. In vitro and in vivo assessment of vitamin A encapsulation in a lipo- some-protein delivery system. J. Liposome Res., 2019, 29(2), 142-152. http://dx.doi.org/10.1080/08982104.2018.1502314 PMID: 30187807
75. Lee, S.B.; Martin, C.R. Electromodulated molecular transport in gold-nanotube membranes. J. Am. Chem. Soc., 2002, 124(40), 11850-11851. http://dx.doi.org/10.1021/ja027494f PMID: 12358519
76. Jafari, S.M.; Katouzian, I.; Rajabi, H.; Ganje, M. Bioavailability and release of bioactive components from nanocapsules. Nanoen- capsulation Technologies for the Food and Nutraceutical Indus- tries; Jafari, S.M., Ed.; Academic Press: London, UK, 2017, pp. 494-523. http://dx.doi.org/10.1016/B978-0-12-809436-5.00013-6
77. Wei, H.C.; Lin, L. L. Antibacterial activity of liposome containing curry plant essential oil against Bacillus cereus in rice. J. Food Saf., 2017, 37, 12302. http://dx.doi.org/10.1111/jfs.12302
78. Mohammadi, A.; Hashemi, M.; Hosseini, S.M. Nanoencapsulation of Zataria multiflora essential oil preparation and characterization with enhanced antifungal activity for controlling Botrytis cinerea, the causal agent of gray mould disease. Innov. Food Sci. Emerg. Technol., 2015, 28, 73-80. http://dx.doi.org/10.1016/j.ifset.2014.12.011.
79. EFSA Scientific Committee. Scientific Opinion on Guidance on the risk assessment of the application of nanoscience and nanotechnologies in the food and feed chain. EFSA J., 2011, 9(5), 2140. http://dx.doi.org/10.2903/j.efsa.2011.2140
80. EFSA Scientific Committee. Scientific opinion of the Scientific Committee on a request from the European Commission on the potential risks arising from nanoscience and nanotechnologies on food and feed safety. EFSA J., 2009, 958, 1-39.

SECTION 2

CROSS-LINKED SYSTEMS FOR DRUG DELIVERY

Part A: Strategies for Hyaluronic Acid-Based Hydrogel Design in Drug Delivery.

Part B: Preparation, characterization and in vitro evaluation of resveratrol-loaded nanospheres potentially useful for human breast carcinoma.

Part C: Gelatin and Glycerine-Based Bioadhesive Vaginal Hydrogel.

Part D: Polysaccharides and proteins-based hydrogels for tissue engineering applications

PART A

Strategies for Hyaluronic Acid-Based Hydrogel Design in Drug Delivery

Abstract

Hyaluronic acid (HA) is a natural, linear, endogenous polysaccharide that plays important physiological and biological roles in the human body. Nowadays, among biopolymers, HA is emerging as an appealing starting material for hydrogels design due to its biocompatibility, native biofunctionality, biodegradability, non-immunogenicity, and versatility. Since HA is not able to form gels alone, chemical modifications, covalent crosslinking, and gelling agents are always needed to obtain HA-based hydrogels. Therefore, in the last decade, different strategies for the design of physical and chemical HA hydrogels have been developed, such as click chemistry reactions, enzymatic and disulfide crosslinking, supramolecular assembly via inclusion complexation, and so on. HA-based hydrogels turn out to be versatile platforms, ranging from static to smart and stimuli-responsive systems, and for these reasons, they are widely investigated for biomedical applications like drug delivery, tissue engineering, regenerative medicine, cell therapy, and diagnostics. Furthermore, the overexpression of HA receptors on various tumor cells makes these platforms promising drug delivery systems for targeted cancer therapy. The aim of the present review is to highlight and discuss recent advances made in the last years on the design of chemical and physical HA-based hydrogels and their application for biomedical purposes, in particular, drug delivery. Notable attention is given to HA hydrogel-based drug delivery systems for targeted therapy of cancer and osteoarthritis.

Keywords: hyaluronic acid; hydrogel; cancer; drug delivery; click chemistry; biomaterial

1. Introduction

Hydrogels are three-dimensional, hydrated polymeric networks, formed by crosslinked hydrophilic polymers with a high affinity for water and biological fluids, capable of absorbing from 10% up to thousands of times their dry weight in water [1]. In recent years, thanks to their unique properties such as biocompatibility, biodegradability, flexibility, softness, etc., hydrogels have been widely investigated for biomedical applications like cell therapy, tissue engineering, drug delivery, and diagnostics [2]. For example, hydrogels made of pectin, carboxymethylcellulose and propylene glycol or polyethylene glycol (PEG) and propylene glycol are used as wound dressings [3,4], keratin- or polyvinyl alcohol-based hydrogels as scaffolds for cell growth [5,6], PEG-based hydrogel (DEXTENZA®), recently approved by the Food and Drug Administration, as ophthalmic inserts, etc. [7]. Among biopolymers, hyaluronic acid (HA) represents one of the most used in the design of hydrogels for biomedical applications due to its biocompatibility, native biofunctionality, biodegradability, non-immunogenicity, and versatility. HA is a natural linear polysaccharide that consists of alternating units of d-glucuronic acid and *N*-acetyl-d-glucosamine, connected by β-1,3- and β-1,4-glycosidic blonds. HA is a non-sulfated glycosaminoglycan that is widely found in the epithelial and connective tissues of vertebrates, and it is the major component of the extracellular matrix (ECM) [8]. It is synthesized by hyaluronan synthase at the plasma membrane, and it is then extruded to the extracellular matrix [9]. HA is found in a wide range of molecular weights from 20,000 up to several million Daltons, depending on the enzyme that catalyzes its synthesis. Around 30% of HA present in the body is rapidly degraded by hyaluronidases and oxidative species, while the remaining 70% is catabolized by liver and lymphatic vessels endothelial cells, with tissue half-lives going from minutes in the bloodstream to weeks in cartilage [10]. Upon physiological conditions, HA is a polyanion associated with extracellular cations (Na+, Ca2+, Mg 2+, K+) known as hyaluronan [11]. HA important physiological and biological roles in the human body. In the extracellular matrix of most tissues it contributes to maintain the tissue's mechanical integrity, homeostasis, viscoelasticity and lubrication thanks to its high molecular weight and its capacity to absorb a high quantity of water [12]. Furthermore, it also plays an important role in intracellular functions; in fact, it is able to regulate, due to its binding to cell surface specific receptors (such as CD44 or RHAMM), cell adhesion, migration, proliferation, and differentiation

and, consequently, processes like inflammation, wound healing, tissue development, morphogenesis, tumor progression, and metastasis [13].

For these reasons, in recent years, hydrogels built from HA have been developed and investigated for biomedical applications like tissue regeneration, tissue engineering, drug delivery, gene therapy, diagnostics, etc. Nowadaybs several HA-based hydrogels are already used in medicine as dermal fillers, viscosupplements, wound dressings, etc., and the market is continuously increasing worldwide. They are now progressing in their design to be responsive to several triggers, to have various features like stability, complex structures, and biochemical cues. The aim of the present review is to highlight and discuss recent advances made in the last years on the design of chemical and physical HA-based hydrogels and their application for biomedical purposes drug delivery.

2. Physical and Chemical Hydrogels

Hydrogels can be classified into “physical” and “chemical” gels, depending on the type of bond that is formed between the polymer chains from which they derive. Hydrogels are called “reversible” or “physical” if the networks are formed as a result of weak physical interactions between the macromolecular chains such as ionic, H-bonding, Van der Waals interactions, hydrophobic forces, or molecular entanglements [14]. Physical hydrogels can be synthesized by warming or cooling polymer solution, mixing solution of polyanion and polycation, combining polyelectrolyte with multivalent ions of opposite charge, etc. [1]. Physical hydrogels are often heterogeneous, unstable, and reversible; in fact, they are not able to maintain their structural integrity and dissolve easily by changing environmental factors like temperature, pH, etc. Instead, hydrogels are called “permanent” or “chemical” if the polymeric chains are connected by covalent bonds [15]. For this reason, these materials, after swelling, retain their structural integrity, even if it is possible a degradation when particular bonds, sensitive to chemical or enzymatic hydrolysis, are present in the structure. Chemical hydrogels can be generated by crosslinking polymers with radiations, chemical crosslinkers, polyfunctional compounds, free radical generating compounds, etc. [1]. Consequently, these systems have a better chemical, mechanical, and thermal stability compared to physical hydrogels. Even though HA, due to its conformation and molecular weight, can form molecular networks in solution, it is not able to form physical gel alone. For this reason, chemical modifications, covalent crosslinking, and gelling agents are needed to obtain HA hydrogels.

HA turns out to be a functional and suitable polymer for chemical modification with reactive species due to its chemical structure; in particular, the chemical modifications concern three functional groups: the carboxylic acid group, the hydroxyl group, and the amino group (after deacetylation) [16]. This section reviews the different modified HA macromers and chemical techniques described in the literature in the last years used for the design of physical and chemical HA-based hydrogels.

2.1 Chemical Hydrogels

Chemical crosslinking turns out to be a versatile method to obtain hydrogels with excellent chemical, mechanical and thermal stability. However, this approach presents some limitations like the use of metal catalysts, photoinitiators, low reaction yield, etc. [17]. Regarding the chemical approach, HA-based hydrogels can be obtained via condensation reactions, enzymatic crosslinking, disulfide crosslinking, click chemistry, polymerization, etc. HA can be directly crosslinked by divinyl sulfone [18], glutaraldehyde [19], carbodiimide [20], bisepoxide [21], etc.; however, direct crosslinking cannot be considered suitable for hydrogels design since it requires harsh reaction condition, toxic by-products can be formed and the crosslinking agents used are cytotoxic. Nowadays, one of the most promising strategies for hydrogels preparation turns out to be click chemistry due to its high specificity, high yield, bioorthogonality, and mild reaction conditions [22].

2.1.1 Diels Alder Reaction (Click Chemistry)

In recent years, a particular interest has been addressed to the Diels–Alder reaction between furan and maleimide moieties for hydrogels design due to its selectivity, efficiency, and thermoreversibility [23].In this regard, Fisher *et al.* recently developed a HA-based hydrogel with tunable properties to use as a platform to investigate breast cancer cells invasion. The hydrogel was obtained via a Diels–Alder click reaction between furan modified HA and bismaleimide functional peptides with the aim of mimicking ECM [24]. A similar approach was reported by Yu et al. in order to obtain a 3D patterned hydrogel. In this work Diels–Alder click chemistry has been used in order to get a HA-based hydrogel that can be subsequently subjected to thiol-ene photocoupling allowing its spatiotemporal patterning [25].

2.1.2 Azide-Alkyn Huisgen Cycloaddition (Click Chemistry)

The Huisgen reaction is a cycloaddition between an azide and an alkyne to produce triazoles which requires the presence of a catalyst (Cu+) as reported by Rostovtsev et al. [26]. In recent years it has become one of the most used strategies for hydrogels preparation thanks to its high yield, efficiency, excellent bioorthogonality, fast reaction rate, etc. [27,28]. For example, Manzi et al. fabricated nanohydrogels based on derivatives of HA and riboflavin obtained by Cu+ catalyzed Huisgen cycloaddition [29]. Despite the various advantages offered by this reaction, the use of copper as a catalyst can be problematic since it is a cytotoxic element. However, recently, it has been observed that cyclooctyne functionalized molecules are able to react rapidly with azide without the presence of copper [30]. This alternative reaction, called strain-promoted azide-alkyne cycloaddition, is currently more used for hydrogels design since it presents biosafety as well as the advantages of the previous reaction. On this matter, Fu et al. fabricated an injectable HA-PEG based hydrogel [31]. In particular, cyclooctyne modified HA was synthesized by reacting HA with 2-(aminoethoxy) cyclooctyne (Figure 1); subsequently, it was reacted with azide functionalized PEG in order to obtain the hydrogel. Interestingly, the resulting hydrogel showed fast gelation time, excellent mechanical properties, and high stability.

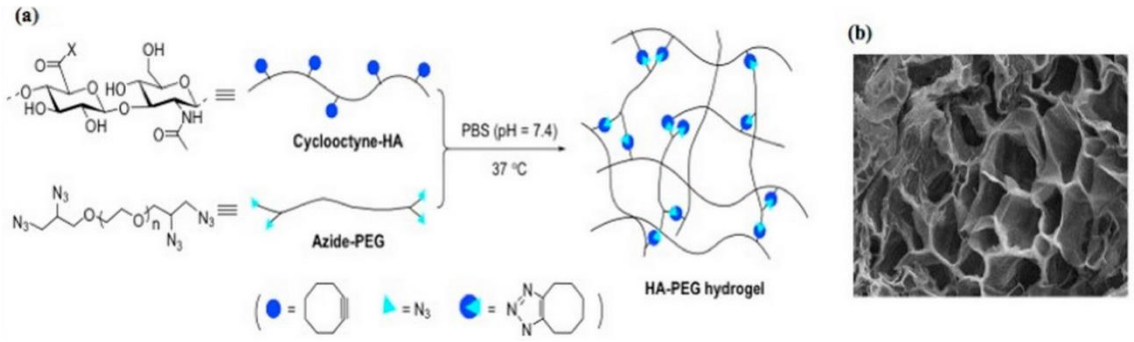

Figure 1. Preparation of the HA-PEG hydrogel (**a**), SEM image of the hydrogel (**b**) [31]. Reproduced with permission from Elsevier, 2017

2.1.3 Thiol-ene Photocoupling (Click Chemistry)

The thiol-ene reaction consists of a radical addition (induced by light) between a thiol and enes which has a high yield, efficiency, specificity, and a fast reaction rate [32]. This method is particularly attractive for hydrogels preparation because it is solvent free and allows the hydrogels spatiotemporal control; for this reason, it is particularly investigated for the design of hydrogels to use as scaffolds for tissue engineering and cell culture or as drug delivery systems [33,34]. Different vinyl groups are employed for thiol-ene click chemistry like norbornene [35], vinyl sulfone [36], maleimide, etc. The thiol-norbornene reaction is characterized by greater specificity compared to the use of other functional groups. For example, Gramlich et al. employed this method for the synthesis of a photopatterned HA-based hydrogel by reacting norbornene modified HA (NorHA) with dithiothreitol (Figure 2) [37]. Hydrogels with an elastic modulus ranging from 1000 Pa to 70,000 Pa were obtained by varying the quantity of crosslinker. Furthermore, they reported that a secondary thiol-norbornene reaction can be performed to the hydrogel by reducing the initial amount of crosslinker.

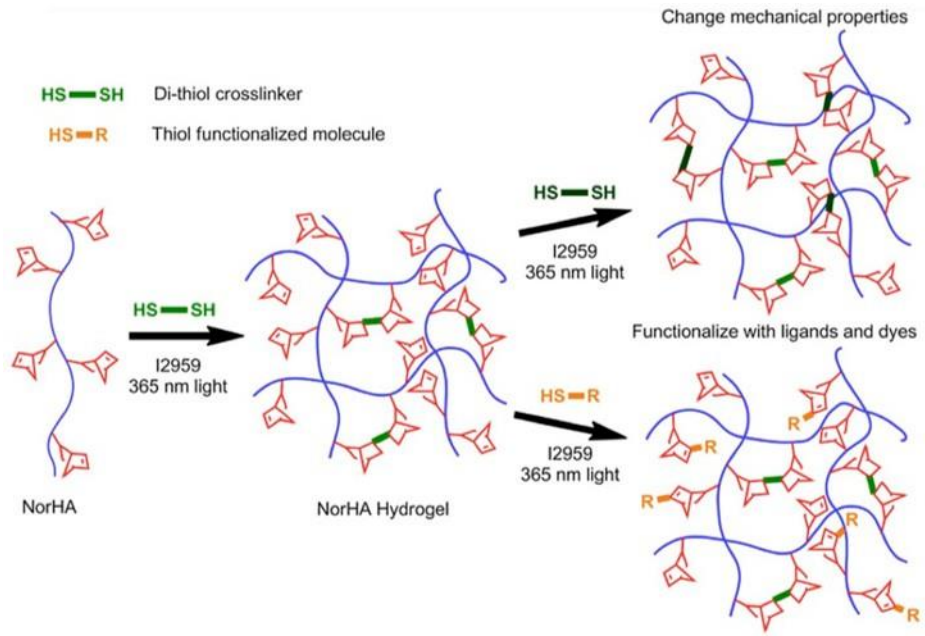

Figure 2. Synthesis scheme of hydrogel [37]. Reproduced with permission from Elsevier, 2013.

In this context, we also find the thiol-Michael addition which, however, is characterized by lower orthogonality. In this regard, Khetan et al. designed and prepared a 3D hydrogel via a two step crosslinking process: firstly, via a thiol-Michael addition between methacrylate-maleimide functionalized HA and thiols of peptides and, subsequently, via methacrylates photopolymerization [38].

2.1.4 Aldehyde-Hydrazide Coupling (Click Chemistry)

The aldehyde-hydrazide reaction has currently attracted interest in hydrogels design due to its high efficiency, cytocompatibility, simplicity, reversibility, and mild reaction conditions [39–41]. In particular, covalent hydrazone crosslinked hydrogels seem to be a promising approach for tissue engineering. In this regard, Chen et al. recently developed an injectable HA-pectin based hydrogel, by reacting HA adipic dihydrazide with biofunctionalized pectin-dialdehyde, and investigated its use as a scaffold for cartilage tissue engineering (Figure 3) [42]. Interestingly, the resulting hydrogel exhibited a fast gelation rate, good mechanical properties, biocompatibility, and cytocompatibility that make it a potential platform suitable for tissue regeneration. To further improve the structural integrity of hydrazone crosslinked hydrogels, Wang et al. recently reported the design and the preparation of an elastin-like protein/HA-based hydrogel by combining two different crosslinking processes (covalent and thermal) [43]. Firstly, the hydrogel was obtained via an aldehyde-hydrazide coupling between hydrazine modified elastin-like protein and aldehyde modified HA; the use of a thermoresponsive protein allowed a secondary thermal crosslinking that improved its structural integrity and stability. The resulting hydrogel showed shear-thinning and self-healing properties, easy injectability and protection of cells from the mechanical stress of injection and for these reasons can be considered a promising candidate for stem cells delivery.

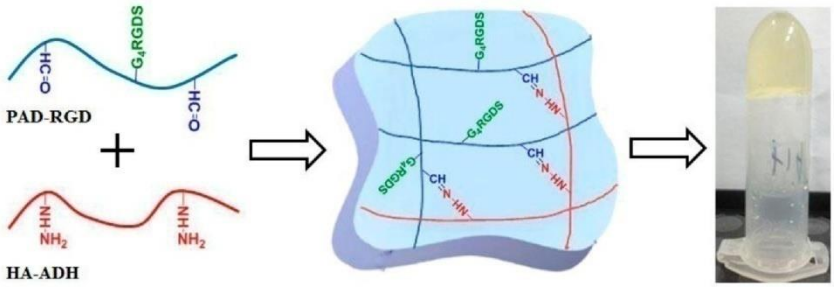

Figure 3. Hydrogels synthetic scheme [42]. Reproduced with permission from Elsevier, 2017.

2.1.5 Enzymatic Crosslinking

Enzymatic crosslinking represents an interesting approach for HA-based hydrogels preparation because it is characterized by mild reaction condition, fast gelation rate and leads to obtaining hydrogels with excellent mechanical properties [44,45]. Among different enzymes, horseradish peroxidase (HRP) turns out to be one of the most employed; it is usually employed in combination with hydrogen peroxide and the reaction can be summarized as follows: $2Ph + H_2O_2 \rightarrow 2Ph\cdot + H_2O$ [46]. In literature are reported various tyramine modified HA-based hydrogels which are formed as a result of an enzymatic crosslinking process that occurs through oxidation of tyramine which causes the formation of di-tyramine bonds [47]. In this regard, Xu et al. designed and fabricated HA-tyramine hydrogels by crosslinking tyramine moieties of HA in the presence of HRP and hydrogen peroxide (Figure 4) [48]. By varying the amounts of the enzyme and hydrogen peroxide, hydrogels with different mechanical strength were formed and were investigated in order to obtain a stable scaffold for stem cells culture. Interestingly, it was observed that the hydrogel with an elastic modulus of 350 Pa supported the proliferation of stem cells. A similar approach was reported by Raia et al. that enzymatically crosslinked tyramine functionalized HA and silk fibroin in order to increase the mechanical strength and the stability of tyramine-HA-based hydrogels [49]. By changing polymers concentration, hydrogels with tunable properties were obtained, resulting in versatile platforms that can be employed for various applications in tissue engineering.

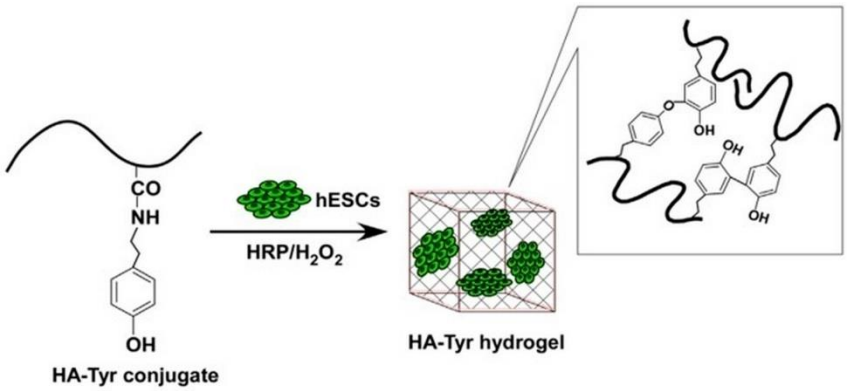

Figure 4. Schematic representation of hydrogels preparation and of encapsulation of human embryonic stem cells (hESCs) [48]. Reproduced with permission from Elsevier, 2015

2.1.6 Disulfide Crosslinking

In the last years, disulfide crosslinked hydrogels have attracted growing attention because this crosslinking method presents various advantages such as biosafety, ease of execution, reversibility and permits to obtain hydrogels with *in-situ* gelation properties and responsiveness to reductant stimuli. Generally, disulfide bonds are formed via oxidation of thiols induced by air or oxidating agents like Cu (II)SO_4 [50]. Disulfide crosslinked HA hydrogels are currently investigated for tissue regeneration thanks to their degradability since they can be cleaved enzymatically by hyaluronidase and by physiological reductants like glutathione and cysteine [51]. For example, Bian et al. proposed self-crosslinking HA-based hydrogels as scaffolds for cell culture (Figure 5) [52]. They were prepared through exposition to air of different thiolated HA derivatives which were obtained by varying the degree of thiol substitution and molecular weights of HA. Gelation rate, mechanical properties, swelling degree, and degradation were investigated, and the resulting hydrogel showed excellent biocompatibility, degradation behavior and, consequently, a great potential for applications in tissue engineering.

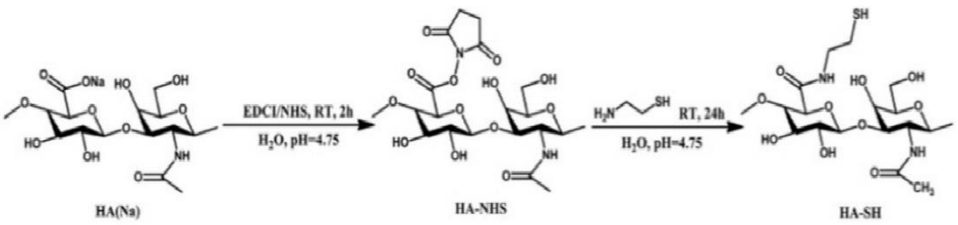

Figure 5. Synthesis scheme of thiol modified HA [52]. Reproduced with permission from Elsevier, 2016.

However, disulfide crosslinking presents some disadvantages like long reaction times, the presence of strong oxidants, etc. To overcome these limitations, an interesting strategy for disulfide crosslinked HA hydrogels preparation has been recently proposed by Velasco et al. [53]. Herein, the authors investigated the effects of the presence of various electron-withdrawing groups at the β position of thiol modified HA (cysteine, *N*-acetyl-l-cysteine). Interestingly, HA functionalized with cysteine or *N*-acetyl-l-cysteine showed fast gelation rate at physiological pH, while HA-thiol did not form any gel in the same conditions. Furthermore, the resulting hydrogels showed excellent mechanical properties and hydrolytic stability.

2.1.7 Crosslinking by Radical Polymerization

Hydrogels can be formed via radical polymerization of monomers in the presence of crosslinking agents and an initiator like a redox pair or a photoinitiator [54]. Methacrylates represent the most common groups used for HA-based hydrogels preparation and they can be introduced to HA by reacting it with glycidyl methacrylate or methacrylic anhydride [55,56]. An advantage of methacrylated HA-based hydrogels is that it is possible to tune their properties by varying HA molecular weight, the concentration of the functional monomer, the degree of substitution, etc. [57]. In this regard, Tavsanli et al. developed silk/HA-based hydrogels and investigated their mechanical properties [58]. The hydrogels were prepared by reacting methacrylated HA (MeHA) and silk fibroin (SF) in aqueous solution in the presence of *N*,*N*,*N*j,*N*j-tetramethylethylenediamine (TEMED), ammonium persulfate (APS), and *N*,*N*-dimetylacrylamide (DMMA) which has the function of connecting methacrylated HA macromers via their vinyl groups (Figure 6). Interestingly, the resulting hydrogels showed bicompatibility, excellent mechanical properties and stability thanks to the presence of SF since its β-sheet domains act as physical crosslinks.

(a)

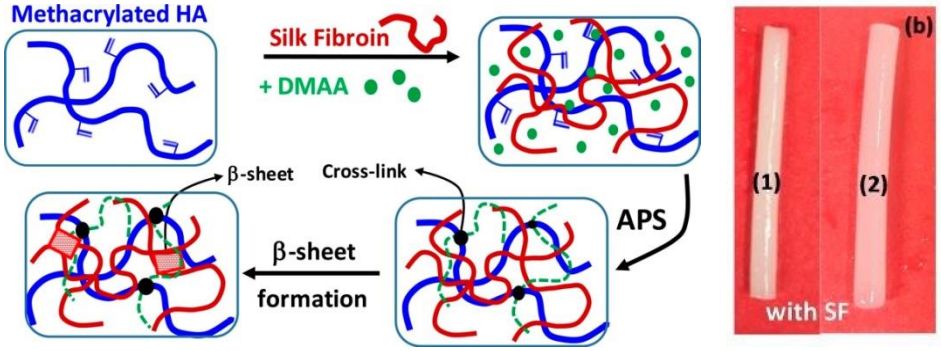

Figure 6. Schematic formation of HA-SF based hydrogel (**a**) and photographs of hydrogels with SF (**b**) [58]. Adapted with permission from Elsevier, 2019.

2.1.8 Crosslinking by Condensation Reactions

Condensation reactions are often applied for hydrogels synthesis. Considering the chemical structure of HA, among the different condensation reactions, esterification turns out to be one of the most employed for hydrogels design. In this regard, Larrañeta et al. recently developed an attractive eco-friendly strategy for the synthesis of HA-based hydrogels [59]. For this purpose, Gantrex S97 was used as crosslinking agent and the hydrogels were obtained via esterification between the hydroxyl groups of HA and the carboxylic groups of Gantrex S97 (Figure 7). Since the reaction takes place in solid phase inside a microwave or an oven, the process can be considered green because it does not need organic solvents or toxic substances. Furthermore, the release capabilities and the antimicrobial properties were investigated. Interestingly, the resulting hydrogel showed a sustained release and anti-infective properties resulting in a promising candidate for the design of drug delivery systems and wound dressings.

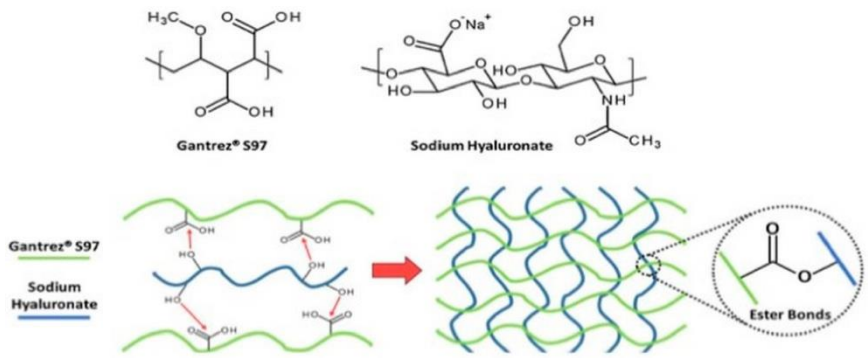

Figure 7. Schematic crosslinking mechanism between sodium hyaluronate and Gantrez® S97 [59]. Reproduced with permission from Elsevier, 2018.

2.2 Physical Hydrogels

In recent years, non-covalent bonds and supramolecular interactions have been widely investigated for hydrogels design thanks to their singular features. First of all, since these interactions are reversible, the non-covalent assembly allows to obtain hydrogels with tunable properties and responsivity to various cues like light, pH, temperature, etc. [60,61]. In contrast to covalent crosslinking, physical crosslinking leads to the formation of less mechanically and chemically stable hydrogels. However, this aspect can be considered an advantageous feature since it can be exploited to obtain hydrogels with shear-thinning and self-healing properties [17]. In this context, inclusion complexation represents one of the most used strategies for the preparation of physical gels. It can be considered the result of supramolecular interactions and structural complementarity between two molecules called "host" and "guest" [62]. Cyclodextrins are one of the most widely employed hosts which have hydrophobic cavities with a high affinity for hydrophobic guests. Several guest molecules employed in pair with cyclodextrins have been reported in literature and among these the most representative is adamantane. In this regard, Rodell et al. designed a self-assembling HA hydrogel based on supramolecular interactions between adamantane functionalized HA and β-cyclodextrin functionalized HA [63]. Hydrogel formation occurred rapidly by mixing host and guest molecules in aqueous solution. Physical properties were investigated, and it has been observed that were dependent on the crosslink density and structure that can be modified by varying host and guest concentrations, molar ratio, etc. The obtained hydrogel displayed shear-thinning properties resulting in a promising injectable system. Another investigated pair for inclusion complexation broadly reported in literature is represented by α- or β-cyclodextrin and azobenzenes since *trans*-azobenzene has a high binding affinity for α- or β-cyclodextrin, while *cis*-azobenzene has a low binding affinity for them. On this subject, Rosales et al. recently developed a supramolecular HA-based hydrogel using HA functionalized with β-cyclodextrin and azobenzene [64]. It has been shown that it is possible to modulate hydrogel properties with light; in fact, upon irradiation (λ = 365 nm), isomerization of azobenzene occurs changing the binding affinity between host/guest molecules and, consequently, the network connectivity and the elastic modulus of the hydrogel. Furthermore, the release capabilities were investigated, highlighting the possibility to tune drugs release profile with light exposure. A similar approach was reported by Rowland et

al. using cucurbit [8] uril and cysteine-phenylalanine as host/guest pair to obtain a supramolecular HA-based hydrogel [65]. Another interesting non-covalent approach for HA-based hydrogels design is represented by functionalization of HA with hydrophobic molecules to render it amphiphilic and consequently determine the macromers self assembly in nanogels. In this regard, Montanari et al. designed HA-based hydrogels via self-assembly of macromers in water after the functionalization of HA with cholesterol [66]. In particular, the self-assembly of macromers occurs due to the hydrophobic interactions between the cholesterol cores and the hydrophilic interactions between the shells formed by HA. Moreover, the use of gelling agents in combination with HA can be considered a valid strategy for HA physical hydrogels design. For example, Jung et al. recently reported the preparation of a thermosensitive hydrogel based on HA and Pluronic F-127 [67]. Pluronic F-127 is a triblock copolymer able to form rapidly thermoresponsive hydrogels which, however, are unstable in physiological conditions due to their low mechanical strength. To overcome this problem, in this study HA was mixed with Pluronic F-127 in water to obtain a hydrogel with improved structural integrity and stability due to the hydrophobic interactions that occur between acetyl groups of HA and methyl groups of Pluronic F-127. Interestingly, the resulting hydrogel not only showed an increased mechanical strength but also a sustained drug release, reducing the typical burst release observed in Pluronic F-127-based hydrogels.

3. HA-Based Hydrogels for Biomedical Applications

Currently, HA-based hydrogels are widely investigated for biomedical purposes like drug delivery, tissue engineering, regenerative medicine thanks to their biocompatibility, biodegradability, non–immunogenicity, responsivity to various cues, and tunable properties [68–70]. This section reviews the main biomedical applications of HA-based hydrogels reported in literature in the last few years, focusing on drug delivery.

3.1 Drug Delivery

HA-based hydrogels are particularly interesting for drug delivery since, in addition to above cited features, allow to have a controlled and targeted drug release in response to different triggers that turns out to be attractive when aiming for targeted therapy [71,72].

3.1.1 Stimuli-Responsive Hydrogels

Various smart hydrogels responsive to different environmental factors such as pH, temperature, light, biochemical molecules have been developed as drug delivery systems. Regarding stimuli-responsive platforms, physical crosslinking is preferred since supramolecular interactions are reversible and consequently results easier to tune hydrogels properties. In this context, Highley et al. recently proposed an interesting strategy for the design of a near infrared light (NIR)/temperature responsive platform [73]. In this study, the platform was prepared in a microfluidic mixing device by combining gold nanorods with a HA supramolecular hydrogel obtained via the inclusion complexation of β-cyclodextrin and adamantin. The presence of nanorods caused heating in response to NIR irradiation causing consequently the breakage of supramolecular interactions and the networks disruption. The release capability of the resulting platform in response to different NIR exposures was evaluated, and interestingly it has been observed that the drug release can be modulated by varying two parameters: irradiation time, and light intensity; specifically, the quantity of the molecule released from the platform increased with increasing power and irradiation time. Inclusion complexation employing azobenzene/cyclodextrin as host/guest pair has been broadly investigated for photoresponsive hydrogels design since the supramolecular host/guest interactions can be disrupted upon *trans-cis* photoisomerization of azobenzene induced by ultraviolet (UV) light [74].

An interesting example of a photoresponsive drug delivery platform has been described by Rosales et al. [64]. Thus, HA was functionalized with azobenzene and β-cyclodextrin to obtain self-assembled hydrogels. The resulting hydrogels showed reversible changes in crosslink density and, consequently, in mesh size, upon UV exposures. These changes were exploited to modulate drug release profiles and, therefore, the release capability upon different UV irradiations was evaluated. In particular, a fluorescently labeled protein was loaded as a model drug and it has been observed that upon irradiation hydrogels released a double amount of protein compared to the non irradiated ones. Even if physical crosslinking is preferred for smart hydrogels preparation, also the chemical approach has been recently investigated. In this regard, Kwon et al. reported the preparation of pH-sensitive hydrogels based on hydroxyethyl cellulose and hyaluronic acid and investigated their potential use as transdermal delivery systems for the treatment of skin lesions [75].

In this study, the hydrogels were synthesized via Michael addition between HA and hydroxyethyl cellulose by using divinyl sulfone as crosslinking agent and their physicochemical properties were investigated. Hydrogels were then loaded with isoliquiritigenin, which has antimicrobial activity, and its release efficiency has been investigated by in vitro measurements at different values of pH. Experimental data showed that the quantity of isoliquiritigenin released increased with increasing pH beyond 7 due to electrostatic repulsions between the carboxylate groups of HA that cause consequently an increase of mesh size.

3.1.2 HA-Based Hydrogels for Targeted Cancer Treatment

As already reported, HA regulates different cellular functions such as cell adhesion, differentiation, migration, proliferation, etc., which arise as a result of HA binding to specific membrane surface receptors, called hyaldherins, like CD44, LYVE-1, and RHAMM [76]. In particular, CD44 is the main receptor involved in cellular proliferation, differentiation, and migration pathways and consequently in tumor progression and metastasis; moreover, it is overexpressed in various types of tumors like melanoma, chondrosarcoma, breast, gastrointestinal, prostate, bladder, lung, and pancreatic cancers, and different studies have reported a relationship between CD44 expression and poor prognosis [77]. For these reasons, HA has recently emerged as a promising molecule for the design of anticancer drug delivery systems for active targeting of malignant tumors [78]. Comprehensive reviews by Huang et al. and Choi et al. supply an interesting description of HA-based drug delivery systems developed for targeted cancer treatment [79,80]. In the last years, several HA-based hydrogels have been studied for the delivery of different antitumor drugs such as doxorubicin, paclitaxel, cisplatin, etc., in order to improve their antitumor activity and reduce their systemic side effects [81,82]; some of the most interesting and recent examples will now be presented. Aiming at preparing a suitable drug delivery platform for the targeted release of doxorubicin, Yang et al. prepared various HA-based nanogels via copolymerization of methacrylated HA with di (ethylene glycol) diacrylate [83]. Nanogels with a diameter of about 70 nm and a spherical shape were obtained, which were then loaded with doxorubicin by an incubation method. In vitro studies showed a CD44-dependent cellular uptake and consequently a greater internalization of nanogels in tumor cell lines that overexpress CD44 receptor (Figure 8).

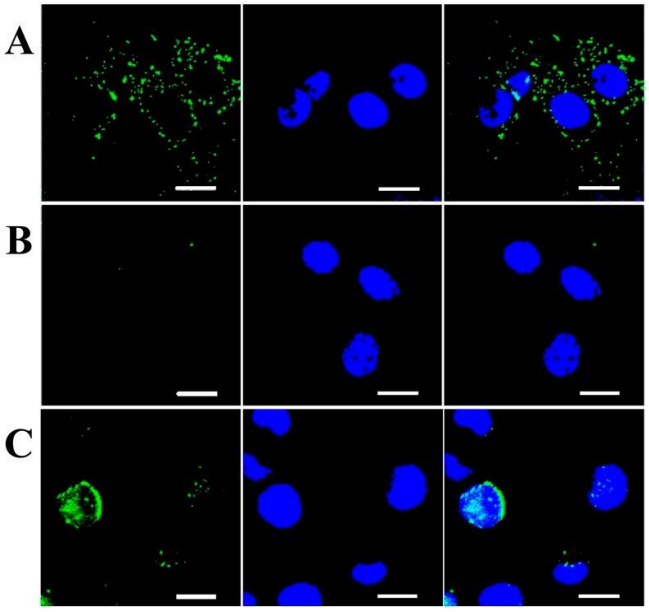

Figure 8. Confocal laser scanning microscopy of (**a**) A549, (**b**) NIHT3T, and (**c**) H22 cells incubated with FITC-labeled HA nanogels [83], The scale bar =10μm. Reproduced with permission from Elsevier, 2015.

Furthermore, the nanogels showed higher accumulation in the tumor site and a superior antitumor activity compared with the free doxorubicin, resulting in a promising drug delivery system for cancer therapy. A noteworthy further example of doxorubicin delivery platform has been reported by Jhan et al. [84]. In this study, injectable thermosensitive hydrogels based on Pluronic F-127 and HA-doxorubicin nanocomplexes were prepared via physical mixing and their physiochemical properties were investigated. The doxorubicin release profile was studied in vitro, while nanogels antitumor activity both in vivo and in vitro. Experimental data showed a pH sensitive and sustained release of doxorubicin from hydrogels with a faster release rate at tumoral pH. Moreover, hydrogels showed an excellent cytotoxic activity against tumor cell lines that overexpress CD44 receptor and a high affinity targeting to the lymphonodes, resulting in promising injectable formulations for the treatment of local and metastatic tumors.

Furthermore, in this context, an efficient approach for metastatic breast cancer treatment has been recently described by Chen et al. [85]. In particular, the authors prepared saporin loaded epidermal growth factor receptor (EGFR) and CD44 dual targeted HA nanogels by combining inverse nanoprecipitation and tetrazole-alkene photocoupling. Nanogels with a diameter of about 160 nm and a spherical shape were obtained and evaluated for the treatment of metastatic breast cancer. In vitro studies showed an excellent internalization of nanogels in 4T1 breast cancer cell line that overexpresses both EGFR and CD44. Furthermore, in vivo studies in metastatic 4T1-luc breast tumor bearing mice displayed that the nanogels enhanced the therapeutic efficacy of saporin, showing an excellent inhibition of tumor growth and lung metastasis. Currently intraperitoneal (IP) chemotherapy is emerging as an efficient strategy for the treatment of solid tumors present in the peritoneal cavity [86].

However, the delivery systems suitable for the IP chemotherapy should have some requirements like biocompatibility, biodegradability, non-immunogenicity, and the capacity to control the drug release. Since HA hydrogels have these features, they are now also studied for the design of drug delivery platforms for IP chemotherapy. In this regard, Cho et al. recently reported the design of in situ crosslinkable HA-based gels and evaluated their potential use as IP carriers of platinum for the treatment of ovarian cancer [87]. Firstly, they prepared platinum loaded nanoparticles that were incorporated in HA-based hydrogels obtained via the aldehyde-hydrazide coupling. The obtained platforms showed sustained platinum release, good anti-tumor activity and a long permanence in the peritoneal cavity resulting attractive for IP chemotherapy of ovarian cancer. Unfortunately, one problem that can occur sometimes when using hydrogels as drug delivery systems is the burst release [88]; with the attempt to reduce the burst release of drugs from hydrogels, Zhang et al. proposed an innovative strategy for HA-based hydrogels design [89].

In this regard, they prepared multilayer hydrogel capsules based on chitosan, HA and doxorubicin via the ionotropic crosslinking method. Release studies concerning these hydrogels showed a pH-sensitive, controlled release of doxorobucin with a notable reduction of the burst release due to their particular structure; in fact, the multilayer structure reduced the drug concentration gradient between the capsules external layer and the surrounding environment limiting the release of doxorubicin adsorbed on the surface of the hydrogels.

3.1.3 HA-Based Hydrogels for Osteoarthritis Treatment

Osteoarthritis is an inflammatory, chronic joint disorder characterized by progressive cartilage erosion. Currently, osteoarthritis treatment is limited to anti-inflammatory drugs administration, viscosupplementation and, if necessary, prosthesis graft at the last stage [90].

As already reported, HA performs multiple biological functions: at the articular level, thanks to its viscoelasticity, it acts as a lubricant, increasing the viscosity of the synovial fluid, and as a cushioning, allowing the separation of the articular surfaces under load. HA presents also chondroprotective and anti-inflammatory effects [91]. Furthermore, some studies reported the overexpression of CD44 receptor on human articular chondrocytes [92]. For these reasons, HA-based hydrogels are widely investigated and used as viscosupplements and delivery platforms for osteoarthritis treatment. In this regard, Jung et al. recently reported the preparation of an injectable thermosensitive hydrogel via physical mixing of HA and Pluronic F-127 [67]. As previously reported, Pluronic F-127 is a gelling agent able to rapidly form thermoresponsive hydrogels that however are instable in physiological conditions due to their low mechanical strength. To overcome this problem, in this study, HA was physically mixed with Pluronic F-127 in order to obtain a hydrogel with improved structural integrity and stability due to the hydrophobic interactions that occur between HA and Pluronic. The hydrogel was then loaded with piroxicam and evaluated for the treatment of osteoarthritis. In Vitro release studies showed 10 days sustained and slow release of piroxicam from HA-Pluronic F-127 hydrogel, while Pluronic F-127 based hydrogels displayed a faster release behavior (Figure 9). Furthermore, in vivo pharmacokinetic studies reported an increase of drug bioavailability and half-life in comparison to a commercial Paclitaxel formulation.

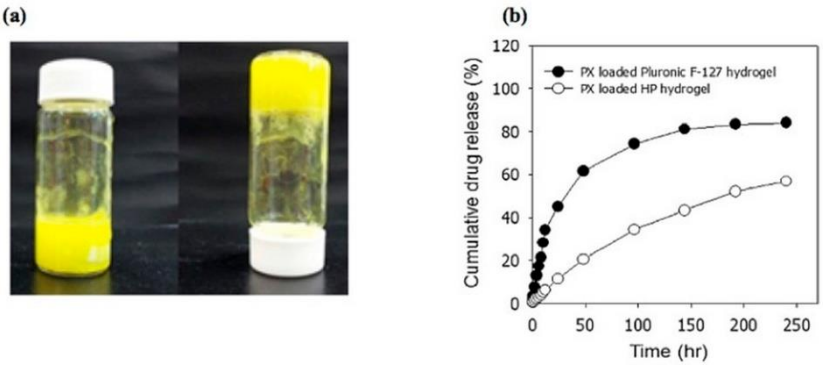

Figure 9. Photographs of the hydrogel (**a**) and in vitro Paclitaxel release from Pluronic F-127 and Pluronic F-127/HA-based hydrogels (**b**) [67]. Reproduced with permission from Elsevier, 2016.

In addition to the classical therapeutic approaches, nowadays gene silencing of signal molecules, proteins, enzymes, that play an important role in osteoarthritis degenerative events, is emerging as a promising strategy for osteoarthritis treatment.In this regard, Cai et al. recently developed a HA-based hydrogel loaded with gapmer antisense oligonucleotides that was studied for silencing target gene expression in osteoarthritis [93]. In particular, the hydrogel was prepared via Schiff reaction between aldehyde modified HA and chitosan, and subsequently, it was loaded with a gapmer oligonucleotide, obtaining a high encapsulation efficiency (~97%), to reduce COX-2 expression. In vitro studies showed a sustained release of COX-2 gapmer up to five days with a low burst release and, furthermore, a 10–14 days long COX-2 gene silencing activity in osteoarthritis chondrocytes. A similar approach was recently reported by Garcia et al. to obtain a HA-based hydrogel for the delivery of chondrocytes and antisense oligonucleotides [94]. In this case hydrogels made of HA and fibrin were loaded with an antisense oligonucleotide in order to modulate the expression of genes that codify for ADAMTS (A Disintegrin and Metallo Proteinase with Thrombospondin Motifs) enzymes which showed to play a key role in causing proteoglycans loss in osteoarthritis [95]; chondrocytes were also incorporated in the scaffolds in order to have both regenerative and therapeutic effects. In Vitro studies showed 14-day long sustained release and an efficient and long genes inhibition in both incorporated and resident chondrocytes. These features make this platform a potential formulation for osteoarthritis treatment.

4. Conclusions

In recent decades, HA has emerged as an attractive molecule for hydrogels design thanks to its biocompatibility, native biofunctionality, biodegradability, non-immunogenicity, and versatility. Nowadays, several HA-based hydrogels are already used in medicine as dermal fillers, viscosupplements, wound dressings, etc., and the market is continuously increasing worldwide. Since HA is not able to form gels alone, new crosslinking methods, like click chemistry reactions, disulfide crosslinking, enzymatic crosslinking, or supramolecular assembly methods like inclusion complexation, functionalization with lipophilic molecules, etc., have been widely investigated resulting in efficient strategies for chemical and physical hydrogels design. However, these current synthetic strategies present several advantages as well as some limitations. For example, various chemical crosslinking techniques often require organic solvents, metal catalysts, reaction by-product can be formed, etc. Thus, in this respect, research is aimed at developing new advantageous synthetic strategies. HA-based hydrogels turn out to be versatile platforms ranging from passive and static matrices to smart, stimuli-responsive platforms with tunable properties and consequently they showed to have great potential as drug delivery systems, scaffolds for tissue engineering and regenerative medicine, and so on. In particular, their tunability is exploited for the design of platforms for controlled and targeted drug delivery; in this regard, a notable attention is given to inclusion complexation employing cyclodextrin and azobenzene as a host/guest pair, which allows obtaining phototoresponsive drug delivery systems. Furthermore, since HA receptors were found to be overexpressed on various tumor cells and on chondrocytes, different HA-based hydrogels have been broadly developed for these purposes, showing promising results for targeted cancer and osteoarthritis therapies. Nowadays, one of the main goals is the design of intelligent hydrogels with various features like stability, complex structures, biochemical cues and responsive to several triggers that, surely, will find a place into clinical practice.

References

Trombino S.; Servidio C., Curcio F.; Cassano R. Strategies for Hyaluronic Acid-Based Hydrogel Design in Drug Delivery. *Pharmaceutics*, 2019, 12;11(8):407.

1. Hoffman, A.S. Hydrogels for biomedical applications. *Adv. Drug Deliv. Rev.* 2012, *64*, 18–23.
2. Seliktar, D. Designing cell-compatible hydrogels for biomedical applications. *Science* 2012, *336*, 1124–1128.
3. ConvaTec Website. Available online: https://www.convatec.it/ (accessed on 12 June 2019).
4. Covidien Website. Available online: https://www.covidien.com/ (accessed on 12 June 2019).
5. Blanchard, C.R.; Timmons, S.F.; Smith, R.A. Keratin-Based Hydrogel for Biomedical Applications and Method of Production. U.S. Patent 6,379,690 B2, 30 April 2002.
6. Kumar, A. Hydrogel scaffolds for tissue engineering. U.S. Patent 2013/0236971 A1, 12 September 2013.
7. Ocular Therapeutix Website. Available online: https://www.ocutx.com/products/dextenza/ (accessed on 12 June 2019).
8. Fraser, J.R.E.; Laurent, T.C.; Laurent, U. Hyaluronan: Its nature, distribution, functions and turnover. *J. Intern. Med.* 1997, *242*, 27–33
9. Prehm, P. Hyaluronate is synthesized at plasma membranes. *Biochem. J.* 1984, *220*, 597–600.
10. Fallacara, A.; Baldini, E.; Manfredini, S.; Vertuani, S. Hyaluronic acid in the third millennium. *Polymers* 2018,*10*, 701.
11. Laurent, T.C.; Fraser, J. Hyaluronan. *FASEB J.* 1992, *6*, 2397–2404.
12. Dicker, K.T.; Gurski, L.A.; Pradhan-Bhatt, S.; Witt, R.L.; Farach-Carson, M.C.; Jia, X. Hyaluronan: A simple polysaccharide with diverse biological functions. *Acta Biomater.* 2014, *10*, 1558–1570.
13. Toole, B.P. Hyaluronan: From extracellular glue to pericellular cue. *Nat. Rev. Cancer* 2004, *4*, 528.
14. Ahmed, E.M. Hydrogel: Preparation, characterization, and applications: A review. *J. Adv. Res.* 2015,*6*, 105–121.

15. Caló, E.; Khutoryanskiy, V.V. Biomedical applications of hydrogels: A review of patents and commercial products. *Eur. Polym. J.* 2015, *65*, 252–267.
16. Schanté, C.E.; Zuber, G.; Herlin, C.; Vandamme, T.F. Chemical modifications of hyaluronic acid for the synthesis of derivatives for a broad range of biomedical applications. *Carbohydr. Polym.* 2011, *85*, 469–489.
17. Appel, E.A.; del Barrio, J.; Loh, X.J.; Scherman, O.A. Supramolecular polymeric hydrogels. *Chem. Soc. Rev.*2012, *41*, 6195–6214.
18. Ibrahim, S.; Kang, Q.K.; Ramamurthi, A. The impact of hyaluronic acid oligomer content on physical, mechanical, and biologic properties of divinyl sulfone-crosslinked hyaluronic acid hydrogels. *J. Biomed. Mater. Res. Part A* 2010, *94*, 355–370.
19. Crescenzi, V.; Francescangeli, A.; Taglienti, A. New gelatin-based hydrogels via enzymatic networking. *Biomacromolecules* 2002, *3*, 1384–1391.
20. Kuo, J.W.; Swann, D.A.; Prestwich, G.D. Chemical modification of hyaluronic acid by carbodiimides.*Bioconj. Chem.* 1991, *2*, 232–241.
21. Segura, T.; Anderson, B.C.; Chung, P.H.; Webber, R.E.; Shull, K.R.; Shea, L.D. Crosslinked hyaluronic acid hydrogels: A strategy to functionalize and pattern. *Biomaterials* 2005, *26*, 359–371.
22. Jiang, Y.; Chen, J.; Deng, C.; Suuronen, E.J.; Zhong, Z. Click hydrogels, microgels and nanogels: Emerging platforms for drug delivery and tissue engineering. *Biomaterials* 2014, *35*, 4969–4985.
23. Gandini, A. The furan/maleimide Diels–Alder reaction: A versatile click–unclick tool in macromolecular synthesis. *Prog. Polym. Sci.* 2013, *38*, 1–29.
24. Fisher, S.A.; Anandakumaran, P.N.; Owen, S.C.; Shoichet, M.S. Tuning the microenvironment: Click-crosslinked hyaluronic acid-based hydrogels provide a platform for studying breast cancer cell invasion. *Adv. Funct. Mater.* 2015, *25*, 7163–7172.
25. Yu, F.; Cao, X.; Li, Y.; Chen, X. Diels–Alder click-based hydrogels for direct spatiotemporal postpatterning via photoclick chemistry. *ACS Macro Lett.* 2015, *4*, 289–292.
26. Rostovtsev, V.V.; Green, L.G.; Fokin, V.V.; Sharpless, K.B. A stepwise huisgen cycloaddition process: Copper (I)-catalyzed regioselective “ligation” of azides and terminal alkynes. *Angew. Chem. Int. Ed.* 2002, *41*, 2596–2599.

27. Pahimanolis, N.; Sorvari, A.; Luong, N.D.; Seppälä, J. Thermoresponsive xylan hydrogels via copper-catalyzed azide-alkyne cycloaddition. *Carbohydr. Polym.* 2014, *102*, 637–644.
28. Gong, T.; Adzima, B.J.; Baker, N.H.; Bowman, C.N. Photopolymerization reactions using the photoinitiated Copper (I)-Catalyzed Azide-Alkyne Cycloaddition (CuAAC) reaction. *Adv. Mater.* 2013, *25*, 2024–2028.
29. Manzi, G.; Zoratto, N.; Matano, S.; Sabia, R.; Villani, C.; Coviello, T.; Matricardi, P.; Di Meo, C. "Click" hyaluronan based nanohydrogels as multifunctionalizable carriers for hydrophobic drugs. *Carbohydr. Polym.* 2017, *174*, 706–715.
30. Laughlin, S.T.; Baskin, J.M.; Amacher, S.L.; Bertozzi, C.R. In vivo imaging of membrane-associated glycans in developing zebrafish. *Science* 2008, *320*, 664–667.
31. Fu, S.; Dong, H.; Deng, X.; Zhuo, R.; Zhong, Z. Injectable hyaluronic acid/poly (ethylene glycol) hydrogels crosslinked via strain-promoted azide-alkyne cycloaddition click reaction. *Carbohydr. Polym.* 2017, *169*, 332–340.
32. Hoyle, C.E.; Lee, T.Y.; Roper, T. Thiol–enes: Chemistry of the past with promise for the future. *J. Polym. Sci. Part A Polym. Chem.* 2004, *42*, 5301–5338.
33. Sawicki, L.A.; Kloxin, A.M. Design of thiol–ene photoclick hydrogels using facile techniques for cell culture applications. *Biomater.Sci.* 2014, *2*, 1612–1626.
34. Yang, C.; Mariner, P.D.; Nahreini, J.N.; Anseth, K.S. Cell-mediated delivery of glucocorticoids from thiol-ene hydrogels. *J. Controll. Release* 2012, *162*, 612–618.
35. Fairbanks, B.D.; Schwartz, M.P.; Halevi, A.E.; Nuttelman, C.R.; Bowman, C.N.; Anseth, K.S. A versatile synthetic extracellular matrix mimic via thiol-norbornene photopolymerization. *Adv. Mater.* 2009, *21*, 5005–5010.
36. Lutolf, M.; Hubbell, J. Synthetic biomaterials as instructive extracellular microenvironments for morphogenesis in tissue engineering. *Nat. Biotechnol.* 2005, *23*, 47.
37. Gramlich, W.M.; Kim, I.L.; Burdick, J.A. Synthesis and orthogonal photopatterning of hyaluronic acid hydrogels with thiol-norbornene chemistry. *Biomaterials* 2013, *34*, 9803–9811.
38. Khetan, S.; Guvendiren, M.; Legant, W.R.; Cohen, D.M.; Chen, C.S.; Burdick, J.A. Degradation-mediated cellular traction directs stem cell fate in covalently crosslinked three-dimensional hydrogels. *Nat. Mater.* 2013, *12*, 458.
39. Yan, S.; Wang, T.; Feng, L.; Zhu, J.; Zhang, K.; Chen, X.; Cui, L.; Yin, J. Injectable in situ self-cross-linking hydrogels based on poly (L-glutamic acid) and alginate for

cartilage tissue engineering. *Biomacromolecules* 2014, *15*, 4495–4508. Tian, W.; Zhang, C.; Hou, S.; Yu, X.; Cui, F.; Xu, Q.; Sheng, S.; Cui, H.; Li, H. Hyaluronic acid hydrogel as Nogo-66 receptor antibody delivery system for the repairing of injured rat brain: In vitro. *J. Controll. Release* 2005, *102*, 13–22.

40. Ito, T.; Fraser, I.P.; Yeo, Y.; Highley, C.B.; Bellas, E.; Kohane, D.S. Anti–inflammatory function of an in situ cross–linkable conjugate hydrogel of hyaluronic acid and dexamethasone. *Biomaterials* 2007, *28*, 1778–1786. Chen, F.; Ni, Y.; Liu, B.; Zhou, T.; Yu, C.; Su, Y.; Zhu, X.; Yu, X.; Zhou, Y. Self–crosslinking and injectable hyaluronic acid/RGD–functionalized pectin hydrogel for cartilage tissue engineering. *Carbohydr. Polym.* 2017, *166*, 31–44.
41. Wang, H.; Zhu, D.; Paul, A.; Cai, L.; Enejder, A.; Yang, F.; Heilshorn, S.C. Covalently adaptable elastin-like protein–hyaluronic acid (ELP–HA) hybrid hydrogels with secondary thermoresponsive crosslinking for injectable stem cell delivery. *Adv. Funct. Mater.* 2017, *27*, 1605609.
42. Kurisawa, M.; Lee, F.; Wang, L.S.; Chung, J.E. Injectable enzymatically crosslinked hydrogel system with independent tuning of mechanical strength and gelation rate for drug delivery and tissue engineering. *J. Mater. Chem.* 2010, *20*, 5371–5375. Tran, N.Q.; Joung, Y.K.; Lih, E.; Park, K.M.; Park, K.D. Supramolecular hydrogels exhibiting fast in situ gel forming and adjustable degradation properties. *Biomacromolecules* 2010, *11*, 617–625.
43. Roberts, J.J.; Naudiyal, P.; Lim, K.S.; Poole–Warren, L.A.; Martens, P.J. A comparative study of enzyme initiators for crosslinking phenol–functionalized hydrogels for cell encapsulation. *Biomater. Res.* 2016, *20*, 30. [CrossRef]
44. Rizzuto, F.; Spikes, J.D. The eosin-sensitized photooxidation of substituted phenylalanines and tyrosines. *Photochem. Photobiol.* 1977, *25*, 465–476. [CrossRef]
45. Xu, K.; Narayanan, K.; Lee, F.; Bae, K.H.; Gao, S.; Kurisawa, M. Enzyme–mediated hyaluronic acid–tyramine hydrogels for the propagation of human embryonic stem cells in 3D. *Acta Biomater.* 2015, *24*, 159–171.
46. Raia, N.R.; Partlow, B.P.; McGill, M.; Kimmerling, E.P.; Ghezzi, C.E.; Kaplan, D.L. Enzymatically crosslinked silk–hyaluronic acid hydrogels. *Biomaterials* 2017, *131*, 58–67.
47. Su, J. Thiol–mediated chemoselective strategies for in situ formation of hydrogels. *Gels* 2018, *4*, 72.

48. Choh, S.-Y.; Cross, D.; Wang, C. Facile synthesis and characterization of disulfide–cross–linked hyaluronic acid hydrogels for protein delivery and cell encapsulation. *Biomacromolecules* 2011, *12*, 1126–1136.
49. Bian, S.; He, M.; Sui, J.; Cai, H.; Sun, Y.; Liang, J.; Fan, Y.; Zhang, X. The self–crosslinking smart hyaluronic acid hydrogels as injectable three–dimensional scaffolds for cells culture. *Coll. Surf. B Biointerfaces* 2016, *140*, 392–402.
50. Bermejo-Velasco, D.; Azémar, A.; Oommen, O.P.; Hilborn, J.N.; Varghese, O.P. Modulating Thiol pKa promotes disulfide formation at physiological pH: An elegant strategy to design disulfide cross–linked hyaluronic acid hydrogels. *Biomacromolecules* 2019, *20*, 1412–1420.
51. Hennink, W.E.; van Nostrum, C.F. Novel crosslinking methods to design hydrogels. *Adv. Drug Deliv. Rev.*2012, *64*, 223–236.
52. Ibrahim, S.; Kothapalli, C.; Kang, Q.; Ramamurthi, A. Characterization of glycidyl methacrylate–crosslinked hyaluronan hydrogel scaffolds incorporating elastogenic hyaluronan oligomers. *Acta Biomater.* 2011, *7*, 653–665.
53. Poldervaart, M.T.; Goversen, B.; De Ruijter, M.; Abbadessa, A.; Melchels, F.P.; Öner, F.C.; Dhert, W.J.; Vermonden, T.; Alblas, J. 3D bioprinting of methacrylated hyaluronic acid (MeHA) hydrogel with intrinsic osteogenicity. *PloS ONE* 2017, *12*, e0177628.
54. Burdick, J.A.; Chung, C.; Jia, X.; Randolph, M.A.; Langer, R. Controlled degradation and mechanical behavior of photopolymerized hyaluronic acid networks. *Biomacromolecules* 2005, *6*, 386–391.
55. Tavsanli, B.; Okay, O. Mechanically robust and stretchable silk/hyaluronic acid hydrogels. *Carbohydr. Polym.*2019, *208*, 413–420.
56. Larrañeta, E.; Henry, M.; Irwin, N.J.; Trotter, J.; Perminova, A.A.; Donnelly, R.F. Synthesis and characterization of hyaluronic acid hydrogels crosslinked using a solvent–free process for potential biomedical applications. *Carbohydr. Polym.* 2018, *181*, 1194–1205.
57. Zheng, Z.; Hu, J.; Wang, H.; Huang, J.; Yu, Y.; Zhang, Q.; Cheng, Y. Dynamic softening or stiffening a supramolecular hydrogel by ultraviolet or near–infrared light. *ACS Appl. Mater. Interfaces* 2017, *9*, 24511–24517.
58. Rombouts, W.H.; de Kort, D.W.; Pham, T.T.; van Mierlo, C.P.; Werten, M.W.; de Wolf, F.A.; van der Gucht, J. Reversible temperature–switching of hydrogel stiffness

of coassembled, silk–collagen–like hydrogels. *Biomacromolecules* 2015, *16*, 2506–2513.

59. Chen, G.; Jiang, M. Cyclodextrin–based inclusion complexation bridging supramolecular chemistry and macromolecular self–assembly. *Chem. Soc. Rev.* 2011, *40*, 2254–2266.
60. Rodell, C.B.; Kaminski, A.L.; Burdick, J.A. Rational design of network properties in guest–host assembled and shear–thinning hyaluronic acid hydrogels. *Biomacromolecules* 2013, *14*, 4125–4134.
61. Rosales, A.M.; Rodell, C.B.; Chen, M.H.; Morrow, M.G.; Anseth, K.S.; Burdick, J.A. Reversible control of network properties in azobenzene–containing hyaluronic acid–based hydrogels. *Bioconj. Chem.* 2018, *29*, 905–91.
62. Rowland, M.J.; Atgie, M.; Hoogland, D.; Scherman, O.A. Preparation and supramolecular recognition of multivalent peptide–polysaccharide conjugates by cucurbit [8] uril in hydrogel formation. *Biomacromolecules* 2015, *16*, 2436–2443.
63. Montanari, E.; D'arrigo, G.; Di Meo, C.; Virga, A.; Coviello, T.; Passariello, C.; Matricardi, P. Chasing bacteria within the cells using levofloxacin–loaded hyaluronic acid nanohydrogels. *Eur. J. Pharm. Biopharm.* 2014, *87*, 518–523.
64. Jung, Y.-S.; Park, W.; Park, H.; Lee, D.-K.; Na, K. Thermo–sensitive injectable hydrogel based on the physical mixing of hyaluronic acid and Pluronic F–127 for sustained NSAID delivery. *Carbohydr. Polym.* 2017, *156*, 403–408.
65. Huang, G.; Huang, H. Application of hyaluronic acid as carriers in drug delivery. *Drug Deliv.* 2018,*25*, 766–772.
66. Hemshekhar, M.; Thushara, R.M.; Chandranayaka, S.; Sherman, L.S.; Kemparaju, K.; Girish, K.S. Emerging roles of hyaluronic acid bioscaffolds in tissue engineering and regenerative medicine. *Int. J. Biol. Macromol.* 2016, *86*, 917–928.
67. Liu, Z.; Tang, M.; Zhao, J.; Chai, R.; Kang, J. Looking into the future: Toward advanced 3D biomaterials for stem-cell-based regenerative medicine. *Adv. Mater.* 2018, *30*, 1705388.
68. Dosio, F.; Arpicco, S.; Stella, B.; Fattal, E. Hyaluronic acid for anticancer drug and nucleic acid delivery.*Adv. Drug Deliv. Rev.* 2016, *97*, 204–236.
69. Li, J.; Mooney, D.J. Designing hydrogels for controlled drug delivery. *Nat. Rev. Mater.* 2016, *1*, 16071.

70. Highley, C.B.; Kim, M.; Lee, D.; Burdick, J.A. Near–infrared light triggered release of molecules from supramolecular hydrogel–nanorod composites. *Nanomedicine* 2016, *11*, 1579–1590.
71. Yamaguchi, H.; Kobayashi, Y.; Kobayashi, R.; Takashima, Y.; Hashidzume, A.; Harada, A. Photoswitchable gel assembly based on molecular recognition. *Nat. Commun.* 2012, *3*, 603.
72. Kwon, S.S.; Kong, B.J.; Park, S.N. Physicochemical properties of pH–sensitive hydrogels based on hydroxyethyl cellulose–hyaluronic acid and for applications as transdermal delivery systems for skin lesions. *Eur. J. Pharm. Biopharm.* 2015, *92*, 146–154.
73. Mattheolabakis, G.; Milane, L.; Singh, A.; Amiji, M.M. Hyaluronic acid targeting of CD44 for cancer therapy: From receptor biology to nanomedicine. *J. Drug Target.* 2015, *23*, 605–618.
74. Chen, C.; Zhao, S.; Karnad, A.; Freeman, J.W. The biology and role of CD44 in cancer progression: Therapeutic implications. *J. Hematol. Oncol.* 2018, *11*, 64.
75. Rao, N.V.; Yoon, H.Y.; Han, H.S.; Ko, H.; Son, S.; Lee, M.; Lee, H.; Jo, D.-G.; Kang, Y.M.; Park, J.H. Recent developments in hyaluronic acid–based nanomedicine for targeted cancer treatment. *Expert Opin. Drug Deliv.* 2016, *13*, 239–252.
76. Choi, K.Y.; Han, H.S.; Lee, E.S.; Shin, J.M.; Almquist, B.D.; Lee, D.S.; Park, J.H. Hyaluronic acid–based activatable nanomaterials for stimuli-responsive imaging and therapeutics: Beyond CD44-mediated drug delivery. *Adv. Mater.* 2019, 1803549.
77. Huang, G.; Huang, H. Hyaluronic acid–based biopharmaceutical delivery and tumor–targeted drug delivery system. *J. Controll. Release* 2018, *278*, 122–126.
78. Fu, C.; Li, H.; Li, N.; Miao, X.; Xie, M.; Du, W.; Zhang, L.-M. Conjugating an anticancer drug onto thiolated hyaluronic acid by acid liable hydrazone linkage for its gelation and dual stimuli–response release. *Carbohydr. Polym.* 2015, *128*, 163–170.
79. Bajaj, G.; Kim, M.R.; Mohammed, S.I.; Yeo, Y. Hyaluronic acid–based hydrogel for regional delivery of paclitaxel to intraperitoneal tumors. *J. Controll. Release* 2012, *158*, 386–392.
80. Yang, C.; Wang, X.; Yao, X.; Zhang, Y.; Wu, W.; Jiang, X. Hyaluronic acid nanogels with enzyme–sensitive cross–linking group for drug delivery. *J. Controll. Release* 2015, *205*, 206–217.

81. Jhan, H.-J.; Liu, J.-J.; Chen, Y.-C.; Liu, D.-Z.; Sheu, M.-T.; Ho, H.-O. Novel injectable thermosensitive hydrogels for delivering hyaluronic acid–doxorubicin nanocomplexes to locally treat tumors. *Nanomedicine* 2015, *10*, 1263–1274.
82. Chen, J.; He, H.; Deng, C.; Yin, L.; Zhong, Z. Saporin–loaded CD44 and EGFR dual–targeted nanogels for potent inhibition of metastatic breast cancer in vivo. *Int. J. Pharm.* 2019, *560*, 57–64.
83. Dakwar, G.R.; Shariati, M.; Willaert, W.; Ceelen, W.; De Smedt, S.C.; Remaut, K. Nanomedicine–based intraperitoneal therapy for the treatment of peritoneal carcinomatosis—Mission possible? *Adv. Drug Deliv. Rev.* 2017, *108*, 13–24.
84. Cho, E.J.; Sun, B.; Doh, K.-O.; Wilson, E.M.; Torregrosa-Allen, S.; Elzey, B.D.; Yeo, Y. Intraperitoneal delivery of platinum with in–situ crosslinkable hyaluronic acid gel for local therapy of ovarian cancer. *Biomaterials* 2015, *37*, 312–319.
85. Qiu, Y.; Park, K. Environment–sensitive hydrogels for drug delivery. *Adv. Drug Deliv. Rev.* 2001, *53*, 321–339.
86. Zhang, W.; Jin, X.; Li, H.; Wei, C.-X.; Wu, C.-W. Onion–structure bionic hydrogel capsules based on chitosan for regulating doxorubicin release. *Carbohydr. Polym.* 2019, *209*, 152–160.
87. Goldring, M.B.; Berenbaum, F. Emerging targets in osteoarthritis therapy. *Curr. Opin. Pharmacol.* 2015,*22*, 51–63.
88. Dougados, M. Sodium hyaluronate therapy in osteoarthritis: Arguments for a potential beneficial structural effect. *Semin. Arthr. Rheum.* 2000, *30*, 19–25.
89. Ishida, O.; Tanaka, Y.; Morimoto, I.; Takigawa, M.; Eto, S. Chondrocytes are regulated by cellular adhesion through CD44 and hyaluronic acid pathway. *J. Bone Mineral Res.* 1997, *12*, 1657–1663.
90. Cai, Y.; López-Ruiz, E.; Wengel, J.; Creemers, L.B.; Howard, K.A. A hyaluronic acid–based hydrogel enabling CD44–mediated chondrocyte binding and gapmer oligonucleotide release for modulation of gene expression in osteoarthritis. *J. Controll. Release* 2017, *253*, 153–159.
91. Garcia, J.P.; Stein, J.; Cai, Y.; Riemers, F.; Wexselblatt, E.; Wengel, J.; Tryfonidou, M.; Yayon, A.; Howard, K.A.; Creemers, L.B. Fibrin–hyaluronic acid hydrogel–based delivery of antisense oligonucleotides for ADAMTS5 inhibition in co–delivered and resident joint cells in osteoarthritis. *J. Controll. Release* 2019, *294*, 247–258.

92. Verma, P.; Dalal, K. ADAMTS-4 and ADAMTS-5: Key enzymes in osteoarthritis. *J. Cell. Biochem.* 2011, *112*, 3507–3514.

PART B

Preparation, characterization and in vitro evaluation of resveratrol-loaded nanospheres potentially useful for human breast carcinoma

Abstract

The aim of the present work was the preparation and characterization of nanospheres based on antioXidants resveratrol and epigallocatechin gallate useful for site-specific release of resveratrol to breast cancer cells. Nanospheres were prepared via microemulsion technique and were characterized by light scattering, FT-IR spectrophotometry and Electronic Scanning Microscopy. Spherical particles with a diameter of about ~400 nm have been obtained. Resveratrol was then 100% loaded into nanoparticles and its release profile was evaluated by in vitro studies at pH 7.4, in order to simulate the physiological environment, and at pH 6.2 to simulate the tumor environment. Experimental data displayed a slow and continous release of resveratrol from nanoparticles at both pHs. Nanospheres also showed a strong antioXidant activity against lipid peroXidation induced in rat liver microsomal membranes. Finally, the effects of increasing doses of the resveratrol-epigallocatechin gallate based nanospheres on the proliferation and viability of MDA-MB 231 human breast carcinoma cells were evaluated. The data showed a significant reduction of cell survival. In particular, it has been observed that resveratrol loaded microparticles acted more effectively than the empty ones. All the obtained results suggest that these platforms, thanks to their release profile, biocompatibility, antioXidant and antitumor activity, could be a sui- table approach for breast cancer treatment and prevention.

Keywords: Resveratrol, Epigallocatechin gallate, Nanoparticles, Breast cancer, Biomaterial

1. Introduction

Breast cancer represents the most common and frequently diagnosed cause of death among women worldwide [1]. Unfortunately, conventional anticancer treatments attack both cancerous and non- cancerous cells causing consequently side effects such as hair loss, gastrointestinal disorders, neutropenia, and depressed immunity [2] that negatively impact health-related quality of life. Over the past decade a growing interest has been addressed to nanomedicine. In particular, the use of nanotechnological platforms (nanoparticles, liposomes, micelles etc.) as drug delivery systems presents, with respect to conventional cancer therapies, various advantages: targeted delivery of drugs to cancer cells with consequent reduction of systemic toXicity, improvement of physicochemical and pharmacokinetic properties (stability, solubility, half life etc.) of therapeutic molecules, sustained and controlled drug release kinetics etc. [3,4]. The main advantage turn out to be the ability to direct the release of drugs into tumor sites thus reducing their distribution in other body districts. This objective can be achieved through two strategies: passive targeting and active targeting [5,6]. Passive targeting occurs due to intrinsic properties of nano- particles and is based on the EPR effect (Enhanced Permeability and Retention) which leads to accumulation, retention of nanoparticles and consequently release and action of drugs in tumor tissues [7]. Natural compounds are often used for the design and fabrication of these carriers [8–10]. In particular, phytochemicals represent one of the most promising active substances for cancer prevention and adjuvant treatments. Of particular interest, are resveratrol and epigallocatechin gallate which were chosen as starting materials for the preparation of the na- noparticles object of the present study. Resveratrol, a non-flavonoid polyphenol, present in several plant- based foods including grapes, berries, soybeans, pomegranate and peanuts, provides a wide range health beneficial effects. In particular, it shows antioxidant and antitumor activities [11–14]. The idea to utilize also the flavonoid epigallocatechin gallate for the preparation of the particles is due both to its pharmaceutical potential and anti- proliferating effect on carcinoma cells [15,16] and its antioxidant efficacy [17]. On the basis of this assumption and our previous studies [18–20], demonstrating the protective role of antioXidants covalently linked to the carrier matrix on the encapsulated molecules, we hypothesized that resveratrol and epigallocatechin gallate, used for na- nospheres preparation, could protect each other, also explicating a synergistic antioXidant activity and, at the same time, preserving the resveratrol loaded in the same

nanospheres. In particular, when the resveratrol and epigallocatechin gallate are used in combination, there is the possibility of cooperative mechanisms among these molecules in biological systems. Infact, the combined addition of the two anti-oxidants can strongly inhibit MDA production. Furthermore, literatura data higlight the possibility that these phenolic compounds could regenerate the loaded resveratrol reduced active form, from the oxidized one [18–20]. In this study we designed and prepared resveratrol and epigalloca- techin gallate (ECGC) based nanospheres and investigated their suit- ability for breast cancer adjuvant treatment and prevention. Nanoparticles were prepared by polymerizing resveratrol methacrylate and ECGC dimethacrylate via microemulsion technique and their physico-chemical properties were investigated by dynamic light scattering, scanning electron microscopy, swelling degree and Fourier transform infrared. Potential applications for breast cancer treatment and pre- vention were evaluated by considering their encapsulation efficiency, release behavior, antioXidant and antitumor activities.

2. Methodology

2.1 Chemicals

All solvents, analytical grade, were purchased from Carlo Erba Reagents (Milan, Italy): acetone, methanol, n-hexane, chloroform (CHCl3), diethyl ether, tetrahydrofuran (THF), dimethylsulfoxide (DMSO). Resveratrol, epigallocatechin gallate (ECGC), methacrylic acid (MAA), tetramethylethylenediamine (TMEDA), persfulfate ammonium (APS), dicyclohexylcarbodiimide (DCC), dimethylaminopyridine (DMAP), sorbitane monooleate (Span 80), polyethylene glycol (PEG), Milli-Q water and polyoxyethylenesorbitan monooleate (Tween 80) were purchased from Sigma Aldrich. MDA-MB-231 were purchased from American Type Culture Collection. The cells were cultured in DMEM/F-12 containing 10% Fetal Bovine Serum (FBS).

2.2 Apparatus

FT-IR spectra were measured by means of a Jasco 4200 IR spectophotometer (Mary's Court Easton, MD, USA) using KBr disks. 1HNMR spectra were recorded on a Bruker Avance

spectrometer (Bruker Nano Inc.415 N. Quay Street, Kennewick, WA 99336, USA; the chimica shifts were expressed as δ-values (ppm) and referred to the solvent. The
UV–vis spectra were carried out using a Jasco UV-530 spectrophotometer (Mary's Court Easton, MD, USA) Scanning electron microscopy (SEM) analysis was performed with JEOL JSMT 300 A microscope (JEOL USA, Inc.11 Dearborn Road, Peabody, MA USA); the surface of the samples was made conductive by deposition of a thin gold layer in a vacuum chamber. Dimensional analysis of nanoparticles was carried through light scattering using a Brookhaven 90 Plus Particle Size Analyzer (Brookhaven Instruments Corporation, New York, USA) at 25 °C by measuring the autocorrelation function at 90° scattering angle.

2.3 Acrylation of resveratrol and epigallocatechin gallate with methacrylic acid

Acrylation was carried out according to Steglich esterification. In a three-necked flask, equipped with a reflux condenser and a magnetic stirrer, accurately flamed and maintained under inert atmosphere, 0.036 ml of MAA (0.427 mmol) was dissolved in 50 ml of dry chloro-form, and then, 170 mg of DCC (0.824 mmol) and 5 mg of DMAP (0.041 mmol) were added. After 15 min, 100 mg of EGCG (0.218 mmol) were added to the reaction mixture that was kept in a cold-water bath, under stirring for 12 h. The progress of the reaction was monitored by Thin Layer Chromatography (TLC) using chloroform: methanol (90:10) as eluent mixture. At the end of the reaction the solvent was removed under vacuum while dicyclohexylurea (DCU) by using methanol. The product was then dried with a mechanical pump and subsequently purified by flash chromatography on silica gel using chloroform: me- thanol (95:5) as eluent mixture. The product was characterized by FT- IR spectroscopy and ^{1}HNMR. Resveratrol methacrylate was synthesized following the same pro- cedure but with different quantities of reagents. 0.11 ml of MAA (1.30 mmol) was dissolved in 50 ml of dry chloroform and then 85 mg of DCC (0.411 mmol), 25 mg of DMAP (20.46 mmol) and, after 15 min, 300 mg of resveratrol (1.31 mmol) were added. The product was characterized by FT-IR spectroscopy and ^{1}H NMR.

2.4 Preparation of nanospheres based on resveratrol methacrylate and epigallocatechin gallate dimethacrylate

The reaction was carried out according to the procedure described in literature [21]. A cylindrical glass reactor, equipped with a me- chanical stirrer, dropping funnel, and a screw cap with puncture-proof rubber septum, was flamed under nitrogen flow and, after cooling, was immersed in a thermostatically controlled bath at 40 °C. Then, 20 mL of n-hexane and 18 mL of chloroform (dispersing phase) were poured into the reactor. The dispersing phase was kept under stirring for 30 min 91 mg of resveratrol methacrylate (0,307 mmol) and 71 mg of epigallocatechin gallate dimethacrylate (0,119 mmol) were dissolved in 3 mL of distillate water and then, this solution, and 15 mg of ammonium persulfate (0,065 mmol), which acts as a radical initiator, were added to the reaction miXture under N2 bubbling. The density of the organic phase was adjusted with the addition of chloroform or n-hexane in order to obtain an equlibrium between the two phases. Then, 10 µl of sorbitane monooleate (Span 80), 5 µl of polyoXyethylenesorbita monooleate (Tween 80) and 15 µl of tetramethylenediamine (TMEDA) were added under nitrogen stream. The system was kept under stirring for 1 h at 40 °C. The obtained nanospheres were filtered, washed with 50 ml of n-propanol, 50 ml of acetone, 50 ml of ethanol and 50 ml of diethyl ether.

2.5 Nanospheres characterization

Dimensional analysis of nanospheres was performed by dynamic light scattering (DLS) and their polydispersity index (PDI), i.e the measurement of nanoparticles population distribution [21], was also evaluated. The obtained samples were also characterized by FT-IR spectrophotometry and scanning electron microscopy (SEM).

2.6 Swelling studies

Nanospheres affinity towards the aqueous environment was de- termined by studying their swelling degree (WR%). Tipically, aliquots (25 mg) of dried material were placed in glass filters (porosity G2/3), previously wetted. These last were then centrifuged (2000 rpm for 5 min) and weighed. Subsequently, the filters were put in contact with a solution of phosphate buffer at pH 6.2 (in order to simulate the tumor environment) and at pH 7.4 (in order to simulate the physiological enviroment) at 37 °C. At predetermined times (1 h, 3 h, 6 h, 24 h,

48 h, 72 h) the excess of water was removed from the filters by percolation at atmospheric pressure. Subsequently, the filters were centrifuged (3500 rpm for 15 min) and then weighed. The weights recorded to the times listed above were averaged and used to calculate the swelling degree by the f ollowing equation:

$$\frac{WR\% = (Ws \quad Wd)}{100} \qquad \text{Equation 1}$$

where Ws and Wd are the weights of swollen and dried nanospheres respectively [22].

2.7 Impregnation of the nanospheres with resveratrol

The preformed resveratrol- and epigallocatechin gallate-based ma- triX (100 mg) was placed in contact with a solution obtained by dis- solving 20 mg of resveratrol in 8 mL of distilled water. Impregnation was carried out under stirring at room temperature for 3 days, during which, the solution was absorbed by the matriX with consequent matriX swelling [22–24]. Finally, the solvent was removed by filtration and the nanoparticles were dried. The analysis of filtrated water by UV–Vis spectrophotometry allowed to calculate drug entrapment percentage (EE%) by using the following equation:

$$\frac{EE\% = (MiMf\ )}{100} \quad \text{Equation 2}$$

where Mi represents the mass of drug in the solution before loading and Mf represents the mass of drug in the solution after entrapment.

2.8 Release studies

10 mg of dried nanoparticles were dispersed in 1.5 mL of phosphate buffer (at pH 7.4 and at pH 6.2) in glass filters (porosity G2). The filters were mantained at 37 °C in an horizontal shaking bath. At pre- determined interval, a certain volume was removed and analyzed by UV–Vis spectrophotometry at 270 nm (ε = 6998.9 (ml/mg) cm−1). The release was evaluated as cumulative drug release percentage over a time interval of 72 h [23,25].

2.9 Malono aldehyde assay

1 mL of microsomal suspension was added to a solution consisting of 3 mL of trichloroacetic acid (TCA) at 0.5%, 0.5 mL of thiobarbituric acid (TBA) and 0.07 ml of butylated hydroXytoluene (BHT) 0.2% in 95% ethanol. The samples, represented by a control (untreated membranes) and treated membranes with antioXidants and resveratrol loaded nanoparticles, were then incubated in a bath at 80 °C for 30 min and then centrifuged. After incubation, the thiobarbituric acid-mal- ondialdehyde (TBA-MDA) complex was detected by spectrophotometry UV–Vis at 535 nm [18].

2.10 MTT assay

MDA-MB-231 cells were seeded in 24-well multiwell culture plates at the concentration of 3 × 104 cell/mL and, before the treatment, the serum was removed for 24 h. The cells were treated with vehicle, re- severatrol (10 μM–20 μM - 50 μM) and two types of microspheres, loaded or not with resveratrol (10 μM–20 μM - 50 μM) for 72 h. The MTT assay was carried out as described below: 100 μL of MTT (2 mg/ mL) (Sigma Aldrich, Milan, Italy) were added to each well and the samples were incubated for 2 h at 37 °C. After incubation 500 μL of DMSO were added to each well. Absorbance was measured at 570 nm [26].

2.11 Hemolytic study

Hemolysis test was performed by spectrophotometric measurement of hemoglobin release after exposure to nanoparticles. The performance of hemolysis assay was tested by the negative control polyethylene glycol (PEG) and Milli-Q water positive control that causes the total lysis of red blood cells.

2.12 Statistical analysis

Each datum point represents the mean ± SD of three different experiments. Data were analyzed by Student's t-test using the GraphPad Prism 4 software program. $P < 0.05$ was considered as statistically significant.

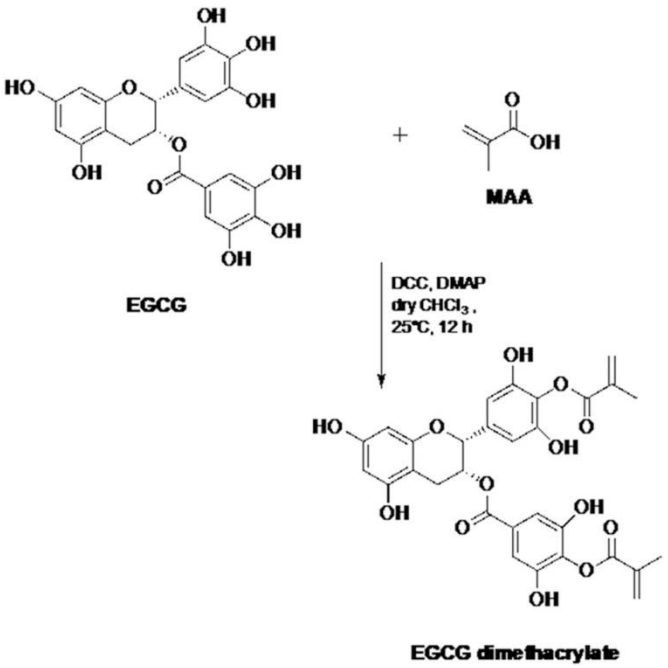

Scheme 1. Route for preparation of EGCG dimethacrylate.

3. Results and discussion

3.1 Acrylation of resveratrol and epigallocatechin gallate with methacrylic acid

Resveratrol methacrylate and epigallocatechin gallate dimethacry- late were obtained via Steglich esterification. In particular, this reaction is based on the esterification of the hydroXyl groups of EGCG (Scheme 1) and resveratrol (Scheme 2) with the carboXylic group of MAA. DCC was used as crosslinking agent since it binds to the oXygen of the car- boXylic group of MAA increasing its electrophilicity and susceptibility towards the attack by the hydroXyl group of epigallocatechin gallate and resveratrol. DMAP was also employed in the reaction because it acts as a base, neutralizing any decrease in pH, and as a catalyst since it is able to remove hydrogen from the hydroXyl group of both ECGC and resveratrol, with consequent formation of alcoholate (-O-) that is more reactive and nucleophilic towards the carbonyl group of MAA. Dicy- clohexylurea (DCU), a reaction byproduct, was dissolved in hot me- thanol and removed by filtration. Finally the obtained product was purified by column

chromatography, dried and characterized by FT-IR (epigallocatechin gallate dimethacrylate in Fig. 2 a and resveratrol methacrylate in Fig. 2b) and ^{1}H NMR.

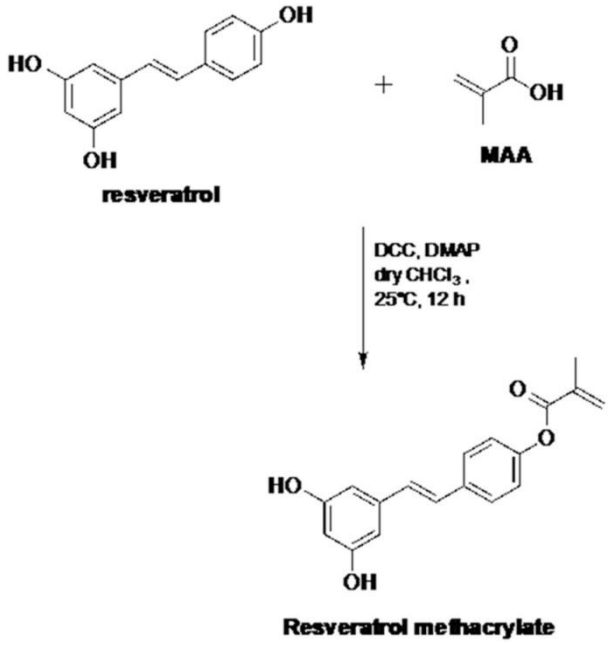

Scheme 2. Route for preparation of resveratrol methacrylate.

3.2 Epigallocatechin gallate dimethacrylate

Yield 87%.

FT-IR (KBr) v (cm−1): 3330 (OH), 3133, 3033 (CH aromatic), 2926, 2850 (CH aliphatic), 1725 (C=O) 1088 (OH), 971, 903 (C=C).

1H NMR (DMSO-d6): 7.65-7.38 (m, 2H), 6.71-6.41 (m, 4H), 6.10-5.59 (m, 4H), 5.29 (ddd, 1H), 5.06 (d, 1H), 2.9 (dd, 1H), 2.8 (dd, 1H), 1.88 (s, 6H).

3.3 Resveratrol methacrylate

Yield 80%.

FT-IR (KBr) v (cm−1): 3325 (OH), 3073, 3033 (CH aromatic), 2931,

2853 (CH aliphatic), 1711 (C=O) 1374 (OH), 948, 906 (C=C).

1H NMR (DMSO-d6): 7.29-7.16 (m, 6H), 6.86 (dd, 2H), 6.23 (dd,

1H), 6.25 (d, 1H), 5.73 (d, 1H), 1.9 (s, 3H).

3.4 Preparation of nanospheres based on resveratrol methacrylate and epigallocatechin gallate dimethacrylate

Nanospheres were prepared using the microemulsion technique. This technique consists in the addition of a monomer aqueous solution (dispersed phase) in an excess of organic solvent immiscible with water (dispersing phase). Small droplets of the dispersed phase are formed under stirring, that, in order to reduce their interfacial free energy, assume a spherical shape. Herein the dispersing phase consists of a miXture of two organic solvents: chloroform (18 mL) and n-hexane (20 mL), while the dispersed phase consists of an aqueous solution (3 mL) of resveratrol methacrylate and epigallocatechin gallate di- methacrylate. The density of the organic phase was adjusted by adding one of the two solvents in order to obtain an equilibrium between the two phases. To prevent particles aggregation, the suspension was kept under constant stirring (1000 rpm). Two surfactants, Span 80 and Tween 80, were added in order to increase particles stability in the organic phase. Polymerization is initiated by the addition, under stir-

ring, of a radical initiator, ammonium persulfate, which decomposes to

form primary radicals at 35–40 °C. Then, after 10 min of stirring, TMEDA was added, acting as an accelerator for the decomposition of ammonium persulfate. Herein, radicals react with the methacrylic functions present on derivatized epigallocatechin gallate and resvera- trol determining a progressive crosslinking. The main advantage of radical polymerization [21] in microemulsion is that the crosslinking process takes place by means of covalent bonds between carbon atoms; this confers to the system more stability compared to systems in which chains are linked by weak interactions and/or easily hydrolysable bonds. The size of particles generally obtained with this technique ranges from different hundreds of nm to a few μm. It is possible to affirm that particles average diameter is directly proportional to the interfacial tension between the two liquid phases and the volume fraction of the disphersed phase, while it is inversely proportional to the density of the monomers droplets, the size of blades and the speed of agitation. However, particle size is affected by different parameters

such as the nature and the ratio of the substances used and reactor's charateristics like speed and type of agitation, shape and size. At the end of the reaction the obtained nanospheres were washed with: 2- propanol, ethanol, acetone and diethyl ether.

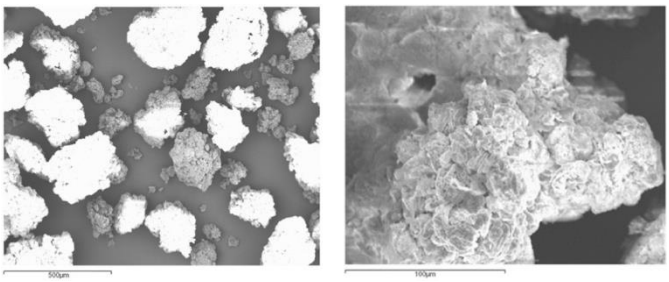

Fig. 1. Photomicrography of empty nanospheres observed by scanning electron microscopy (SEM).

3.5 Nanospheres characterization

The obtained nanospheres were characterized by dimensional and morphological analyses and FT-IR spectrometry. The results of DLS confirmed the presence of nanoparticles with an average diameter of about 400 nm and a PDI of 0.03 which is indicative of an excellent homogeneity in particle size distribution. DLS results were confirmed also by SEM analysis which highlighted the presence of nanoparticles with spherical shape (Fig. 1).

Nanoparticles formation was confirmed also by FT-IR spectrometry, in particular the absence of the peak (Fig. 2c) corresponding to the double bond of the acrylic group confirms that polymerization has occurred.

3.6 Studies of swelling

To assess nanoparticles affinity towards aqueous media, their swelling degree (α%), at two different pH values (6.2 and 7.4) and at different time intervals (1 h, 3 h, 6 h, 24 h, 48 h, 72 h), was evaluated. Table 1 shows the α% values at each studied pH and time intervals. The results showed that the swelling degree at pH 6.2 is greater than that at pH 7.4.

3.7 Impregnation of nanoparticles with resveratrol

Resveratrol incorporation into nanoparticles was carried out by using soaking procedure. The entrapment of the drug into the polymeric matriX is attributable to weak, non-covalent interactions such as hy- drogen bonds, Van der Waals interactions etc. Due to the chemical nature of the drug and matriX, the active substance interacts more with nanoparticles surfaces. During impregnation, the polymeric matriX in- creases in its volume, but it retains its three-dimensional structure without breaking up since it is insoluble in water. Nanoparticles showed an excellent entrapment efficiency of about 100%.

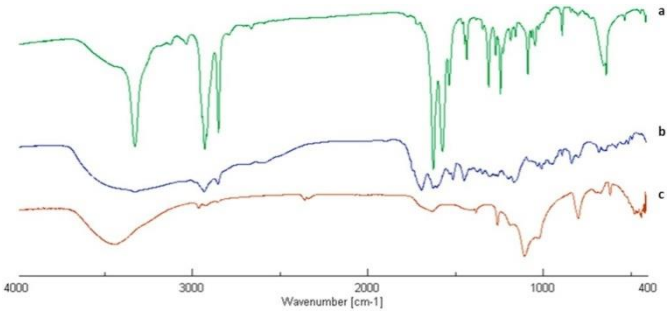

Fig. 2. IR Spectra of epigallocatechin gallate dimethacrylate (a), resveratrol methacrylate (b) and nanospheres (c).

3.8 Release studies

Resveratrol release studies from nanoparticles were conducted at pH 7.4 (in order to simulate the physiological enviroment) and at pH 6.2 (in order to simulate the tumor environment), at different time intervals (1 h, 3 h, 6 h, 24 h, 72 h). Nanoparticles were kept under stirring in an horizontal shaking bath at 37 °C. Drug release profile was determined by spectrophotometric analysis and expressed as percen- tage of drug released respect to the effectively entrapped total dose as a function of time (Fig. 3).

Data showed a pH-sensitive and sustained release of resveratrol from nanoparticles indicating that it is possible to use this delivery system for resveratrol site specific release both in pathological and physiological conditions. In particular, resveratrol release efficiency increased with increasing pH; this could be attributable to electrostatic repulsions due to the increase of dissociated groups which cause an increase of meshes size. However, it was not easy to predict the release profile of resveratrol. In fact this phenomenon is influenced by

various parameters: interactions between drug and matriX, chemo-physical proprieties of loaded drug, temperature of release media, speed of water penetration into polymeric matriX, nanoparticles crosslinking degree etc.

Crosslinking degree is a very important parameter because it affects the swelling degree and consequently t\he mechanism of release and the diffusion rate of the drug. The prevalence of one of these factors on the others may determine the outcome but, generally, the result comes from a particular combination of these parameters. Release profile could also be affected by the loading procedure; for example when molecules can easily penetrate into nanoparticles meshes, stronger and more stable interactions will occur and, therefore, the drug will be released in smaller amounts.

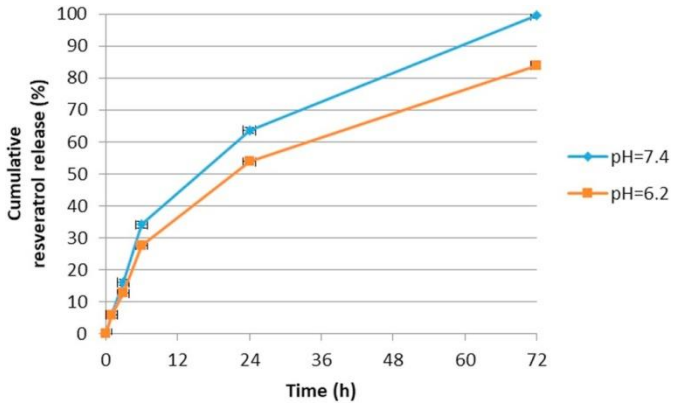

Fig. 3. Resveratrol release from nanospheres evaluated within 72 h. Data are expressed as the mean ± S.D. of at least three independent experiments.

3.9 Evaluation of nanoparticles antioxidant activity

Nanoparticles ability to inhibit lipid peroXidation induced by t- BOOH was examined in rat liver microsomal membranes, in an in- cubation period of 120 min. The antioXidant activity of resveratrol and epigallocatechin gallate was also evaluated in the same conditions. In Fig. 4 is shown that all the tested compounds are able to inhibit lipid peroXidation in a time-dependent manner.

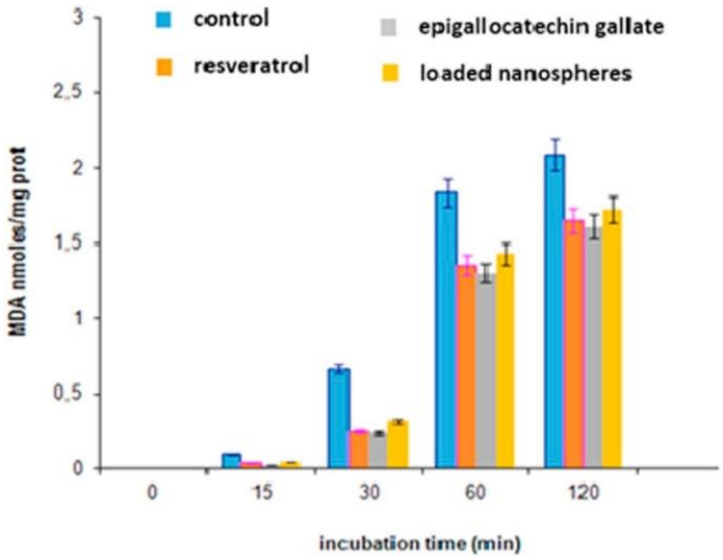

Fig. 4. Antioxidant activity evaluation as inhibition of malondialdehyde (MDA). Data are expressed as the mean ± S.D. of at least three independent experiments.

3.10 MTT assay

In this experiment we evaluated the effects of increasing doses of two different types of nanoparticles based on resveratrol and epigallocatechin gallate on the proliferation and vitality of MDA-MB 231 human breast cancer cell line. This analysis was carried out via MTT assay treating cells with increasing concentrations (10- 20–50 μM) of resveratrol or nano- particles (empty or loaded with reseveratrol) for 72 h.

Results showed that all the samples tested reduced significantly cell survival already from the concentration of 10 μM compared to the untreated control. In particular, nanoparticles at the concentration of 20–50 μM, show a greater inhibition of cell survival compared to re- sveratrol alone. Moreover, resveratrol loaded nanoparticles act more effectively than the empty ones starting from the concentration of 20 μM (Fig. 5).

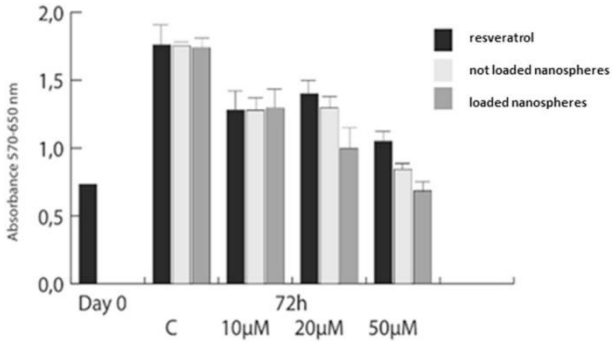

Fig. 5. Effect of nanoparticles on MDA-MB 231 human breast cancer cell via- bility. *p < 0.05 compared to control (resveratrol). Data are expressed as the mean ± SD of at least three independent experiments.

3.11 Hemolytic study

Hemolytic study was performed to evaluate not loaded or loaded resveratrol nanoparticles effects on erythrocytes. The lysis was detected by observing the increasing absorbance value due to the release of the hemoglobin in the solution. As shown in Fig. 6 the microspheres did not produce the release of hemoglobin as evidenced by the similar absor- bance with the negative control.

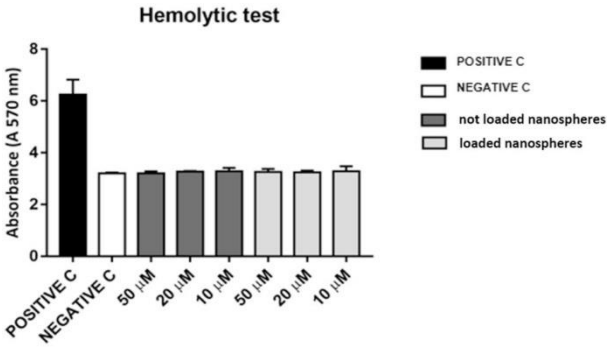

Fig. 6. Percentage of hemoglobin released after addition of treatment as in- dicated. EXperiment was conducted in triplicate.

4. Conclusions

The aim of this work was the preparation and characterization of nanoparticles based on resveratrol and epigallocatechin gallate, useful for site-specific release of resveratrol to breast cancer cells. Resveratrol and EGCG were successfully derivatized with MAA in order to obtain active substances able to undergo radical polymerization. Nanoparticles with a spherical shape and an average diameter of about 400 nm were obtained via microemulsion technique; these dimensions allow nano- spheres accumulation into tumor sites due to the EPR effect. Nanospheres were then loaded with resveratrol by soaking technique obtaining an excellent encapsulation efficiency of about 100%. So, resveratrol release profiles in media that simulate physiological as well as tumor environ- ment were evaluated and the results showed a pH-sensitive and sustained release of resveratrol from nanoparticles. Nanospheres also showed ex- cellent antioXidant properties and the ability to preserve the antioXidant activities of both resveratrol and ECGC. Moreover, loaded nanoparticles are more effective than both resveratrol and empty nanospheres in inhibiting human breast cancer cells viability in vitro. In conclusion, these platforms thanks to their excellent biocompatibility, antioXidant and antitumor activities turn out to be promising candidates for the devel- opment of potential systems for breast cancer treatment.

References

R. Cassano, F. De Amicis, C. Servidio, F. Curcio, S. Trombino. Preparation, characterization, and in vitro evaluation of resveratrol-loaded nanospheres potentially useful for human breast carcinoma, *Journal of Drug Delivery Science and Technology*, 2020, 57, 101748.

[1] F. Bray, J. Ferlay, I. Soerjomataram, R.L. Siegel, L.A. Torre, A. Jemal, GLOBOCAN estimates of incidence and mortality worldwide for 36 cancers in 185 countries, Ca - Cancer J. Clin. 68 (2018) 394–424.

[2] J. LemieuX, E. Maunsell, L. Provencher, Chemotherapy-induced alopecia and effects on quality of life among women with breast cancer: a literature review, Psycho Oncol. 17 (2008) 317–332.

[3] D. Peer, J.M. Karp, S. Hong, O.C. Farokhzad, R. Margalit, R. Langer, Nanocarriers as an emerging platform for cancer therapy, Nat. Nanotechnol. 2 (2007) 751–760.

[4] R.K. Jain, T. Stylianopoulos, Delivering nanomedicine to solid tumors, Nat. Rev. Clin. Oncol. 7 (2010) 653–664.

[5] R. Bazak, M. Houri, S. El Achy, S. Kamel, T. Refaat, Cancer active targeting by nanoparticles: a comprehensive review of literature, J. Canc. Res. Clin. Oncol. 141 (2015) 769–784.

[6] F. Danhier, O. Feron, V. Préat, To exploit the tumor microenvironment: passive and active tumor targeting of nanocarriers for anti-cancer drug delivery, J. Contr. Release 148 (2010) 135–146.

[7] J. Fang, H. Nakamura, H. Maeda, The EPR effect: unique features of tumor blood vessels for drug delivery, factors involved, and limitations and augmentation of the effect, Adv. Drug Deliv. Rev. 63 (2011) 136–151.

[8] D. Dheer, D. Arora, S. Jaglan, R.K. Rawal, R. Shankar, Polysaccharides based na-nomaterials for targeted anti-cancer drug delivery, J. Drug Target. 25 (2017) 1–16.

[9] S. Serini, R. Cassano, P.A. Corsetto, A.M. Rizzo, G. Calviello, S. Trombino, Omega-3 PUFA loaded in resveratrol-based SolidLipid nanoparticles: physicochemical prop- erties and antineoplastic activities in human colorectal cancer cells in vitro, Int. J. Mol. Sci. 19 (2018) 586–605.

[10] S. Jana, A. Gandhi, K.K. Sen, S.K. Basu, Natural polymers and their application in drug delivery and biomedical field, J. PharmaSciTech 1 (2011) 16–27.

[11] A. Bishayee, Cancer prevention and treatment with resveratrol: from rodent studies to clinical trials, Canc. Prev. Res. 2 (2009) 409–418.

[12] L.G. Carter, J.A. D'Orazio, K.J. Pearson, Resveratrol and cancer: focus on in vivo evidence, Endocr. Relat. Canc. 21 (2014) 209–225.

[13] D. Sinhaa, N. Sarkar, J. Biswas, Anupam Bishayee. Resveratrol for breast cancer prevention and therapy: preclinical evidence and molecular mechanisms, Semin. Canc. Biol. 40 (2016) 209–232.

[14] Y. Zu, Y. Zhang, W. Wang, X. Zhao, X. Han, K. Wang, Y. Ge, Preparation and in vitro/in vivo evaluation of resveratrol-loaded carboXymethyl chitosan nano- particles, J. Drug Del. 23 (2016) 971–981.

[15] N. Fu, Z. Zhou, T.B. Jones, T.Y. Tan, W.D. Wu, S. XuqiLin, X.D. Chen, P.Y. Chan, Production of monodisperse epigallocatechin gallate (EGCG) microparticles by spray drying for high antioXidant activity retention, Int. J. Pharm. 413 (2011) 155–166.

[16] G.J. Du, Z. Zhang, X.D. Wen, C. Yu, T. Calway, C.S. Yuan, C.Z. Wang, Epigallocatechin gallate (EGCG) is the most effective cancer chemopreventive polyphenol in green tea, Nutrients 4 (2012) 1679–1691.

[17] M. Nikoo, M. Joe, R. Hassan, A. Gavlighi, AntioXidant and antimicrobial activities of (-) -Epigallocatechin-3-gallate (EGCG) and its potential to preserve the quality and safety of foods, Compr. Rev. Food Sci. Food Saf. 17 (2018) 732–754.

[18] S. Trombino, S. Serini, F. Di Nicuolo, L. Celleno, S. Andò, N. Picci, G. Calviello, P. Palozza, AntioXidant effect of ferulic acid in isolated membranes and intact cells: synergistic interactions with α-tocopherol, β-carotene, and ascorbic acid, J. Agric. Food Chem. 21 (2004) 2411–2420.

[19] R. Cassano, S. Mellace, M. Marrelli, F. Conforti, S. Trombino, α-Tocopheryl lino-lenate solid lipid nanoparticles for the encapsulation, protection, and release of the omega-3 polyunsaturated fatty acid: in vitro anti-melanoma activity evaluation, Colloids Surf. B Biointerfaces 1 (2017) 128–133.

[20] R. Cassano, S. Trombino, R. Muzzalupo, L. Tavano, N. Picci, A novel dextran hydrogel linking trans-ferulic acid for the stabilization and transdermal delivery of vitamin E, Eur. J. Pharm. Biopharm. 72 (2009) 232–238.

[21] D.E.J. Koppel, Analysis of macromolecular polydispersity in intensity correlation spectroscopy: the method of cumulants, Chem. Phys. 57 (1972) 4814–4820.

[22] S. Trombino, R. Cassano, A. Cilea, T. Ferrarelli, R. Muzzalupo, N. Picci, Synthesis of pro-drugs L-lysine based for 5-aminosalicylic acid and 6-mercaptopurine colon specific release, Int. J. Pharm. 420 (2011) 290–296.

[23] R. Cassano, S. Trombino, T. Ferrarelli, A.R. Bilia, M.C. Bergonzi, F. De Amicis, N. Picci, Preparation, characterization and in vitro activities evaluation of curcumin based microspheres for azathioprine oral delivery, React. Funct. Polym. 72 (2012) 446–450.

[24] F. Iemma, G. Spizzirri, Puoci, F.R. Muzzalupo, S. Trombino, R. Cassano, S. Leta, N. Picci, pH-Sensitive hydrogels based on bovine serum albumin for oral drug de- livery, Int. J. Pharm. 312 (2006) 151–157.

[25] V.D. Wolthuis, O. Franssen, H. Talsma, J.J. Kettens-van den Bosch, Synthesis, characterization, and polymerization of glycidyl methacrylate derivatized dextran, Macromolecules 28 (1995) 6317–6322.

[26] J. SuY, S.Y. Huang, Y.H. Ni, K.F. Liao, S.S. Chiu, Anti-tumor and radiosensitization effects of N-butylidenephthalide on human breast cancer cells, Molecules 23 (2018) 240–250.

PART C

Gelatin and Glycerine-Based Bioadhesive Vaginal Hydrogel

Abstract

The work's aim was the preparation and characterization of a hydrogel based on gelatin and glycerine, useful for site-specific release of benzydamine, an anti-inflammatory drug, able to attenuate the inflammatory process typical of the vaginal infection. The obtained hydrogel has been characterized by electronic scanning microscopy (SEM) and differential scanning calorimetry (DSC). In addition, due to the precursor properties, the hydrogel exhibits a relevant mucoadhesive activity. The swelling degree was evaluated at two different pHs and at defined time intervals. In particular, phosphate buffers were used at pH 6.6, in order to mimic the typical conditions of infectious diseases at the vaginal level, particularly for HIV-seropositive pregnant women, and pH 4.6, to simulate the physio-logical environment. The obtained results revealed that the hydrogel swells up well at both pHs. Release studies conducted at both pathological and physiological pHs have shown that benzydamine is released at the level of the vaginal mucosa in a slow and gradual manner. These data support the hypothesis of the hydrogel use for the site-specif release of benzydamine in the vaginal mucosa.

Keywords: Gelatin, glycerine, hydrogel, mucoadhesive, vaginal.

1. Introduction

The need to find new pharmacological approaches for the treatment of various diseases has led to an increasing interest in the “Drug Delivery System” (DDS). DDSs represent a particularly promising technology to improve the *in vivo* and *in vitro* efficacy of biologically active 145ssesse145 to circum- scribe the effect on a specific cell typology, improving its efficacy, prolonging its permanence period and reducing the therapy toxicity.

Polymer carrier technology offers a new approach to drug delivery. In fact, by coupling a drug to a carrier such as microspheres, nanoparticles, liposomes, etc., it is possible to modulate the release characteristics of the same drug. In conventional drug release, after being absorbed, it is distrib- uted in the organism through the 145ssesse circulation. For most drugs, only a small part will manage to reach the af- fected organ. Instead, in the targeted release, the drug con- centrates in the tissue of interest, thus reducing the concentration in the remaining tissues, improving efficacy and re- ducing the side effects [1-4].

A possible application of DDS concerns the treatment of the disease related to the female genital apparatus, ranging from simple bacterial infection to contraceptive treatment or to infertility treatment in women. Regarding vaginal drug delivery, the optimization of formulations will require more attention; in particular, the characteristics such as hydrophil- icity, distribution, viscosity and bio-adhesion should be fo- cused [5-13].

The most common problems of vaginal administration drugs are due to the lack of mucoadhesion, which corre- sponds to poor bioavailability. In this 145ssess, the objective of this work was the design, preparation and study of a new mucoadhesive carrier based on gelatin and glycerine for vaginal administration of benzydamine, a non-steroidal anti-inflammatory drug, in order to reduce its 145ssesse toxicity [14].

145ssesse145145t a protein derived from the collagen that has been extensively used for the development of mucoadhesive hydrogels useful as controlled drug delivery systems [15, 16]. In particular, gelatin-based hydrogels were used to de- velop vaginal suppositories for the controlled delivery of drugs and also in the treatment of vaginal dryness [17-20]. On the other hand, glycerine is a non-toxic and water-soluble polyol, found in many lipids known as glycerides. It is widely used as hydrating/wetting eccipient

in various phar- maceutical preparations for the delivery of bioactive agents in the vagina [21, 22]. Taking inspiration from this, it seems justified to develop gelatin-glycerin based hydrogels. In particular, a hydrogel, based on gelatin and glycerine, loaded with benzydamine was prepared (Fig. **1**). Through the prepa- ration of the hydrogel, a high molecular weight carrier and a high mucus adhesiveness was obtained, in order to allow the targeted release of benzydamine in the vaginal environment. Moreover, thanks to the mucoadhesive properties, this carrier could increase the residence time *in situ*, thus reducing the number of conventional pharmaceutical applications. Ideally, the formulation will be retained on the biological surface and the drug will release near the absorbent membrane, with con- sequent improvement of bioavailability. This carrier could be potentially useful for the treatment of *Candida* colonization of the vagina that is a risk factor in pregnancy, especially for HIV-seropositive and HIV-seronegative pregnant women [23].

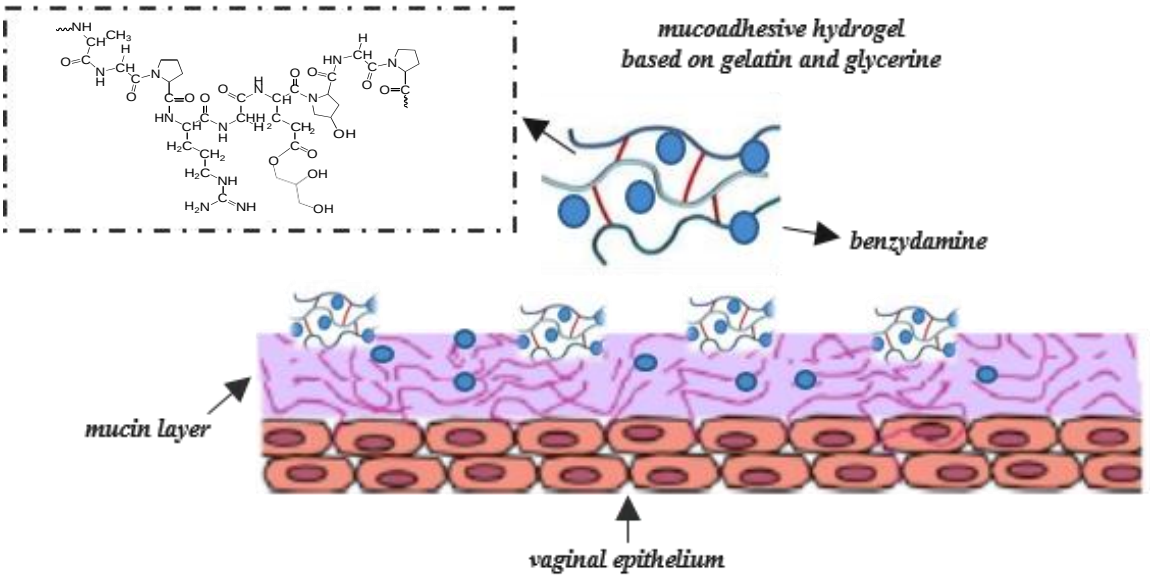

Fig. (1). Schematic representation of interation of mucoadhesive hydrogel with mucin layer. The three-dimensional network is composed of both gelatin (blue line) and glycerine (red line). (*A higher resolution / colour version of this figure is available in the electronic copy of the article*).

2. Experimental

2.1 Materials

The analytical grade solvents used were purchased from Carlo Erba Reagenti (Milan, Italy): acetone, chloroform, ethanol, n-hexane, 2-propanol, ethyl ether. *N*-hexane and chloroform were purified with standard procedures. In par- ticular, *N*-hexane was pre-dried by refluxing with $LiAlH_4$ and subsequent distillation and then dried by refluxing with sodium and re-distilled; CCl_4 was dried by refluxing with sodium sulfate and subsequent distillation. In addition, ben- zydamine salt (MW 309.41 g/mol), gelatin (mixture type A and B with 160 Bloom grams and unknown molecular weight), glycerine (PM 92.09 g/mol), sorbitan trioleate (Span 85), polyoxymethylene sorbitan (tween 85), *N, N'*- dicyclohexylcarbodimide (DCC), 4-dimethylaminopyridine (DMAP) were purchased from Sigma-Aldrich (Sigma Chemical Co, St. Louis, MO, USA).

2.2 Instrumentation

The infrared spectra were performed using a Perkin- Elmer 1720 FT-IR spectrophotometer, in the range 4000-400 cm^{-1} (number of scans 16). UV-Vis spectra were made using a JASCO UV-530 spectrophotometer. The compounds were

lyophilized using a "Freezing-drying" Micro modulyo, Ed- wards apparatus. The hydrogel was observed by electronic scanning microscopy (SEM) JEOL JSMT 300 A. The sur- face of the sample was made conductive by the deposition of a gold-layer carried out under vacuum. The transition tem- perature was evaluated using DSC-NETZSCH 200 operating under nitrogen with defined heating (10°C min^{-1}) and cool- ing rates (5°C min^{-1}).

2.3 Preparation of Benzydamine

Benzydamine was obtained from the corresponding salt. Briefly, 1 g of benzydamine hydrochloride salt was dissolved in 400 ml of distilled water. The solution was then placed under stirring and heated to 100°C. Subsequently, NaOH was added to promote the precipitation of benzydamine. The precipitate was then recovered by filtration, using a Pyrex™ 60mm glass Büchner filter 147ssess with porosity 4, dried at the mechanical pump

and subsequently characterized by FT- IR.

2.4 Preparation of the Hydrogel Based on Gelatin and Glycerine

A glass cylindrical reactor (100-150 ml) equipped with a mechanical stirrer, was flamed in a nitrogen stream and after cooling, it was immersed in a thermostated bath at 60°C. Then, *n*-hexane (20 ml) and chloroform (18 ml) were in- serted (dispersing phase), and gelatin was added (1g/$1.17 \cdot 10^{-3}$ mol). The polymerization reaction was performed in terms of an interfacial polycondensation (water/oil). The dispersing phase and the gelatin were kept under mechanical stirring for 30 minutes. After that, a predetermined quantity of glycerine (0.086 g, 0.068 ml/$9.36 \cdot 10^{-4}$ mol) was appropriately solubi- lized in distilled water 4 ml, heating for few minutes to aid the dissolution process and added into the reactor with 0.24 g of *N, N'*-dicyclohexylcarbidimide (DCC) and $1.43 \cdot 10^{-3}$g of 4- dimethylaminopyridine (DMAP) [24-25]. Then, 150 µl of sorbitan trioleate (Span 85) were added, and after 10 minutes, 150 µl of polyoxymethylene sorbitan trioleate (Tween 85) was added too. The system was kept under stirring for 1 h and at a temperature of 60°C. The reactor content was finally filtered and subsequently washed in succession with 50 ml of isopropanol, 50 ml of ethanol, 50 ml of acetone and 50 ml of ethyl ether. The filtrate was dried by a membrane pump and then characterized by FT-IR spectrophotometry, dimensional analysis, differential scanning calorimetry (DSC), electronic scanning micrograph (SEM), and measurement of the 148sses- ling degree in aqueous solution at different Ph values.

2.5 Swelling Studies

To assess the hydrophilic affinity of the hydrogel to the aqueous environment, its swelling degree was determined (WR%). Aliquots of dry material (25 mg) were inserted in glass filters (porosity G2/3) previously wet, centrifuged (5 minutes at 2000 g/min) and then weighed. Subsequently, they were put in contact with a buffer solution 5 Ml (Na_2HPO_4, NaH_2PO_4), at Ph 4.6 and 6.6 (to mimic the physiological and pathological conditions of the vaginal en- vironment) at temperature of 37°C until the swelling balance between the polymer elasticity and the osmotic forces deter- mined by the polymer affinity to the solvent was reached. This condition was achieved when the weight of the swollen hydrogel was constant.

At pre-established intervals time (1h, 3h, 6h, 9h, 24h), the buffer excess was removed from the filters by percolation at atmospheric pressure. Subsequently, the filters were cen- trifuged at 3500 rpm for 15 minutes and weighed. This pro- cedure was repeated 3 times at all of the time points.

The weights recorded at the times listed above were used to calculate the swelling using the following equation 1:

$$A\% = \frac{(Ws - Wd)}{Wd} \times 100$$

where Ws and Wd respectively represent the weights of the swollen and dried hydrogel [26-29].

2.6. Impregnation of Hydrogel with Benzydamine

The preformed matrix (about 100 mg) was placed in contact with a solution of known drug concentration obtained by dissolving 20 mg of benzydamine in 10 ml of distilled water. The impregnation was performed under stirring at room temperature for 3 days, during which the drug solution was absorbed by the hydrogel [29]. Finally, the solvent was removed by filtration, using a Pyrex™ 2.5mm glass Büchner filter funnel with porosity 4, and the particles were dried to constant weight. The analysis of the filtrated water, using a UV spectrophotometer, allowed to calculate the percentage of active principle adsorbed by the matrix (LE%) using equa- tion 2:

$$LE\% = \frac{(Ai - Af)}{Ai} \times 100$$

where Ai was the drug concentration in the solution before loading and Af the drug concentration in the solution after loading.

2.7 Release Study

The drug release profile [28] from the matrix was evalu- ated by placing an aliquot of loaded hydrogel (10 mg) in 1.5 ml of buffer solutions, at Ph 4.6 and 6.6, respectively contained in glass flasks. The flasks were kept under horizontal stirring at a temperature of 37°C. There was no loss of re- lease medium due to evaporation. In fact, the flasks used for release studies were covered with laboratory film (Parafilm) to prevent this phenomenon. At predetermined time inter- vals, the entire volume (1.5 ml) was taken from the release solution, replaced with the same volume of fresh fluid, and analyzed by UV-Vis spectrophotometry using a calibration plot (ε=800.15 (ml/mg) cm^{-1}) and λ=254 nm). Sink condition was maintained throughout the experiment.

The percentage of the released drug was expressed in relation to the absorbance. The release test was completed within 24 hours. The release studies were carried out in triplicate and the results agreed with ±5% standard error.

2.8 Mucoadhesion Studies

The mucin was dispersed in a buffer solution (1mg/Ml) and kept at 37°C for 24h under stirring (150 rpm). Then, an appropriate amount of each sample or poly 150ssess acid (se-

lected as positive control) was added to the mucin dispersion (mucina/polymer weight ratio of 1) and each sample was incubated at 37°C (150 rpm) while stirring for 2, 4, or 24h. After each stirring time, the mixture was centrifuged at 2000 rpm/min for 2 minutes and the transmittance (%) of each sample was recorded at 650 nm. Transmittance was meas- ured for samples composed by the sample to be tested plus 151ssesse151 dispersion. Mucin dispersions alone were used as blank. A reduction in transmittance indicates a greater inter- action between the tested sample and mucin. Thus, lower transmittance equals to higher interaction. The mucoadhe- sion of the tested samples was reported with respect to the polyacrylic acid chosen as 100% of mucoadhesive force. Each experiment was performed three times, and the results were reported as mean ± SD.

2.9. Statistical Analysis

Data are expressed as the mean ± S.D. of at least three independent experiments. Statistical analysis was performed using Student's t-test. P-Values ≤0.05 were considered statis- tically significant.

3. **Results and discussion**

3.1 Characterization of the Hydrogel (*FT-IR)*

The hydrogel based on gelatin and glycerine was prepared using the reverse phase emulsion polymerization technique and characterized by FT-IR spectrophotometry which confirmed the formation of the hydrogel FT-IR (KBr) v (cm^{-1}): 3416 (OH), 2936 (CH), 2878 (CH), 1744, 1727 (C= O). FT-IR spectrum of the hydrogel is presented in Fig. (3b). Polymeric network shows FT-IR, a spectrum different from that of pure gelatin (Fig. 3a) and glycerine (Fig. 3c). Some changes can be observed mainly in the 3500 3000 cm^{-1} and 1800 1600 cm^{-1} regions. After gelatin crosslinking with glycerine, new 151ssesse151151t peaks were found at 1744 and 1727 cm^{-1}, which indicated the ester 151ssesse formation (Fig. **2b**) due to the presence of glycerine hydroxyl groups with gelatin association. Furthermore, the area between 3000 and 3500 cm^{-1} (Fig. **2b** versus Fig. **3°** and **2c**) resulted as much more intense, hypothesizing the insertion of glycerin on the skeleton of gelatin.

This result may be attributed to the –OH of the hydroxyl group. Absorption bands in the regions of 2950-2940 and 2935-2900 cm^{-1} correspond to asymmetric and symmetric

stretching of the –CH2 groups. Additionally, the absorption band at 2890-2760 cm^{-1} is characteristic stretching -CH group of the matrix. On the other hand, as literature data confirmed [30], FT-IR spectrum of the underivatized gelatin (Fig. **3**°) showed peaks at 3445 and 3420 cm^{-1} substantially due to N-H stretching of secondary amide, a C=O stretching peak at 1680 and 1640 cm^{-1}, and N-H bending peak between 1550 and 1500 cm^{-1}. Therefore, it can be concluded that the free carboxylic groups of gelatin have been esterified.

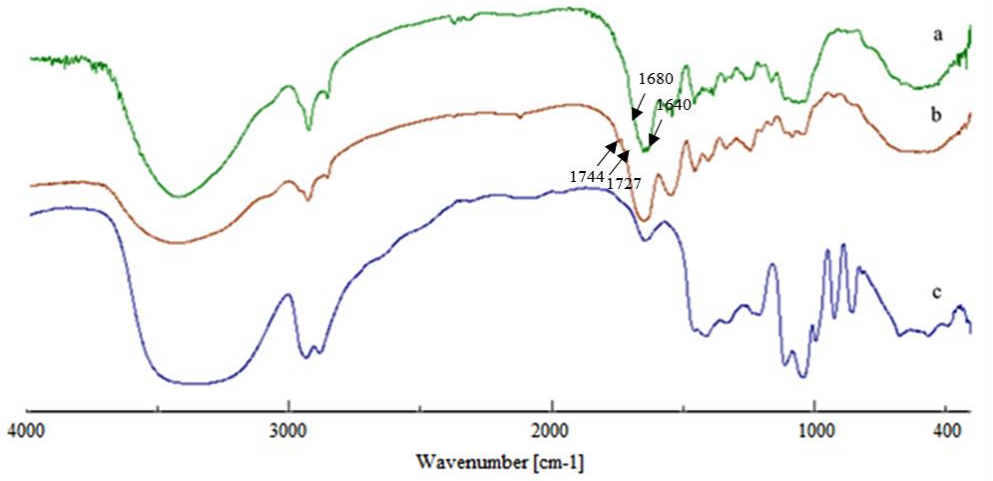

Fig. (2). FT-IR spectra overlapping of gelatin (**a**), hydrogel (**b**), glycerine (**c**) showing changes mainly in the 3500 3000 cm^{-1} and 1800 1600 cm^{-1} regions. (A higher resolution/colour version of this figure is available in the electronic copy of the article).

3.2 Swelling Studies

To assess the affinity of the hydrogel to the aqueous me- dia, its degree of swelling (α%) was determined, through swelling studies, at two different pHs (4.6 and 6.6) and at definite time intervals (1h, 3h, 6h, 8h, 24h). Data reported in Table 1 illustrate the water uptake at each studied Ph and time (Table 1).

The obtained results indicate that the prepared hydrogel swells to both pHs. In chemically crosslinked hydrogel, not much difference was observed in the swelling ratio at the acidic

medium when the Ph was raised from 4.6 to 6.6 even if the hydrogel swells more at Ph 4.6. The main difference in the behavior of the hydrogel at the two different pHs lies is the time required to reach the swelling balance. In fact, Table 1 shows that the time taken to achieve swelling equilibrium of the hydrogel was at least 8-24 h at Ph 6.6 and 1-8 h at Ph 4.6. At Ph 6.6, the water transport was more rate-controlled than at Ph 4.6. This behavior is probably due to the resis- tance of the polymer to a sudden increase in volume to a higher Ph that should lead to a more gradual release of the loaded benzydamine.

A %	Ph	Time (h)				
		1	**3**	**6**	**8**	**24**
	4.6	1240 ± 42	1320 ± 51	1356 ± 58	1412 ± 62	1452 ± 69
	6.6	756±23	936±28	1072±29	1228±35	1250±40

Table 1. Hydrogel swelling behavior. Data are expressed as the mean±S.D. of at least three independent experiments $p<0.05$.

3.3 Calorimetric Analysis

The calorimetric analysis was carried out in order to evaluate the transition temperatures. In particular, the transi- tion temperature of both hydrogel and its precursors was evaluated.

Thermograms were acquired after keeping hydrogel for two weeks in a vacuum oven until constant weights. The calorimetric analysis was performed by heating the samples from 25°C to 200°C under nitrogen with a flow rate of 25 ml/min and heating of 5°C min^{-1}.

Their thermograms were analyzed in detail and com- pared. Fig. (**3**) shows the gelatin thermograms (Fig. **3b**) and the gelatin- and glycerine-based hydrogel (Fig. **3a**). In par- ticular, an exothermic peak at 81.9°C was observed in the DSC of gelatin, while the gelatin- and glycerine-based hy- drogel showed an exothermic peak at 71.4°C. Glycerine, on the other hand, exhibited a transition temperature of around 20°C (thermogram not shown). The peak at 71.4°C did not appear in the DSC thermogram of pure gelatin, indicating the existence of cross-linking among the glycerine and gelatin.

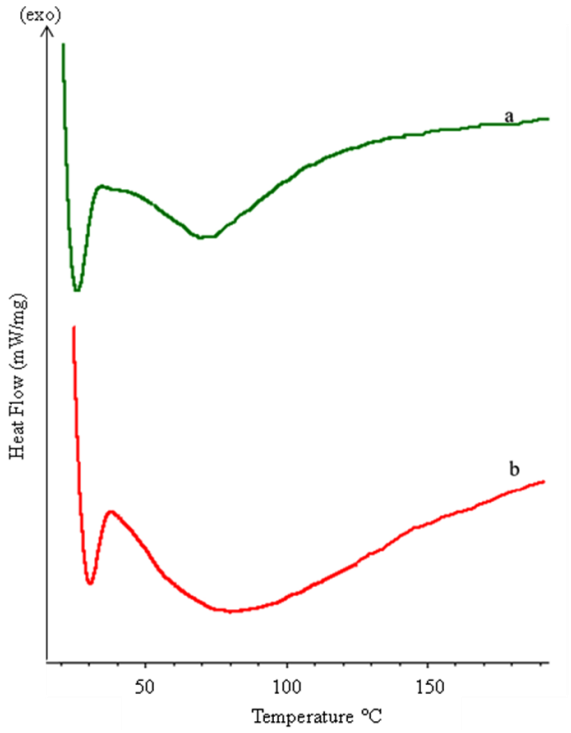

Fig. (3). DSC thermograms of glycerine-based hydrogel (**a**) showing an exothermic peak at 71.4°C and of gelatin (**b**) showing an exothermic peak at 81.9°C. (*A higher resolution / colour version of this figure is available in the electronic copy of the article*).

3.4 Morphological Analysis

The morphological characterization of the hydrogel was performed using electronic scanning microscopy (SEM). In particular, as shown in Fig. (**4**), the hydrogel exhibited sev- eral pores. This porous structure, attributable to the pres- ence of hydrophilic groups in the hydrogel, facilitates the permeation of water or biological fluids and explains the high degree of swelling at both pathological and physio- logical pHs.

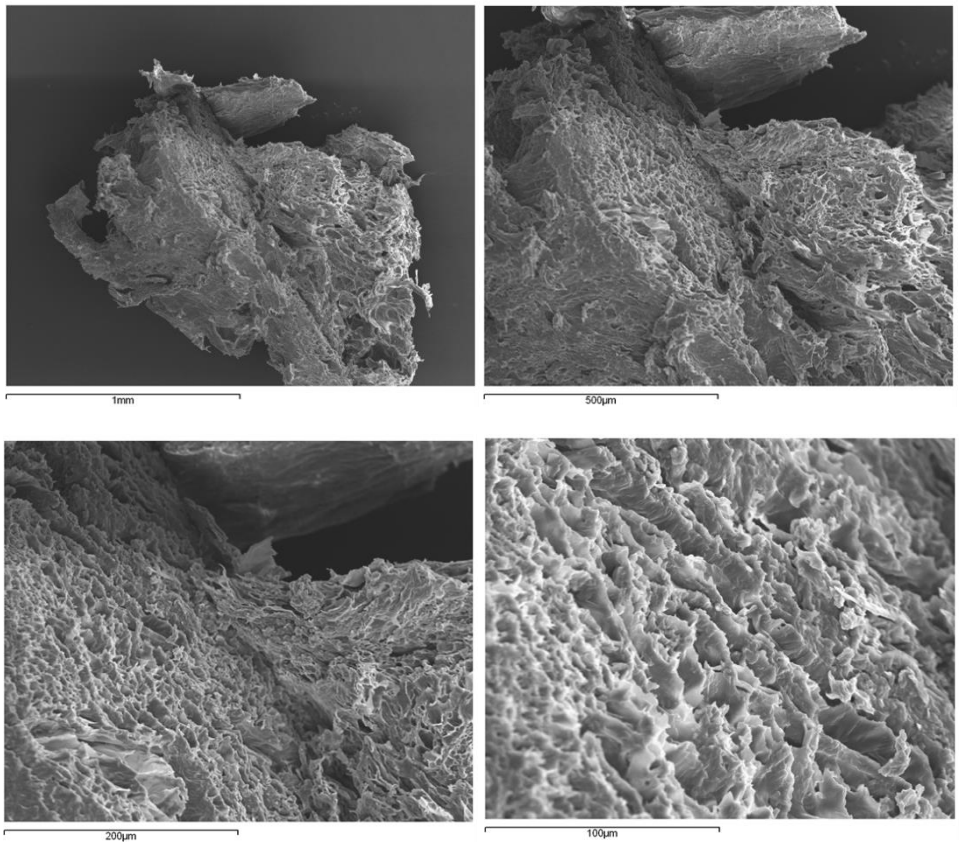

Fig. (4). SEM photomicrographs of hydrogel recorded at different magnification showing porous surface.

3.5 Impregnation of the Hydrogel with Benzydamine

The excellent results obtained by analyzing the structural properties and evaluating the swelling capacity in aqueous medium at different Ph values have suggested a possible use of gelatin-based polymers as systems for the delivery of ac- tive ingredients [15-22]. For this purpose, the benzydamine release profile at Ph 6.6 was evaluated. Its loading within the hydrogel was performed allowing the hydrogel to swell, till equilibrium, just in a benzydamine solution. Drug loading is due to various factors such as cross-linking density of the polymeric matrix, the interaction between polymer and sol- vent, etc. During the impregnation, the synthesized polymer increases in volume, but retains its three-dimensional struc- ture without disintegrating, due to its insolubility in water. The impregnation involves the interaction of an exact amount of matrix (100 mg) in a volume of 10 ml (8 ml of ethanol and 2 ml of distilled water) at a known concentration of active principle for 72 hours at 25°C. The percentage of adsorbed benzydamine (LE%) and therefore, the loading efficiency of the hydrogel was found to be 97.6%.

3.6 Release Studies

The release studies were carried out using 10 mg of hy- drogel containing benzydamine at Ph 6.6 and at different time intervals (1h, 3h, 5h 24h), using a thermo- stated bath which keeps stirring at a temperature of 37°C hydrogel. The choice of this Ph is due to the hydrogel resis- tance to a rapid volume increase at this value that corre- sponds to a diffusion, within it, of the selected medium, more controlled than that observed at Ph 4.4. This behavior should ensure a gradual and controlled release of the benzy- damine. Furthermore, this Ph is also typical of the inflammatory state at the vaginal level [23]. The ability of the polymer matrix to release the drug encapsulated into it was evaluated by spectrophotometric analysis. The drug release profile was expressed as a cumulative percentage of drug released in relation to the total dose trapped in the matrix, as a function of time (Fig. **5**).

The experimental data suggest that the situation that bet- ter mimics the vaginal surroundings in the presence of in- flammation was observed at Ph 6.6. This result was due to a benzydamine gradual and controlled release that potentially avoids its systemic absorption. The obtained results showed that benzydamine was re- leased slowly and gradually over time. These data indicated the possibility of using gelatin and glycerine hydrogel for the topical release of benzydamine in an inflammatory site, re- ducing the 156ssesse toxicity of the latter. However, it must be considered that the released drug quantity by the gelatine and glycerine based hydrogel and the progress 156ssesse by the release were not easily foreseeable elements. In fact, this phenomenon depends on numerous factors, such as the speed of water penetration into the system, which allows the poly- mer 156ssesse156156to pass from a dehydrated state to a swollen state (swelling capacity); drug-matrix interactions; the 156ssesse-physical properties of the loaded drug; the tem- perature of the release medium and the crosslinking degree of the hydrogel. This last factor, governing the swelling, in- 156ssesse the diffusion rate of the active ingredient in the fluid surrounding the hydrogel. The withdrawal of one of these factors can determine the 156ssesse156 of the release but, more likely, the final result arises from the particular combination of the aforementioned parameters that is established for each individual case. It 156ssesse necessary to consider the loading phase of the drug on the hydrogel: when the active ingredient easily succeeds in penetrating the carrier mesh, establishes with it more stable interactions and consequently, released to a lesser extent.

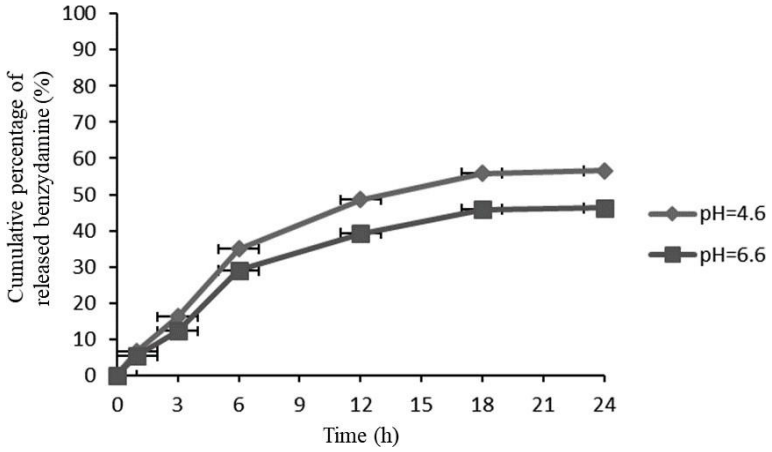

Fig. (5). Benzydamine release profile. The release studies were carried out at Ph 4.6 and 6.6 and at different time intervals (1h, 3h, 5h 24h). Data are expressed as the mean±S.D. of at least three independent experiments $p<0.05$.

3.7 Mucoadhesion Studies

The mucoadhesive capacity of the prepared hydrogels was 157ssesse157 for 2, 4 and 24h, at two different Ph values, using polyacrylic acid as a positive control. The obtained results revealed that hydrogel is more mucoadhesive than polyacrylic acid, considered as 100% mucoadhesive at Ph 6.6, typical of the vagina in inflammatory conditions (Fig. **6**). Instead, at physiological Ph, it was less mucoadhesive than polyacrylic acid (Fig. **7**).

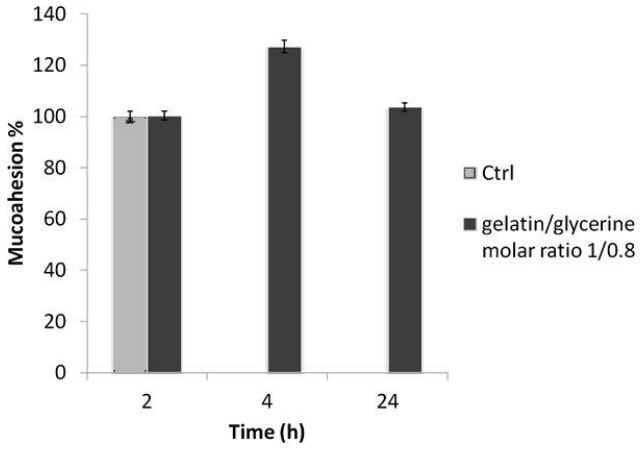

Fig. (6). Mucoadhesion % at Ph 6.6. The mucoadhesion studies were carried out at 2, 4

and 24h, at two different Ph values. Data are expressed as the mean±S.D. of at least three independent ex- periments $p<0.05$.

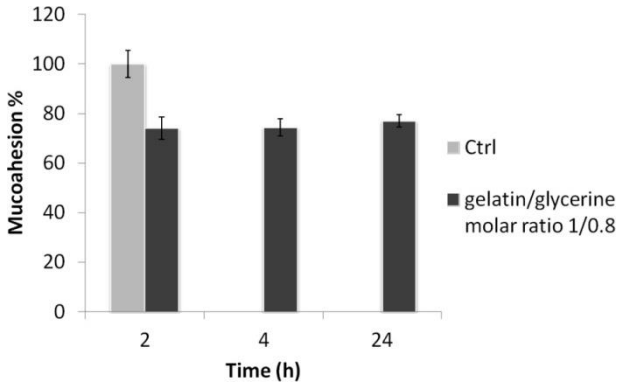

Fig. (7). Mucoadhesion % at physiological Ph. The mucoadhesion studies were carried out at 2, 4 and 24h, at two different Ph values. Data are expressed as the mean±S.D. of at least three independent experiments $p<0.05$.

4. CONCLUSION

The human vagina represents a compartment subjected to Candida colonization especially among HIV-seropositive and HIV-seronegative pregnant women [23-31]. At present, available dosage forms such as creams, gels, foams, irriga- tions, tablets and suppositories, used as vaginal drug delivery systems, show various limitations primarily due to short residence time of the drug that leads to loss of therapeutic efficacy. For this reason, in order to prolong the permanence of drug in the vaginal cavity, novel pharmaceutical forms (i.e., liposomes, vaginal rings and hydrogels) have been developed. Particularly interesting, they turned out to be bioadhesive therapeutic systems, especially in the form of hydrogels that are able to guarantee a prolonged contact between the drug and the vaginal mucosa. This work precisely focused on the preparation and characterization of a mucoadhesive hydrogel based on gelatine and glycerine that are the excipients of choice used in the preparation of conventional pharmaceutical forms, useful for the topical release of drugs at the vaginal level. The hydrogel was loaded with benzydamine, a drug able to attenuate the in- flammatory process typical of the infection. This material, which exhibits a relevant mucoadhesive activity, has been characterized

through FT-IR, electronic scanning micros- copy (SEM) and differential scanning calorimetry (DSC). Furthermore, its degree of swelling has been 159ssesse by swelling studies conducted at two different pHs and at de- fined time intervals. In particular, phosphate buffers were used at Ph 6.6, to mimic the typical conditions of infectious diseases at the vaginal level, and Ph 4.6, to simulate the physiological environment. The obtained results revealed that the hydrogel swells up well at both pHs. Release studies conducted at both pathological and physiological pHs have shown that benzydamine released in a slow and gradual manner. Therefore, all the reported data support the hypothe- sis for the use of hydrogel for site-specific release of benzy- damine into the vaginal mucosa.

REFERENCES

Roberta Cassano, Federica Curcio, Delia Mandracchia, Adriana Trapani, Sonia Trombino. Gelatin and Glycerine-Based Bioadhesive Vaginal Hydrogel, Curr Drug Deliv. 2020. 17(4):303-311.

[1] Hoare, T.R.; Kohane, D.S. Hydrogels in drug delivery: Progress and challenges. Polymer (Guildf.), 2008, 49, 1993.

[2] http://dx.doi.org/10.1016/j.polymer.2008.01.027

[3] Qiu, Y.; Park, K. Environment-sensitive hydrogels for drug deliv- ery. Adv. Drug Deliv. Rev., 2001, 53(3), 321-339.

[4] http://dx.doi.org/10.1016/S0169-409X(01)00203-4 PMID: 11744175

[5] Peppas, N.A.; Bures, P.; Leobandung, W.; Ichikawa, H. Hydrogels in pharmaceutical formulations. Eur. J. Pharm. Biopharm., 2000, 50(1), 27-46.

[6] http://dx.doi.org/10.1016/S0939-6411(00)00090-4 PMID: 10840191

[7] Gupta, P.; Vermani, K.; Garg, S. Hydrogels: from controlled re- lease to pH-responsive drug delivery. Drug Discov. Today, 2002, 7(10), 569-579.

[8] http://dx.doi.org/10.1016/S1359-6446(02)02255-9 PMID: 12047857

[9] Hussain, A.; Ahsan, F. The vagina as a route for systemic drug delivery. J. Control. Release, 2005, 103(2), 301-313.

[10] http://dx.doi.org/10.1016/j.jconrel.2004.11.034 PMID: 15763615

[11] Friend, D.R. Advances in vaginal drug delivery. Drug Deliv. Transl. Res., 2011, 1(3), 183-184.

[12] http://dx.doi.org/10.1007/s13346-011-0030-6 PMID: 25788238

[13] Vermani, K.; Garg, S. The scope and potential of vaginal drug delivery. Pharm. Sci. Technol. Today, 2000, 3(10), 359-364.

[14] http://dx.doi.org/10.1016/S1461-5347(00)00296-0 PMID: 11050460

[15] de Araújo Pereira, R.R.; Bruschi, M.L. Vaginal mucoadhesive drug delivery systems. Drug Dev. Ind. Pharm., 2012, 38(6), 643-652.

[16] http://dx.doi.org/10.3109/03639045.2011.623355 PMID: 21999572

[17] Jiménez-Castellanos, M.R.; Zia, H.; Rhodes, C.T. Mucoadhesive drug delivery

systems. Drug Dev. Ind. Pharm., 1993, 19, 143.

[18] http://dx.doi.org/10.3109/03639049309038765

[19] das Neves, J.; Bahia, M.F. Gels as vaginal drug delivery systems.

Int. J. Pharm., 2006, 318(1-2), 1-14.

[20] http://dx.doi.org/10.1016/j.ijpharm.2006.03.012 PMID: 16621366

[21] Khanvilkar, K.; Donovan, M.D.; Flanagan, D.R. Drug transfer through mucus. Adv. Drug Deliv. Rev., 2001, 48(2-3), 173-193.

[22] http://dx.doi.org/10.1016/S0169-409X(01)00115-6 PMID:

11369081

[23] Woodley, J. Bioadhesion: new possibilities for drug administra- tion? Clin. Pharmacokinet., 2001, 40(2), 77-84.

[24] http://dx.doi.org/10.2165/00003088-200140020-00001 PMID:

11286325

[25] Mathiowitz, E.; Chickering, D.; Jacob, J.S.; Santos, C. Bioadhesive drug delivery system. In: Mathiowitz, E., Encyclopedia of control- ler. Drug Deliv., 1999, 1, 9-44.

[26] Stelmachów, J.; Sawicki, W.; Śpiewankiewicz, B.; Cendrowski, K. Efficacy and tolerance of benzydamine in the treatment of vaginal infections. Med. Sci. Monit., 1998, 4(6), 1040-1042.

[27] Khade, S.M.; Behera, B.; Sagiri, S.S.; Singh, V.K.; Thirugnanam, A.; Pal, K.; Ray, S.S.; Pradhan, D.K.; Bhattacharya, M.K. Iran. Gelatin-PEG based metronidazole-loaded vaginal delivery systems: preparation, characterization, and in vitro antimicrobial efficiency. Polym. J., 2014, 23, 171.

[28] Van Den Bulcke, A.I.; Bogdanov, B.; De Rooze, N.; Schacht, E.H.; Cornelissen, M.; Berghmans, H. Structural and rheological proper- ties of methacrylamide modified gelatin hydrogels. Biomacro- molecules, 2000, 1(1), 31-38.

[29] http://dx.doi.org/10.1021/bm990017d PMID: 11709840

[30] Morimoto, K.; Katsumata, H.; Yabuta, T.; Iwanaga, K.; Kakemi, M.; Tabata, Y.; Ikada, Y. Evaluation of gelatin microspheres for nasal and intramuscular administrations of salmon calcitonin. Eur. J. Pharm. Sci., 2001, 13(2), 179-185.

[31] http://dx.doi.org/10.1016/S0928-0987(01)00094-X PMID:

11297902

[32] Price, J.H.; Ismail, H.; Gorwill, R.H.; Sarda, I.R. Effect of the suppository base on progesterone delivery from the vagina. Fertil. Steril., 1983, 39(4), 490-493.

[33] http://dx.doi.org/10.1016/S0015-0282(16)46938-4 PMID: 6832405

[34] Bruce, A.W.; Reid, G.; McGroarty, J.A.; Taylor, M.; Preston, C. Preliminary study on the prevention of recurrent urinary tract infec- tion in adult women using intravaginal lactobacilli. Int. Urogyne- col. J. Pelvic Floor Dysfunct., 1992, 3, 22.

[35] http://dx.doi.org/10.1007/BF00372644

[36] Acartürk, F. Mucoadhesive vaginal drug delivery systems. Recent Pat. Drug Deliv. Formul., 2009, 3(3), 193-205.

[37] http://dx.doi.org/10.2174/187221109789105658 PMID: 19925443

[38] Garg, S.; Tambwekar, K.; Vermani, K.; Garg, A.; Kaul, C.L.; Zaneveld, L.J.D. Compendium of pharmaceutical excipients for vaginal formulations. Pharm. Technol., 2001, 25, 14.

[39] Fernández, A.; Garcia, A.; Martin, R.H.; Olaechea, M.I.; Igartua, M.; Muñoz, J.P.; Gascón, A.R. Semi-solid mucoadhesive formula- tions., 2010.

[40] Ebhodaghe, B.I.; Ako-Nai, K.A.; Aderoba, A.K.; Anderson, W.A.; Kassim, O.O. Candida colonization of the vagina of HIV- seropositive pregnant women and their seronegative counterparts at selected health-care centers in Akure, Ondo State, Nigeria. Ann. Trop. Med. Public Health, 2016, 9, 381.

[41] http://dx.doi.org/10.4103/1755-6783.193934

[42] Cassano, R.; Trombino, S.; Ferrarelli, T.; Muzzalupo, R.; Tavano, L.; Picci, N. Synthesis and antibacterial activity evaluation of a novel cotton fiber (Gossypium barbadense) ampicillin derivative. Carbohydr. Polym., 2009, 78, 639.

[43] http://dx.doi.org/10.1016/j.carbpol.2009.05.030

[44] Cassano, R.; Trombino, S.; Ferrarelli, T.; Barone, E.; Arena, V.; Mancuso, C.; Picci, N. Synthesis, characterization, and anti- inflammatory activity of diclofenac-bound cotton fibers. Biomac- romolecules, 2010, 11(7), 1716-1720.

[45] http://dx.doi.org/10.1021/bm100404q PMID: 20536117

[46] Iemma, F.; Spizzirri, U.G.; Puoci, F.; Muzzalupo, R.; Trombino, S.; Cassano, R.; Leta, S.; Picci, N. pH-sensitive hydrogels based on bovine serum albumin for oral drug delivery. Int. J. Pharm., 2006, 312(1-2), 151-157.

[47] http://dx.doi.org/10.1016/j.ijpharm.2006.01.010 PMID: 16490328

[48] Cassano, R.; Trombino, S.; Muzzalupo, R.; Tavano, L.; Picci, N. A novel dextran hydrogel linking trans-ferulic acid for the stabiliza- tion and transdermal delivery of vitamin E. Eur. J. Pharm. Bio- pharm., 2009, 72(1), 232-238.

[49] http://dx.doi.org/10.1016/j.ejpb.2008.10.003 PMID: 18976708

[50] Cassano, R.; Trombino, S.; Ferrarelli, T.; Mauro, M.V.; Giraldi, C.; Manconi, M.;

Fadda, A.M.; Picci, N. Respirable rifampicin-based microspheres containing isoniazid for tuberculosis treatment. J. Biomed. Mater. Res. A, 2012, 100(2), 536-542.

[51] http://dx.doi.org/10.1002/jbm.a.33302 PMID: 22162280

[52] Trombino, S.; Cassano, R.; Bloise, E.; Muzzalupo, R.; Tavano, L.; Picci, N. Synthesis and antioxidant activity evaluation of a novel cellulose hydrogel containing trans-ferulic acid. Carbohydr. Po- lym., 2008, 75, 184.

[53] http://dx.doi.org/10.1016/j.carbpol.2008.05.018

[54] Bhowmik, S.; Islam, J.M.M.; Debnath, T.; Miah, M.Y.; Bhattachar- jee, S.; Khan, M.A. Reinforcement of Gelatin-Based Nanofilled Polymer Biocomposite by Crystalline Cellulose from Cotton for Advanced Wound Dressing Applications. Polymers (Basel), 2017, 9(6), 222.

[55] http://dx.doi.org/10.3390/polym9060222 PMID: 30970900

[56] Hay, P.; Czeizel, A.E. Asymptomatic trichomonas and candida colonization and pregnancy outcome. Best Pract. Res. Clin. Obstet. Gynaecol., 2007, 21(3), 403-409.

[57] http://dx.doi.org/10.1016/j.bpobgyn.2007.02.002 PMID: 17512254

PART D

Polysaccharides and proteins-based hydrogels for tissue engineering applications

Abstract

Tissue engineering is a branch of science that studies the possibility of repairing organs and tissues of the human body, such as muscles, bones, cartilage, and skin, damaged by a disease, accident, or aging, restoring its integrity and functionality without resorting to transplants or prostheses, thus ensuring a better quality of life for patients. To achieve this, it is necessary to integrate biological components, such as cells and growth factors, with biomaterials. In particular, implants made up of living cells are designed to proliferate on biocompatible and bioabsorbable materials. Among these, materials of natural origin are more interesting because they are characterized by several very important properties to create a favorable microenvironment for the healing process. This chapter fits into this context and aims to describe the polysaccharides- and protein-based biomaterials particularly useful for tissue engineering and their major applications**.**

Keywords: Biomaterials, polysaccharides hydrogels, proteins hydrogels, tissue engineering applications.

1. Introduction

In recent years, the need for biomaterials useful for the promotion, regeneration, or replacement of damaged tissues has increased considerably. Tissue engineering represents a new frontier for the biomedical field and its primary purpose is to repair or even replace damaged tissues and organs such as muscles, bones, and cartilages (Langer and Vacanti, 1993; Saunders and Ma, 2019) from diseases, trauma, or aging, restoring their integrity and functionality, thus permitting a better quality of life. The purpose of tissue engineering is to use scaffold matrices to fill the tissues and/or cells and, therefore, treat the tissues after a transplant (Howard et al., 2008). Tissue scaffolds cannot only cover the wound and provide a physical barrier but can also offer a cellular skin with excretive biological components to stimulate re-epithelialization and formation of granulation tissue (Yadav and Chauhan, 2017). Various materials can be used as scaffolds for distinct tissue. Among them, natural polymers are most attractive; thanks to their bioactive properties such as antimicrobial, immunomodulatory, cell proliferative, and angiogenic for their similarieties with the extracellular matrix (ECM), biodegradability, and good biological performance (Mano et al., 2007). All these factors are very important to create a favorable microenvironment for the healing process (Velema and Kaplan, 2006; Sahana and Rekha, 2018). In this context, polysaccharides and proteins are natural biomaterials, which have found many applications in tissue regeneration. In particular, polysaccharides are characterized by functional groups that are essential for the development of materials applicable in tissue regeneration as well as exhibiting a high biocompatibility and biodegradability. Biomaterials, based on proteins, have also been explored for tissue engineering. Although proteins are highly biocompatible, they are also characterized by rapid degradation and low mechanical resistance that cause a lack of structural support during the formation of the new tissue (Khan and Ahmad, 2013). Among the most promising biomaterials used in biomedical field are hydrogels, a class of materials with three-dimensional (3D) network of hydrophilic polymers chains capable of retaining a significant amount of water (Peppas and Hoffman, 2020). Hydrogels have good biocompatibility, production flexibility, variable composition, and physical properties (Lee and Kim, 2018) that enable to mimic the highly hydrated ECM and to facilitate nutrients and oxygen transport due to their porous structure (Lee and Mooney, 2012; Caló and Khutoryanskiy, 2015; Saunders and Ma, 2019).

The present chapter aims to describe hydrogels based on polysaccharides such as chitosan, cellulose, alginate, hyaluronic acid, and proteins such as collagen, gelatin, elastin, and their various applications in the field of tissue engineering will be highlighted (Figure 8.1).

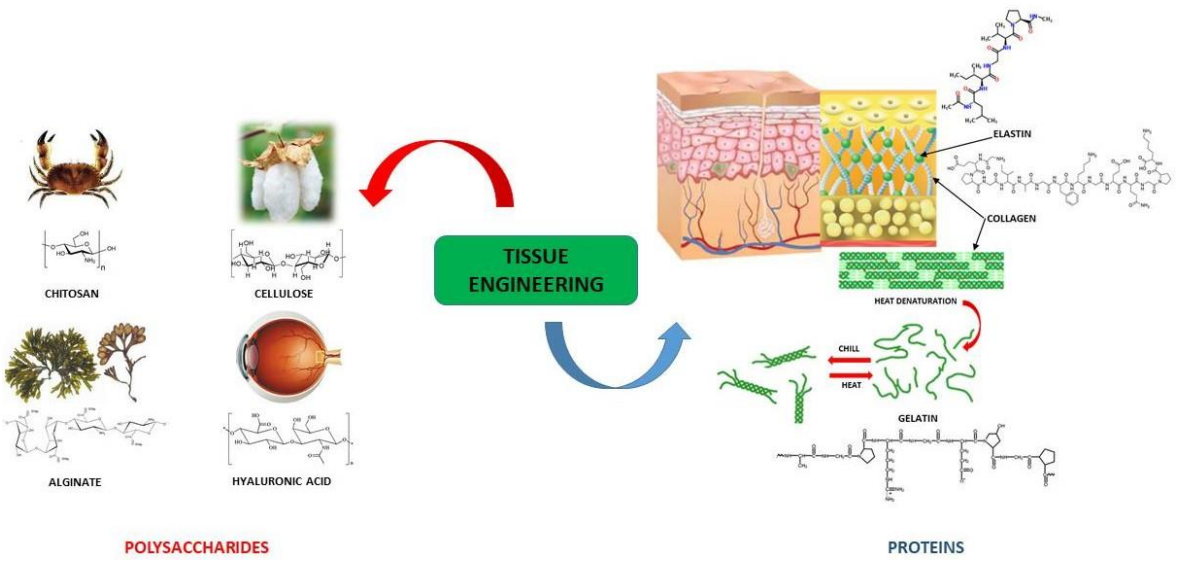

Figure 8.1: Natural sources of biomaterials for tissue engineering.

2. Polysaccharide-based Biomaterials

Polysaccharides are macromolecules with excellent properties including biodegradability and biocompatibility that are the precious features of polymers application for biomaterial applications (Zhu at al., 2019). For this reason, polysaccharides have recently gained increasing attention from numerous researchers owing to their applications in pharmaceuticals and biomedical field. In this section, the principal polysaccharides used in tissue engineering will be described.

2.1 Chitosan

Chitosan is a linear polysaccharide composed of (1–4)-2-acetamido-2-deoxy-b-D-glucan (*N*-acetyl- D-glucosamine) and (1–4)-2-amino-2-deoxy-*b*-D-glucan (D-glucosamine) units (Figure 8.2) that can be easily derived from the partial deacetylation of chitin (Rinaudo, 2006).

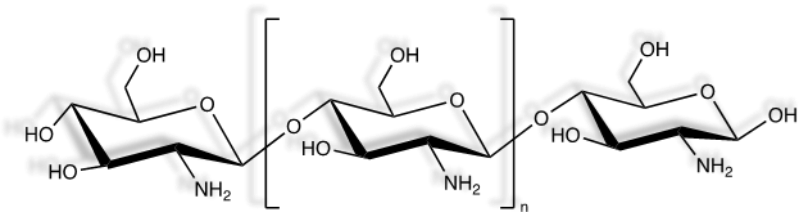

Figure 8.2: Chitosan chemical structure.

Chitosan has drawn considerably more attention due to its environmentally friendly nature, biocompatibility, biodegradability, and availability (Baranwal et al., 2018). It is also particularly interesting in bone regeneration because it facilitates the attachment and proliferation of osteoblasts

as well as the process of bone mineralization (Sheehy et al., 2013). Furthermore, this polysaccharide can be enzymatically degraded by lysozyme (Varum et al., 1997; Pangburn et al., 1982), a polycationic protein present in the ECM of human cartilage (Moss et al., 1997; Greenwald et al., 1972) and, for this reason, it is able to modulate chondrocyte morphology, differentiation, and stimulating chondrogenesis. Furthermore, compared to many synthetic polymers, chitosan degradation products are nontoxic (Levengood and Zhang, 2014). Therefore, various methodologies have been developed to obtain chitosan hydrogels and foams as 3D scaffolds particularly useful for tissue engineering (Croisier and Jérôme, 2013).

Several injectable chitosan-based hydrogels have been developed for cartilage repair (Choa et al., 2004; Hong et al., 2007; Chena and Chen, 2006). These hydrogels can be prepared by both physical and chemical cross-linking methods. Reversible physical interactions in poly(*N*-isopropylacrylamide) (PNIPAM)- or polyethylene glycol (PEG)-grafted chitosan derivatives have been used to obtain physically cross-linked hydrogels (Bhattarai et al., 2005; Berger et al., 2004). These physical gels are generally characterized by a low stability, low mechanical strength, and rapid degradation. Chemically cross-linked injectable chitosan hydrogels are prepared using redox-initiated cross-linking (Hong et al., 2006) and photoinitiated cross-linking (Amsden et al., 2006). Furthermore, the properties of these chemically cross-linked hydrogels such as gelation time, gel modulus, and hydrogel degradability can be tuned by changing the molecular weight of polymers and the cross-linking densities. In fact, Hong et al. (2007) reported the preparation of

methacrylated chitosan-based hydrogels using ammonium persulfate and *N*,*N*,*N*′,*N*′-tetramethylethylenediamine with increased concentration of the initiator. Consequently, the gelation time could be reduced, and the enzymatic degradation of the resulting hydrogels could be decreased.

Naderi-Meshkin et al. (2014) proposed the synthesis of a chitosan-beta glycerophosphate-hydroxyethyl cellulose (CH-GP-HEC) scaffold with a sol–gel transition at 37 °C. Chondrogenic factors or mesenchymal stem cells (MSCs) were included in the hydrogel. Subsequently, in order to correct the defects of the cartilage tissue, the CH-GP-HEC hydrogel was injected into the lesion site and the viability of the encapsulated MSCs was assessed by coloring with iodide-fluorescein diacetate and propidium. After inducing a differentiation process with the growth factor tβ3, the chondrogenic differentiation capacity of the encapsulated human MSC (hMSC) was determined. These cells, inserted inside the CH-GP-HEC hydrogel, showed excellent survival and proliferation rates during the 28 days of observation. The CH-GP-HEC hydrogel also provided suitable conditions for chondrogenic differentiation of the encapsulated hMSCs.

Another interesting study was proposed in 2014 by Choi et al. They investigated the incorporation of type II collagen (Col II) and chondroitin sulfate (CS) in chitosan-based injectable hydrogels gelled after exposure, in the presence of riboflavin, to visible blue light (VBL). Infact, Col II and CS are components of the cartilage ECM that play a crucial role in chondrogenesis. Unfortunately, the direct use of scaffolds for cartilage regeneration is limited due to their instability and rapid enzymatic degradation. For this reason, Choi and collaborators thought of incorporating Col II and CS into a chitosan hydrogel. Since the unmodified hydrogel was able to promote the multiplication and placement of cartilaginous ECMs allowed by encapsulated chondrocytes and MSCs, the idea of incorporating Col II or CS into the chitosan hydrogels has contributed to increasing the process of chondrogenesis, especially by Col II. This is attributable to the binding of integrin α10 to Col II, which promoted an increased cell-matrix adhesion, thus favoring the cartilage regeneration.

In 2018, Wu et al. obtained PNIPAM-g-chitosan injectable and thermosensitive hydrogel characterized by the absence of toxicity. They are characterized by high biocompatibility, biodegradability and, after injection, show a rapid phase transition, therefore are ideal candidates as vectors of cells or implanted scaffolding. To strengthen its mechanical properties, Wu and collaborators have thought of covalently bonding thiol side chains in

chitosan through the conjugation of *N*-acetylcysteine by carbodiimide. After oxidation of the thiols in disulfide bonds, the hydrogels showed a better compression modulus.

Through in vitro proliferation studies, a great biocompatibility of hydrogels toward MSCs, fibroblasts, and osteoblasts has been shown allowing the encapsulation of cells without toxicity. These results suggested the potentiality of the thiol-modified thermosensitive polysaccharide hydrogels as cell-laden biomaterial for tissue regeneration.

An interesting work was also proposed by Xu and collaborators in 2018. They made a biodegradable composite carboxymethyl chitosan (CMCS) hydrogel conductive by in situ chemical polymerization using poly(3,4-ethylendioxythiophene) (PEDOT) as a conductive polymer layer. This hydrogel has proven to be potentially useful for nerve tissue engineering. In dependence of the different contents of PEDOT, the physicochemical and electrochemical properties of the conductive hydrogels (PEDOT/CMCS) were analyzed. In addition, in vitro studies have shown the lack of toxicity of the PEDOT/CMCS hydrogels, the adhesive capacity, the viability, and cell proliferation. In particular, after a culture for 9 days, the PEDOT layer of the conductive hydrogels improved the diffusion and proliferation of pheochromocytoma cells in rat-like neurons even in the absence of electrical stimulation. Furthermore, the inclusion of PEDOT in the CMCS hydrogels allowed the hydrogel to have both greater mechanical strength and conductivity and to preserve their biocompatibility. These results suggested the use of these conductive hydrogels (PEDOT/CMCS) as nerve regeneration scaffold materials. An injectable chitosan-based hydrogel, useful for bone tissue engineering, was developed by Saekhor and colleagues. In particular, they wanted to obtain a water- soluble and thixotropic chitosan particularly useful as an injectable liquid with the ability to form a hydrogel under physiological conditions. For this reason, chitosan was reacted with carboxymethyl chloride to obtain CMCS. The latter was conjugated with α-cyclodextrin (α-CD) to produce CMCSCD. This conjugation improved the solubility, in knowledge, of the hydrophobic cavity to produce as cross-linking points by forming an inclusion complex with PEG. The sol–gel transition was formed within 450 ± 10 min to obtain a complete (yellow) soft gel. Through the scanning electron microscope, both the surface and cross-section were observed, showing an interconnected porous structure of the gel, making it suitable for transport of extracellular fluid and nutrients and hormones to cells and waste removal.

Moreover, in vitro experiment with sarcoma osteogenic (SaOS-2) cell line indicated that this injectable hydrogel was potentially compatible, nontoxic to the SaOS-2 cells, and capable to promote cell proliferation. Based on all obtained results, the CMCSCD/PEG demonstrated to be a promising scaffold for bone tissue engineering. Very recently also, Nezhad-Mokhtari et al. have developed a new injectable hydrogel based on collagen, aldehyde modified-nanocrystalline cellulose, and chitosan loaded with gold nanoparticles (collagen/ADH- CNCs/CS-Au) for tissue engineering applications (Nezhad-Mokhtari et al., 2020). In particular, solutions of collagen/CS-Au and ADH-CNCs were mixed resulting in an intermacromolecular Schiff base cross-linking reaction, obtaining a rapid formation of the hydrogel. With the aim to control the microscopic morphology, swelling degree, gelation time, and degradation rate, various molar blending ratio of collagen/CNCs/CS-Au were used. The MTT assay, performed with mouse fibroblast cells (NIH 3T3), highlighted the effectiveness and nontoxicity of the obtained hydrogel. In addition, the reinforcing with the addition of CNCs and CS-Au, to form the hydrogel, was an interesting approach to improve the mechanical strength and degradation resistance of the scaffold. It could be concluded that also this hydrogel may be a good candidate as a new biomaterial for tissue engineering applications.

2.2 Cellulose

Cellulose (Figure 8.3) is a glucose polysaccharide that has a straight chain consisting of several (1– 4) linked D-glucose units. It is the most plentiful biopolymer on earth and found in the cell wall of green plants, many algae, and other microorganisms such as oomycetes or bacteria (Novotna et al., 2013).

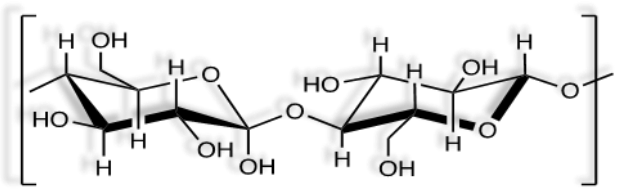

Figure 8.3: Cellulose chemical structure.

Bacterial cellulose (BC) is an interesting material as implant and scaffold in tissue engineering (Peterson and Gatenholm, 2011). In fact, it is notable for biocompatibility, mechanical resistance, and ability to be structurally and chemically engineered at nano-, micro-, and macroscales. BC hydrogels are promising materials for making dressings thanks to its properties such as purity, maintaining adequate humidity, and flexibility in adapting to any wound, forming a tight barrier between the wound itself and the external environment, thus avoiding bacterial infections (Valle et al., 2017).

Cellulose (CB) hydrogels can be obtained from pure and native cellulose by dissolving with LiCl/dimethylacetamide (DMAc), *N*-methylmorpholine-*N*-oxide (NMMO), ionic liquids (ILs), alkalis/urea (or thiourea), or producing them from BC (Shen et al., 2016). Cellulose derivatives usually include esters such as cellulose acetate phthalate (CAP) [e.g., cellulose acetate (CA), cellulose acetate trimellitate], hydroxypropyl methylcellulose phthalate, cellulose acetate butyrate (CAB), or ethers [e.g., methyl cellulose (MC), ethyl cellulose (EC), hydroxyethyl cellulose (HEC), carboxymethyl cellulose (CMC), sodium carboxymethyl cellulose (NaCMC), hydroxypropyl cellulose, and hydroxypropyl methylcellulose (HPMC)]. Other types of hydrogels are constituted from mixtures of natural polymers, polyvinyl alcohol, polyelectrolyte complexes, interpenetrating polymer network, and inorganic hybrid cellulose hydrogels (Chang and Zhang, 2011; Onofrei and Filimon, 2016; Sannino et al., 2009). These hydrogels are being studied for possible biomedical applications and, in particular, in tissue engineering (Kabir et al., 2018).

The capacity of a hydrogel made of BC/acrylic acid (AA) to release human epidermal keratinocytes and dermal fibroblasts (DFs), useful for the full-thickness skin lesions treatment, was evaluated by Loh and collaborators (Loh et al., 2018). Through in vitro studies, they proved the excellent cell attachment of the BC/AA hydrogel, the maintaining of cell viability with a narrow migration, and allowing a cell transfer. In vivo studies, histological, immunohistochemistry, and transmission electron microscopy analysis indicated that hydrogel alone and hydrogel with cells (HCs) accelerated wound healing compared to the untreated controls. Therefore, the BC/AA hydrogel could be an interesting cellular vector for the release of keratinocytes and fibroblasts, thus promoting wound healing. In the same year, Boyer et al. have made a composite hydrogel containing a small amount of nanoreinforced clay, called laponite, which can stick within the hydroxypropyl methylcellulose (Si- HPMC) silicate hydrogel structure. Therefore, composite hydrogels were made by mixing laponites with Si-HPMC thus, developing a hybrid interpenetrating network that increased their mechanical properties. The in vitro investigations showed no

side effects from the laponites. Furthermore, through in vivo studies, conducted for 6 weeks using nude mice, the capacity of the hybrid scaffold, made with composite hydrogel and chondrogenic cells, to form cartilage tissue was evaluated. Histological studies showed that the new cartilage-like tissue was characterized by an ECM including glycosaminoglycans (GAGs) and collagens. These results indicated the possibility of using the composite hydrogel for the treatment of cartilage defects. With the aim to obtain a biomaterial to treat tissue defects, Ghorbani and Roshangar have prepared and characterized injectable hydrogels based on collagen and modified nanocrystalline cellulose [cellulose nanocrystals (CNCs)] (Ghorbani and Roshangar, 2019). The surface of CNCs was functionalized with aldehyde groups using an oxidation manner of nanocrystalline cellulose in water with sodium periodate. The surface morphology of hydrogels with different ratios of CNCs has been analyzed evaluating the macroscopic physical properties and microscopic internal structure. Swelling tests showed that the hydrogels maintain their structure over the course of 60 days and were, thus, suitable for longer term applications. The results of toxicity studies for CNCs, aldehyde-modified CNCs, and the CNC-reinforced hydrogels support the potential application of these materials for biomedical applications.

Recently, Li et al. have proposed a green and simple method to prepare a series of all-natural chitosan-dialdehyde bacterial cellulose (CS-DABC) hydrogels. In particular, for the first time, to prepare these hydrogels, was used ascorbic acid as solvent to dissolve chitosan and the natural fiber DABC as reinforcing and cross-linking agent (Li et al., 2020). The disadvantage of the use of acetic acid and other toxic cross-linking agents was bypassed making these hydrogels biocompatible. Moreover, due to the supporting of DABC nanofibers and introduction of dynamic balance of the Schiff base structure in the cross-linked network, these hydrogels exhibited good mechanical properties, self-healing ability, and injectability. Consequently, these hydrogels can be used as good, sustained release systems of drugs to promote wound healing indicating great potential in the field of wound dressings or tissue engineering. Among the latest interesting research on cellulose-based hydrogels for tissue engineering applications, there is the work of Gupta and his collaborators (2020). They proposed a green synthesis to prepare nanoparticles using eco-friendly chemicals such as silver, a broad spectrum natural antimicrobial substance, and curcumin a natural polyphenol with healing properties. The hydrophobicity of curcumin was bypassed by its microencapsulation in hydroxypropyl-cyclodextrins, which, in turn, were then loaded into BC hydrogels. These hydrogels demonstrated broad-spectrum

antimicrobial activity against three common pathogenic microbes that infect wounds such as *Staphylococcus aureus*, *Pseudomonas aeruginosa*, and *Candida auris*. They showed also with antioxidant properties, high cytocompatibility, with the tested cell lines. In addition, the high moisture content and the good level of transparency of the hydrogels indicated a possible application in the management of chronic wounds with high microbial bioburden.

2.3 Alginate

Alginate (Figure 8.4) is a natural anionic and hydrophilic polysaccharide typically obtained from brown seaweed and bacteria. It contains blocks of β-(1→4)-linked-D-mannuronic acid (M) and α- (1→4)-linked-L-guluronic acid (G) monomers (Figure 8.4). Alginate is interesting for many biomedical applications due to its excellent biocompatibility, low toxicity, low cost, and for its ability to gel in the presence of bivalent cations such as Ca^{2+} (Langer and Vacanti, 1993; Lee and Mooney, 2012). In particular, alginate hydrogels have a structural resemblance to the extracellular matrices of living tissues. In fact, alginate-based treatments could maintain a physiologically moist microenvironment, minimize bacterial infection at the wound site, and facilitate healing.

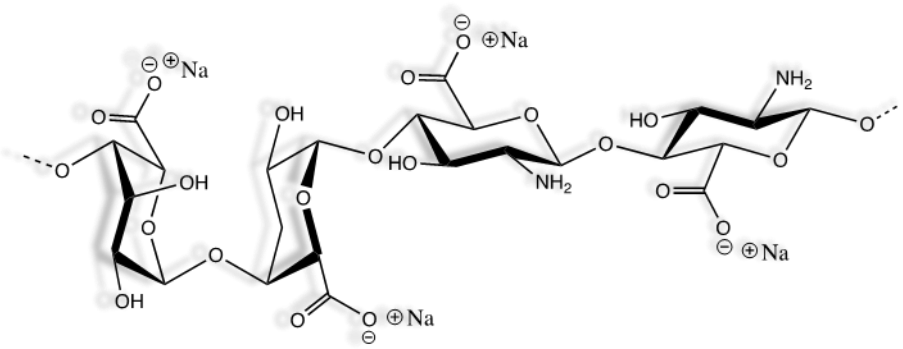

Figure 8.4: Alginate chemical structure.

Furthermore, alginate is an appropriate material for several tissue engineering applications such as cell encapsulations and biofabrications (Li et al., 2006; Song at al., 2011). Nevertheless, alginate is not able to promote cell attachment due to poor cell–material interactions, causing slow degradation with unfavorable degradation kinetics (Gao et al., 2009). To overcome these drawbacks, specific proteins have been considered for their similarity to the ECM to enhance cellular interaction and to improve degradability, biocompatibility, and the availability of alginate hydrogel (Wang and Shansky, 2012).

To this aim, Silva et al. (2014) developed a hybrid hydrogel based on alginate and keratin extracted from wool. This hydrogel was made in 2D and 3D conformations and was characterized by chemical–physical analyses. Studies on primary human umbilical vein endothelial cells have also been performed to highlight the ability of these hybrid hydrogels to promote cell attachment, proliferation, diffusion, and viability. It has been shown that the cells seeded on the 2D hydrogel surface remained viable for up to 10 days of culture, forming a monolayer and showing the typical endothelial morphology, instead the encapsulated cells remained viable for up to 4 weeks. During this culture time, the number and mitochondrial activity of the cells increased, and the cells started to propagate. Hence, hybrid alginate/keratin hydrogels could be promising biomaterial for regenerative medicine applications.

In 2017, Chen et al. developed a drug-loaded hydrogel, produced using ion cross-linking, for use in oral bone tissue regeneration (Chen et al., 2017). This hydrogel was made of calcium alginate at different concentrations (12.5, 25, and 50 mg/mL) and displayed a high plastic behavior and biological properties suitable for promoting the regeneration of oral bone tissue. The swelling degree, degradation time, and release rate of bovine serum albumin were also assessed. Human periodontal ligament cells and bone marrow stromal cells were maintained in culture together with calcium alginate hydrogen and polylactic acid as control and then the cellular proliferation was examined. Inflammatory-related factor gene expressions of human periodontal ligament cells and osteogenesis-related gene expressions of bone marrow stromal cells were observed. The materials, implanted in the subcutaneous tissue of the rabbits, showed a favorable biocompatibility. The results of the studies demonstrated that calcium alginate hydrogels caused less inflammation than the polylactic acid and had superior osteoinductive bone ability to the polylactic acid. The drug- loadable calcium alginate hydrogel system could represent an interesting approach for bone defect reparation and, thus, useful in clinical dental applications.

With the aim to verify the mineralization and differentiation potential of human dental pulp stem cells (DPSCs) seeded onto scaffolds based on alginate and nanohydroxyapatite, it has been previously described and evaluated by Turco et al (2009). Sancilio and collaborators (2018), in their work, made use of hydroxyapatite (HAp) as inorganic strengthening and osteoconductive element of alginate/HAp composite scaffolds. These scaffolds are actually valued as possible strategy in bone tissue engineering because they can efficiently support the adhesion, colonization, and matrix deposition of osteoblast-like cells without any supplementary chemical alginate modification.

In particular, Sancilio and collaborators inserted the HAp in an alginate solution and the internal gelation was generated by the addition of delta-lactone of the D-gluconic acid which induced the slow hydrolysis of the acid with consequent direct calcium ion release from HAp. Human DPSCs are clonogenic cells capable of differentiating in multiple lineages. To this end, the components of the ECM, the vitality parameters, and oxidative stress, as well as the gene expression profile of the markers related to both early and late mineralization process, were assessed and analyzed.

So, Sancilio et al. have demonstrated that DPSCs expressed osteogenic differentiation-related markers and promoted calcium deposition and biomineralization when growing onto alginate/HAp scaffolds.Therefore, these alginate/HAp scaffolds have proven to be composite materials suitable for tissue engineering, as they are able to promote specific tissue regeneration as well as the formation of mineralized matrices and the regeneration of natural bone.

More recently, Reakasame and Boccaccini described, in their review, the possibility of using oxidized alginate (OA)-based hydrogels that have drawn considerable importance as a biodegradable material for tissue engineering applications due to the higher degradation rate and the presence in OA of more reactive groups than native alginate (Reakasame and Boccaccini, 2018). So, the OA-based hydrogel could be successfully used in various engineering tissue applications such as repair of bone, cartilage, cornea, blood vessel, and other soft tissues. With the aim to mimic the complex inorganic/organic structure of bone, Diaz-Roriguez et al. synthesized new biomimetic hydrogels based on mineralized calcium alginate following the addition of biomineral calcium carbonate microparticles obtained from mussels or oysters (OYs) shells. This innovative strategy also has the advantage of exploiting natural components, since alginate would have the function of forming the biodegradable polymer matrix while the calcium carbonate stimulating cell differentiation by mimicking the nanostructure of the tissue. Alginate hydrogels containing 7 mg/mL of OY particles promoted the osteogenic differentiation of hMSCs. Thus, the incorporation of calcium carbonate particles in alginate networks was able to modulate cell differentiation. Furthermore, the presence of calcium carbonate in alginate matrix could improve long-term stability of alginate hydrogels. So, Roriguez et al. highlighted the importance of the type of alginate and the origin of calcium carbonate to obtain valid systems for the engineering of bone tissue capable of modulating both mechanical properties and cell differentiation.

In 2019, Homaeigohar et al. functionalized graphite nanofilaments to get better, mechanical, electrical, and biological properties of an alginate hydrogel and accelerated nerve regeneration. CA functionalization by a green and simple approach permitted to induce the formation of oxygen containing functional groups on the surface of graphite nanofilaments, thereby ensuring their uniform distribution within the alginate matrix. Its biocompatibility has even been enhanced as shown by the use of in vitro MSCs. The uniformly distributed nanofilaments increased the mechanical stability of the nanocomposite hydrogel compared to pure one by up to three times. Furthermore, the nanofilaments were able to give electrical contact and intercellular signaling stimulating their biological activity. In vivo tests highlighted the applicability of the nanocomposite hydrogel for implantation within body showing no adverse reaction and no inflammatory responses after 2 weeks after its implant. The obtained results demonstrated that the electroactive nanocomposite hydrogel, stimulating nerve generation, could be potentially useful for neural tissue engineering applications.

In 2020, Shafei and coworkers designed and realized an alginate-based hydrogel loaded with exosomes (EXOs), nano-size membrane vesicles isolated from cultured adipose-derived stem cells that could promote migration, proliferation, and angiogenesis process in skin wound through modulation of the secretory activity of DFs and could improve the synthesis and secretion of collagen/elastin with a better re-epithelialization (Shafei et al., 2020). The degradability evaluation of EXOs-loaded hydrogel and cell viability studies confirmed the favorable properties of hydrogel for in vitro and in vivo applications. Moreover, the release of EXO from alginate hydrogel indicated that this structure was suitable for controlled release of small bioactive molecules including secreted EXO derivatives and growth factors. Consequently, alginate hydrogel could enhance wound closure, collagen synthesis, and vessel formation in the wound area, and it could represent a good therapeutic strategy for skin wounds healing. Recently, Ehterami and collaborators also developed a vitamin D3-loaded alginate hydrogel for wounds healing. Various vitamin D3 concentrations were added to sodium alginate and cross-linked by calcium carbonate in combination with D- gluconolactone. The swelling behavior, weight loss, microstructure, and cyto- and hemocompatibility of obtained hydrogels were assessed. Furthermore, the therapeutic efficacy of prepared materials was evaluated in the full-thickness dermal wound model. The hydrogels study through scanning electron microscopy (SEM) showed their highly porosity and the presence of interconnected pores. In addition, the hydrogels resulted in biodegradable (being its weight loss percentage of about 89% in 14 days) hemo-

and cytocompatible. In particular, in vivo studies indicated that the alginate hydrogel/3,000 IU vitamin D3 exhibited more highest capacity of wound closure, best performance, and induced highest re-epithelialization and granular tissue formation. These results indicated that alginate hydrogels with 3000 IU of vitamin D3 could be useful as a dressing to treat skin wounds (Ehterami et al., 2020).

2.4 Hyaluronic Acid

Hyaluronic acid (HA) (Figure 8.5) is a GAG, composed by repeating disaccharide units of *N*-acetyl- D-glucosamine and D-glucuronic acid, and synthesized in bacteria, birds, and mammals.

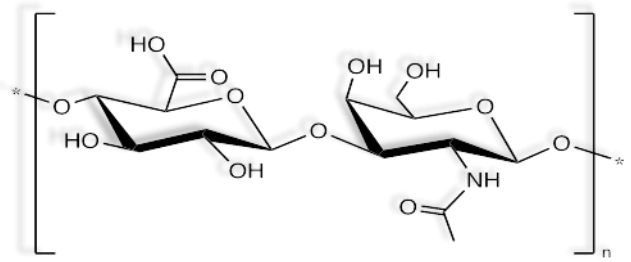

Figure 8.5: Hyaluronic acid chemical structure.

It is found in the body in pericellular matrices, various body fluids, and in specialized tissues such as the vitreous humor of the eye and cartilage. Its physical properties and viscoelastic behavior make HA a precious biomaterial thanks also to the ability of assembly into extracellular and pericellular matrices and its effects on cell signaling (Falcone et al., 2006). HA is characterized by physicochemical properties such as the solubility and the presence of reactive functional groups that allow chemical changes on HA, which makes it attractive for tissue regeneration. Furthermore, these materials do not cause allergies or inflammations and their hydrophilicity which make them particularly interesting also as injectable fillers via the skin and soft tissues (Hemshekhar et al., 2016; Trombino et al., 2019).

Tan et al. reported a new biodegradable and biocompatible hydrogels and composites derived from oxidized HA and water-soluble chitosan after mixing, without the addition, of a chemical cross-linking agent (Tan et al., 2011). Furthermore, the gelation was obtained

by the Schiff base reaction between amino and aldehyde groups of polysaccharide derivatives. In particular, *N*-succinyl chitosan and aldehyde hyaluronic acid were synthesized to prepare composite hydrogel and its potential as an injectable scaffold was shown encapsulating the bovine articular chondrocyte. Therefore, the composite hydrogel promoted cell survival and cells were able to preserve the morphology of the chondrocytes. These characteristics suggested the possibility of using injectable composite hydrogels in tissue engineering.

In 2018, Sani et al. made a elastic, antimicrobial, and adhesive hydrogel composed of methacrylated HA (MeHA) and an elastin-like polypeptide (ELP), which can be rapidly photoreticulated in situ for the purpose of regenerating and repairing different tissues. Therefore, hydrogel hybrids with various physical properties have been designed and modifying the concentrations of MeHA and ELP. In addition, adhesion tests have shown that the MeHA/ELP hydrogels have a greater adhesive force toward the tissue than the commercial tissue adhesives. The incorporation of zinc oxide (ZnO) nanoparticles conferred antimicrobial properties to the hydrogel that inhibited the growth of methicillin-resistant *S. aureus* (MRSA) compared to controls. Furthermore, the MeHA/ELP hydrogels did not induce any significant inflammatory response. They could also be efficiently biodegraded by promoting the integration of new autologous tissue. In a recent paper, Rezaeeyazdi et al. described the preparation of several injectable cryogels based on HA and gelatin. Their idea was to combine both physicochemical characteristics of HA and intrinsic cell adhesion characteristics of gelatin, providing sufficient physical support for attachment, survival, and diffusion of cells. The physical characteristics of gelatin cryogels, such as mechanics and injection, have also improved after copolymerization with HA. The adhesion of mouse fibroblast cell lines (3T3), grown in HA cryogels, was increased when expressed with gelatin. In addition, the cryogels had a minimal effect on the activation of dendritic cells in the bone marrow, underlining their cytocompatibility. In vitro studies have shown that HA-copolymerized gelatin has not significantly changed their intrinsic biological characteristics, so the HA-cogelatin cryogels combine the favorable capacity of single biopolymer giving a strong system from the point of mechanical view, susceptible to cells, with macroporous and injectable structure and, therefore, interesting for tissue engineering applications.

Han et al. proposed a biocompatible and in situ cross-linkable hydrogel arised from HA. The hydrogel was obtained through a bioorthogonal reaction and tested for the regeneration of cartilage in vivo. The gelling reaction is attributable to copper-free click

reactions between an azide and a dibenzyl cyclooctyne (DBCO). In particular, the HA-PEG4-DBCO hydrogel was synthesized and cross-linked through 4-arm PEG azide and the effects of the relationship between HA-PEG4-DBCO and PEG 4-arm azide on gelation time, microstructure, morphology superficial, balance swelling, and compression module were also evaluated. In order to evaluate the in vitro and in vivo capacity of the obtained hydrogel as injectable scaffold, chondrocytes were encapsulated inside it. The obtained results underlined how the hydrogel is capable of supporting cell survival and the cells able to regenerate cartilage tissue confirming the ability of the injectable hydrogel to be used in tissue engineering applications. In 2019, Luo et al. preapared two in situ injectable hydrogels made of gelatin (sc-G) and HA/gelatin (HA/G) for hemorrhage control. In particular, these materials were prepared by cross-linking gelatin and HA with *N*-(3-dimethylaminopropyl)-*N′*-ethylcarbodiimide hydrochloride (EDC) and *N*-hydroxysuccinimide on the surface of the tissue in situ and analyzed by rheological, stability, cytotoxicity, and burst resistance tests. Their hemostatic capacity was assessed in a bleeding rat model of the liver. The sc-G and HA/G hydrogels that were able to gel in the 90s and 50s, respectively, have been shown to be suitable for cell attachment and proliferation. Bursting forces was even greater than that of fibrin glue. The hemostatic power of the HA/G hydrogel was found to be better than that of the sc-G hydrogel and was comparable to that of fibrin. These results indicated a possible use in particular of HA/G hydrogel as tissue sealant for hemorrhage control in clinic. A remarkable study undertaken by Makvandi and coworkers reported the synthesis of thermosensitive and injectable hydrogels synthesis, containing tricalcium phosphate, HA, and corn silk extract-nanosilver (CSE-Ag NPs) for potential use in bone tissue regeneration applications. In particular, spherical silver nanoparticles were synthesized through a microwave-assisted green approach using corn silk extract without using toxic chemical reagents thus, making them more suitable for clinical and biomedical applications. Rheological experiments indicated that the thermosensitive hydrogels had gelification temperature (Tgel) close to body one. The samples containing silver had an antibacterial activity against several gram-positive and gram- negative bacterial strains without cytotoxicity after 24 h. In addition, MSCs inserted in the nanocomposite exhibited high bone differentiation indicating the use of this material as a potential scaffold for bone tissue regeneration. In the same period, Wang et al. developed and characterized a new injectable HA hydrogel functionalized with tyramine through dual-enzymatically cross-linked by horseradish peroxidase and galactose oxidase (GalOX). They evaluated the gelation time, swelling behavior, water content,

mechanical strength, degradation rate, cytotoxicity in vitro, and immune response in vivo. The results of these analyses highlighted that the properties of hydrogel (HT) such as good injectability, favorable cytocompatibility to mice bone marrow mesenchymal stem cells, and low inflammatory response verified by cytotoxicity test in vitro and after in vivo subcutaneous injection in vivo. The authors suggested the possibility of adjusting gelation time, swelling behavior, and degradation rate of the HT hydrogel varying the concentrations of HT and GalOX in a determined range. These interesting results supported the use of these hydrogel for application in 3D stem cell culture and in tissue engineering.

3. Protein-based Biomaterials

Like polysaccharides, proteins are versatile macromolecules that perform essential functions in living systems in almost all biological processes. They are characterized by several interesting properties such as large-scale availability, low cost, biocompatibility, biodegradability, and chemical reactivity. Given their unique properties, proteins have been thoroughly used for the development of innovative materials for biomedical applications (Silva et al., 2018). Moreover, the mechanical and modifiable structural properties of protein-based hydrogels make these scaffolds interesting for tissue engineering and regeneration. With the use of protein structures, it is also possible to insert sequences that facilitate cell adhesion to the substrate and overall cell growth (Schloss et al., 2016). In this section, the most promising proteins-based materials, their properties, and applications in tissue engineeering are described.

3.1 Collagen

Collagen (Figure 8.6) is the most abundant protein in animals. This fibrous protein consists of a right-handed bundle of three parallel and left-handed polyproline II helices. Twenty-eight different types of collagens composed of at least 46 distinct polypeptide chains that have been found in vertebrates and many other proteins also contain collagen domains (Shoulders and Raines, 2009).

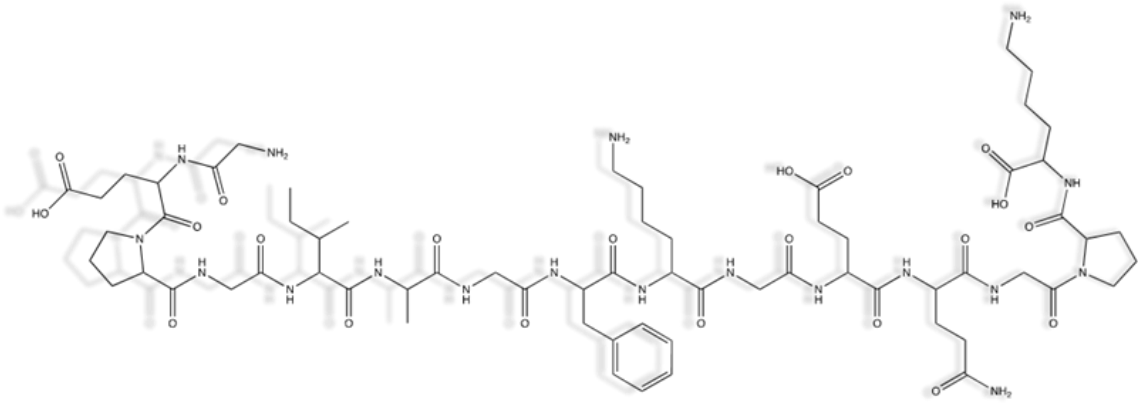

Figure 8.6: Collagen chemical structure.

This protein appealing in medical applications thanks to its presence in all connective tissue and its various properties such as: excellent biocompatibility and safety, biodegradability, and weak antigenicity. The protein contains specific cell adhesion domains including arginine-glycine- aspartic acid. After the integrin receptor on the cell surface binds to the RDG domain on the collagen molecule, cell adhesion is actively induced. The latter interaction allows the progression of cell growth as well as the differentiation and regulation of various cellular functions (Yamada et al., 2014). The main applications of collagen for tissue engineering concern bone substitutes, skin replacement, and artificial blood vessels and valves (Lee at al., 2001). Cahn et al. described a porous 3D collagen scaffold material with uniform pore size of 80 m to support capillary formation in vitro and favor the vascularization when implanted in vivo (Saunders and Ma, 2019). For the synthesis of the scaffolds, type I bovine collagen was utilized. In vitro scaffolds seeded with primary human microvascular endothelial cells suspended in human fibrin gel were able to form CD31-positive capillary-like structures. In vivo, following subcutaneous implantation in mice, the cell-free collagen scaffolds were vascularized by the host neovessels; in the meantime, there was a gradual degradation of the scaffold material for 8 weeks. Moreover, collagen scaffolds, filled with human fibrinogen gel, were implanted in the subcutaneous tissue inside a chamber that enclosed the femoral vessels of the rats. Subsequently, the angiogenic sprouts of the femoral vessels entered the scaffolds and these, after 4 weeks, entirely degraded. In the same model, collagen scaffolds seeded with stem cells derived from human adipose (ASC) compared to cell-free collagen scaffolds. In addition, the collagen scaffolds, obtained by Chan and collaborators, being also

biocompatible, could be used to promote the growth of more strong vascularized tissue engineered grafts with a consequent better survival of the implanted cells.

In 2008, Nocera et al. proposed a collagen isolated printable from the bovine Achilles tendon and evaluated the purity of the collagen isolated by means of electrophoresis on sodium dodecyl sulfate gel and polyacrylamide. They discovered that the bands corresponded to α1, α2, and β chains possessed a little contamination from other small proteins. Collagen gels and solutions have been used to obtain scaffold by means of 3D printing. First, the researchers designed and manufactured an inexpensive 3D printer, then tested collagen printing, and made 3D-printed collagen scaffolds at pH 7. The scaffold porosity was excellent. After observation of the scaffold's microstructure, using SEM, a porous mesh of fibrillar collagen was observed. Moreover, the 3D- printed collagen scaffold was not cytotoxic with cell viability higher than 70% using Vero cell lines (derived from the kidney of an African green monkey) and fibrobalst NIH 3T3. In vitro tests with both cells lines showed that the collagen scaffolds had the capacity to favor the cell attachment and proliferation. Also, a new fibrillar collagen mesh was seen after 2 weeks of culture at 37°C. With the aim to treat patients with renal failure, Lee et al. investigated the possibility to inject collagen hydrogel in renal tissue. The collagen hydrogel was then injected into the kidneys of normal mice and rat kidneys with ischemia/reperfusion injury. Subsequently, the kidneys of both animal models were studied for up to 4 weeks to check for tissue response. The infiltrating host cells present in the injection regions expressed renal stem/progenitor cell markers as well as MSC markers. After this treatment, both glomeruli, significantly higher, were found in the injected regions compared to the normal regions of the renal cortex in both normal- and ischemic-injured kidneys. Furthermore, after the injection of collagen hydrogel, renal activity, after the ischemia/reperfusion injury, was regained. Therefore, the insertion of biomaterials into the kidney can be an excellent strategy to facilitate the regeneration of glomerular and tubular structures in normal and injured kidneys (Lee et al., 2018).

In 2019, Samadian and collaborators prepared and characterized a collagen hydrogel loaded with naringin as scaffold for peripheral nerve damage treatment. The microstructure, biodegradation, swelling behavior, and cyto-/hemocompatibility of the hydrogel were evaluated. Finally, the efficacy of the obtained hydrogel on the sciatic nerve crush injury was studied in the animal model. The characterization tests showed a porous structure of the hydrogel with the presence of interconnected pores and pore average size of 90 μm. The degradation tests proved that a loss of about 70% of the primary weight of

the hydrogel after 4 weeks of storage. In vitro studies revealed a high cell proliferation on collagen/naringin hydrogel higher than the control group (tissue culture plate) at both 48 and 72 h after cell seeding and even significantly higher than pure collagen at 72 h.

Moreover, the animal study confirmed the positive effect of the proposed hydrogels on the healing of the induced nerve injury. All results showed that the prepared collagen/naringin hydrogel could be used as a sophisticated alternative to healing peripheral nerve damages.

In their study, Zhang et al. hypothesized that the use of an ECM collagen I hydrogel loaded with histone deacetylase 7 peptide 7-amino-acid-phosphorylated (7Ap) could hold back ventricular remodeling and improving heart function after heart attack and myocardial infarction (MI) (Zhang et al., 2019). In fact, the phosphorylated form of 7A (7Ap) was reported to promote in situ tissue repair via the mobilization and recruitment of endogenous stem cell antigen-1 positive (Sca-l) stem cells. In this study, an MI model was established through ligation of the left anterior descending coronary artery of C57/B6 mice. In particular, collagen I hydrogel loaded with 7Ap was injected intramyocardially into the infarcted region of the left heart wall. After local delivery, 7Ap collagen increased the formation of neomicrovessels, improved the recruitment and differentiation of antigen-1-positive stem cells, decreasing cell apoptosis, and promoting the progression of the cardiomyocyte cycle. Moreover, 7Ap collagen limited fibrosis in the left ventricle wall, reducing thinning of the infarcted area, and significantly improving cardiac efficiency 2 weeks after heart infart. These results indicated the positive impact of implanting 7Ap-collagen hydrogel as a novel constituent for the myocardial infarction treatment.

Recently, Nabavi et al. proposed an interesting strategy to stimulate bone regeneration, employing a type I collagen hydrogel entrapping tacrolimus, an immunosuppressant drug useful after organ transplantation to reduce the activity of the patient's immune system and, therefore, avoid the risk of organ rejection. For this reason, various amounts of tacrolimus (10 g/mL, 100 g/mL, and 1000 g/mL, respectively) were added to the hydrogel. The drug-loaded hydrogels were characterized. In particular, swelling capacity, porosity, weight loss, blood compatibility, cell proliferation, and drug release were evaluated. The obtained hydrogel, enclosed in a gelatin and polycaprolactone film, was put on the injured part of Wistar rats showing a high porosity and a sufficient degree of swelling, good drug release capacity, and fine hemocompatibility behavior. Also, in vivo studies enhanced the importance of the developed hydrogel for bone healing. Very interesting is also the study proposed by Nilforoushzadeh et al. that fabricated and characterized engineered collagen-fibrin-based scaffold to generate intrinsic microvasculature in a dermal and epidermal skin

substitute to use in patients with hard to heal diabetic wounds. In particular, they characterized hydrogel evaluating the biological compatibility and cell proliferation, migration, and vitality in skin organotypic cell culture. The performance of the prevascularized hydrogel

transplanted on five human subjects as an intervention group with diabetic wounds was analyzed and compared with nonvascularized skin grafts as a control on five patients. There was an important increase in skin thickness and density in the vascular beds of the hypodermis assessed by skin scanner respect to that in the control group. These preliminary data indicated that the hydrogel collagen-fibrin could be a good candidate for accelerating the healing process in patients with hard to heal diabetic wounds.

3.2 Gelatin

Gelatin (Figure 8.7) is a protein-based material derived from the hydrolysis of collagen. It is very useful in biomedical and pharmaceutical fields (Jain and Kumar, 2013; Tonsomboon et al., 2013) due to its biodegradable, biocompatible nature, low immunogenicity, and its commercial availability at low cost. The advantages include its solubility in aqueous systems, a sol–gel transition at 30 °C (Bohidar and Jena, 1994), and the possibilty to be cross-linked or modified with the inclusion of other materials to significantly alter its mechanical and biochemical properties (Jain and Kumar, 2013).

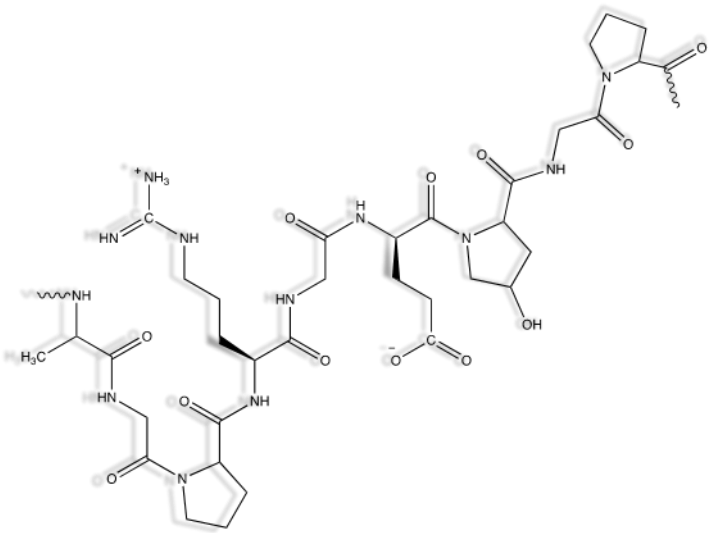

Figure 8.7: Gelatin chemical structure.

In their review, Soman et al. described the possibility to use gelatin methacrylamide as a gel- based system with tunable stiffness, which could be controlled without significantly changing its chemical composition. Generation of gelatin methacrylamide gels of different elastic moduli have been previously demonstrated (Nichol et al., 2010). These materials would be an effective tool for applications in ocular tissue engineering also on the basis of the result shown in other biomedical application such as cartilage repair (Medvedeva et al., 2018) generating blood vessels (Chen et al.,2012) and also cardiac tissue development. With the aim to find inexpensive skin substitutes useful in patients with burn injuries and chronic wounds, Nicholas et al. developed a hydrogel cellularized (PG-1) by using two polymers, pullulan, an economic antioxidant polysaccharide and gelatin. After inserting human fibroblasts and keratinocytes onto PG-1, a cellularized bilayer skin substitute was gained. This new cellularized PG-1 was compared in vivo to one acellular and no hydrogel (control) by means of a mouse excisional skin biopsy template. PG-1 showed an average pore size of 61.69 μm with an ideal elastic modulus, swelling behavior, and biodegradability. In addition, the excellent viability, proliferation, differentiation, and morphology of skin cells were evaluated by means of in vivo/dead assays, 5-bromo-2′-deoxyuridine proliferation assays, and confocal microscopy. Immunohistochemical analyses of excisional wounds treated with cellularized PG-1 showed the formation of a thicker newly formed skin with a higher presence of actively proliferating cells and incorporation of human cells than acellular or control PG-1. Excisional wounds treated with acellular or cellular hydrogels showed significantly less macrophage infiltration and increased angiogenesis 14 days after skin biopsy respect to control. All obtained results suggested that cellularized PG-1 could promote skin regeneration and wound healing.

Dong et al. have designed an injectable PEG gelatin hydrogel with highly tunable properties to enhance stem cell retention useful for wound healing. The hydrogel was obtained from a multifunctional PEG-based hyperbranched polymer and a commercially available thiolated gelatin. This material showed a spontaneous gelation within about 2 min under the physiological condition. In addition, with the aim to support murine adipose-derived stem cells (ASCs) growth and maintain their stemness, Dong and coworkers incapsulated them into the PEG-gelatin hydrogel. Moreover, they tuned hydrogel mechanical properties, biodegradability, and cellular responses by changing the formulation and cell seeding densities. In vivo studies, with old female FVB mice, showed

that in situ hydrogel significantly improved cell retention, enhances angiogenesis, and accelerates wound closure.

The obtained results suggested that injectable PEG-gelatin hydrogel can be used for regulating stem cell behaviors in 3D culture, delivering cells for wound healing to overcome all the limitation of conventional nerve suturing methods such as scar tissue formation, the limited adhesive, and mechanical strength of fibrin-based adhesives. Soucy et al. have engineered composite neurosupportive hydrogels with strong tissue adhesion. These composites were obtained by photocross-linking two natural polymers, gelatin-methacryloyl (GelMA) and methacryloyl- substituted tropoelastin (MeTro). These lasts are characterized by modificable mechanical properties by varying the GelMA/MeTro ratio. Furhermore, GelMA/MeTro hydrogels showed 15- fold higher adhesive strength to nerve tissue *ex vivo* respect to fibrin control. Moreover, the composites were shown to support Schwann cell viability and proliferation as well as neurite extension and glial cell participation in vitro, which are essential cellular components for nerve regeneration. Therefore, subcutaneously implanted GelMA/MeTro hydrogels showed slower degradation in vivo respect to pure GelMA, suggesting its potential to support the growth of slowly regenerating nerves. Thus, GelMA/MeTro composites can be useful as clinically important biomaterials to regenerate nerves and reduce the need for microsurgical suturing during nerve reconstruction.

Recently, Contessi Negrini et al. obtained a 3D-printed hydrogel potentially useful for the regeneration of damaged or missing adipose tissue (AT). 3D-printed hydrogel scaffolds are characterized by macroscopic shape, microarchitecture, extracellular matrix-mimicking structure, degradability, and soft-tissue biomimetic mechanical properties that give them very interesting materials for AT reparation. The authors presented a simple and cost-effective 3D-printing strategy using gelatin-based ink to fabricate scaffolds idoneous for AT engineering. In particular, the ink was prepared by mixing gelatin and *N*,*N*′-methylenebisacrylamide as cross-linker to initiate the reaction. Subsequently, the solution was loaded in the cartridge, at 35 °C, of a pneumatic extrusion- based 3D printer and after printed on a cooled surface with a temperture of 4 °C, in an appropriate time for ink printability, as verified by rheological tests.

The printed gelatin hydrogels were successively cross-linked at different temperatures to optimize their stability and fix the printed structure. The gelatin scaffolds remained stable for 21 days at physiological temperature, with compressive mechanical properties mimicking those of AT and they showed no indirect cytotoxic effects on a 3T3-L1 preadipocyte cell line. In addition, the printed scaffolds successfully promoted adhesion and proliferation of primary human preadipocytes. Moreover, in vitro tests showed no cytotoxic effects and the ability of the gelatin hydrogels to support adhesion, proliferation, and differentiation of primary human preadipocytes toward the adipogenic phenotype thus, demonstrating the potential of the 3D-printed gelatin hydrogels as scaffolds for AT engineering.

Ardhani et al. have developed a gelatin hydrogel membrane mimicking the physicochemical structure of the nerve and furnishing calcium ions in an axonal environment and useful for the regeneration of the nerves. This gelatin membrane has been modified with carbonated hydroxyapatite (CHA), similar in composition to human bone (Eliaz and Metoki, 2017). CHA has been incorporated for improving both the mechanical and scaffolding properties of the gelatin membrane that its stability in physiological conditions. In addition, this scaffold provided an intracellular controlled release to ensure a better axonal environment and promote nerve regeneration. The obtained gelatin membrane showed an ideal microstructure fundamental to prevent the regrowth of the fibrous tissue at the lesion site, allowing an adequate diffusion of glucose and specific proteins. Furthermore, the calcium release into the environment has favored neuronal growth, without suppressing the release of acetylcholine esterase and also the lengthening of neuritis was dramatically higher in the gelatin membrane incorporated with CHA. The preliminary obtained results encourage the use of this CHA-gelatin membrane as a medical device for nerve reconstruction.

3.3 Elastin

Elastin (Figure 8.8) is a key ECM protein that is fundamental for the elasticity and resilience of many vertebrate tissues including large arteries, lungs, ligaments, tendons, skin, and elastic cartilage (Daamen et al., 2007). This protein possesses a hydrophobic structure and is characterized by many interesting properties such as good elasticity, long-term stability, self-assembly, biocompatibility, and biodegradability. This can be applied in biomaterials in different forms such as insoluble fibers, hydrolyzed soluble form, recombinant tropoelastin (fragments), repeats of synthetic peptide sequences, and as block copolymers of elastin, possibly in combination with other biopolymers. It has recently gained attention in the field of biomedical materials and in particular as tissue engineering scaffolds, dermal substitutes, and other biomedical materials (Annabi et al., 2009).

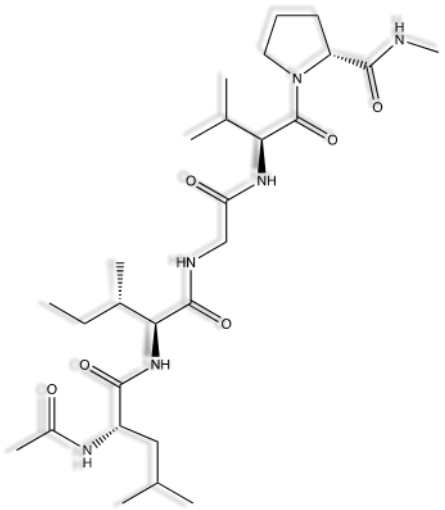

Figure 8.8: Elastin chemical structure.

Annabi et al. have proposed the possibility to make porous α-elastin hydrogels through high pressure CO_2 (Yamada et al., 2014). In particular, α-elastin was chemically cross-linked with hexamethylene diisocyanate that reacts with various functional groups in elastin such as lysine, cysteine, and histidine. High pressure CO_2 affected fabricated hydrogels properties. In fact, the pore size of the hydrogels was enhanced 20-fold when, for example, the pressure was increased from 1 to 60 bar. The swelling ratio of the samples fabricated by high pressure CO_2 resulted also higher compared to that the gels produced under atmospheric pressure. The compression modulus of α-Elastin hydrogels was

increased as the applied strain magnitude was modified from 40% to 80%. The compression modulus of hydrogels produced under high pressure CO_2 was threefold lower than the gels formed at atmospheric conditions due to the increased porosity of the gels produced by high pressure CO_2. The results obtained by Annabi and coworkers demontrated that the large pores within the 3D structures of these elastin-based hydrogels considerably promoted cellular penetration and growth throughout the matrices. Therefore, these hydrogels could be potentially useful for applications in tissue engineering. Although generally used collagen scaffolds have good biochemical properties, they are not beneficial due to their weak mechanical and physical properties. Several studies reported the realization of combined elastin scaffolds with other natural polymers such as HA, alginate, and collagen. Very recent is the work of Saniet et al. that realized an elastic, antimicrobial, and adhesive hydrogel composed of MeHA and an ELP as an adhesive and antimicrobial biomaterial characterized by a possibility to be rapidly photocross-linked in situ for the regeneration and repair of different tissues. So, hybrid hydrogels with a wide range of physical properties were engineered by modifying MeHA and ELP concentrations. Adhesion studies demonstrated that the MeHA/ELP hydrogels exhibited higher adhesive strength with respect to commercially tissue adhesives. Furthermore, through the incorporation of ZnO nanoparticles, MeHA/ELP hydrogels were also rendered antimicrobial and capable to significantly inhibit the growth of MRSA with respect to controls. Moreover, the composite adhesive hydrogels promoted in vitro mammalian cellular growth, spreading, and proliferation. In vivo subcutaneous implantation demonstrated that MeHA/ELP hydrogels did not elicit any significant inflammatory response and could be also biodegraded while promoting the integration of new autologous tissue.

With the aim to reinforce the collagen matrix, characterized by poor mechanical and physical properties, the collagen was linked with ELP to optimize the composite composition using a novel statistical method of response surface methodology (RSM) (Gurumurthy et al., 2018). In particular, a composite prepared using 6 mg/mL collagen and 18 mg/mL ELP showed an optimal combination of all three tensile properties. Physical properties of 6:18 mg/mL composite were compared to 6:0 mg/mL collagen-only hydrogel with a swelling ratio of differential scanning calorimetry and Fourier-transform infrared spectroscopy showed that ELP reduced the amount of residual water in the composites and highlighted the presence of collagen–ELP interactions. SEM images of the collagen-only hydrogel showed a porous and dense fibrillar in the collagen fibrillar microstructure, while

the collagen-ELP composite showed a dense collagen microstructure with characteristic ELP aggregates. Therefore, due to the low water content and dense microstructure, the 6:18 mg/mL collagen-ELP composite exhibited advanced mechanical properties. These composites, prepared by Gurumurthy et al., have formed good quality rigid porous structures that are very useful in the field of tissue engineering.

Silva et al., in their study, produced and characterizated novel hybrid hydrogels based on alginate combined with elastin extracted from bovine neck ligament without the use of cross-linking agents. The properties of elastin were combined with the excellent chemical and mechanical stability of alginate. Two hybrid hydrogels were produced: 2D films obtained using sonication method and 3D microcapsules produced by pressure-driven extrusion. The complete physicochemical characterization demonstrated the positive effect of elastin on the key properties of the alginate-based hydrogels to obtain fibroblast attachment, proliferation, spreading, and viability. The alginate/E hybrid hydrogel can be promising biomaterial for soft-tissue regeneration and suitable for the production of engineering more complex scaffolds, for example, by 3D printing approaches.

Cipriani and collaborators evaluated injectable in situ cross-linkable elastin-like recombinamers (ELRs) to improve cartilage regeneration. ELRs are class of proteinaceous polymers bioinspired by natural elastin and designed using recombinant technologies. They realized both ELR-based hydrogel and ELR-based hydrogel incorporated with rabbit mesenchymal stromal cells (rMSCs) for the regeneration of subchondral defects. The performance of these hydrogel was evaluated in vivo in New Zealand rabbits. In particular, the cylindrical osteochondral defects were filled with an aqueous ELR solution, and the rabbits were sacrificed after 4 months in order to make a histological evaluation of the biomaterial performance such as cell infiltration, the quality of the surrounding matrix, and the new matrix in defects. Both strategies favored cartilage regeneration, but in particular the hydrogel containing rMSC allowed adequate bone regeneration, while the ELR- based HA induced excellent regeneration of hyaline cartilage.

These data suggested that the ELR- based bioactive hydrogel could improve cartilage regeneration both with and without rMSCs embedded supports infiltration and de novo matrix synthesis. In a very recent and interesting review, Sarangthem et al. have highlighted the advantageous role of ELPs for regeneration of skin injuries. Elastin derivatives, in particular, when applied to chronic wounds, can promote wound closure and improve the strength and flexibility of the healed area.

They also can improve the healing process essential for restoration of skin's barrier function in short period after injury. Furthermore, the sol–gel transition of elastin derivatives allows complete coverage of wound area, protecting from external pathogens and incorporation of antibacterial components further accelerate the healing process.

4. Future Prospects

In the last year, the increase in the field of tissue engineering, especially in the production of biocompatible and biodegradable scaffolds, has allowed the regeneration of tissues with similar characteristics to their corresponding natural ones. However, despite the promising results obtained, much remains to be done so that materials with appropriate structure can be produced that allow the cells to spread in all its parts and to grow thanks to the right nutritional contribution. The production of a tissue ex novo requires significantly longer times compared to those for implanting a prosthesis or a traditional implant. Nevertheless, given the premises and the first results, investing in regenerative engineering, as demonstrated by the various literature data, here explained, represent the starting point for possible future applications and for the development of new technologies.

5. Conclusion

The design and application of biomaterials in tissue engineering have made great strides in the last years with extraordinary impact in various clinical applications. In particular, the development of new materials, of natural origin, has made it possible to improve the performance of the scaffolds, positively conditioning both the biological response, and the speed and quality of a new tissue proliferation. Therefore, in this chapter, various and interesting approaches, based on protein and carbohydrate hydrogels, are described, suggesting a very promising future for their application in tissue engineerin

References

Cassano R., Curcio F., Di Gioia M.L., Procopio D., Trombino S. Polysaccharides and proteins-based hydrogels for tissue engineering applications. In: Rajesh K. Kesharwani Raj K. Keservani Anil K. Sharma. *Tissue Engineering Applications and Advancements*. 2021. ISBN: 9781774630204.

Amdsen, B. G., Sukarto, A., Knight, D. K. and Shapka, S. N. Methacrylated glycol chitosan as a photopolymerizable biomaterial. *Biomacromolecules*. 2007, 8: 3758–3766.

Annabi, M., Mithieux, S. M., Boughton, E. A., Ruys, A. J., Weiss, A. S. and Dehghani, F. Synthesis of highly porous cross-linked elastin hydrogels and their interaction with fibroblasts in vitro. *Biomaterials*. 2009, 8: 4550–4557.

Annabi, N., Mithieux, S. M., Weiss, A. S. and Dehghani, F. The fabrication of elastin-based hydrogels using high pressure CO_2. *Biomaterials*. 2009, 2: 1–7.

Ardhani, R., Ana, I. D. and Tabata, Y. Gelatin hydrogel membrane containing carbonate hydroxyapatite for nerve regeneration scaffold. *J Biomed Mater Res*. 2020, 3: 1–13.

Baranwal, A., Kumara, A., Priyadharshinib, A., Oggub, G. S., Bhatnagar, I., Srivastava, A. and Chandra, P. Chitosan: An undisputed biofabrication material for tissue engineering and biosensing applications. *Int J Biol Macromols*. 2018, 110: 110–123.

Berger, J., Reist, M., Mayer, J. M., Felt, O. and Gurny, R. Structure and interactions in chitosan hydrogels formed by complexation or aggregation for biomedical applications. *Eur J Pharm Biopharm*. 2004, 51: 35–52.

Bhattarai, N., Ramay, H. R., Gunn, J., Matsen, F. A. and Zhang, M. PEG-grafted chitosan as an injectable thermosensitive hydrogel for sustained protein release. *J Control Release*. 2005, 103: 609–624.

Bohidar, H. B. and Jena, S. S. Study of sol-state properties of aqueous gelatin solutions. *J Chem Phys*. 1994, 100: 6888–6895.

Boyer, C., Figueiredo, L., Pace, R., Lesoeur, J., Rouillon, T., LeVisage, C. et al. Laponite nanoparticle-associated silated hydroxypropylmethyl cellulose as an injectable reinforced interpenetrating network hydrogel for cartilage tissue engineering. *Acta Biomater*. 2018, 65: 112– 122.

Caló, E. and Khutoryanskiy, V. V. Biomedical applications of hydrogels: a review of patents and commercial products. *Eur Polym J*. 2015, 65: 252–267.

Chan, E. C., Kuo, S. M., Kong, A. M., Morrison, W. A., Dusting, G. J., Mitchell, G. M. et al. Three-dimensional collagen scaffold promotes intrinsic vascularisation for tissue engineering applications. *PLoS One*. 2016, 22: 1–22.

Chang, C. and Zhang, L. Cellulose-based hydrogels: present status and application prospects.
Carbohydr Polym. 2011, 84: 40–53.

Chen, F., Rousche, K. and Tuan, R. Technology insight: adult stem cells in cartilage regeneration and tissue engineering. *Nat Rev Rheumatol*. 2006, 2: 373–382.

Chen, L., Shen, R., Komasa, S., Xue, Y., Jin, B., Hou, Y. et al. Drug-loadable calcium alginate hydrogel system for use in oral bone tissue repair. *Int J Mol Sci*. 2017, 18: 989–1006.

Chen, Y. C., Lin, R. Z., Qi, H., Yang, Y., Bae, H., Melero-Martin, J. M. et al. Functional human vascular network generated in photocross-linkable gelatin methacrylate hydrogels. *Adv Funct Mater*. 2012, 22: 2027–

Choa, J. H., Kim, K. D., Park, K. D., Jung, M. C., Yang, W. I., Han, S. W. et al., Chondrogenic differentiation of human mesenchymal stem cells using a thermosensitive poly(*N*- isopropylacrylamide) and water-soluble chitosan copolymer. *Biomaterials*. 2004, 25: 5743–5751.

Choi, B., Kim, S., Lin, B., Wu, B. M. and Lee, M. Cartilaginous extracellular matrix-modified chitosan hydrogels for cartilage tissue engineering. *ACS Appl Mater Interfaces*. 2014, 6: 20110– 20121.

Cipriani, F., Ariño Palao, B., Gonzalez de Torre, I., Vega Castrillo, A., Aguado Hernández, H. J., Alonso Rodrigo, M. et al. An elastin-like recombinamer-based bioactive hydrogel embedded with mesenchymal stromal cells as an injectable scaffold for osteochondral repair. *Regen Biomater*. 2016, 6: 335–347.

Negrini, N. C., Celikkin, N., Tarsini, P., Farè, S. and Święszkowski, W. Three-dimensional printing of chemically cross-linked gelatin hydrogels for adipose tissue engineering. *Biofabrication*. 2020, 12: 025001–025017.

Croisier, F. and Jérôme, C. Chitosan-based materials for tissue engineering. *Eur Polym J*. 2013, 49: 780–792.

Daamen, W. F., Veerkamp, J. H., Van Hest, J. C. and Van Kuppevelt, T. H. Elastin as a biomaterial for tissue engineering. *Biomaterials*. 2007, 28: 4378–4398.

Diaz-Rodriguez, P., Garcia-Triñanes, P., Echezarret López‐d M. M., Santoveña, A. and Landina, M. Mineralized alginate hydrogels using marine carbonates for bone tissue engineering applications. *Carbohydr Polym*. 2018, 195: 235–242.

Dong, Y., Sigen A., Rodrigues, M., Li, X., Kwon, S. H., Kosaric, N. et al. Injectable and tunable gelatin hydrogels enhance stem cell retention and improve cutaneous wound healing. *Adv Funct Mater*. 2017, 27: 1606619–1606631.

Ehterami, A., Salehi, M., Farzamfar, S., Samadian, H., Vaez, A., Sahrapeyma, H. et al. A promising wound dressing based on alginate hydrogels containing vitamin D3 cross-linked by calcium carbonate/D-glucono-δ-lactone. *Biomed Eng Lett*. 2020, 3: 309–319.

Eliaz, N. and Metoki, N. Calcium phosphate bioceramics: a review of their history, structure, properties, coating technologies, and biomedical applications. *Materials*. 2017, 10: 1–104.

Falcone, S. J., Palmeri, D. and Berg, R. A. Biomedical applications of hyaluronic acid. In: Polysaccharides for Drug Delivery and Pharmaceutical Applications. 2006, 8: 155–174.

Gao, C., Liu, M., Chen, J. and Zhang, X. Preparation and controlled degradation of oxidized sodium alginate hydrogel. *Polym Degrad Stability*. 2009, 94: 1405–1410.

Ghorbani, M. and Roshangar, L. Construction of collagen/nanocrystalline cellulose-based hydrogel scaffolds: synthesis, characterization, and mechanical properties evaluation. *Int J Polym Mater Biomat*. 2019, 3: 1563–1535.

Greenwald, C. R. A. A., Josephson, S., Diamond, H. S. and Tsang, A. Human cartilage lysozyme. *J Clin Invest*. 1972, 51: 2261–2270.

Gupta, A., Briffa, S. M., Swingler, S., Gibson, H., Kannappan, V., Adamus, G. et al. Synthesis of silver nanoparticles using curcumin-cyclodextrins loaded into bacterial cellulose-based hydrogels for wound dressing applications. *Biomacromolecules*. 2020, 21: 1802–1811.

Gurumurthy, B., Griggs, J. A. and Janorkar, A. V. Optimization of collagen-elastin-like polypeptide composite tissue engineering scaffolds using response surface methodology. *J Mech Behav Biomed Mater*. 2018, 84: 116–125.

Han, S. S., Yoon, H. Y., Yhee, J. Y., Cho, M. O., Shim, H. E., Jeong, J. E. et al. In situ cross- linkable hyaluronic acid hydrogels using copper-free click chemistry for cartilage tissue engineering. *Polym Chem*. 2018, 9: 20–27.

Hemshekhar, M., Thushara, R. M., Chandranayaka, S., Sherman, L. S., Kemparaju, K. and Girish,

K. S. Emerging roles of hyaluronic acid bioscaffolds in tissue engineering and regenerative medicine. *Int J Biol Macromol*. 2016, 86: 917–928.

Homaeigohar, S., Tsai, T. Y., Young, T. H., Yang, H. Y. and Ji, Y. R. An electroactive alginate hydrogel nanocomposite reinforced by functionalized graphite nanofilaments for neural tissue engineering. *Carbohydr Polym*. 2019, 224: 115112–115123.

Hong, Y., Mao, Z., Wang, H., Gao, G. and Shen, J. Covalently cross-linked chitosan hydrogel formed at neutral pH and body temperature. *J Biomed Mater Res Part A*. 2006, 79: 913–922.

Hong, Y., Song, H., Gong, Y., Mao, Z., Gao, C. and Shen, J. Covalently cross-linked chitosan hydrogel: properties of in vitro degradation and chondrocyte encapsulation. *Acta Biomater*. 2007, 3: 23–31.

Howard, D., Lee Buttery, D., Shakesheff, K. M. and Roberts, S. J. Tissue engineering: strategies, stem cells, and scaffolds. *J Anat*. 2008, 213: 66–72.

Jain, E. and Kumar, A. Disposable polymeric cryogel bioreactor matrix for therapeutic protein production. *Nat Protoc*. 2013, 8: 821–835.

Kabir, S. M. F., Sikdar, P. P., Haque, B., Bhuiyan, M. A. R., Ali, A. and Islam, M. N. Cellulose- based hydrogel materials: chemistry, properties, and their prospective applications. *Prog Biomater*. 2018, 7: 153–174.

Saekhor, K., Udomsinprasert, W., Honsawek, S. and Tachaboonyakia, W. Preparation of an injectable modified chitosan-based hydrogel approaching for bone tissue engineering. *Int J Biol Macromol*. 2019, 123: 167–173.

Khan, F. and Ahmad, S. R. Polysaccharides and their derivatives for versatile tissue engineering application. *Macromol Biosci*. 2013, 13: 395–421.

Langer, R. and Vacanti, J. P. Tissue engineering. *Science*. 1993, 260: 920–926.

Lee, J. H. and Kim, H. W. Emerging properties of hydrogels in tissue engineering. *J Tissue Eng*.

2018, 9: 1–4.

Lee, K. Y. and Mooney, D. J. Hydrogels for tissue engineering. *Chem Rev*. 2001, 101: 1869–1880. Lee, K. Y. and Mooney, D. J. Alginate: properties and biomedical applications. *Prog Polym Sci*.

2012, 37: 106–126.

Lee, S. J., Wang, H. J., Kim, T. H., Choi, J. S., Kulkarni, G., Jackson, J. D. et al. In situ tissue regeneration of renal tissue induced by collagen hydrogel injection. *Stem Cells Transl Med*. 2018, 7: 241–250.

Levengood, S. K. L. and Zhang, M. Chitosan-based scaffolds for bone tissue engineering. *J Mater Chem B*. 2014, 2: 3161–3184.

Li, H. B., Jiang, H., Wang, C. H., Duan, C. M., Ye, Y., Su, X. P. et al. Comparison of two types of alginate microcapsules on stability and biocompatibility in vitro and in vivo. *Biomed Mater*. 2006, 1: 42–47.

Li, W., Wang, B., Zhang, M., Wu, Z., Wei, J., Jiang, Y. et al. All natural injectable hydrogel with self-healing and antibacterial properties for wound dressing. *Cellulose*. 2020, 27: 2637–2650.

Loh, E. Y. X., Mohamad, N., Fauzi, M. B., Ng, M. H., Ng, S. F. and Amin, M. C. I. M. Development of a bacterial cellulose-based hydrogel cell carrier containing keratinocytes and fibroblasts for full-thickness wound healing. *Sci Rep*. 2018, 8: 2875.

Luo, J. W., Liua, C., Wu, J. H., Lin, L. X., Fan, H. M., Zhao, D. H. et al. In situ injectable hyaluronic acid/gelatin hydrogel for hemorrhage control. *Mater Sci Eng*. 2019, 3: 628–634.

Makvandi, P., Ali, G. W., Della Sala, F., Abdel-Fattah, W. I. and Borzacchiello, A. Hyaluronic acid-/corn silk extract-based injectable nanocomposite: a biomimetic antibacterial scaffold for bone tissue regeneration. *Mater Sci Eng*. 2020, 8: 110195–110205.

Mano, J. F., Silva, G. A., Azevedo, H. S., Malafaya, P. B., Sousa, R. A., Silva, S. S. et al. Natural origin biodegradable systems in tissue engineering and regenerative medicine: present status and some moving trends. *J Royal Soc Interf*. 2007, 17: 999–1030.

Medvedeva, E. V., Grebenik, E. A., Gornostaeva, S. N., Telpuhov, V. I., Lychagin, A. V., Timashev, P. S. et al. Repair of damaged articular cartilage: current approaches and future directions. *Int J Mol Sci*. 2018, 19: 2366–2389.

Moss, J. M., Van Damme, M. P. I., Murphy, W. H., Stanton, P. G., Thomas, P. and Preston, B. N. Purification, characterization, and biosynthesis of bovine cartilage lysozyme isoforms. *Arch Biochem Biophys*. 1997, 339: 172–182.

Nabavi, M. H., Salehi, M., Ehterami, A., Bastami, F., Semyari, H., Tehranchi, M. et al. A collagen- based hydrogel containing tacrolimus for bone tissue engineering. *Drug Deliv Transl Res*. 2020, 10: 108–121.

Naderi-Meshkin, H., Andreas, K., Matin, M. M., Sittinger, M., Bidkhori, H. R., Ahmadiankia, N. et al. Chitosan-based injectable hydrogel as a promising in situ forming scaffold for cartilage tissue engineering. *Cell Biol Int*. 2014, 38: 72–84.

Nezhad-Mokhtari, P., Akrami-Hasan-Kohal, M. and Marjan Ghorbani, M. An injectable chitosan- based hydrogel scaffold containing gold nanoparticles for tissue engineering applications. *Int J Biol Macromol*. 2020, 154: 198–205.

Nichol, J. W., Koshy, S., Bae, H., Hwang, C. M. and Khademhosseini, A. Cell-laden microengineered gelatin methacrylate hydrogels Jason. *Biomaterials*. 2011, 31: 5536–5544.

Nicholas, M. N., Jeschke, M. G. and Amini-Nik, S. Cellularized bilayer pullulan-gelatin hydrogel for skin regeneration. *Tissue Eng*. 2016, 22: 9–10.

Nilforoushzadeh, M. A., Sisakht, M. M., Amirkhani, M. A., Seifalian, A. M., Banafshe, H. R., Verdi, J. et al. Engineered skin graft with stromal vascular fraction cells encapsulated in fibrin–collagen hydrogel: A clinical study for diabetic wound healing. *J Tissue Eng Regen Med*. 2020, 14: 424–440.

Nocera, A. D., Comín, R., Salvatierra, N. A. and Cid, M. P. Development of 3D printed fibrillar collagen scaffold for tissue engineering. *Biomed Microdevices*. 2018, 20: 26–39.

Novotna, K., Havelka, P., Sopuch, T., Kolarova, K., Vosmanska, V., Lisa, V. et al. Cellulose-based materials as scaffolds for tissue engineering. *Cellulose*. 2013, 20: 2263–2278.

Onofrei, M. and Filimon, A. Cellulose-based hydrogels: Designing concepts, properties, and perspectives for biomedical and environmental applications. *Polym Sci Res Adv Pract Appl Edu Aspects*. 2016, 3: 108–120.

Pangburn, S., Trescony, P. and Heller, J. Lysozyme degradation of partially deacetylated chitin, its films and hydrogels. *Biomaterials*. 1982, 3: 105–108.

Peppas, A. N. and Hoffman, A. S. Hydrogels. In: *Biomaterials Science: An Introduction to Materials in Medicine* (4th edition). Wagner, W. R., Sakiyama-Elbert, S. E., Yaszemski, M. J. (Eds). 2020, 1.3.2 E153–166.

Petersen, N. and Gatenholm, P. Bacterial cellulose-based materials and medical devices: current state and perspectives. *Appl Microbiol Biotechnol*. 2011, 91: 1277–1286.

Reakasame, S. and Boccaccini, A. R. Oxidized alginate-based hydrogels for tissue engineering applications: a review. *Biomacromolecules*. 2018, 19: 3–21.

Rezaeeyazdi, M., Colombani, T., Memic, A. and Bencherif, S. A. Injectable hyaluronic acid-co- gelatin cryogels for tissue engineering. *Appl Mater*. 2018, 11: 1374–1388.

Rinaudo, M. Chitin and chitosan: properties and applications. *Prog Polym Sci*. 2006, 31: 603–613.

Sahana, T. G. and Rekha, P. D. Biopolymers: applications in wound healing and skin tissue engineering. *Mol Biol Rep*. 2018, 45: 2857–2867.

Samadian, H., Vaez, A., Ehterami, A., Salehi, M., Farzamfar, S., Sahrapeyma, H. Sciatic nerve regeneration by using collagen type I hydrogel containing naringin. *J Mater Sci Mater Med*. 2019, 30: 107–117.

Sancilio, S., Gallorini, M., Di Nisio, C., Marsich, E., Di Pietro, R., Schweikl, H. alginate/hydroxyapatite-based nanocomposite scaffolds for bone tissue engineering improve dental pulp biomineralization and differentiation. *Stem Cells Int*. 2018, 2018: 1–13.

Sani, E. S., Portillo-Lara, R., Spencer, A., Yu, W., Geilich, B. M., Noshadi, I. et al. Engineering adhesive and antimicrobial hyaluronic acid/elastin-like polypeptide hybrid hydrogels for tissue engineering applications. *ACS Biomater Sci Eng*. 2018, 4: 2528–2540.

Sannino, A., Demitri, C. and Madaghiele, M. Biodegradable cellulose-based hydrogels: design and applications. *Materials*. 2009, 2: 353–373.

Sarangthem, V., Singh, T. D. and Dinda, A. K. Emerging role of elastin-like polypeptides (ELPs) in regenerative medicine. *Adv Wound Care*. 2020, 1: 1–37.

Saunders, L. and Ma, P. X. Healing supramolecular hydrogels for tissue engineering applications.

Macromol Biosci. 2019, 19: 313–324.

Schloss, A. C., Williams, D. M. and Regan, L. J. Protein-based hydrogels for tissue engineering. In: Protein-based Engineered Nanostructures. Cortajarena, A. and Grove, T. (Eds). 2016, 940: 167– 177.

Shafei, S., Khanmohammadi, M., Heidari, R., Ghanbari, H., Nooshabadi, V. T., Farzamfar, S. et al. Exosome-loaded alginate hydrogel promotes tissue regeneration in full-thickness skin wounds: An in vivo study. *J Biomed Mater Res*. 2020, 5: 545–556.

Sheehy, J., Vinardella, T., Buckley, C. T. and Kelly, D. J. Engineering osteochondral constructs through spatial regulation of endochondral ossification. *Acta Biomater*. 2013, 9: 5484–5492.

Shen, X., Shamshina, J. L., Berton, P., Gurau, G. and Rogers, R. D. Hydrogels based on cellulose and chitin: fabrication, properties, and applications. *Green Chem*. 2016, 18: 53–75.

Shoulders, M. D. and Raines, R. T. Collagen structure and stability. *Ann Rev Biochem*. 2009, 78: 929–958.

Silva, R., Singh, R., Sarker, B., Papageorgiou, D. G., Juhasz, J. A., Roether, J. A. et al. Hybrid hydrogels based on keratin and alginate for tissue engineering. *J Mater Chem*. 2014, 2: 5441–5451.

Silva, S. S., Fernandes, E. M., Pina, S., Silva-Correia, J., Vieira, S., Oliveira, J. M. et al. Natural- origin materials for tissue engineering and regenerative medicine. *Comp Biomater II*. 2018, 2: 228– 252.

Soman, P., Chung, P. H., Zhang, A. P. and Chen, S. Digital microfabrication of user-defined 3D microstructures in cell-laden hydrogels. *Biotechnol Bioeng*. 2013, 110: 1–11.

Song, S. J., Choi, J., Park, Y. D., Hong, S., Lee, J. J., Ahn, C. B. et al. Sodium alginate hydrogel- based bioprinting using a novel multinozzle bioprinting system. *Artif Organs*. 2011, 35: 1132–1136.

Soucy, J. R., Sani, E. S., Portillo Lara, R., Diaz, D., Dias, F., Weiss, A. S. et al. Photocross-linkable gelatin/tropoelastin hydrogel adhesives for peripheral nerve repair. *Tissue Eng Part A*. 2018, 24: 17–18.

Tan, H., Chu, C. R., Payne, K. A. and Marra, K. G. Injectable in situ forming biodegradable chitosan–hyaluronic acid-based hydrogels for cartilage tissue engineering. *Biomaterials*. 2009, 30: 2499–2506.

Tonsomboon, K., Strange, D. G. T. and Oyen, M. L. Gelatin nanofiber-reinforced alginate gel scaffolds for corneal tissue engineering. *Proc Eng Med Biol Soc*. 2010, 2013: 6671–6674.

Trombino, S., Servidio, C., Curcio, F. and Cassano, R. Strategies for hyaluronic acid-based hydrogel design in drug delivery. *Pharmaceutics*. 2019, 11: 407–424.

Turco, G., Marsich, E. and Bellomo, F. Alginate/hydroxyapatite biocomposite for bone ingrowth: a trabecular structure with high and isotropic connectivity. *Biomacromolecules*. 2009, 10: 1575–1583.

Valle, L. J. D., Diaz, A. and Puiggali, J. Hydrogels for biomedical applications: cellulose, chitosan, and protein/peptide derivatives. *Gels*. 2017, 27: 1–28.

Varum, K. M., Myhr, M. M., Hjerde, R. J. N. and Smidsrød, O. In vitro degradation rates of partially *N*-acetylated chitosans in human serum. *Carbohyd Res*. 1997, 299: 99–101.

Velema, J. and Kaplan, D. Biopolymer-based biomaterials as scaffolds for tissue engineering. *Adv Biochem Eng Biotechnol*. 2006, 102: 187–238.

Wang, L., Li, J., Zhang, D., Ma, S., Zhang, J., Gao, F. et al. Dual-enzymatically cross-linked and injectable hyaluronic acid hydrogels for potential application in tissue engineering. *RSC Adv*. 2020, 10: 2870–2876.

Wang, L. and Shansky, J. Design and fabrication of a biodegradable, covalently cross-linked shape- memory alginate scaffold for cell and growth factor delivery. *Tissue Eng Part A*. 2012, 18: 2000– 2007.

Wu, S. W., Liua, X., Miller, A. L., Cheng, Y. S., Yeh, M. L. and Lu, L. Strengthening injectable thermosensitive NIPAAm-g-chitosan hydrogels using chemical cross-linking of disulfide bonds as scaffolds for tissue engineering. *Carbohyd Polym*. 2018, 192: 308–316.

Xu, C., Guan, S., Wang, S., Gong, W., Liu, T., Ma, X. et al. Biodegradable and electroconductive poly(3,4-ethylenedioxythiophene)/carboxymethyl chitosan hydrogels for neural tissue engineering. *Mater Sci Eng C*. 2018, 84: 32–43.

Yadav, R. B. and Chauhan, M. K. A review: chitosan as 3D matrix for tissue engineering. *Int J Res Pharm Sci*. 2017, 3: 66–69.

Yamada, S., Yamamoto, K., Ikeda, T., Yanagiguchi, K. and Hayashi, Y. Potency of fish collagen as a scaffold for regenerative medicine. *Biomed Res Int*. 2014, 2014: 1–8.

Zhang, J., Sisley, A. M. G., Anderson, A. J., Taberner, A. J., McGhee, C. N. J. and Dipika, V. Characterization of a novel collagen scaffold for corneal tissue engineering. *Tissue Eng Part C Methods*. 2015, 22: 1–15.

Zhu, T., Mao, J., Cheng, Y., Liu, H., Lv, L., Ge, M. et al. Recent progress of polysaccharide-based hydrogel interfaces for wound healing and tissue engineering. *Adv Mater Interfaces*. 2019, 6: 1–2, 2039.

SECTION 3

BIOPOLYMERIC MATERIALS FOR TARGETED DRUG DELIVERY

Part A: Polymeric Biomaterials for the Treatment of Cardiac Post-Infarction injuries.

Part B: Chitosan membranes filled with Cyclosporine A as possible devices for local administration of drugs in the treatment of breast cancer

Part C: Polymersomes as promising vehicle for controlled drug delivery.

Part A

Polymeric Biomaterials for the Treatment of Cardiac Post-Infarction injuries

Abstract

Cardiac regeneration aims to reconstruct the heart contractile mass, preventing the organ from a progressive functional deterioration, by delivering pro-regenerative cells, drugs, or growth fac- tors to the site of injury. In recent years, scientific research focused the attention on tissue engineering for the regeneration of cardiac infarct tissue, and biomaterials able to anatomically and physiolog- ically adapt to the heart muscle have been proposed as valuable tools for this purpose, providing the cells with the stimuli necessary to initiate a complete regenerative process. An ideal biomaterial for cardiac tissue regeneration should have a positive influence on the biomechanical, biochemical, and biological properties of tissues and cells; perfectly reflect the morphology and functionality of the native myocardium; and be mechanically stable, with a suitable thickness. Among others, engineered hydrogels, three-dimensional polymeric systems made from synthetic and natural biomaterials, have attracted much interest for cardiac post-infarction therapy. In addition, biocompatible nanosystems, and polymeric nanoparticles in particular, have been explored in preclinical studies as drug delivery and tissue engineering platforms for the treatment of cardiovascular diseases. This review focused on the most employed natural and synthetic biomaterials in cardiac regeneration, paying particular attention to the contribution of Italian research groups in this field, the fabrication techniques, and the current status of the clinical trials.

Keywords: cardiac regeneration; tissue engineering; biomaterials; hydrogels; nanoparticles

1. Introduction

Myocardial infarction (MI) represents one of the leading causes of morbidity world- wide, with a mortality rate of 17.9 million people per year [1]. The main limitation to the proper recovery of myocardial functionality after a heart injury lies in the modest endogenous capability to regenerate the damaged tissue, which is usually replaced with unfunctional connective tissue [2]. Thus, there is tremendous interest in finding perma- nent solutions to restore the cardiac functionality while attenuating tissue remodeling and fibrosis [3,4].

The available therapeutic strategies are designed to target one of the five main pro- cesses associated with MI, namely, massive cardiomyocyte death [5], inflammation [6], remodeling of the extracellular matrix (ECM) [7], angiogenesis [8], and cardiomyoge- nesis [9]. In detail, the prevention of cardiomyocyte death can be achieved by either repression of apoptotic processes or stimulation of survival pathways; manipulation of the chemokine/cytokine profile or cellular responses during the inflammation process, which can help in modulating a proper tissue repair; modulation of the balance between the matrix metalloproteinases and tissue residing factors, which can avoid scar formation, thus favoring a desired tissue healing; stimulation of pro-angiogenesis signals, which can stimulate the formation of new blood vessels; and, finally, induction of the prolifera- tion/transplantation of cardiomyocytes, which is a key requirement for the full restoration of cardiac function [10–12]. Cell-based therapy, consisting of the direct injection of an autologous or heterologous cell suspension into the myocardium, is a suitable strategy for repairing or replacing injured cardiac tissue [13]. Human embryonic stem cells (hESC) and induced pluripotent stem cells (iPSC) have been recognized as valuable tools for this purpose, because of their ability to effectively differentiate into cardiomyocytes [14,15]. On the other hand, this therapeutic approach suffers for some drawbacks related to the need to inject a great number of cells due to the low cell survival and poor retention rate (almost 10%). Furthermore, for achieving a proper differentiation into cardiomyocytes and organization of the regenerated tissue, the presence of both biochemical signaling and mechanical support, acting as topographical guidance, is strongly required [16,17].

Cardiac tissue engineering, coupled with regenerative medicine, represents a very useful approach to repair or regenerate damaged tissues or organs and restoring their functions. In the last decades, due to the possibility to design scaffolds with tailored physic- chemical and biomechanical features, biomimetic devices based on synthetic

or natural polymers have attracted much interest in this field [18,19]. The design of a performing biomaterial takes advantage of the collaboration of researchers belonging to different scien- tific areas, from chemistry, physics, and engineering, to technology, biology, and medicine. Depending on the application area, the properties of the final biomaterials can be tailored by selecting the most appropriate polymer, as well as the synthetic and formulation pro- cesses [20], which are the core expertise of Pharmaceutical Technology. Cardiac scaffolds based on natural or synthetic biomaterial can mimic the ECM environment, with the further possibility to combine the cell therapy with the release of bioactive molecules [21]. In this regard, different kinds of systems, either in the form of injectable or implanted scaffolds, have been proposed to date [22,23]. In this review, we aim to overview the recent advances in the development of bioma- terials for cardiac tissue regeneration, paying particular attention to the contribution of Italian research groups in this field. The referenced works were classified according to the nature of the base materials (organic or inorganic, natural, or synthetic), highlighting the adopted synthetic strategy and the main outcomes.

2. Biomaterials for Cardiac Regeneration

Any biomaterial designed for cardiac tissue engineering should possess key properties to prevent the dilation of cardiac muscle, avoid or slow scar formation and fibrosis, while favoring the integration and proliferation of cardiomyocytes [24].

At first, high biocompatibility and non-immunogenicity are required to avoid adverse effects during the healing process [25]. For any kind of in vivo application, an ideal biomaterial should produce a beneficial or neutral response upon interaction with the host tissue or environmental components at the site of application. In the case of cardiac applications, apart from the interaction with all the components of the myocardium (e.g., cardiomyocytes, endothelium, fibroblasts, and perivascular cells) and the compatibility of the metabolic by-products, the blood–material interaction is also a big challenge, since the material's exposure to the blood flow can result in thrombosis or embolism events [25].

The immune response triggered by an implanted biomaterial can results in either posi- tive (tissue regeneration with angiogenesis, remodeling, and restoration of functionality) or negative (tissue repair with fibrosis and scar formation) healing effects [26]; thus, the induction of an immune response favoring tissue regeneration is critical for successful treatments. Although the base mechanisms eliciting a regenerative response are not fully

understood, experimental evidence allows hypothesizing that surface chemistry and degradation rates are pivotal parameters [27]. The kinetics of scaffold degradation should be ideally close to that of new tissue formation, to guarantee adequate space availability for the newly formed tissue and effective regeneration before the scaffold is completely degraded. A fast
degradation rate can result in incomplete host infiltration, further compromising the organ integrity; on the other hand, inhibition of cell remodeling and angiogenesis, together with scar formation, is the main phenomenon accompanying the overly long persistence of the scaffold [28].

Furthermore, an ideal scaffold should possess a porosity degree in the range 50–90%, to promote the diffusion of nutrients, oxygen, and extracellular fluids through the cellular networks—mechanical properties allowing the mechanical strength of the organ to be retained until complete regeneration of heart tissue—as well as the right balance between stiffness and flexibility to support repeated stretch cycles, without constraining the contractions and relaxation of cardiac muscle [25].

As schematically depicted in Figure 1, to promote cell engraftment and reorganization into a 3D tissue, the cardiac scaffold should match the key features of the heart, as well as the unique interplay between the cardiac cells and native cardiac ECM components [29]. It should possess tailored mechanical properties, such as anisotropy, elasticity, and contrac- tility, to provide the required pressure for an effective pump function while withstanding the tensile stress [30]. The surface properties should be tailored with functional niches to provide the cells with anchoring positions promoting attachment, anisotropic alignment, and proliferation [31]. Thus, scaffold stiffness and geometry are important features to be considered, with square pores being more efficient in promoting cell adhesion rather than hexagonal pores [32]. Moreover, biochemical cues, such as growth factors [33], cy- tokines, and adhesion molecules, should be inserted to induce effective maturation of cardiac cells [21]. Finally, in order to produce the optimal material for tissue interfaces, the design of the cardiac biomaterial should fit with the complex electrical pathways of the myocardium [34], obtained by a fine coordination between membrane potential depolarization, pacemaker conduction system, and specific intracellular communication networks [35].

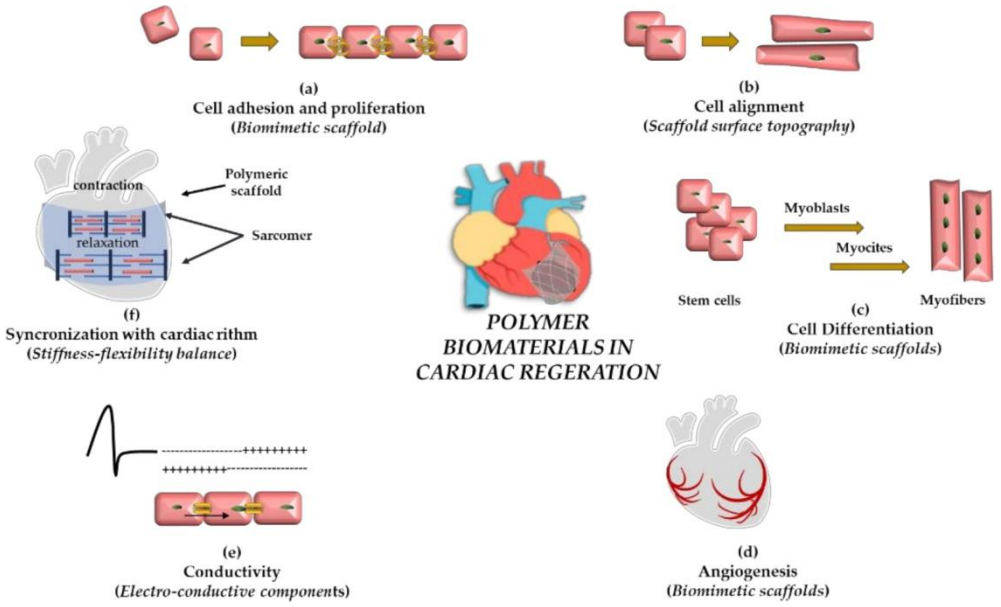

Figure 1. Representation of the biological effects required for myocardial regeneration induced by polymeric biomaterials. (**a**) Increased cell proliferation and adhesion; (**b**) greater cell alignment; (**c**) cell differentiation; (**d**) induction of angiogenesis; (**e**) cellular electrical coupling and enhanced impulse conduction; (**f**) synchronization with cardiac rhythm.

Ultimately, since an ideal cardiac patch should possess features close to that of the cardiac ECM, some clinical trials aimed to investigate the safety and effectiveness of the cardiac patches based on a natural ECM [1]. The ECM cardiac patch CorMatrix® (CorMatrix Cardiovascular, Inc. Vascular surgeon in Roswell, GA, USA) was claimed to promote endogenous cardiac regeneration, although trials were able to prove its safety rather than its effectiveness (ClinicalTrials.gov identifier: NCT02887768) [36]. More encouraging results were obtained with VentriGel™ (Ventrix, Inc., San Diego, CA, USA), a porcine-cardiac ECM-injectable hydrogel, which was found to be safe and improves exercise capacity (ClinicalTrials.gov identifier: NCT02305602) [37].

Among the great number of materials available for the fabrication of cardiac scaffolds mimicking the ECM functionalities, polymers from either natural or synthetic origin well match with the above-described requirements.

Natural polymers, such as polysaccharides and proteins, possess many favorable properties, including biocompatibility and biodegradability, and have been applied as

scaffold in cardiac regeneration because of their similarity with the natural tissues and the ability to facilitate cell adhesion, proliferation, and differentiation [38]. In addition, the presence of many functional groups allows the polymer backbone to be easily functionalized, and the physic-chemical properties to be finely tuned [39]. On the other hand, synthetic polymers are versatile materials with high porosity, durability, and physic-chemical and structural properties, capable to fit with the particular needs of the target tissue [40]. In most cases, to overcome the limitations of each class of polymer, while enhancing their strengths, natural and synthetic polymers can be combined into composite materials with superior properties [41]. Following the same rationale, inorganic or organic/inorganic hybrid scaf- folds were also proposed, in order to mimic either the main inorganic components of natural tissues or their intrinsic properties [42]. For example, considering the electrical properties of native myocardium, conductive fillers can be introduced, facilitating the electrical coupling between adjacent cells within the scaffolds [35]. Organic, inorganic, and hybrid biomaterials can be formulated into different types of constructs, which, for our convenience, are here classified as injectable hydrogels, cardiac patches, and nanoparticles. Injectable hydrogels, three-dimensional hydrophilic polymeric networks with a high water content, are formed by in situ gelation and represent very advantageous devices for tissue engineering and drug delivery [43]. These formulations can be injected directly into the site of interest with a syringe without surgery, enhancing the patient compliance, with the cells loaded into the hydrogel during the gelation process [44,45]. Specifically, for cardiac applications, hydrogels should possess proper mechanical stiffness, as well as the ability to retain cells after transplantation while providing them with a suitable physical and biochemical microenvironment for proliferation [46–48]. A cardiac patch is defined as a piece of in vitro-grown, functioning heart tissue on an engineered support that can replace part of the injured tissue. The cells can be cultured on, or suspended into, the biomaterial matrix, obtaining cell sheets and cell-containing scaffolds, respectively [49]. Finally, nanoparticle systems are well known for their ability to enhance the pharma- cokinetics profiles of any bioactive molecules and are often used as delivery systems to facilitate the healing process of the cardiac tissues [50].

3. Cardiac Scaffolds Fabrication Techniques

Since the scaffolds' effectiveness strictly depends on their properties, it is evident that the choosing the proper fabrication method is a key determining factor. The avail- able techniques for the fabrication of cardiac scaffolds can be divided into conventional and non-conventional methods. The first group includes solvent casting/particulate leaching, thermally-induced phase separation, electrospinning, gas foaming, and freeze drying [24,51].

In the solvent casting/particulate leaching method, the selected polymeric materials are dissolved in a highly volatile solvent in the presence of a suitable porogen (e.g., water-soluble inorganic salts or sugars) and poured into a mold. After solvent evaporation, porogens are leached out by immersing the composite in water with formation of the porous scaffold [52]. In this technique, the porogen amount influences the scaffold porosity, while pore size and geometry can be modulated by varying the particulate size and shape [53]. Thermally induced phase separation is a versatile technique where temperature vari- ation induces a phase separation of a polymer solution into low and high polymer con- centration phases [54]. In a typical procedure, the selected polymer is dissolved at a high temperature in a solvent with a low melting point, and the porous scaffold is obtained after cooling below the solvent melting (liquid–liquid phase separation) or solidification (solid–liquid phase separation) points. In the first case, the solvent is then removed under vacuum, while in the solid–liquid phase separation, solvent crystals are removed by wash- ing with a non-solvent of the polymer and then applying a vacuum-drying or freeze-drying procedure. Pore size is influenced by the cooling temperature and solvent crystallization for liquid–liquid and solid–liquid phase separation, respectively, with the heat transfer conditions greatly influencing the geometry [55,56].

Electrospinning involves the application of a strong electric field (10–20 kV) on a polymer solution placed in a needle [57]. Under these conditions, the polymer solution is charged, and flows at a controlled rate to a collector put at a specific distance from the needle. While moving, the solvent evaporates, with the subsequent deposition of the polymeric fibers with mean diameters in the range of 3 nm to 5 μm [58]. The fiber morphology can be tuned to the varying ambient conditions, such as temperature, humidity,

and air velocity, as well as to the instrumental parameters (e.g., applied voltage, flow rate, needle size, needle-to-collector distance, and collector shape and composition). Moreover, to generate functional scaffolds, the solution properties, such as viscosity, conductivity, surface tension, and polymer molecular weight, should be optimized [59].

In the gas-foaming procedure, polymer discs are firstly exposed to supercritical CO_2, and then the pressure is quickly decreased to atmospheric, leading to the formation of clusters of thermodynamically unstable CO_2 into the polymer structures, and thus pore nucleation occurs. Under these conditions, high porous scaffolds can be obtained, although with the disadvantages of poor pore interconnectivity and the formation of a nonporous layer surface [60].

The freeze-drying process is an advantageous technique allowing the obtainment of porous scaffolds without using high temperatures and avoiding any washing step to remove the porogen. Following this technique, a frozen polymer solution, poured in a mold, is freeze-dried under vacuum, obtaining materials with a porosity depending on the pH and freezing rate [61].

The conventional techniques suffer from some disadvantages related to the difficulty in controlling the scaffold architecture and mimicking the ECM structure, and are often poorly reproducible. Thus, so-called unconventional techniques have been proposed, including three-dimensional (3D) printing, laser ablation, and pressure-assisted microsyringe.

3D printing possesses great potential in producing scaffolds for biomedical applications [62]. The procedure, based on a bottom-up approach, involves a computer-assisted combination of materials in 3D

shape. Among the different 3D printing techniques, Se- lective Laser Sintering (SLS) is the most used for biomedical applications [63]. In SLS, polymer particles are locally fused together into solid structures by the application of a high-powered laser (infrared or CO_2 laser), with the motion of the laser beam being con- trolled by a computer-aided platform. A layer-to-layer overlay allows highly complex and tailored scaffolds to be formed [64]. The method is cost effective due to the possibility to recycle the unused particles, and highly versatile since it allows tuning scaffolds properties by modulating the processing parameters, such as the particle size, laser power, and scan speed [65].

Different natural and synthetic polymers can be shaped into 3D cardiac scaffolds by laser ablation, consisting of the thermal or photochemical removal of materials from

bulk [66], although the high energy required in the process limits the application of this methodology.

Finally, a well-defined scaffold geometry can be obtained by the pressure-assisted microsyringe technique, where a 5–20 μm capillary needle is used to extrude a polymer dissolved into a high volatile solvent. The viscosity of the polymer solution, together with the needle diameter and the applied pressure, contributes to determine the scaffold's morphology and surface properties [67].

4. Natural Polymers in Cardiac Regeneration

Natural polymers are ideal candidates for the preparation of cardiac scaffolds, as documented by an analysis of the current clinical trials in the field [1].

Italian research in this field mainly involves the use of collagen (COL), gelatin (GEL), and silk fibroin (FIB) as the protein materials, while chitosan (CHI), alginate (ALG), heparin (HEP), and hyaluronic acid (HYA) represent the most explored polysaccharides. The main examples of biomaterials based on natural polymers proposed for cardiac regeneration are shown in Table 1.

Table 1. Biomaterials based on natural polymers proposed for cardiac regeneration applications in Italian research.

Composition	Formulation	Preparation	Model		Outcomes		Ref
			In vitro	In vivo	In vitro	In vivo	
COL	Patches	Preformed Sponges	SMC HUVEC CM	Wistar rats	Cell growth and differentiation	Angiogenesis Arteriogenesis	[68]
GEL	Microspheres	Water-in-oil emulsion	CPC	NOD SCID mice	Cell engraftment	Cell accumulation	[69]
FIB	Scaffolds	Freeze-drying Electrospinning	CPC	- - -	Overexpression of cardiac proteins and ECM	- - -	[70]
CHI	Patches	Electrochemical deposition	MS1	- - -	Biocompatibility	- - -	[71]
ALG CHS	Injectable hydrogels	In situ gelation	CM CF	- - -	Cell growth and differentiation	- - -	[72]
ALG	Hydrogels	Ionic gelation	CD14+	Sprague Dawley rats	Biocompatibility	Enhanced wound healing	[73]
HYA	Scaffolds	Preformed scaffolds	MSC	Swine	Cell growth and differentiation Synthesis of VEGF	Cell growth and differentiation Angiogenesis	[74]
COL/CHI	Scaffolds	Electrophoretic deposition	HFF C2Cl2 CM iPSC	- - -	Cell adhesion and orientation Cell growth and differentiation	- - -	[75]
GEL/GLL	Microparticles	Water-in-oil emulsion	CPC Porcine heart	- - -	Cell adhesion Cell growth	- - -	[76]
GEL/GLL	Microparticles	Water-in-oil emulsion	CPC	Wistar rats	Cell adhesion Cell growth Release of IGF-1	Cell growth	[77]
GEL/ALG COL/ALG	Sponges	Ionic and chemical gelation	C2C12	- - -	Cell growth and differentiation	- - -	[78]
GEL/ALG	Scaffolds	Ionic and chemical gelation	C2C12	- - -	Cell growth and differentiation	- - -	[79]
GEL/CHS	Patches	Electrospinning	NHDF HUVEC CF/CM	- - - -	Biocompatibility Cell adhesion Cell growth and differentiation	- - -	[80]

ALG: alginate; C2C12: mouse myoblast; CD14+: CD14 positive human peripheral blood monocytes; CF: cardiac fibroblasts; CHI: Chitosan; CHS: chondroitin sulfate; CM: cardiomyocytes; COL: collagen; CPC: cardiac progenitor cells; FIB: silk fibroin; GEL: gelatin; GLL: gellan; HFF: human foreskin fibroblasts; HUVEC: human umbilical vein endothelial cells; HYA: hyaluronic acid; IGF-1: insulin-like growth factor 1; iPSC: pluripotent stem cells; MS1: mouse endothelial cells; MSC: mesenchymal stem cells; NHDF: normal human dermal fibroblasts; rCM: rat neonatal cardiomyocytes; SMC: vascular smooth muscle cells; VEGF: vascular endothelial growth factor.

COL is the major fibrous protein of the ECM, composed of tropocollagen monomers, formed by three left-handed polypeptide chains rich in glycine, proline, and hydroxypro- line, that join to form a triple right helix [81]. Among the 28 types of collagen, type I is the main component of ECM myocardium and the most investigated in cardiac tissue engineering [82], because of its ability to mimic the native cardiac structure, promoting tissue formation, cell differentiation in vitro, and the maintenance of

myocardial geometry during the cardiac cycle [83,84]. The potential of type I collagen sponge in promoting the neovascularization process was tested both in in vitro and in vivo studies. The collagen scaffolds were applied on the epicardial surface of both cryoinjured and intact rat hearts, finding the complete absorption of the collagen scaffold after 60 days post-injury time and the appearance of new arterioles and capillaries in both experimental models [68].

GEL, the hydrolysis product of collagen, was also used as base materials for cardiac tissue engineering. Gelatin microspheres with a dimensional range of 50–75 µm were prepared by the water-in-oil emulsion process in the presence of glutaraldehyde as crosslinker and proposed as microcarriers of human cardiac progenitor cells (CPC) in the ischemic

myocardium. The microparticles were able to promote in vitro cell attachment, maintaining their cardiogenic potential, while in vivo models of myocardial infarction revealed that the significant increase in cell engraftment in myocardial tissue was not accompanied by an equal improvement in cardiac function, compared to CPC only [69] (Figure 2).

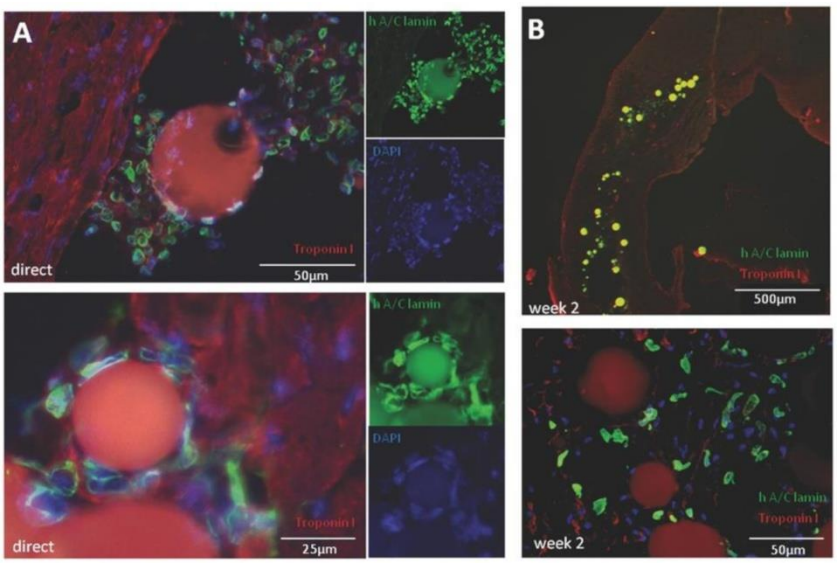

Figure 2. Injection of CPC-laden gelatin MS into murine myocardium. (**A**) Histological analysis. (**B**) Two weeks post-injection. Reproduced with permission from [69], 2016, John Wiley and Sons.

Silk-based materials, such as films, hydrogels, nano- and micro-nets, and sponges [85,86], are a promising class of systems for biomedical application due to their tunable mechanical features, biodegradation, and biocompatibility. Biomaterials based on silk fibroin, obtained by directly treating degummed fibers, have been employed to induce the regeneration of various mammalian tissues, including bone, cartilage, tendon, and skin [87,88].

FIB scaffolds with three different geometries (two sponges with different pore sizes and distributions and an electrospun nanometric net) were prepared and the influence on CPC differentiation and integrin, cardiac, and sarcomere protein expression evalu- ated in vitro [70]. The study demonstrated that the scaffolds embedded with a collagen-containing medium and seeded with CPC can efficiently drive cell commitment, as demonstrated by the high level of sarcomere and cardiac proteins, as well as by the great quantity of ECM observed after 21 days.

Fibrinogen and its enzymatic hydrolysis product, fibrin (FBR), are glycoproteins extensively employed in cardiac tissue engineering by virtue of their peculiar characteristics, such as an improved healing mechanism, protective against myocardial reperfusion injury, and increased cell migration [89–91]. In the literature, there have been reports on the application of fibrin matrices loaded with mesenchymal stem cells [92] and human embryonic stem cells [93] as valuable scaffold materials able to improve left ventricle contraction and prevent heart failure. An FBR cardiac patch was involved in a clinical trial (ClinicalTrials.gov identifier: NCT02057900). Here, cardiac progenitors embedded in the patch were epicardially delivered during a coronary artery bypass procedure. The results showed the ability of the patch to promote the formation of highly purified cardiac progen- itor cells, without the occurrence of arrhythmia phenomena [94].

CHI is another key material explored for cardiac applications because of either its sustainability (it is a by-product of the food industry), biocompatibility, biodegradability, and antibacterial properties, or its cationic nature, promoting the interaction with the anionic glycosaminoglycans and proteoglycans of the cardiac ECM [95]. The latter is a key determining factor for cardiac applications, since the presence of glycosaminoglycan in the cardiac ECM is a critical factor for modulating the functionalities of specific proteins, such as growth factors [96]. Moreover, the high versatility of CHI allows the fabrication of scaffolds with a tunable morphology and chemo-physical properties, including the porosity and pore level [97,98]. A wide range of 3D-printed CHI scaffolds [99,100] have been proposed for skin [101] and bone [102] regeneration, while thin scaffolds crosslinked by either genipin or epichlorohydrin with two different oriented porosities were employed as cardiac patches [71]. The possibility to modulate the available chemical functionalities (e.g., amino and hydroxyl groups for epichlorohydrin and genipin, respectively), together with that to control the porosity and

the micro-channel orientation, were considered as the added value of the proposed scaffolds, since the regeneration of cardiac tissue requires a preferential cell orientation. Saporito et al. have developed an injectable in situ gelling systems based on an anionic polysaccharide, such as ALG, and on chondroitin sulphate (CHS) loaded with platelet lysate (PL), to improve the survival rate of the cardiomyocytes after myocardial infarction. The choice of ALG as base material for repairing myocardial infarction, cardiac regeneration, supporting heart vascularization, re-cellularization, and restoring electrical conductivity [103], is related to its ability to form high viscous solutions due to long-range interactions within the polymer chains [104], thus allowing the formation of hydrogels in mild conditions. The results of in vitro studies on fetal heart cells showed that the system is able to maintain a prolonged residence time of the PL, allowing a high degree of cardiac cells survival (either cardiomyocytes or cardiac fibroblasts) after oxidative damage [72]. Bloise et al. hypothesized that the activation of immune-mediated mechanisms of heart repair by the release of a colony-stimulating factor and anti-inflammatory interleukins 4/6/13 from a Ca^{2+} crosslinked ALG hydrogel can stimulate wound healing and restore myocardial function after the infarct [73].

The suitability of ALG injectable hydrogels for cardiac regeneration was proved by three different clinical trials. A bio-absorbable ALG hydrogel (IK-5001, Bellerophon BCM LLC) injected into the infarct-related artery was found to be totally safe, even if the treat- ment did not reduce heart remodeling (ClinicalTrials.gov identifier: NCT01226563) [105]. On the other hand, a significant improvement in cardiac function parameters (e.g., ejection fraction, end-systolic and diastolic volumes, and average wall thickness) was recorded after treatment with acellular ALG hydrogels (Algisyl-LVR^{TM}, LoneStar Heart Inc., (Mission Viejo, CA, USA) ClinicalTrials.gov identifier: NCT0084796) [106]. The same hydrogel was also tested on 78 patients with dilated cardiomyopathy, obtaining a remarkable ameliora- tion of the exercise capacity (ClinicalTrials.gov identifier: NCT01311791) [47].

HYA, a fundamental component of the ECM, is involved in cellular proliferation and differentiation, and thus in many biological processes, including wound repair and inflam-mation [107]. Muscari et al. investigated the transplantation of autologous mesenchymal stem cells (MSC) with a hyaluronan-based knitted scaffold to restore the functionality of the infarcted myocardium via induction of neo-angiogenesis and histological modifications of the cardiac cells [74]. The advantage of inserting HYA in a cardiac scaffold originates

from its role in angiogenesis and inflammation modulation, thus allowing neovascularization of cardiac tissue and increasing the capillary density and normalizing left ventricular function in an infarcted heart [108]. Contrast-enhanced ultrasound studies showed that the native tissue interacted positively with the scaffold by modifying the extracellular matrix with a reduced presence of collagen and an increased content of proteoglycans. As a result, a lower degree of cardiomyocyte damage was observed, with the absence of any trace of inflammatory process at the infarct site, probably due to the action of the grafted MSC attenuating cellular infiltration.

As before mentioned, proteins and polypeptides were often combined with polysaccharides in order to obtain composite systems mimicking the ECM composition and able to promote cell division and growth during the tissue regeneration process [109].

A blend of COL and CHI, obtained by electrophoretic deposition, was proposed as a highly biocompatible 3D-scaffold to support fibroblast as well as cardiomyocyte adhesion and proliferation. The attachment, spreading, and orientation of cardiomyocytes were affected by the blend of the composition, showing the suitability of the proposed material for promoting cardiac tissue regeneration [75].

The water-in-oil emulsion method was employed to fabricate GEL-GLL microparticles as injectable scaffolds to repair the infarcted myocardium. The systems showed good injectability and persistence at the injection site. Moreover, by in vitro cell culture assays, the influence of particle diameter on cardiac progenitor cells was demonstrated, indicating a preferential cell adherence to microparticles with a smaller size [76]. After loading with insulin-like growth factor-1 (IGF-1) by absorption, in vivo experiments were performed, finding an attenuated chamber dilatation and myocardial damage and fibrosis, together with an improved cell homing [77].

ALG was used as a polysaccharide counterpart in the synthesis of GEL- or COL-based blends crosslinked both by Ca^{2+} ions and by glutaraldehyde for cardiac regeneration [78]. Different ALG-to-GEL weight ratios were tested and the best results in terms of cell prolifer- ation using C2C12 myoblasts were obtained for the blends containing more than 60% GEL, with the ALG/GEL ratio of 20:80 showing the ability to promote cell differentiation [79].

Heart patches based on GEL and CHS were prepared by means of electrospinning and proposed as fibrous implants to improve heart recovery after corrective surgery for critical congenital heart defects. CHS improved the mechanical properties of the system,

increasing the elasticity and reducing the stiffness. The nanofibrous scaffolds were loaded with PL as a source of growth factors to enhance the tissue repair. Interestingly, the patches appeared to selectively favor the proliferation of cardiomyocytes rather than cardiac fibroblasts, thus reducing the fibrosis phenomena [80]. A 3D-printed biocomplex, composed of a HYA/GEL matrix system and CPC, was transplanted into a mouse model of myocardial infarction, leading to a significant reduction in adverse remodeling and preservation of cardiac performance, as evidenced by both magnetic resonance imaging and histology. In addition, the matrix supported the long-term in vivo survival and engraftment of CPC, which exhibited a temporal increase in cardiac and vascular differentiation markers overthe course of the 4-week follow-up period.

5. Synthetic Polymers in Cardiac Regeneration

Several biodegradable polymers, such polyethylene glycol (PEG), poly(εcaprolactone) (PCL), poly (glycerol sebacate) (PGS), poly(l-lactide) (PLA), poly(lactic-co-glycolic acid) (PLGA), biodegradable polyurethanes (PUR), and poly(butylene succinate) (PBS), gainedconsiderable interest for cardiac regeneration [110] (Table 2).

Table 2. Biomaterials based on synthetic polymers proposed for cardiac regeneration applications in Italian research.

Composition	Formulation	Preparation	Model		Outcomes		Ref
			In vitro	In vivo	In vitro	In vivo	
PGS/PCL	Fibers	Electrospinning/ soft lithography	C2C12 rCM	- - -	Cells orientation and morphology dependent on fibers topography	- - -	[111]
PPDL	Fibers	Electrospinning	H9C2	- - -	Cell adhesion and proliferation	- - -	[112]
P(BSmTESn)	Film	Compression moulding	H9C2	- - -	Cell adhesion and differentiation depending on comonomer ratio	- - -	[113]
	Nanoparticles	Water-in oil miniemulsion	DMT release experiments in physiological conditions		Encapsulation and kinetic release depending on comonomer ratio		
PUR	Porous scaffolds	Thermally-Induced Phase Separation	H9C2	- - -	Cell viability dependent from PUR composition	- - -	[114]
PUR	Porous scaffolds	Melt-extrusion	CPC	- - -	Cell adhesion and proliferation	- - -	[115]
PUR-LN-1	Biomimetic scaffold	melt-extrusion / carbodiimide chemistry	CPC	FVB Mice	Cell adhesion and proliferation	Angiogenesis	[51]
PUR	Patches	electrospinning	- - -	Lewis rats	- - -	Angiogenesis / Scar formation inhibition / Left ventricle wall thinning inhibition	[116]
PUR/SiO/AT	Film	Sol-gel reaction	C2C12	- - -	Electro-conductivity / Cell adhesion and proliferation		[117]
PLA-co-TMC	Fibers	Electrospinning	CM	- - -	Cell proliferation / Morphology preservation	- - -	[118]
PLA- GCSF	Fibers	Electrospinning	- - -	Rabbits	- - -	Angiogenesis / Reorganization of the ECM architecture	[119]
PLGA	Injectable hydrogel	Emulsion solvent extraction-evaporation	ADSC	- - -	Cell growth and differentiation	- - -	[120]
PVA	Scaffolds	gas foaming/ freeze drying	iPSC	- - -	Cell growth and differentiation	- - -	[121]
Polypeptide-RGD	Injectable hydrogel	Self-assembling	rCPC	Wistar rats	Cell differentiation	Reduced heart damage	[122]
P(3HB-co-4HB)- RGD	Fibers	Electrospinning/aminolysis	H9C2	- - -	Cell adhesion and proliferation	- - -	[123]
PMEMA-co-DEAMA-coated PCL	Preformed discs coating	Dip-coating	VIC	- - -	Cell growth	- - -	[124]

ADSC: human adipose-derived stem cells; AT: aniline tetramer; C2C12: mouse myoblast; CM: cardiomyocites; CPC: human cardiac progenitor cells; DMT: dexamethasone; ECM: extracellular matrix; GCSF: granulocyte colony-stimulating factor; H9C2: heart myoblast; iPSC: pluripotent stem cells; LN-1; laminin-1; [P(3HB-co-4HB)]: Poly(3-hydroxybutyrate-co-4-hydroxybutyrate); P(BSmTESn): poly(butylene/triethylene succinate); PCL: poly(εcaprolactone); PGS: Poly(glycerol sebacate); PLGA: poly(lactic-co-glycolic acid); P(L)LA-co-TMC: polylactide-trimethylcarbonate; PMEMA-co-DEAMA: poly(methoxyethylmethacrylate-co-diethylaminoethylmethacrylate); PPDL: poly(ω-pentadecalactone); PUR: polyurethanes; rCM: rat neonatal cardiomyocytes; rCPC: rat cardiac progenitor cells; PVA: poly(vinyl alcohol); RGD: arginine-glycine-aspartic acid; SiO:siloxane; VIC: valve interstitial cells.

To promote cardiac cell alignment, PGS and PCL were combined in patterned electrospun fibers, simulating the architecture of cardiac tissue. Since nano- and micro-scale topographical features of the fibers play a critical role in the induction and maintenance of various cellular properties and functions, different surface topographies were inves- tigated, such as squares and grooves, with constant or different interspatial distances. The results of in vitro cell culture assays showed that the surface topography influenced the cardiomyocytes' orientation and morphology, without affecting the cells' viability [111]. Sub-micrometric fibers of poly(ω-pentadecalactone) obtained by electrospinning were proposed as biocompatible scaffolds characterized by long degradation times. The ad- hesion and proliferation of rat cardiac H9C2 cells on the scaffold surface was evaluated, verifying that the cells retained their morphology and form a confluent monolayer [112]. In a more recent work, a series of random PBS-based copolymers containing PEG-like sequences of triethylene succinate (TES) was synthesized by melt polycondensation and tested as scaffolds for embryonic rat cardiac H9C2 cell adhesion and proliferation and as delivery devices of the anti-inflammatory drug dexamethasone (DMT). It was found that by varying the molar percentage of TES in the copolymer, the thermal and mechanical properties, surface wettability, and hydrolysis rate of the material can be easily modified. In addition, the proposed biomaterials showed good biocompatibility properties, with the copolymers containing up to 20 mol% of TES co-units, sustaining a better cell adhesion and proliferation as well as the highest encapsulation capability and the fastest DMT release kinetics [113].

Among the different types of synthetic polymers used for the preparation of cardiac devices, PUR shows high versatility, because of the biocompatibility and the elastic properties necessary to avoid plastic deformation or failure, and the large number of macrodiols, diiso- cyanates, and chain extenders available for the preparation. Silvestri et al. reported on the synthesis of four biodegradable scaffolds by thermally-induced phase separation, adding poly (ester urethanes) and poly (ether ester urethanes) from PCL and PEG as macrodiols, 1,4-diisocyanatobutane as a diisocyanate, L-lysine ethyl ester, and alanine–alanine–lysine peptide as chain extenders, to confer enzymatic degradability to the final system. Elastase degradation tests demonstrated the possibility to finely tune the biodegradation rate, while the best results in terms of cell proliferation were obtained with the scaffold containing the lowest amount of PEG, probably for the more adequate microstructure favoring cell attachment [114]. PUR bi-layered scaffolds,

endowed with elastomeric-like behavior, were prepared by melt-extrusion additive manufacturing using PCL as the diol, BDI as the diisocyanate, and L-lysine ethyl ester dihydrochloride as the chain extender. The resulting scaffolds were found to efficiently support CPC adhesion and spreading, although a poor proliferation was observed after a 1–14 days culture time [115]. The same PUR system was functionalized by plasma-mediated grafting with laminin-1 (LN1), a protein protecting CPC from apoptosis and stimulating their proliferation [52]. Compared to pristine PUR and the system obtained using GEL as the functionalizing protein, the resulting PUR-LN1 scaffold showed an increased cell density, an improved cell protection against apoptosis, and enhanced CPC proliferation, stimulating their differentiation into cardiomyocytes, endothelial cells, and smooth muscle cells [51].

In order to investigate the influence of scaffold anisotropy and ECM incorporation on the pathological remodeling process initiated by myocardial infarction, three different microfibrous, biodegradable patches composed of poly (ester carbonate urethane)urea were prepared. The results showed that the bi-layered patch containing ECM promoted angio- genesis, inhibiting scar formation and left ventricle wall thinning, typical key phenomena of maladaptive remodeling following myocardial infarction. On the other hand, the patches with the stiffer direction parallel to the heart circumferential direction (orthogonal group) and with the longitudinal direction of the heart (longitudinal group) did not produce significant effects on echocardiographic function, wall thinning, or scar formation [116].

Electrically conductive polyurethane/siloxane networks, containing different amounts of aniline tetramer (AT) as conductive moieties, were proposed for cardiac tissue engineering application. Castor oil was employed as the biodegradable source of polyols whereas siloxane domains guaranteed mechanical strength properties. The results of the biologi- cal experiments demonstrated that AT affects the attachment and proliferation of C2C12 myoblasts, confirming the potential application of the materials as a cardiac patch [117]. Polylactic acid (PLA) derives from polycondensation of lactic acid, a monomer of natural origin produced by the bacterial fermentation of carbohydrates, or by ring opening polymerization of the cyclic dimer lactide [125]. PLA can be easily obtained in the form of fibers, films, and sheets that can be used not only as scaffolds for tissue regeneration but also as drug delivery vehicles [126,127]. In cardiac tissue engineering, PLA is widely used because it is a cytocompatible and biodegradable material with

different physical-chemical, mechanical, and thermal properties, depending on the stereo-regularities obtained from the L or D enantiomers of lactic acid during polymerization [128,129]. Moreover, it is often combined with other synthetic polymers in order to obtain materials with optimized biomechanical properties [130].

A commercial copolymer of (L)-lactic acid with trimethylene carbonate (PLA-co-TMC), well known for its interesting thermal, mechanical, and degradation behaviors, was em- ployed as starting material to obtain a biomimetic electrospun scaffold, and its performance compared with a PLA homopolymer scaffold. PLA-co-TMC modified its mechanical properties by varying the surrounding temperature, being a glassy rigid material at room temperature and a rubber-like soft material at 37 °C, and when seeded with cardiomy- ocytes, efficiently promoted cell proliferation, preserving cell morphology [118]. A PLA electrospun scaffold releasing granulocyte colony-stimulating factor (GCSF) was tested as a ventricular patch in a rabbit chronic model of myocardial infarction. It was found that the scaffold efficiently integrated into a chronic infarcted myocardium, and that the function- alization of the biopolymer with GCSF led to increased fibroblast-like vimentin-positive cellular colonization and reduced inflammatory cell infiltration within the micrometric fiber mesh in comparison to nonfunctionalized scaffold. Moreover, a PLLA/GCSF polymer induced an angiogenetic process with a statistically significant increase in the number of neovessels compared to the nonfunctionalized scaffold and, when implanted at the infarcted zone, induced a reorganization of the ECM architecture, leading to connective tissue deposition and scar remodeling. These findings were combined with a reduction in end-systolic and end-diastolic volumes, indicating a preventive effect of the scaffold on ventricular dilation, and an improvement in cardiac performance [119].

The main limitation in the use of PLA is its degradation products, in particular, lactic acid, which is a relatively strong acid that can cause an inflammatory response when it accumulates internally, accelerating the degradation of the implant and the loss of its mechanical integrity. Thus, different approaches have been proposed to mitigate the shortcomings of this synthetic polymer, including the preparation of a copolymer of lactic acid and glycolic acid: poly (lactic-co-glycolic acid) (PLGA) [131]. PLGA microparticles were used as a carrier of growth factors to simulate cell proliferation and organization in vessels [132]. When applied in cardiac regeneration, PLGA microparticles loaded with human adipose-derived stem cells, hepatocyte growth factor,

and IGF-1 were incorporated into an injectable hydrogel, to obtain a multifunctional system able to stimulate the survival and/or differentiation of the grafted cells toward a cardiac phenotype. Following the growth factors release, an enhanced synthesis of cardiac differentiation markers was observed, as well as an accelerated cell cycle progression. Moreover, the addition of the thermosensitive P407 hydrogel to the microparticulate system led to an improvement of its elasticity properties and an increase in junction connections in human adipose-derived stem cells [120].

Between the many biopolymer-based scaffolds already studied, poly (vinyl alcohol) (PVA) devices have a great potential for cardiac tissue engineering because of their excellent mechanical properties, such as stability and flexibility, conferring an adaptive behavior towards the strain changes caused by cardiac contractions [133]. Moreover, PVA retain a significant amount of water or biological fluids, swelling without dissolving. Dattola

et al. reported on the fabrication of a biocompatible, porous PVA scaffold, employing a combination of gas-foaming and freeze-drying processes, avoiding any cross-linking agents. An analysis of the stress–strain curves proved that the obtained scaffolds were characterized by an elastic behavior similar to that of the muscle ECM, while the potential applicability as a cardiac device was confirmed by the ability to support human-induced pluripotent stem cell growth and differentiation into cardiomyocytes [121].

A useful approach to stimulate cell activity is the surface conjugation of scaffolds with the RGD (R: arginine; G: glycine; D: aspartic acid) peptide, a well-established cell adhesion motif. RGD is a tri-amino acid constituting a variety of ECM proteins, playing a pivotal role in the regulatory functions of many biological activities [134]. In an interest- ing work, Burgess et al. reports on an alternative approach to promote the delivery and retention of cardiac progenitor cells into the heart based on an injectable self-assembling peptide hydrogel functionalized with RGD. The results of the study demonstrated that CPC cultured in vitro within the hydrogel spontaneously differentiated towards adult cardiac for one-week phenotypes. Furthermore, after injection, the hydrogel on its own resulted in a reduction in heart damage, and when loaded with CPC, was able to retain them for up to 10 days at the injury site, with a significant reduction in left ventricular dilation [122]. The RGD peptide was immobilized by aminolysis on a scaffold based on poly(3-hydroxybutyrate-co-4-

hydroxybutyrate) [P(3HB-co-4HB)], a bacterial copolymer with desirable mechanical and physical properties, demonstrating that the surface modifi- cation enhanced the hydrophilicity of the system, promoted the cell–scaffold interaction, and enhanced the attachment and proliferation of H9C2 myoblast cells [123] (Figure 3).

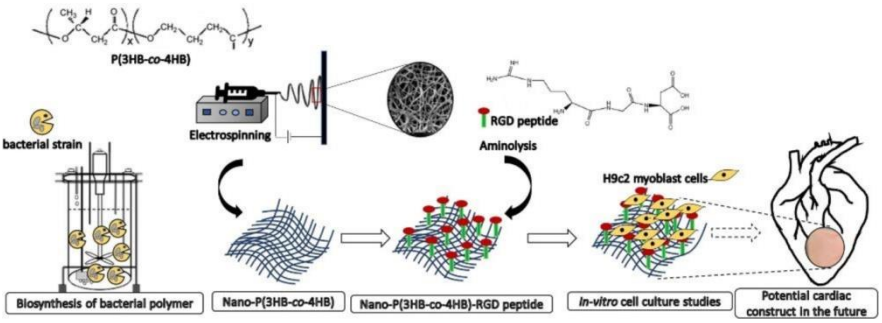

Figure 3. Schematic representation of the nano-P(3HB-co-4HB) scaffold. Reproduced from [123], 2020, Frontiers.

Finally, non-degradable polyacrylate copolymers were proposed as useful materials in the valve scaffold manufacturing process. The interest towards this class of copolymer is derived from their highly tunable mechanical properties, high biocompatibility, and the possibility to be functionalized with various biologics, such as adhesion molecules, binding repeats, extracellular matrix components, and cytokines. Poly (methoxyethylmethacrylate-co-diethylaminoethylmethacrylate) was used as a coating agent of non-woven PCL scaffold and seeded with valve interstitial cells (VIC). The authors observed that VIC increased the secretion of the elastin-maturing component and of other valve-specific extracellular matrix components, proving the effectiveness of the proposed valve implants in promoting VIC adherence and growth, and avoiding their evolution toward a pro-calcific phenotype [124].

6. Composite and Hybrid Systems in Cardiac Applications

An ideal scaffold for cardiac regeneration should be highly biocompatible, support cell proliferation, and possess adequate elasticity to not compromise heart contractile function. To fully satisfy these requirements, composite and hybrid systems are often proposed, to combine the key properties of the individual components [135,136] (Table 3).

Table 3. Composite and hybrid biomaterials for cardiac regeneration applications in Italian research.

Composition	Formulation	Preparation	Model		Outcomes		Ref
			In vitro	In vivo	In vitro	In vivo	
PEG-FBN	Patches	Radical Polymerizarion	iPSC	NOD SCID mice	Cell growth and differentiation	Cell growth and differentiation Angiogenesis	[137]
BSA-MPs@PEG-CHS-FIB	Injectable Hydrogel	Radical Polymerizarion	CMSC	- - -	Cell growth and differentiation	- - -	[138]
BSA-MBs@PEG-FBR	Hydrogel	Radical Polymerizarion	HFF CPC	- - -	H_2S release	- - -	[139]
PEtU-PDMS/FBR	Hydrogel	Spray phase inversion	AMSC	- - -	Cell growth and differentiation	- - -	[140]
PNIPAAm/HEMAHex -ALG/GEL	Scaffolds	Micromolding	C2C12	- - -	Cell adhesion and growth	- - -	[141]
ALG/GEL-PCL	Scaffolds	Molding	H9C2	- - -	Cell growth and differentiation	- - -	[142]
ALG/GEL-PDO	Scaffolds	Ionic and chemical gelation	CPC	Rat	Cell growth and differentiation	Restoring of cardiac functions	[143]
PLGA/GEL	Scaffolds	Solvent casting	MSC	- - -	Cell Adhesion and alignment Cell growth and differentiation		[144]
PEG-HEP	Hydrogel	Radical Polymerizarion	MSC MCS	Sprague Dawley rats	Biocompatibility Angiogenesis	Cell retention and engraftment Cell growth Angiogenesis	[145]
PVA/DEX/βCD	Hydrogel	Molding	3T3 H9C2	- - -	Biocompatibility Cell growth	- - -	[146]
CHI/PCP	Scaffolds	Freeze-drying	SH-SY5Y	- - -	Electrical conductivity Biocompatibility	- - -	[147]
GEL/SWCNT	Scaffolds	Chemical gelation	H9C2	- - -	Electrical conductivity Biocompatibility	- - -	[148]
PSHU−PNIPAAm/ MWCNT	Scaffolds	Condensation	NRVM	- - -	Long term cells survival Cell growth and differentiation	- - -	[149]
PLA/MNP	Films	Spin-coated assisted deposition	H9C2	- - -	Biocompatibility Cell adhesion Cell growth and differentiation	- - -	[150]
CaP	Nanoparticles	Precipitation	HL-1 CM	Mice	Biocompatibility	MiRNA delivery	[151]
SiO_2	Nanoparticles	Water-in-oil microemulsion	MSC	- - -	Cell adhesion Cell growth and differentiation	- - -	[152]

3T3: mouse fibroblast; ALG: Alginate; AMSC: human amniotic mesenchymal stromal cells; BSA: Bovine Serum Albumin; C2C12: mouse myoblast; CaP: calcium phosphate; CD: Cyclodextrin; CHS: chondroitin sulfate; CMSC: Cardiac Mesenchymal Stem Cells; CPC: Cardiac progenitor cells; DEX: Dextran; FBN: Fibrinogen; FBR: Fibrin; FIB: Fibroin; GEL: Gelatin; H9C2: Rat embryo ventricular cardiomyocytes; HEMAHex: 2-hydroxyethylmethacrylate-6-hydroxyhexanoate; HEP: Heparin; HFF: human foreskin fibroblasts; HL-1: Cardiac Muscle Cell Line; iPSC: pluripotent stem cells; MBs: Microbubbles; MCS: Mononuclear cells from Sprague Dawley rats; MNP: magnetic nanoparticles; MPs: Microparticles; MSC: Mesenchymal stem cells; MWCNT: Multi-Walled Carbon Nanotubes; PNIPAAm: Poly-N-isopropylacrylamide; NRVM: Neonatal Rat Ventricular Myocytes; PCL: polycaprolactone; PCP: pyrolysed cork powder; PLA: poly(lactic acid); PLGA: poly(lactic-co-glycolic acid); PDMS: polydimethylsiloxane; PDO: Polydioxanone; PEG: poly(ethylene glycol); PEtU: poly(ether)urethane;PSHU: poly(serinol hexamethylene urea);PVA: polyvinylalcohol; SH-SY5Y: Neuroblastoma cell line; SHU: serinol hexamethylene urea; SWCNT: Single-Walled Carbon Nanotubes.

7. Composite Materials

Pure fibrinogen or fibrin scaffolds often suffer from some limitations related to their poor mechanical properties that may restrict their field of use [153]. Thus, fibrinogen or fibrin were combined with synthetic polymers in order to reinforce the whole structure, improve the elasticity, and the resistance to deformation forces [154].

Poly (ethylene glycol)-fibrinogen scaffolds were loaded with iPSC cells bioengineered to secrete placental growth factor and matrix metalloproteinase 9 factors involved in vascularization and engraftment processes. When injected in infarcted rat myocardium, an improved revascularization and hemodynamic parameters were recorded, together with an interesting functional integration of allograft-derived cells and host myocardium [137]. Hydrogels based on FIB and polyethylene-glycol-diacrylated were prepared by photopolymerization and proposed as sponge-like scaffolds and injectable carriers for cardiac mesenchymal stem cell differentiation. Bovine serum albumin microspheres were added to the hydrogel system to increase the porosity and cell-adhesive properties of the material. Good viability and expression of proteins characteristic of the initial phases of the cardiac muscle differentiation process were recorded, with a further increase in the cell viability after the addition of chondroitin sulfate into the scaffolds [138].

In another work, enzyme-coated bovine serum albumin microbubbles able to catalyze the H_2S release were loaded into a polyethylene glycol–fibrinogen hydrogel in order to favor the proliferation and differentiation of human Sca-1 pos cardiac progenitor cells (hCPC), with micropores within the scaffold serving as biological cues to promote cell attachment and maintain cell morphology. The authors claimed the possibility to employ this H_2S-releasing 3D scaffolds to minimize the ischemic effects and reperfusion damages in the implant site thanks to the properties of the H_2S [139]. In addition, FBR layers were reinforced with poly(ether)urethane–polydimethylsiloxane, obtaining a semi-interpenetrating polymeric network with desirable elastic properties and able to sustain growth and differentiation of human amniotic mesenchymal stromal cells [140].

The combination of an ALG/GEL blend with poly(N-isopropylacrylamide)-co-2-hydroxyethylmethacrylate-6-hydroxyhexanoate by the micromolding technique carried out to the fabrication of 3D scaffolds with cardiac ECM-like microarchitecture. Due to their favorable properties, such as superficial microporosity, elastic behavior, and anisotropic properties similar to that of an adult human left ventricular myocardium, the

materials were proposed as effective scaffolds for myoblast proliferation and differentiation [141]. In order to reinforce the performances of the 20:80 ALG/GEL sponge blend and improve the sutur- ing properties of the final system [78], fibrous structures based on polycaprolactone (PCL) were inserted. The resulting material perfectly combined the hydrophilicity of the natural blend and the mechanical properties of the synthetic polymer without compromising the biocompatibility [142].

Polydioxanone was also investigated as a reinforcing agent of an ALG/GEL blend functionalized with IGF-1, using the avidin–biotin-binding strategy, with the in vitro and in vivo biological characterization demonstrating the enhanced cell adhesion and long- term retention after implantation on the damaged myocardium, together with an improved suture ability [143].

A PLGA/GEL-based biomaterial with controlled degradation kinetics was proposed as a scaffold for human MSC. The system, mimicking the anisotropic structure and the mechanical properties of cardiac tissue, has found to promote adhesion, long-term viabil- ity, and ordered disposition of MSC, as a confirmation of its suitability in restoration of myocardium viability [144]. Ciuffreda et al. proposed a hydrogel system based on PEG and acrylated heparin (HEP) as a synthetic substitute for the extracellular matrix, with the aim to couple the well-known treatments of ischemic heart disease by MSC transplantation with the ability of heparinized biomaterials to stimulate angiogenesis in both subcutaneous implants and wound healing models. The authors found a significant increase in MSC engraftment, a reduction in ventricular remodeling, stimulation of neo-vasculogenesis, and an increase in several pro-angiogenic factors [145]. Zuluga et al. proposed the delivery of Astaxanthin, an FDA approved xanthophyll carotenoid derivative, by a composite hydrogel consisting of polyvinyl alcohol/dextran/cyclodextrins. Astaxanthin allows the mitigation of oxidative stress in the heart by blocking ROS and reducing the myofibril stress [146].

8. Hybrid and Inorganic Materials

In order to improve the performance of the cardiac scaffolds in terms of mechanical, electrical, and functional properties, inorganic counterparts were combined to natural or synthetic polymers to obtain hybrid systems with superior features.

The work of Scalera et al. was designed to address the limitation of the low electro-conductivity of CHI-based materials [147]. In detail, due to the well-known

possibility to improve the conductivity of different types of biomaterials by incorporation of carbon nanostructures [155], the authors focused their attention on the production of graphitic materials from natural sources, and from pyrolyzed cork in particular. The investigation of the scaffold properties clearly proved the enhanced conductivity and mechanical properties of CHI materials upon incorporation of inorganic carbon, without affecting the high biocompatibility and the degradation patterns. Interestingly, a sample containing 1% (by weight) of carbon filler was found to possess electro-conductivity close to that of cardiac muscle, while the pyrolyzed cork is intended to match with the objectives of the European Green Deal.

Another therapeutic approach is the mitigation of the oxidative stress in the infarcted heart. In this regard, Hao et al. explored the possibility to use fullerenol nanoparticles loaded into an injectable ALG hydrogel network as an antioxidant vehicle for cell release [156]. The presence of fullerenol was found to be able to scavenge superoxide anions and hydroxyl radicals, thus ensuring cardiomyogenic differentiation of brown adipose tissue. Single-walled carbon nanotubes (SWCNT) were embedded in a GEL crosslinked matrix and used as scaffolds for the H9C2 cell line. By varying the SWNCT amount, the mechanical, electrical, and biological behaviors of the hybrid system could be tuned, while the phenotypical changes in the H9C2 cell line was evaluated by modifying the culture medium composition. In particular, the best result in terms of cell differentiation was obtained with fetal bovine serum and all-trans retinoic acid concentrations of 1% and 50 nm, respectively [148]. Hybrid injectable biomimetic scaffolds were obtained by the covalent functionalization of lysine-derivatized poly(serinol hexamethylene urea)-co- poly(N-isopropylacrylamide) (RGT-lysine) with multi-walled carbon nanotubes (MWCNT). The copolymer guaranteed a sol-gel phase transition near to body temperature, ideal for biomedical applications, whereas the MWCNT improved the rheological and electrical properties. The results of the biological assays suggested that the chemical conjugation of MWCNT to RGT-lysine enhanced the biocompatibility of the system, with the obtained hybrid scaffold showing an improved long-term cardiac cell survival (up to 21 d), prolifer- ation, and function compared to the same material obtained in absence of MWCNT [149]. Magnetic nanoparticles (MNPs) were also employed as inorganic counterparts of

PLA to obtain ultrathin nanofilms. Since the MNP content affected the roughness and wettability of the scaffold, different materials were prepared and the effect of the

surface properties on cytocompatibility, adhesion, proliferation, and differentiation of H9C2 eval- uated. It was found that the MNPs did not compromise cell viability, improving their adhesion, proliferation, and differentiation properties [150].

Totally inorganic nanoparticles were investigated as scaffolds or delivery systems of bioactive materials into cardiac tissue. Due to the similarity with the main inorganic compo- nent of bones, teeth, and some pathological calcification, calcium phosphate nanoparticles were proposed as a promising platform for in vitro and in vivo miRNA delivery in po- larized tissue, such as the heart. The advantage of using this kind of material lies in their high biocompatibility and pH-sensitive stability, allowing for the complete release of their payload in biological acidic environments, such as endosomes and lysosomes [151]. In another approach, the ability of silica nanoparticles (SiO_2-NP) to facilitate stem cell adhesion capability on cardiac tissue was investigated. SiO_2-NP treatment increases the surface expression of the gap junctions on MSC, increasing the intercellular communications with cardiomyoblasts in an ischemia-like environment [152].

9. Conclusions and Perspectives

Irreversible damage to cardiac tissue after myocardial infarction is the main cause of a progressive loss of organ function that often evolves into heart failure and death. Cardiac tissue regeneration based on biomaterial scaffolds represents an emerging therapeutic strategy to repair the injured heart and improve heart function. Natural or synthetic polymers have attracted much interest for the development of biocompatible supports able to promote the direct transplantation of cells into the injured environment, act as replacement tissues, stimulate the organ in the regeneration of damaged tissues through direct administration of growth factors, and ensure the implantation of polymeric sup- ports able to recruit and stimulate the patient's own cells. This review paper covers the broad range of polymeric materials used for cardiac regeneration purposes developed by the Italian scientific community, highlighting the formulation strategies as well as main outcome results.

The majority of studies dealt with the evaluation of cardiac scaffolds and patches as cell delivering systems, promoting stem cell proliferation and differentiation. The high similarity with the ECM makes the polysaccharides/protein composites the most widely proposed starting materials, with most studies covering alginate and gelatin derivatives. Furthermore, synthetic polymers and inorganic nanoparticles are often added

to the natural system to modulate the mechanical and rheological properties and confer electrical conduc- tivity, respectively. The outcomes of the studies are at a preliminary but promising stage, underlining the huge interest in the field, as well as that a more exhaustive and critical eval- uation of the preclinical data is required before setting up clinical trials. The main issues are the mechanical stability, immunogenic responses, and a proper integration within the host myocardium. A possible answer to these challenges could be the design of a cardiac patch able to treat the harmful consequences of MI and, at the same time, to restore proper cardiac functionalities by delivering specific biological cues.

It should be also underlined that the results of the current clinical trials demonstrated the safety of the proposed patched, while not fully showing their effectiveness in terms of cardiac regeneration, as recorded in the preclinical studies. Clearly, the presence of a gap between the preclinical studies and clinical applications could be filled by the proper exchange of information and synergy between scientists working in different research areas, including technologists, engineers, and clinicians. Only by matching the biomedical requirements with tailored formulation protocols would it be possible to provide insight and valuable strategies that might lead to the lab-bench-to-clinic translation of cardiac biomaterials.

References

Curcio F., Trombino S., Cassano R., Curcio M., Cirillo G., Iemma, F. Polymeric Biomaterials for the Treatment of Cardiac Post-Infarction injuries. *Pharmaceutics*, 2021, 13, 1038.

1. Bar, A.; Cohen, S. Inducing Endogenous Cardiac Regeneration: Can Biomaterials Connect the Dots? *Front. Bioeng. Biotech.* 2020, *8*, 126.
2. Jopling, C.; Sleep, E.; Raya, M.; Marti, M.; Raya, A.; Belmonte, J.C.I. Zebrafish heart regeneration occurs by cardiomyocyte dedifferentiation and proliferation. *Nature* 2010, *464*, 606–609.
3. Esquivel, L.E.P.; Zhang, B.Y. Application of Cell, Tissue, and Biomaterial Delivery in Cardiac Regenerative Therapy. *ACS Biomater. Sci. Eng.* 2021, *7*, 1000–1021.
4. Radisic, M.; Christman, K.L. Materials Science and Tissue Engineering: Repairing the Heart. *Mayo Clin. Proc.* 2013, *88*, 884–898.
5. Abbate, A.; Bussani, R.; Amin, M.S.; Vetrovec, G.W.; Baldi, A. Acute myocardial infarction and heart failure: Role of apoptosis. *Int. J. Biochem. Cell B* 2006, *38*, 1834–1840.
6. Ong, S.B.; Hernandez-Resendiz, S.; Crespo-Avilan, G.E.; Mukhametshina, R.T.; Kwek, X.Y.; Cabrera-Fuentes, H.A.; Hausenloy, D.J. Inflammation following acute myocardial infarction: Multiple players, dynamic roles, and novel therapeutic opportunities. *Pharm. Ther.* 2018, *186*, 73–87.
7. Stuart, S.D.F.; De Jesus, N.M.; Lindsey, M.L.; Ripplinger, C.M. The crossroads of inflammation, fibrosis, and arrhythmia following myocardial infarction. *J. Mol. Cell Cardiol.* 2016, *91*, 114–122.
8. Renault, M.A.; Losordo, D.W. Therapeutic myocardial angiogenesis. *Microvasc. Res.* 2007, *74*, 159–171.
9. Mohamed, T.M.A.; Ang, Y.S.; Radzinsky, E.; Zhou, P.; Huang, Y.; Elfenbein, A.; Foley, A.; Magnitsky, S.; Srivastava, D. Regulation of Cell Cycle to Stimulate Adult Cardiomyocyte Proliferation and Cardiac Regeneration. *Cell* 2018, *173*, 104–116.
10. Lupu, I.E.; De Val, S.; Smart, N. Coronary vessel formation in development and disease: Mechanisms and insights for therapy *Nat. Rev. Cardiol.* 2020, *17*, 790–

806.

11. Wysoczynski, M.; Bolli, R. A realistic appraisal of the use of embryonic stem cell-based therapies for cardiac repair. *Eur. Heart J.* 2020, *41*, 2397–2404.
12. Maghin, E.; Garbati, P.; Quarto, R.; Piccolil, M.; Bollini, S. Young at Heart: Combining Strategies to Rejuvenate Endogenous Mechanisms of Cardiac Repair. *Front. Bioeng. Biotech.* 2020, *8*, 447.
13. Mancuso, A.; Barone, A.; Cristiano, M.C.; Cianflone, E.; Fresta, M.; Paolino, D. Cardiac Stem Cell-Loaded Delivery Systems: A New Challenge for Myocardial Tissue Regeneration. *Int. J. Mol. Sci.* 2020, *21*, 7701.
14. He, L.H.; Chen, X.B. Cardiomyocyte Induction and Regeneration for Myocardial Infarction Treatment: Cell Sources and Administration Strategies. *Adv. Healthc. Maters* 2020, *9*, 202001175.
15. Gude, N.A.; Sussman, M. Cardiac regenerative therapy: Many paths to repair. *Trends Cardiovas. Med.* 2020, *30*, 338–343.
16. Smagul, S.; Kim, Y.; Smagulova, A.; Raziyeva, K.; Nurkesh, A.; Saparov, A. Biomaterials Loaded with Growth Factors/Cytokines and Stem Cells for Cardiac Tissue Regeneration. *Int. J. Mol. Sci.* 2020, *21*, 5952.
17. Garbayo, E.; Pascual-Gil, S.; Rodriguez-Nogales, C.; Saludas, L.; de Mendoza, A.E.H.; Blanco-Prieto, M.J. Nanomedicine and drug delivery systems in cancer and regenerative medicine. *Wires Nanomed. Nanobiotechnol.* 2020, *12*, e1637.
18. d'Avanzo, N.; Bruno, M.C.; Giudice, A.; Mancuso, A.; De Gaetano, F.; Cristiano, M.C.; Paolino, D.; Fresta, M. Influence of Materials Properties on Bio-Physical Features and Effectiveness of 3D-Scaffolds for Periodontal Regeneration. *Molecules* 2021, *26*, 1643.
19. Yang, Q.B.; Fang, J.T.; Lei, Z.Y.; Sluijter, J.P.G.; Schiffelers, R. Repairing the heart: State-of the art delivery strategies for biological therapeutics. *Adv. Drug Deliv. Rev.* 2020, *160*, 1–18.
20. Vigani, B.; Rossi, S.; Sandri, G.; Bonferoni, M.C.; Caramella, C.M.; Ferrari, F. Hyaluronic acid and chitosan-based nanosystems: A new dressing generation for wound care. *Expert. Opin. Drug Del.* 2019, *16*, 715–740.
21. Jang, Y.; Park, Y.; Kim, J. Engineering Biomaterials to Guide Heart Cells for Matured Cardiac Tissue. *Coatings* 2020, *10*, 925.

22. Patino-Guerrero, A.; Veldhuizen, J.; Zhu, W.Q.; Migrino, R.Q.; Nikkhah, M. Three-dimensional scaffold-free microtissues engineered for cardiac repair. *J. Mater. Chem. B* 2020, *8*, 7571–7590.
23. Sisso, A.M.; Boit, M.O.; De Forest, C.A. Self-healing injectable gelatin hydrogels for localized therapeutic cell delivery. *J. Biomed. Mater. Res. A* 2020, *108*, 1112–1121.
24. Roshandel, M.; Dorkoosh, F. Cardiac tissue engineering, biomaterial scaffolds, and their fabrication techniques. *Polym. Adv. Technol.* 2021, *32*, 2290–2305.
25. Kaiser, N.J.; Coulombe, K.L.K. Physiologically inspired cardiac scaffolds for tailored in vivo function and heart regeneration. *Biomed. Mater.* 2015, *10*, 034003.
26. Mantovani, A.; Sica, A.; Sozzani, S.; Allavena, P.; Vecchi, A.; Locati, M. The chemokine system in diverse forms of macrophage activation and polarization. *Trends Immunol.* 2004, *25*, 677–686.
27. Mariani, E.; Lisignoli, G.; Borzi, R.M.; Pulsatelli, L. Biomaterials: Foreign Bodies or Tuners for the Immune Response? *Int. J. Mol. Sci.* 2019, *20*, 636.
28. Brown, B.N.; Badylak, S.F. Extracellular matrix as an inductive scaffold for functional tissue reconstruction. *Transl. Res.* 2014, *163*, 268–285.
29. Kato, B.; Wisser, G.; Agrawal, D.K.; Wood, T.; Thankam, F.G. 3D bioprinting of cardiac tissue: Current challenges and perspectives. *J. Mater. Sci. Mater. Med.* 2021, *32*, 54.
30. Schwach, V.; Passier, R. Native cardiac environment and its impact on engineering cardiac tissue. *Biomater. Sci.* 2019, *7*, 3566–3580.
31. Vasanthan, V.; Hassanabad, A.F.; Pattar, S.; Niklewski, P.; Wagner, K.; Fedak, P.W.M. Promoting Cardiac Regeneration and Repair Using Acellular Biomaterials. *Front. Bioeng. Biotech.* 2020, *8*, 291.
32. Karam, J.P.; Muscari, C.; Montero-Menei, C.N. Combining adult stem cells and polymeric devices for tissue engineering in infarcted myocardium. *Biomaterials* 2012, *33*, 5683–5695.
33. Bavaro, T.; Tengattini, S.; Rezwan, R.; Chiesa, E.; Temporini, C.; Dorati, R.; Massolini, G.; Conti, B.; Ubiali, D.; Terreni, M. Design of epidermal growth factor immobilization on 3D biocompatible scaffolds to promote tissue repair

and regeneration. *Sci. Rep.* 2021, *11*, 2629.

34. Mousavi, A.; Vahdat, S.; Baheiraei, N.; Razavi, M.; Norahan, M.H.; Baharvand, H. Multifunctional Conductive Biomaterials as Promising Platforms for Cardiac Tissue Engineering. *ACS Biomater. Sci. Eng.* 2021, *7*, 55–82.
35. Solazzo, M.; O'Brien, F.J.; Nicolosi, V.; Monaghan, M.G. The rationale and emergence of electroconductive biomaterial scaffolds in cardiac tissue engineering. *APL Bioeng.* 2019, *3*, 041501.
36. Nelson, J.S.; Heider, A.; Si, M.S.; Ohye, R.G. Evaluation of Explanted CorMatrix Intracardiac Patches in Children With Congenital Heart Disease. *Ann. Thorac. Surg.* 2016, *102*, 1329–1335.
37. Traverse, J.H.; Henry, T.D.; Dib, N.; Patel, A.N.; Pepine, C.; Schaer, G.L.; De Quach, J.A.; Kinsey, A.M.; Chamberlin, P.; Christman, K.L. First-in-Man Study of a Cardiac Extracellular Matrix Hydrogel in Early and Late Myocardial Infarction Patients. *JACC Basic Transl. Sci.* 2019, *4*, 659–669.
38. Chandika, P.; Heo, S.Y.; Kim, T.H.; Oh, G.W.; Kim, G.H.; Kim, M.S.; Jung, W.K. Recent advances in biological macromolecule based tissue-engineered composite scaffolds for cardiac tissue regeneration applications. *Int. J. Biol. Macromol.* 2020, *164*, 2329–2357.
39. Curcio, M.; Cirillo, G.; Rouaen, J.R.C.; Saletta, F.; Nicoletta, F.P.; Vittorio, O.; Lemma, F. Natural Polysaccharide Carriers in Brain Delivery: Challenge and Perspective. *Pharmaceutics* 2020, *12*, 1183.
40. Moorthi, A.; Tyan, Y.C.; Chung, T.W. Surface-modified polymers for cardiac tissue engineering. *Biomater. Sci.* 2017, *5*, 1976–1987.
41. Casagrande, S.; Tiribuzi, R.; Cassetti, E.; Selmin, F.; Gervasi, G.L.; Barberini, L.; Freddolini, M.; Ricci, M.; Schoubben, A.; Cerulli, G.G.; et al. Biodegradable composite porous poly (DL-lactide-co-glycolide) scaffold supports mesenchymal stem cell differentiation and calcium phosphate deposition. *Artif. Cell Nanomed. B* 2018, *46*, S219–S229.
42. Sekula-Stryjewska, M.; Noga, S.; Dzwigonska, M.; Adamczyk, E.; Karnas, E.; Jagiello, J.; Szkaradek, A.; Chytrosz, P.; Boruczkowski, D.; Madeja, Z.; et al. Graphene-based materials enhance cardiomyogenic and angiogenic differentiation capacity of human mesenchymal stem cells in vitro—Focus on cardiac tissue

regeneration. *Mater. Sci. Eng. C Mater.* 2021, *119*, 111614.

43. Cirillo, G.; Spizzirri, U.G.; Curcio, M.; Nicoletta, F.P.; Iemma, F. Injectable Hydrogels for Cancer Therapy over the Last Decade. *Pharmaceutics* 2019, *11*, 486.
44. Kretlow, J.D.; Klouda, L.; Mikos, A.G. Injectable matrices and scaffolds for drug delivery in tissue engineering. *Adv. Drug Deliv.Rev.* 2007, *59*, 263–273.
45. Palumbo, F.S.; Fiorica, C.; Di Stefano, M.; Pitarresi, G.; Gulino, A.; Agnello, S.; Giammona, G. In situ forming hydrogels of hyaluronic acid and inulin derivatives for cartilage regeneration. *Carbohyd. Polym.* 2015, *122*, 408–416.
46. Bejleri, D.; Streeter, B.W.; Nachlas, A.L.Y.; Brown, M.E.; Gaetani, R.; Christman, K.L.; Davis, M.E. A Bioprinted Cardiac Patch Composed of Cardiac-Specific Extracellular Matrix and Progenitor Cells for Heart Repair. *Adv. Healthc. Mater.* 2018, *7*, 1800672.
47. Anker, S.D.; Coats, A.J.S.; Cristian, G.; Dragomir, D.; Pusineri, E.; Piredda, M.; Bettari, L.; Dowling, R.; Volterrani, M.; Kirwan, B.A.; et al. A prospective comparison of alginate outcomes in patients with advanced heart failure (AUGMENT-HF trial). *Eur. Heart J.* 2015, *36*, 2297–2309.
48. Jia, J.; Jeon, E.J.; Li, M.; Richards, D.J.; Lee, S.; Jung, Y.; Barrs, R.W.; Coyle, R.; Li, X.Y.; Chou, J.C.; et al. Evolutionarily conserved sequence motif analysis guides development of chemically defined hydrogels for therapeutic vascularization. *Sci. Adv.* 2020, *6*,eaaz5894.
49. Zhang, J. Engineered Tissue Patch for Cardiac Cell Therapy. *Curr. Treat. Options Cardiovasc. Med.* 2015, *17*, 37.
50. Sapir, Y.; Polyak, B.; Cohen, S. Nanomaterials for cardiac tissue engineering. *Nanomater. Tissue Eng.* 2013, *56*, 244–277.
51. Boffito, M.; Di Meglio, F.; Mozetic, P.; Giannitelli, S.M.; Carmagnola, I.; Castaldo, C.; Nurzynska, D.; Sacco, A.M.; Miraglia, R.; Montagnani, S.; et al. Surface functionalization of polyurethane scaffolds mimicking the myocardial microenvironment to support cardiac primitive cells. *PLoS ONE* 2018, *13*, e0199896.
52. Subia, B.; Kundu, J.; Kundu, S.C. Biomaterial scaffold fabrication techniques for potential tissue engineering applications. *Tissue Eng.* 2010, *524*, 141–157.
53. Hokmabad, V.R.; Davaran, S.; Ramazani, A.; Salehi, R. Design and fabrication

of porous biodegradable scaffolds: A strategy for tissue engineering. *J. Biomater. Sci.Polym. E* 2017, *28*, 1797–1825.

54. Zeinali, R.; del Valle, L.J.; Torras, J.; Puiggali, J. Recent Progress on Biodegradable Tissue Engineering Scaffolds Prepared by Thermally-Induced Phase Separation (TIPS). *Int. J. Mol. Sci.* 2021, *22*, 3504.
55. Colucci, F.; Mancini, V.; Mattu, C.; Boffito, M. Designing Multifunctional Devices for Regenerative Pharmacology Based on 3D Scaffolds, Drug-Loaded Nanoparticles, and Thermosensitive Hydrogels: A Proof-of-Concept Study. *Pharmaceutics* 2021, *13*, 464.
56. Martinez-Perez, C.A.; Olivas-Armendariz, I.; Castro-Carmona, J.S.; Garcia-Casillas, P.E. Scaffolds for Tissue Engineering Via Thermally Induced Phase Separation. In *Advances in Regenerative Medicine*; InTech: Rijeka, Croatia, 2011; pp. 275–294.
57. Budai-Szucs, M.; Ruggeri, M.; Faccendini, A.; Leber, A.; Rossi, S.; Varga, G.; Bonferoni, M.C.; Valyi, P.; Burian, K.; Csanyi, E.; et al. Electrospun Scaffolds in Periodontal Wound Healing. *Polymer* 2021, *13*, 307.
58. Kumbar, S.G.; James, R.; Nukavarapu, S.P.; Laurencin, C.T. Electrospun nanofiber scaffolds: Engineering soft tissues. *Biomed. Mater.* 2008, *3*, 034002.
59. Pham, Q.P.; Sharma, U.; Mikos, A.G. Electrospinning of polymeric nanofibers for tissue engineering applications: A review. *Tissue Eng.* 2006, *12*, 1197–1211.
60. Costantini, M.; Colosi, C.; Mozetic, P.; Jaroszewicz, J.; Tosato, A.; Rainer, A.; Trombetta, M.; Swiszkowski, W.; Dentini, M.; Barbetta, A. Correlation between porous texture and cell seeding efficiency of gas foaming and microfluidic foaming scaffolds. *Mater. Sci.Eng. C Mater.* 2016, *62*, 668–677.
61. Giannitelli, S.M.; Mozetic, P.; Trombetta, M.; Rainer, A. Combined additive manufacturing approaches in tissue engineering. *Acta Biomater.* 2015, *24*, 1–11.
62. Qasim, M.; Haq, F.; Kang, M.H.; Kim, J.H. 3D printing approaches for cardiac tissue engineering and role of immune modulation in tissue regeneration. *Int. J. Nanomed.* 2019, *14*, 1311–1333.
63. Tamay, D.G.; Usal, T.D.; Alagoz, A.S.; Yucel, D.; Hasirci, N.; Hasirci, V. 3D and 4D Printing of Polymers for Tissue Engineering Applications. *Front. Bioeng. Biotechnol.* 2019, *7*, 164.
64. Liu, J.; Yan, C. 3D Printing of Scaffolds for Tissue Engineering. In *3D Printing*;

IntechOpen: London, UK, 2018.

65. Savalani, M.M.; Hao, L.; Dickens, P.M.; Zhang, Y.; Tanner, K.E.; Harris, R.A. The effects and interactions of fabrication parameters on the properties of selective laser sintered hydroxyapatite polyamide composite biomaterials. *Rapid Prototyp. J.* 2012, *18*, 16–27.
66. Gittard, S.D.; Narayan, R. Laser direct writing of micro- and nano-scale medical devices. *Expert Rev. Med. Devices* 2010, *7*, 343–356.
67. Mattioli-Belmonte, M.; Vozzi, G.; Kyriakidou, K.; Pulieri, E.; Lucarini, G.; Vinci, B.; Pugnaloni, A.; Biagini, G.; Ahluwalia, A. Rapid-prototyped and salt-leached PLGA scaffolds condition cell morpho-functional behavior. *J. Biomed. Mater. Res. A* 2008, *85a*, 466–476.
68. Callegari, A.; Bollini, S.; Iop, L.; Chiavegato, A.; Torregrossa, G.; Pozzobon, M.; Gerosa, G.; De Coppi, P.; Elvassore, N.; Sartore, S. Neovascularization induced by porous collagen scaffold implanted on intact and cryoinjured rat hearts. *Biomaterials* 2007, *28*, 5449–5461.
69. Feyen, D.A.M.; Gaetani, R.; Deddens, J.; van Keulen, D.; van Opbergen, C.; Poldervaart, M.; Alblas, J.; Chamuleau, S.; van Laake, L.W.; Doevendans, P.A.; et al. Gelatin Microspheres as Vehicle for Cardiac Progenitor Cells Delivery to the Myocardium. *Adv. Healthc. Mater.* 2016, *5*, 1071–1079.
70. Di Felice, V.; Serradifalco, C.; Rizzuto, L.; De Luca, A.; Rappa, F.; Barone, R.; Di Marco, P.; Cassata, G.; Puleio, R.; Verin, L.; et al. Silk fibroin scaffolds enhance cell commitment of adult rat cardiac progenitor cells. *J. Tissue Eng. Regen. Med.* 2015, *9*, E51–E64.
71. Altomare, L.; Guglielmo, E.; Varoni, E.M.; Bertoldi, S.; Cochis, A.; Rimondini, L.; De Nardo, L. Design of 2D chitosan scaffolds via electrochemical structuring. *Biomatter* 2014, *4*, e29506.
72. Saporito, F.; Baugh, L.M.; Rossi, S.; Bonferoni, M.C.; Perotti, C.; Sandri, G.; Black, L.; Ferrarit, F. In Situ Gelling Scaffolds Loaded with Platelet Growth Factors to Improve Cardiomyocyte Survival after Ischemia. *ACS Biomater. Sci. Eng.* 2019, *5*, 329–338.
73. Bloise, N.; Rountree, I.; Polucha, C.; Montagna, G.; Visai, L.; Coulombe, K.L.K.; Munarin, F. Engineering Immunomodulatory Biomaterials for Regenerating the Infarcted Myocardium. *Front. Bioeng. Biotechnol.* 2020, *8*,

292.

74. Muscari, C.; Bonafe, F.; Martin-Suarez, S.; Valgimigli, S.; Valente, S.; Fiumana, E.; Fiorelli, F.; Rubini, G.; Guarnieri, C.; Caldarera, C.M.; et al. Restored perfusion and reduced inflammation in the infarcted heart after grafting stem cells with a hyaluronan-based scaffold. *J. Cell Mol. Med.* 2013, *17*, 518–530.
75. Benzoni, P.; Ginestra, P.; Altomare, L.; Fiorentino, A.; De Nardo, L.; Ceretti, E.; Dell'Era, P. Biomanufacturing of a chitosan/collagen scaffold to drive adhesion and alignment of human cardiomyocyte derived from stem cells. *Proc. Cirp* 2016, *49*, 113–120.
76. Rosellini, E.; Barbani, N.; Frati, C.; Madeddu, D.; Massai, D.; Morbiducci, U.; Lazzeri, L.; Falco, A.; Lagrasta, C.; Audenino, A.; et al. Influence of injectable microparticle size on cardiac progenitor cell response. *J. Appl. Biomater. Funct. Mater.* 2018, *16*, 241–251.
77. Rosellini, E.; Barbani, N.; Frati, C.; Madeddu, D.; Massai, D.; Morbiducci, U.; Lazzeri, L.; Falco, A.; Graiani, G.; Lagrasta, C.; et al. IGF-1 loaded injectable microspheres for potential repair of the infarcted myocardium. *J. Biomater. Appl.* 2021, *35*, 762–775.
78. Rosellini, E.; Zhang, Y.S.; Migliori, B.; Barbani, N.; Lazzeri, L.; Shin, S.R.; Dokmeci, M.R.; Cascone, M.G. Protein/polysaccharide- based scaffolds mimicking native extracellular matrix for cardiac tissue engineering applications. *J. Biomed. Mater. Res. A* 2018, *106*, 769–781.
79. Rosellini, E.; Cristallini, C.; Barbani, N.; Vozzi, G.; Giusti, P. Preparation and characterization of alginate/gelatin blend films for cardiac tissue engineering. *J. Biomed. Mater. Res. A* 2009, *91*, 447–453.
80. Saporito, F.; Sandri, G.; Bonferoni, M.C.; Rossi, S.; Malavasi, L.; Del Fante, C.; Vigani, B.; Black, L.; Ferrari, F. Electrospun Gelatin-Chondroitin Sulfate Scaffolds Loaded with Platelet Lysate Promote Immature Cardiomyocyte Proliferation. *Polymers* 2018, *10*, 208.
81. Asgari, M.; Latifi, N.; Heris, H.K.; Vali, H.; Mongeau, L. In vitro fibrillogenesis of tropocollagen type III in collagen type I affects its relative fibrillar topology and mechanics. *Sci. Rep.* 2017, *7*, 1392.
82. Blackburn, N.J.R.; Sofrenovic, T.; Kuraitis, D.; Ahmadi, A.; McNeill, B.; Deng, C.; Rayner, K.J.; Zhong, Z.Y.; Ruel, M.; Suuronen, E.J. Timing underpins the

benefits associated with injectable collagen biomaterial therapy for the treatment of myocardial infarction. *Biomaterials* 2015, *39*, 182–192.

83. Goldsmith, E.C.; Borg, T.K. The dynamic interaction of the extracellular matrix in cardiac remodeling. *J. Card. Fail.* 2002, *8*, S314–S318.
84. Vunjak-Noyakovic, G.; Lui, K.O.; Tandon, N.; Chien, K.R. Bioengineering Heart Muscle: A Paradigm for Regenerative Medicine. *Annu. Rev. Biomed. Eng.* 2011, *13*, 245–267.
85. Fini, M.; Motta, A.; Torricelli, P.; Glavaresi, G.; Aldini, N.N.; Tschon, M.; Giardino, R.; Migliaresi, C. The healing of confined critical size cancellous defects in the presence of silk fibroin hydrogel. *Biomaterials* 2005, *26*, 3527–3536.
86. Wang, Y.Z.; Kim, H.J.; Vunjak-Novakovic, G.; Kaplan, D.L. Stem cell-based tissue engineering with silk biomaterials. *Biomaterials*, 2006, *27*, 6064–6082.
87. Bondar, B.; Fuchs, S.; Motta, A.; Migliaresi, C.; Kirkpatrick, C.J. Functionality of endothelial cells on silk fibroin nets: Comparative study of micro- and nanometric fibre size. *Biomaterials* 2008, *29*, 561–572.
88. Unger, R.E.; Sartoris, A.; Peters, K.; Motta, A.; Migliaresi, C.; Kunkel, M.; Bulnheim, U.; Rychly, J.; Kirkpatrick, C.J. Tissue- like self-assembly in cocultures of endothelial cells and osteoblasts and the formation of microcapillary-like structures on three-dimensional porous biomaterials. *Biomaterials* 2007, *28*, 3965–3976.
89. Barsotti, M.C.; Felice, F.; Balbarini, A.; Di Stefano, R. Fibrin as a scaffold for cardiac tissue engineering. *Biotechnol. Appl. Biochem.* 2011, *58*, 301–310.
90. Sireesha, M.; Babu, V.J.; Ramakrishna, S. Biocompatible and biodegradable elastomer/fibrinogen composite electrospun scaffolds for cardiac tissue regeneration. *RSC Adv.* 2015, *5*, 103308–103314.
91. Caiado, F.; Carvalho, T.; Silva, F.; Castro, C.; Clode, N.; Dye, J.F.; Dias, S. The role of fibrin E on the modulation of endothelial progenitors adhesion, differentiation and angiogenic growth factor production and the promotion of wound healing. *Biomaterials* 2011, *32*, 7096–7105.
92. Petzelbauer, P.; Zacharowski, P.A.; Miyazaki, Y.; Friedl, P.; Wickenhauser, G.; Castellino, F.J.; Groger, M.; Wolff, K.; Zacharowski, K. The fibrin-derived peptide B beta(15–42) protects the myocardium against ischemia-reperfusion injury. *Nat. Med.* 2005, *11*, 298–304.

93. Wiedemann, D.; Schneeberger, S.; Friedl, P.; Zacharowski, K.; Wick, N.; Boesch, F.; Margreiter, R.; Laufer, G.; Petzelbauer, P.; Semsroth, S. The Fibrin-Derived Peptide B beta(15–42) Significantly Attenuates Ischemia-Reperfusion Injury in a Cardiac Transplant Model. *Transplantation* 2010, *89*, 824–829.

94. Menasche, P.; Vanneaux, V.; Hagege, A.; Bel, A.; Cholley, B.; Parouchev, A.; Cacciapuoti, I.; Al-Daccak, R.; Benhamouda, N.; Blons, H.; et al. Transplantation of Human Embryonic Stem Cell-Derived Cardiovascular Progenitors for Severe Ischemic Left Ventricular Dysfunction. *J. Am. Coll. Cardiol.* 2018, *71*, 429–438.

95. Toong, D.W.Y.; Toh, H.W.; Ng, J.C.K.; Wong, P.E.H.; Leo, H.L.; Venkatraman, S.; Tan, L.P.; Ang, H.Y.; Huang, Y.Y. Bioresorbable Polymeric Scaffold in Cardiovascular Applications. *Int. J. Mol. Sci.* 2020, *21*, 3444.

96. Hortells, L.; Johansen, A.K.Z.; Yutzey, K.E. Cardiac Fibroblasts and the Extracellular Matrix in Regenerative and Nonregenerative Hearts. *J. Cardiovasc. Dev. Dis.* 2019, *6*, 29.

97. Venkatesan, J.; Kim, S.K. Chitosan Composites for Bone Tissue Engineering-An Overview. *Mar. Drugs* 2010, *8*, 2252–2266.

98. Rodriguez-Vazquez, M.; Vega-Ruiz, B.; Ramos-Zuniga, R.; Saldana-Koppel, D.A.; Quinones-Olvera, L.F. Chitosan and Its Potential Use as a Scaffold for Tissue Engineering in Regenerative Medicine. *Biomed. Res. Int.* 2015, *2015*, 821279.

99. Intini, C.; Elviri, L.; Cabral, J.; Mros, S.; Bergonzi, C.; Bianchera, A.; Flammini, L.; Govoni, P.; Barocelli, E.; Bettini, R.; et al. 3D-printed chitosan-based scaffolds: An in vitro study of human skin cell growth and an in-vivo wound healing evaluation in experimental diabetes in rats. *Carbohyd. Polym.* 2018, *199*, 593–602.

100. Elviri, L.; Foresti, R.; Bergonzi, C.; Zimetti, F.; Marchi, C.; Bianchera, A.; Bernini, F.; Silvestri, M.; Bettini, R. Highly defined 3D printed chitosan scaffolds featuring improved cell growth. *Biomed. Mater.* 2017, *12*, 045009.

101. Bergonzi, C.; Di Natale, A.; Zimetti, F.; Marchi, C.; Bianchera, A.; Bernini, F.; Silvestri, M.; Bettini, R.; Elviri, L. Study of 3D-printed chitosan scaffold features after different post-printing gelation processes. *Sci. Rep.* 2019, *9*, 362.

102. Parisi, L.; Galli, C.; Bianchera, A.; Lagonegro, P.; Elviri, L.; Smerieri, A.;

Lumetti, S.; Manfredi, E.; Bettini, R.; Macaluso, G.M. Anti-fibronectin aptamers improve the colonization of chitosan films modified with D-(+) Raffinose by murine osteoblastic cells. *J. Mater. Sci. Mater. Med.* 2017, *28*, 163.

103. Cattelan, G.; Gerboles, A.G.; Foresti, R.; Pramstaller, P.P.; Rossini, A.; Miragoli, M.; Malvezzi, C.C. Alginate Formulations: Current Developments in the Race for Hydrogel-Based Cardiac Regeneration. *Front. Bioeng. Biotechnol.* 2020, *8*, 414.

104. Puscaselu, R.G.; Lobiuc, A.; Dimian, M.; Covasa, M. Alginate: From Food Industry to Biomedical Applications and Management of Metabolic Disorders. *Polymers* 2020, *12*, 2417.

105. Rao, S.V.; Zeymer, U.; Douglas, P.S.; Al-Khalidi, H.; Liu, J.Y.; Gibson, C.M.; Harrison, R.W.; Joseph, D.S.; Heyrman, R.; Krucoff, M.W. A randomized, double-blind, placebo-controlled trial to evaluate the safety and effectiveness of intracoronary application of a novel bioabsorbable cardiac matrix for the prevention of ventricular remodeling after large ST-segment elevation myocardial infarction: Rationale and design of the PRESERVATION I trial. *Am. Heart J.* 2015, *170*, 929–937.

106. Lee, L.C.; Wall, S.T.; Klepach, D.; Ge, L.; Zhang, Z.H.; Lee, R.J.; Hinson, A.; Gorman, J.H.; Gorman, R.C.; Guccione, J.M. Algisyl- LVR (TM) with coronary artery bypass grafting reduces left ventricular wall stress and improves function in the failing human heart. *Int. J. Cardiol.* 2013, *168*, 2022–2028.

107. Collins, M.N.; Birkinshaw, C. Hyaluronic acid based scaffolds for tissue engineering—A review. *Carbohyd. Polym.* 2013, *92*, 1262–1279.

108. Bonafe, F.; Govoni, M.; Giordano, E.; Caldarera, C.M.; Guarnieri, C.; Muscari, C. Hyaluronan and cardiac regeneration. *J. Biomed. Sci.* 2014, *21*, 100.

109. Pitarresi, G.; Palumbo, F.S.; Cavallaro, G.; Fare, S.; Giammona, G. Scaffolds based on hyaluronan crosslinked with a polyaminoacid: Novel candidates for tissue engineering application. *J. Biomed. Mater. Res. A* 2008, *87*, 770–779.

110. McMahan, S.; Taylor, A.; Copeland, K.M.; Pan, Z.; Liao, J.; Hong, Y. Current advances in biodegradable synthetic polymer based cardiac patches. *J. Biomed. Mater. Res. A* 2020, *108*, 972–983.

111. Tallawi, M.; Dippold, D.; Rai, R.; D'Atri, D.; Roether, J.A.; Schubert, D.W.; Rosellini, E.; Engel, F.B.; Boccaccini, A.R. Novel PGS/PCL electrospun fiber mats with patterned topographical features for cardiac patch applications. *Mater. Sci. Eng. C Mater.* 2016, *69*, 569–576.

112. Focarete, M.L.; Gualandi, C.; Scandola, M.; Govoni, M.; Giordano, E.; Foroni, L.; Valente, S.; Pasquinelli, G.; Gao, W.; Gross, R.A. Electrospun Scaffolds of a Polyhydroxyalkanoate Consisting of omega-Hydroxylpentadecanoate Repeat Units: Fabrication and In Vitro Biocompatibility Studies. *J. Biomater. Sci. Polym. E* 2010, *21*, 1283–1296.

113. Fabbri, M.; Guidotti, G.; Soccio, M.; Lotti, N.; Govoni, M.; Giordano, E.; Gazzano, M.; Gamberini, R.; Rimini, B.; Munari, A. Novel biocompatible PBS-based random copolymers containing PEG-like sequences for biomedical applications: From drug delivery to tissue engineering. *Polym. Degrad. Stabil.* 2018, *153*, 53–62.

114. Silvestri, A.; Sartori, S.; Boffito, M.; Mattu, C.; Di Rienzo, A.M.; Boccafoschi, F.; Ciardelli, G. Biomimetic myocardial patches fabricated with poly(epsilon-caprolactone) and polyethylene glycol-based polyurethanes. *J. Biomed. Mater. Res. B* 2014, *102*, 1002–1013.

115. Chiono, V.; Mozetic, P.; Boffito, M.; Sartori, S.; Gioffredi, E.; Silvestri, A.; Rainer, A.; Giannitelli, S.M.; Trombetta, M.; Nurzynska, D.; et al. Polyurethane-based scaffolds for myocardial tissue engineering. *Interface Focus* 2014, *4*, 20130045.

116. D'Amore, A.; Yoshizumi, T.; Luketich, S.K.; Wolf, M.T.; Gu, X.Z.; Cammarata, M.; Hoff, R.; Badylak, S.F.; Wagner, W.R. Bi-layered polyurethane—Extracellular matrix cardiac patch improves ischemic ventricular wall remodeling in a rat model. *Biomaterials*2016, *107*, 1–14.

117. Baheiraei, N.; Gharibi, R.; Yeganeh, H.; Miragoli, M.; Salvarani, N.; Di Pasquale, E.; Condorelli, G. Electroactive polyurethane/siloxane derived from castor oil as a versatile cardiac patch, part I: Synthesis, characterization, and my- oblast proliferation and differentiation (vol 104, pg 775, 2016). *J. Biomed. Mater. Res. A* 2016, *104*, 1570.

118. Mukherjee, S.; Gualandi, C.; Focarete, M.L.; Ravichandran, R.; Venugopal, J.R.; Raghunath, M.; Ramakrishna, S. Elastomeric electrospun scaffolds of poly (l-lactide-co-trimethylene carbonate) for myocardial tissue engineering. *J.*

Mater. Sci. Mater. Med. 2011, *22*, 1689–1699.

119. Spadaccio, C.; Nappi, F.; De Marco, F.; Sedati, P.; Taffon, C.; Nenna, A.; Crescenzi, A.; Chello, M.; Trombetta, M.; Gambardella, I.; et al. Implantation of a Poly-l-Lactide GCSF-Functionalized Scaffold in a Model of Chronic Myocardial Infarction. *J. Cardiovasc. Transl.* 2017, *10*, 47–65.
120. Karam, J.P.; Muscari, C.; Sindji, L.; Bastiat, G.; Bonafe, F.; Venier-Julienne, M.C.; Montero-Menei, N.C. Pharmacologically active microcarriers associated with thermosensitive hydrogel as a growth factor releasing biomimetic 3D scaffold for cardiactissue-engineering. *J. Control. Release* 2014, *192*, 82–94.
121. Dattola, E.; Parrotta, E.I.; Scalise, S.; Perozziello, G.; Limongi, T.; Candeloro, P.; Coluccio, M.L.; Maletta, C.; Bruno, L.; De Angelis, M.T.; et al. Development of 3D PVA scaffolds for cardiac tissue engineering and cell screening applications. *RSC Adv.* 2019, *9*, 4246–4257.
122. Burgess, K.A.; Frati, C.; Meade, K.; Gao, J.; Diaz, L.C.; Madeddu, D.; Graiani, G.; Cavalli, S.; Miller, A.F.; Oceandy, D.; et al. Functionalised peptide hydrogel for the delivery of cardiac progenitor cells. *Mater. Sci. Eng. C Mater.* 2021, *119*, 111539.
123. Vigneswari, S.; Chai, J.M.; Kamarudin, K.H.; Amirul, A.A.; Focarete, M.L.; Ramakrishna, S. Elucidating the Surface Functionality of Biomimetic RGD Peptides Immobilized on Nano-P(3HB-co-4HB) for H9c2 Myoblast Cell Proliferation. *Front. Bioeng. Biotechnol.* 2020, *8*, 1253.
124. Santoro, R.; Venkateswaran, S.; Amadeo, F.; Zhang, R.; Brioschi, M.; Callanan, A.; Agrifoglio, M.; Banfi, C.; Bradley, M.; Pesce, M. Acrylate-based materials for heart valve scaffold engineering. *Biomater. Sci.* 2017, *6*, 154–167.
125. Santoro, M.; Shah, S.R.; Walker, J.L.; Mikos, A.G. Poly(lactic acid) nanofibrous scaffolds for tissue engineering. *Adv. Drug Deliv. Rev.* 2016, *107*, 206–212.
126. Hu, J.A.; Sun, X.A.; Ma, H.Y.; Xie, C.Q.; Chen, Y.E.; Ma, P.X. Porous nanofibrous PLLA scaffolds for vascular tissue engineering. *Biomaterials* 2010, *31*, 7971–7977.
127. Farto-Vaamonde, X.; Auriemma, G.; Aquino, R.P.; Concheiro, A.; Alvarez-Lorenzo, C. Post-manufacture loading of filaments and 3D printed PLA scaffolds with prednisolone and dexamethasone for tissue regeneration

applications. *Eur. J. Pharm. Biopharm.* 2019, *141*, 100–110.

128. Lasprilla, A.J.R.; Martinez, G.A.R.; Lunelli, B.H.; Jardini, A.L.; Maciel, R. Poly-lactic acid synthesis for application in biomedical devices—A review. *Biotechnol. Adv.* 2012, *30*, 321–328.
129. Lopes, M.S.; Jardini, A.L.; Maciel, R. Poly (lactic acid) production for tissue engineering applications. *Procedia Eng.* 2012, *42*, 1402–1413.
130. Pisani, S.; Croce, S.; Chiesa, E.; Dorati, R.; Lenta, E.; Genta, I.; Bruni, G.; Mauramati, S.; Benazzo, A.; Cobianchi, L.; et al. Tissue Engineered Esophageal Patch by Mesenchymal Stromal Cells: Optimization of Electrospun Patch Engineering. *Int. J. Mol. Sci.* 2020, *21*, 1764.
131. Gentile, P.; Chiono, V.; Carmagnola, I.; Hatton, P.V. An Overview of Poly(lactic-co-glycolic) Acid (PLGA)-Based Biomaterials for Bone Tissue Engineering. *Int. J. Mol. Sci.* 2014, *15*, 3640–3659.
132. D'Angelo, I.; Oliviero, O.; Ungaro, F.; Quaglia, F.; Netti, P.A. Engineering strategies to control vascular endothelial growth factor stability and levels in a collagen matrix for angiogenesis: The role of heparin sodium salt and the PLGA-based microsphere approach. *Acta Biomater.* 2013, *9*, 7389–7398.
133. Teixeira, M.A.; Amorim, M.T.P.; Felgueiras, H.P. Poly (Vinyl Alcohol)-Based Nanofibrous Electrospun Scaffolds for Tissue Engineering Applications. *Polymers* 2020, *12*, 7.
134. Colombo, M.; Bianchi, A. Click Chemistry for the Synthesis of RGD-Containing Integrin Ligands. *Molecules* 2010, *15*, 178–197.
135. Dvir, T.; Timko, B.P.; Brigham, M.D.; Naik, S.R.; Karajanagi, S.S.; Levy, O.; Jin, H.W.; Parker, K.K.; Langer, R.; Kohane, D.S. Nanowired three-dimensional cardiac patches. *Nat. Nanotechnol.* 2011, *6*, 720–725.
136. Tan, Y.; Richards, D.; Xu, R.Y.; Stewart-Clark, S.; Mani, S.K.; Borg, T.K.; Menick, D.R.; Tian, B.Z.; Mei, Y. Silicon Nanowire-Induced Maturation of Cardiomyocytes Derived from Human Induced Pluripotent Stem Cells. *Nano Lett.* 2015, *15*, 2765–2772.
137. Bearzi, C.; Gargioli, C.; Baci, D.; Fortunato, O.; Shapira-Schweitzer, K.; Kossover, O.; Latronico, M.V.G.; Seliktar, D.; Condorelli, G.; Rizzi, R. PlGF-MMP9-engineered iPS cells supported on a PEG-fibrinogen hydrogel scaffold possess an enhanced capacity to repair damaged myocardium. *Cell Death Dis.*

2014, *5*, e1053.

138. Ciocci, M.; Cacciotti, I.; Seliktar, D.; Melino, S. Injectable silk fibroin hydrogels functionalized with microspheres as adult stem cells-carrier systems. *Int. J. Biol. Macromol.* 2018, *108*, 960–971.
139. Mauretti, A.; Neri, A.; Kossover, O.; Seliktar, D.; Di Nardo, P.; Melino, S. Design of a Novel Composite H2S-Releasing Hydrogel for Cardiac Tissue Repair. *Macromol. Biosci.* 2016, *16*, 847–858.
140. Lisi, A.; Briganti, E.; Ledda, M.; Losi, P.; Grimaldi, S.; Marchese, R.; Soldani, G. A Combined Synthetic-Fibrin Scaffold Supports Growth and Cardiomyogenic Commitment of Human Placental Derived Stem Cells. *PLoS ONE* 2012, *7*, e0034284.
141. Rosellini, E.; Vozzi, G.; Barbani, N.; Giusti, P.; Cristallini, C. Three-dimensional microfabricated scaffolds with cardiac extracellular matrix-like architecture. *Int. J. Artif. Organs* 2010, *33*, 885–894.
142. Rosellini, E.; Lazzeri, L.; Maltinti, S.; Vanni, F.; Barbani, N.; Cascone, M.G. Development and characterization of a suturable biomimetic patch for cardiac applications. *J. Mater. Sci. Mater. Med.* 2019, *30*, 126.
143. Frati, C.; Graiani, G.; Barbani, N.; Madeddu, D.; Falco, A.; Quaini, F.; Lazzeri, L.; Cascone, M.G.; Rosellini, E. Reinforced alginate/gelatin sponges functionalized by avidin/biotin-binding strategy: A novel cardiac patch. *J. Biomater. Appl.* 2020, *34*, 975–987.
144. Cristallini, C.; Rocchietti, E.C.; Gagliardi, M.; Mortati, L.; Saviozzi, S.; Bellotti, E.; Turinetto, V.; Sassi, M.P.; Barbani, N.; Giachino, C. Micro- and Macrostructured PLGA/Gelatin Scaffolds Promote Early Cardiogenic Commitment of Human Mesenchymal Stem Cells In Vitro. *Stem Cells Int.* 2016, *2016*, 7176154.
145. Ciuffreda, M.C.; Malpasso, G.; Chokoza, C.; Bezuidenhout, D.; Goetsch, K.P.; Mura, M.; Pisano, F.; Davies, N.H.; Gnecchi, M. Syn- thetic extracellular matrix mimic hydrogel improves efficacy of mesenchymal stromal cell therapy for ischemic cardiomyopathy. *Acta. Biomater.* 2018, *70*, 71–83.
146. Zuluaga, M.; Gregnanin, G.; Cencetti, C.; Di Meo, C.; Gueguen, V.; Letourneur, D.; Meddahi-Pelle, A.; Pavon-Djavid, G.; Matricardi, P. PVA/Dextran hydrogel patches as delivery system of antioxidant astaxanthin: A cardiovascular approach. *Biomed. Mater.* 2018, *13*, 015020.
147. Scalera, F.; Monteduro, A.G.; Maruccio, G.; Blasi, L.; Gervaso, F.; Mazzotta,

E.; Malitesta, C.; Piccirillo, C. Sustainable chitosan- based electrical responsive scaffolds for tissue engineering applications. *Sustain. Mater. Technol.* 2021, *28*, e00260.

148. Cabiati, M.; Vozzi, F.; Gemma, F.; Montemurro, F.; De Maria, C.; Vozzi, G.; Domenici, C.; Del Ry, S. Cardiac tissue regeneration: A preliminary study on carbon-based nanotubes gelatin scaffold. *J. Biomed. Mater. Res. B* 2018, *106*, 2750–2762.
149. Pena, B.; Bosi, S.; Aguado, B.A.; Borin, D.; Farnsworth, N.L.; Dobrinskikh, E.; Rowland, T.J.; Martinelli, V.; Jeong, M.; Taylor, M.R.G.; et al. Injectable Carbon Nanotube-Functionalized Reverse Thermal Gel Promotes Cardiomyocytes Survival and Maturation. *ACS Appl. Mater. Interfaces* 2017, *9*, 31645–31656.
150. Ventrelli, L.; Fujie, T.; Del Turco, S.; Basta, G.; Mazzolai, B.; Mattoli, V. Influence of nanoparticle-embedded polymeric surfaces on cellular adhesion, proliferation, and differentiation. *J. Biomed. Mater. Res. A* 2014, *102*, 2652–2661.
151. Di Mauro, V.; Iafisco, M.; Salvarani, N.; Vacchiano, M.; Carullo, P.; Ramirez-Rodriguez, G.B.; Patricio, T.; Tampieri, A.; Miragoli, M.; Catalucci, D. Bioinspired negatively charged calcium phosphate nanocarriers for cardiac delivery of MicroRNAs. *Nanomedicine* 2016, *11*, 891–906.
152. Popara, J.; Accomasso, L.; Vitale, E.; Gallina, C.; Roggio, D.; Lannuzzi, A.; Raimondo, S.; Rastaldo, R.; Alberto, G.; Catalano, F.; et al. Silica nanoparticles actively engage with mesenchymal stem cells in improving acute functional cardiac integration. *Nanomedicine* 2018, *13*, 1121–1138.
153. Prasadh, S.; Wong, R.C.W. Unraveling the mechanical strength of biomaterials used as a bone scaffold in oral and maxillofacial defects. *Oral Sci. Int.* 2018, *15*, 48–55.
154. Rajangam, T.; An, S.S.A. Fibrinogen and fibrin based micro-and nano scaffolds incorporated with drugs, proteins, cells and genes for therapeutic biomedical applications. *Int. J. Nanomed.* 2013, *8*, 3641–3662.
155. Cirillo, G.; Pantuso, E.; Curcio, M.; Vittorio, O.; Leggio, A.; Iemma, F.; De Filpo, G.; Nicoletta, F.P. Alginate Bioconjugate and Graphene Oxide in Multifunctional Hydrogels for Versatile Biomedical Applications. *Molecules* 2021, *26*, 1355.

156. Hao, T.; Li, J.J.; Yao, F.L.; Dong, D.Y.; Wang, Y.; Yang, B.G.; Wang, C.Y. Injectable Fullerenol/Alginate Hydrogel for Suppression of Oxidative Stress Damage in Brown Adipose-Derived Stem Cells and Cardiac Repair (vol 11, pg 5474, 2017). *ACS Nano* 2018, *12*, 10564.

PART B

Chitosan membranes filled with Cyclosporine A as possible devices for local administration of drugs in the treatment of breast cancer

Abstract

The aim of this work is the design, preparation and characterization of membranes based on cyclosporine A (CsA) and chitosan carboxylate (CC) to be used as an implantable subcutaneous medical device for a prolonged therapeutic effect in the treatment of breast cancer. The choice to use CsA is due to literature data that have demonstrated its possible antitumor activity on different types of neoplastic cells. To this end, CsA was bound to CC through an amidation reaction to obtain a prodrug to be dispersed in a chitosan-based polymeric membrane. The reaction intermediates and the final product were characterized by Fourier transform infrared spectroscopy (FT-IR) and proton nuclear magnetic resonance (1H-NMR). Membranes were analyzed by differential scanning calorimetry (DSC) and scanning electron microscopy (SEM). The data obtained showed the effective formation of the amide bond between CsA and CC and the complete dispersion of CsA inside the polymeric membrane. Furthermore, preliminary tests, conducted on MDA-MB-231, a type of breast cancer cell line, have shown a high reduction in the proliferation of cancer cells. These results indicate the possibility of using the obtained membranes as an interesting strategy for the release of cyclosporin-A in breast cancer patients.

Keywords: membrane; cyclosporine A; chitosan; carboxylated chitosan; breast cancer

1.Introduction

Breast cancer is one of the most diffused neoplastic diseases among women, whose therapeutic approach is based on various methods that include surgical removal, chemo- or radiotherapy and treatment with monoclonal antibodies. Innumerable are the side effects deriving from these therapies, and some of them are related to the cytotoxic activity of drugs that act indistinctly both on cancer cells and on healthy ones. The severe side effects, such as nausea, vomiting, diarrhea, mucositis and myelosuppression, decrease the life quality of the patients. One approach to reduce side effects is to localize the drug to tumors and cancer cells. Local administration of anticancer drugs is already clinically applied. [1] In this approach it is beneficial to increase the residence time of a drug at the administration site. This can be achieved through a carrier matrix that remains at the site of administration and releases therapeutic substances in a controlled manner. Examples of systems for local administration are injectable in situ gelling materials [2–4], beads [5], inhalable particles [6–8], nanocarriers that remain at the site of administration [9–11], microneedles [12,13], liquid crystalline phases [14], creams and ointments [15,16] and metal drug releasing implants [17,18]. Nowadays, in the literature, it is reported that the use of subcutaneous implants as drug delivery systems allows to prolong the release of drugs with different characteristics in various parts of the body [19–21]. Moreover, to be functional, these devices must show a certain biocompatibility with the reference tissues [22,23]. Natural or synthetic polymeric materials are often used, and possess a high degree of biocompatibility, reduced toxicity, and considerable biodegradability [24–26]. For this reason, the aim of this work was to design implantable dense polymeric membranes, able to prolong the release of a drug directly to the site of action, to guarantee a homogeneous distribution of the same and be able to minimize side effects. In this approach, a dense membrane can act as a vector for the prolonged release of a drug when placed in contact with a neoplastic lesion. Dense membranes consist of a dense structure in which the drug can be transported by diffusion under the driving force of a pressure, concentration, or electrical potential gradient. One of the main physical methods to control the release using a polymeric system is membrane permeation controlled (MPC) release. In this system, the drug is

incorporated into a polymeric membrane and the rate of drug release depends on its diffusion through the membrane. The drug used in this work was CsA, which is a neutral cyclic polypeptide that is considered a powerful immunosuppressant and used in clinical practice in the prevention and treatment of rejection of organ transplants. For many years it was used as a drug of choice in the topical and systemic treatment of dermatological pathologies (psoriasis, atopic dermatitis, alopecia), of autoimmune ones (lupus), of rheumatoid arthritis and of autoimmune uveitis [27,28]. Recent studies have also demonstrated the possible antitumor activity of this molecule on different types of neoplastic cells [29]. The mechanism of action by which CsA inhibits the proliferation of tumor cells is based on an inhibition of their glycolytic process due to the absence of energy. It exerts a down regulation against the enzyme pyruvate kinase M2, responsible to produce ATP in the final stages of glycolysis [30]. For this reason, as the energy reserves of the cancer cell cease to exist, it is unable to perform the normal functions of the cell cycle, which stops in the G1/S phase, causing cell death. Being a classical immunosuppressant, systemic administration of CsA in patients with breast tumors can compromise the host's anticancer responses and be harmful. Unfortunately, cyclosporine, a lipophilic drug, is characterized by low solubility and consequent poor oral bioavailability. It also has a narrow therapeutic index and therefore the potential to induce renal toxicity. In this context, an effective, non-toxic, stable and patient-friendly formulation may be useful because it could inhibit the proliferation of breast cancer without affecting general immunity and reducing nephrotoxicity. In particular, the local application of cyclosporine appears to be advantageous as it compromises the suppressive function of the regulatory CD4+, CD25+ and Foxp3 T lymphocytes that infiltrate into tumor tissues [30]. However, this drug, due to its high molecular weight, is unable to distribute evenly and penetrate the stratum corneum of the skin and reach the target site unaffected after its administration. In this regard, the polymer used, chitosan, allows the administration of highly lipophilic drugs, such as CsA, not only orally but also topically. [31]. In particular, the chitosan, a natural polymer derived from chitin, causes an increase in the permeability of the epithelial membrane that favors the permanence of the drug at the absorption site and its paracellular transport [32–34]. Specifically, in this work, CsA, after being covalently linked with the carboxylated chitosan, was dispersed inside a polymeric matrix based on chitosan which was subsequently subjected to contact with the target site, facilitating the dispersion of

the drug thanks to a high permeability and flow. The reaction intermediates and the final product were characterized by means of Fourier transform infrared spectroscopy and proton nuclear magnetic resonance. The membranes were analyzed by differential scanning calorimetry and scanning electron microscopy. The obtained data showed the effective formation of the amide bond between the CsA and CC and complete dispersion of the CsA inside the polymeric membrane. Preliminary tests conducted on MDA-MB-231, a highly aggressive, invasive and poorly differentiated triple negative breast cancer (TNBC) cell line, have demonstrated antitumor activity considering the high reduction in tumor cell proliferation.

2. Materials and Methods

2.1 Materials

For the synthesis of the prodrug, the following materials were used: medium-molecular-weight chitosan purchased from Sigma Aldrich (St. Louis, MO, USA), orthophosphoric acid (H_3PO_4) 85% purchased from Carlo Erba Reagenti (Milan, Italy), nitrite of sodium ($NaNO_2$), 85% formic acid, bromoacetyl bromide purchased from Sigma Aldrich, sodium bicarbonate ($NaHCO_3$), sodium sulfate (Na_2SO_4), dimethylaminopyridine (DMAP), dimethylformamide (DMF), phosphate buffer (PBS), sodium azide, diisopropylethylamine (DIPEA), dicyclohexylcarbodiimide (DCC), ethyl 1– 3 dimethylaminopropylcarbodiimide (EDC), hydrochloric acid (HCl), sodium chloride (NaCl), and triphenylphosphine purchased from Fluka Chemika-Biochemika (Buchs, Switzerland). The solvents used were dichloromethane, chloroform, tetrahydrofuran, diethyl ether, ethanol, methanol, acetone and cold ethyl ether, purchased from VWR Chemicals Prolabo (Milano, Italy), Fluka Chemika-Biochemika (Buchs, Switzerland) and LabScan Analytical Sciences (Gliwice, Poland). Methylene blue was purchased from BDH Analytical Chemicals (Ontario, Canada). Ciclosporin (molecular weight 1202.61 g/mol) was purchased from Farmalabor Srl (Bari, Italy). For the preparation of the membranes, the chitosan (average molecular weight) purchased from Aldrich (St. Louis, MO, USA), PVA (Polyvinyl alcohol 13,000–23,000 Dalton, 98% hydrolyzed, Sigma Aldrich), acetic acid purchased from VWR Chemicals Prolabo, multi-well plates purchased from thermo-scientific (Milano, Italy) and distilled water

were used.

2.2 Cell Culture

Human breast cancer MDA-MB-231 were acquired from Interlab Cell Line Collection (ICLC, Genova, Italy), where they were authenticated. Cells were stored according to supplier's instructions and used within 6 months after frozen aliquot resuscitations. MDA-MB-231 were cultured in Dulbecco's Modified Eagle's medium-F12 plus glutamax containing 5% fetal bovine serum (Invitrogen, Carlsbad, CA, USA), and 1 mg/mL penicillin–streptomycin at 37 °C with 5% CO_2 air. Mycoplasma negativity was tested monthly (MycoAlert, Lonza, Basel, Switzerland).

2.3 Instruments

The ^{1}H-NMR spectra were realized through a Bruker VM 30 spectrophotometer (Bruker, Ettlingen, Germany). The FT-IR spectra were processed through a Jasco 4200 spectrophotometer (Jasco Europe S.R.L, Lecco, Italy). The spectra UV-Vis were recorded with a Jasco V-530 UV/Vis spectrophotometer (Thermo Fisher Scientific, Monza, Italy). Differential scanning calorimetry (DSC) was performed with a DSC 200 PC Netzsch instrument (NETZSCH-Gerätebau GmbH, Verona, Italy). The micrographs of the membranes were carried out using an electronic scanning microscope (SEM) (FELMI-ZFE, Graz, Austria) FEI Quanta 200, FEG (field emission gun) with a 0.5–30 Kv voltage and an EDX Oxford Inca 300 system. The samples were sputtered with gold before the SEM analysis. The solvents were removed using a Buchi Rotavapor R II (Buchi, Cornaredo, Italy), while the lyophilization of some compounds was carried out through an Edwards "Freezing-drying" Micro Modulyo (Thermo Electron Corporation, Gormley, ON, Canada). The evaporation of the membranes and their complete drying were carried out with a stove for vacuum drying (Thermo Fisher Scientific; Waltham; MA; USA).

2.4 Synthesis of Carboxylated Chitosan (CC)

In a three-necked flask fitted with a reflux condenser, magnetic stirrer, meticulously flamed under a nitrogen stream (inert atmosphere), 1 g of chitosan and 40 mL of H_3PO_4 at 85% were added. After 1 h, 3 g of sodium nitrite (0.043 mol) were added, and the solution was kept under

vigorous stirring for about 5 min. The addition of 3 g of sodium nitrite (0.043 mol) was repeated twice more, keeping everything under magnetic stirrer for 1 h and 15 min. At the end of the third addition, 10 mL of formic acid was added to neutralize the sodium nitrite excess. The compound was then precipitated with 400 mL of cold ethyl ether and 100 mL of acetone under stirring for 30 min and was filtered and washed with distilled H_2O and ethanol (100 mL). Subsequently, a further washing was carried out with diethyl ether and methanol to obtain a product which was dried under vacuum and characterized by FT-IR [39].

2.5 Determination of Carboxylic Groups Content

The carboxylate chitosan (0.05 g) was suspended in a solution consisting of 2.5 mL of phosphate buffer (pH 8.0) and 2.5 mL of aqueous methylene blue solution and then was filtered, acidified with 1 mL of HCl 0.1 N, and added with 8 mL of distilled water. The determination of the carboxylic groups was performed using a UV-Vis spectrophotometer through a method that involves the analysis of the test sample containing methylene blue. This sample bind carboxyl groups and tends to decrease its concentration within the solution; the resulting amount of unabsorbed methylene blue has been used in the following equation 1 to determine the actual content of carboxyl groups [40]:

$$\text{mmol COOH / g dry sample} = \frac{(7{,}5-A)x\ 0{,}00313}{E}$$

A = non-absorbed amount of methylene blue.

E = CC amount in grams.

2.6 Synthesis of CSA- CC

In a two-necked flask under magnetic stirrer for about 1 h, 0.06 g ($4.98 \times 10{-}5$ mol) of CsA, 1 mL of bromoacetyl bromide (0.013 mol) and 0.03 g of dimethylaminopyridine ($2.45\times 10{-}4$ mol) were added. The progression of the reaction was monitored by TLC (silica gel) using chloroform-methanol (6:4) as eluent mixture. At the same time, an aqueous solution containing 7.5 mL of distilled water and 1.15 g of NaHCO3 (0.0136 mol) was prepared. This last was added to the compound contained in the flask. The two phases were separated by performing an extraction with dichloromethane (6 mL). After that, the organic phase was

treated with Na2SO4 to remove the residual water, washed with dichloromethane and then filtered. The product was evaporated, lyophilized, characterized to ^{1}H-NMR to give 0.578 g. Successively, 0.578 g (4.4×10^{-4} mol) of product were added to 20 mL of DMF and 0.0310 g (4.78×10^{-4} mol) of sodium azide, to obtain a solution which was left under magnetic stirrer for 24 h. The mixture was evaporated, and the residue was dispersed in dichloromethane (60 mL) and washed with an aqueous solution containing NaCl. Then, the organic phase was a hydride with Na_2SO_4, filtered and evaporated. The residue was dried and dissolved in 2 mL of dry tetrahydrofuran under magnetic stirrer. In the mixture, 0.000143 g (5.45×10^{-7} mol) of tri-phenyl phosphine and 41 μL of distilled water were added and stirred for 18 h. The solvent was evaporated, and the obtained residue was dissolved in 100 mL of ether and in a cold solution of HCl in ether to facilitate its precipitation. The residue was dissolved in ethyl ether and n- hexane, evaporated, frozen and lyophilized. At the obtained product, 125 mL (1.95 mol) of dichloromethane, 0.37 mL (2.12×10^{-3} mol) of DIPEA, 0.044 g (2.83×10^{-4} mol) of EDC, 0.162 g (7.86×10^{-4} mol) and 0.172 g of CC were added. The reaction was kept under magnetic stirring for 24 h, then the product was filtered and dried under vacuum [41,42].

2.7 Preparation of Chitosan (CM) and Membranes Chitosan (CMCsCC) Membranes

Dense membranes consist of dense structure presenting no detectable pore at the limits of electron microscopy. A mixture of molecules is transported through dense membranes by diffusion under the driving force of a pressure, concentration, or electrical potential gradient. Dense membranes may have a symmetric or an asymmetric structure. Dense membranes were prepared by phase inversion induced by solvent evaporation. A mixture of 0.15 g of chitosan in 5 mL of acetic acid solution (3%) was stirred for 24 h in a vial placed inside an oil bath at 40 °C. One milliliter of this solution was then placed in a multi-well plate and dried at 80 °C for 4 h [43]. Table 1 shows other examples of membranes made with this procedure.

Table 1. Membranes based on chitosan and other components.

Membranes	Chitosan	Acetic acid Solution (ml)	CsACC
CM*[1]	0.15 g	5 mL	-
CM*[2] + Csacc	0.15 g	5 mL	0.017 g

*[1] Chitosan Membranes. *[2] Chitosan Membranes + Ciclosporine A-Carboxylated Chitosan.

2.8 In Vitro Skin Permeation Studies

Skin permeation studies were performed by using Franz diffusion cells apparatus with cellulose acetate membranes and pig skin (furnished from local butcher) for 24 h. The apparatus was maintained at 37 °C to mimic physiological conditions. Receptor chambers (7.0 mL) were filled with NaCl 0.9% solution containing ethanol (20%) and kept under stirring. Unloaded chitosan membranes were used as control. At specific time intervals (1, 2, 4, 8, 10, and 24 h) an aliquot (1 mL) of each sample was withdrawn from receptor chambers and replaced with fresh release medium. Samples were analyzed through UV- Vis spectrophotometry and drug release profiles were expressed as percentage of drug released respective to the total loaded amount in function of time.

2.9 Localization of CsA in Skin (CLSM Study)

Confocal laser scanning microscopy (CLSM) (Leica Microsystems Srl, Milan, Italy) was carried out to see the depth of permeation of a fluorescent lipophilic substance as a model drug like coumarine-6. The dye loaded membranes were applied on the pig skin and kept for 24 h in the permeation experiment. At the end of the experiment, the excess formulation was removed from the skin surface. The skin was washed 3 times with phosphate buffer (pH 7.4) and dried. Specimens were embedded in optimal cutting temperature compound (Tissue-Tek, Sakura Finetek Europe, Alphen aan den Rijin, The Netherlands) and stored at −80 °C. Cryostat-cut skin sections (16 μm thick) were mounted on slides and nuclei counterstained with Vectashield solution containing 1.5 μg/mL 4′,6- diamidino2-phenylindole (DAPI; Vector Laboratories, Burlingame, CA, USA). Images were acquired using a confocal microscope (Leica TC-SP2 Confocal System, Leica Microsystem Srl, Milan, Italy).

2. 10 Cell Proliferation Assays

MDA-MB-231 cells were seeded, in triplicate, in 6-well plates in a regular growth medium. On the second day, the cells were synchronized in serum free media (SFM) for 24 h, so that most of the cells belonged to a population in the same cell cycle phase, to avoid growth differences among cells. The following day, cells were put in contact with chitosan, CsA, carboxylated chitosan, CsACC and membrane based on chitosan + CsACC. After 72 h, MDA-MB-231 cells were harvested by trypsinization and collected in Eppendorf. All collected samples were incubated in a 0.5% trypan blue solution for 1 min at room temperature. Cell viability was determined by Countess Automated Cell Counter (NucleoCounter® NC-202, Gydevang, Denmark) [44].

3.Results and Discussion

3.1 CsACC Synthesis and Characterization

CsACC was obtained through an amidation reaction that favored the covalent bond between the derivatized CsA and the carboxylated chitosan. Cyclosporin A (1) was initially esterified with bromoacetyl-bromide in the presence of DMAP to form the corresponding ester (2).

Subsequently, with the addition of sodium azide in the presence of DMF, the bromine atom was replaced by a azide anion (3) to then be reduced to the amine form after addition of triphenyl phosphine, water, and anhydrous tetrahydrofuran (4). The amino group, in the presence of DIPEA, DCC and EDC, showed the formation of a bond with the CC carboxyl group (5) (Figure 1).

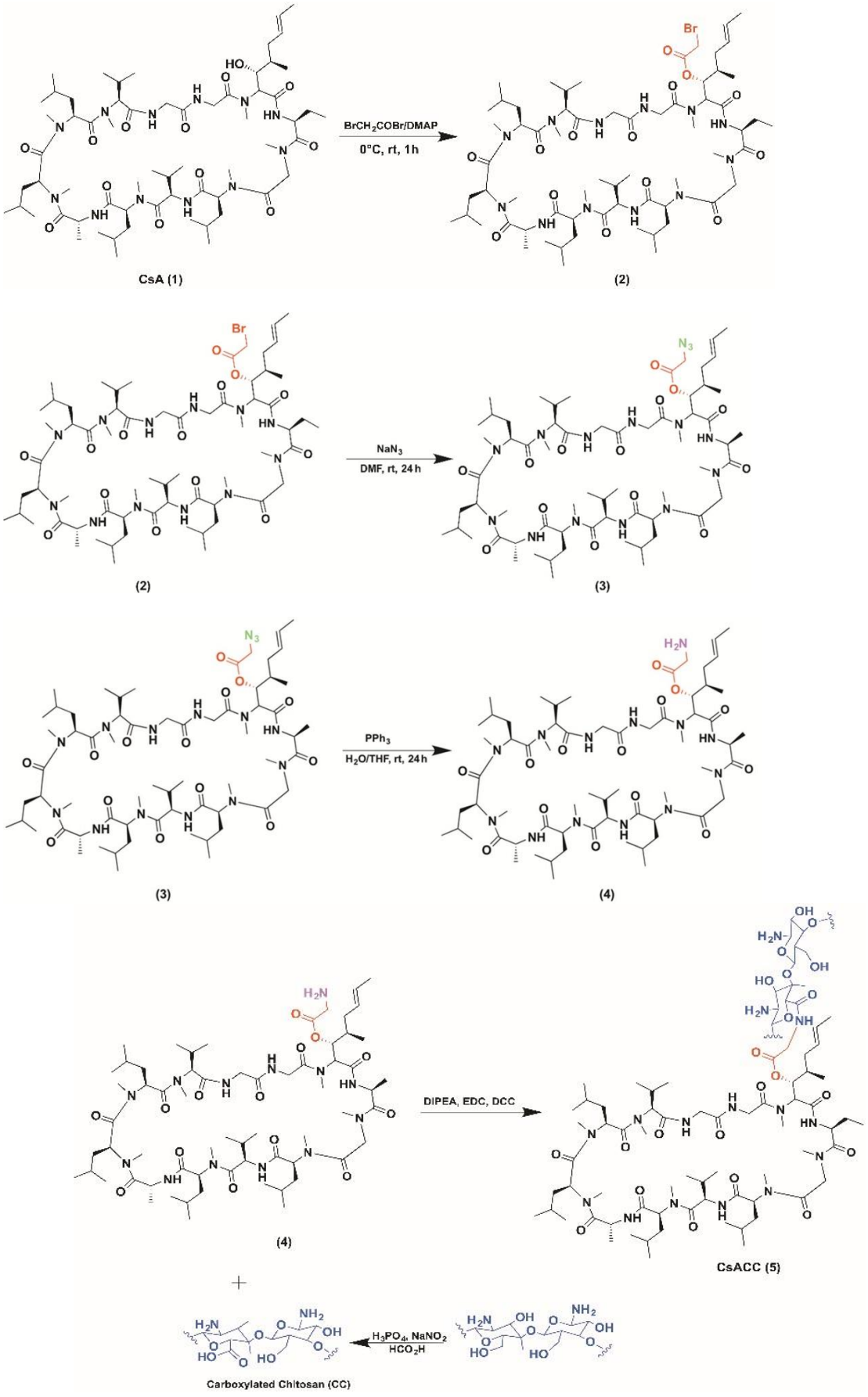

Figure 1. Scheme of CsACC synthesis.

The intermediates of the reaction were characterized. The CC was characterized by spectroscopic techniques. FT-IR (KBr) v (cm−1): 3435 (OH), 2925, 2855, 2833 (CH aliphatics), 1719(C=O) 1362 (OH) (Figure 2b). ^{1}H-NMR (DMSO-d6): 11.2 (bs, 1H), 5.54 (m, 1H), 5.04 (bs, 2H), 4.40 (m, 1H), 3.50 (m, 1H), 3.02 (m, 1H), 2.21 (m, 1H). Yield: 0.8 g. The CsACC

derivate was also characterized by FT-IR and ^{1}H-NMR. FT-IR spectrum shows the presence of a new band at 1621 cm^{-1} correlated to the stretching vibration of the C=O amide (Figure 2a). ^{1}H-NMR analysis has provided a very broad and complex spectrum in $CDCl_3$ in which the signals of the *N*-methyl groups (3 ppm) and those related to CH_3 in the side chain of different amino acid residues (1 ppm) are evident (Figure 3). In this spectrum, the signals of CH_2 and CH of chitosan between 3–4 ppm are also evident. The DSC curves of the carboxylated chitosan (b) and the CsACC derivative (a) are shown in Figure 4. The CC showed an endothermic peak at 205 °C, the amide derivate at 207 °C, and the CsA (curve not shown) at 244 °C.

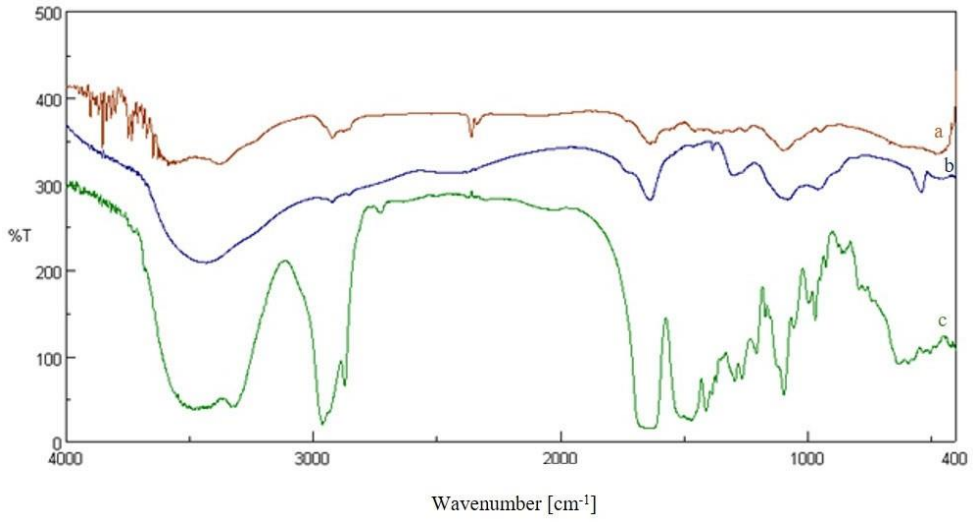

Figure 2. FT-IR of CsACC (**a**), CC (**b**), CsA (**c**).

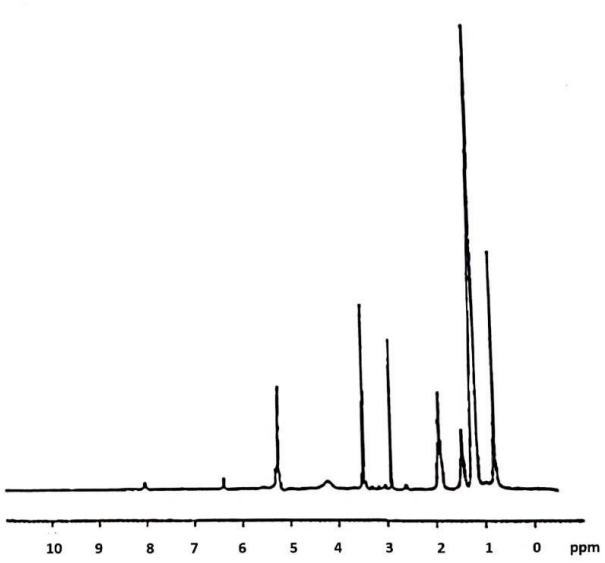

Figure 3. 1H-NMR spectrum of CsACC.

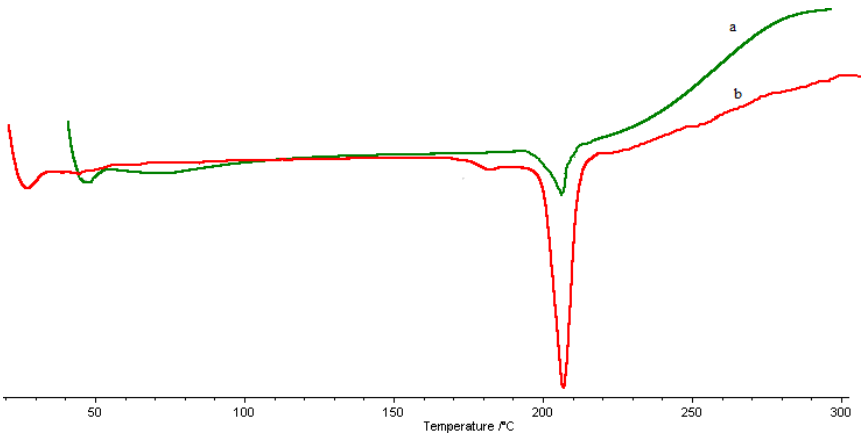

Figure 4. DSC curve of CsACC (a), CC (b).

The membranes were characterized by FT-IR and electronic scanning microscopy (SEM). Characterization by FT-IR revealed that the spectrum of chitosan did not change, despite the composition of the membranes being modified (Figure 5).

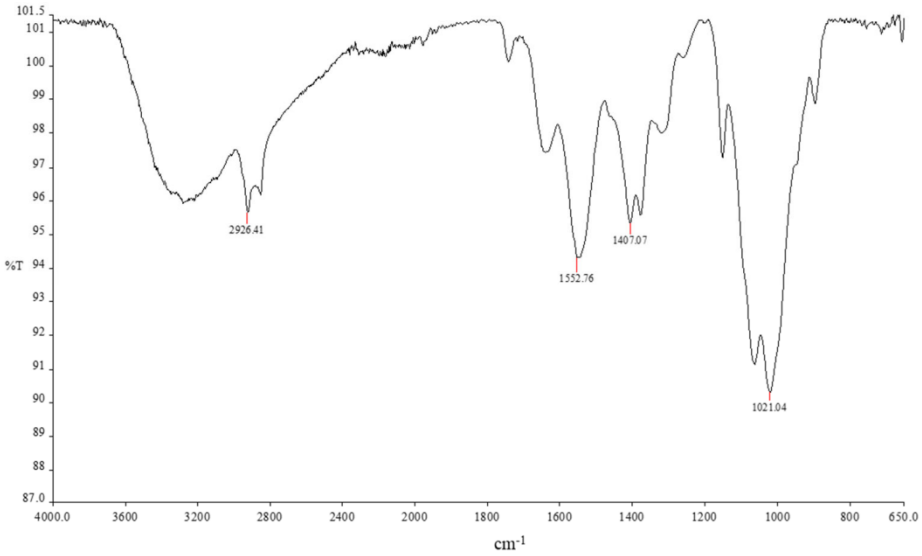

a

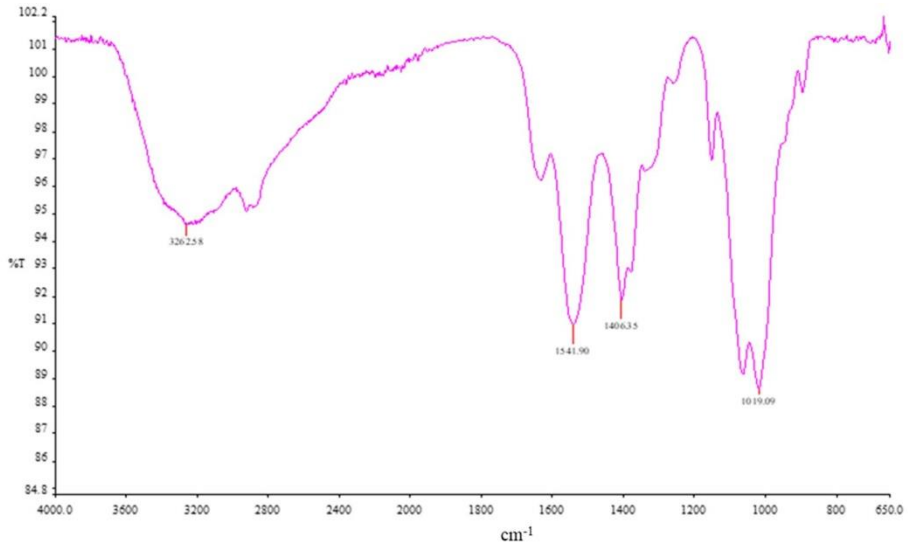

b

Figure 5. FT-IR of membrane based on chitosan (**a**), chitosan + CsACC (**b**).

3.2 Characterization of Membranes

The obtained membranes were characterized by SEM micrographies. The results showed that the membrane based on chitosan (a), and chitosan + CsaCC (b) appear dense. However, from figure (b) is evident the presence of the CsACC derivative that appears like filaments that protrude from the membranes (Figure 6).

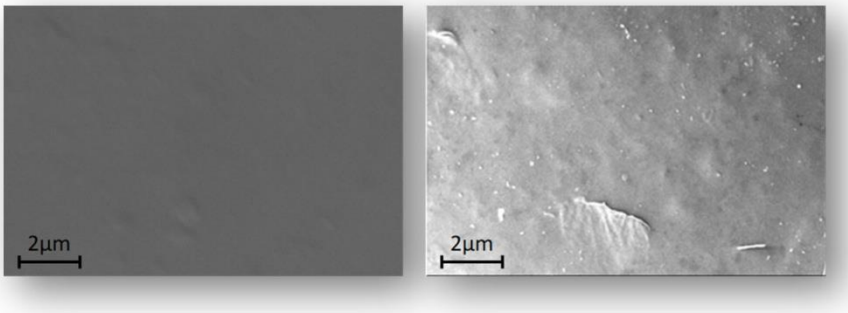

a b

Figure 6. SEM photomicrographies of the membrane based on chitosan (**a**), and chitosan + CsACC (**b**). The images are taken at 10 K× magnification.

3.3 Skin Permeation Studies

To have dermatological formulations and further modulate CsA release, this drug and its prodrug were used to obtain various membranes of chitosan that were then subjected to transdermal release studies to evaluate their potential application and efficacy in oncological diseases treatment. Drug release profiles were evaluated by using Franz diffusion cells with membranes or pigskin. Synthetic membranes, in addition to pig skin, were used because cyclosporine is characterized by a specific absorbance range (λ = 195–215 nm) and, therefore, can interfere with several skin components, such as lipid and proteins, that adsorb at similar wavelengths [35,36]. The presence of skin components in receptor chambers can be attributed to the release medium composition (0.9% NaCl/ethanol 20%) since ethanol can promote

phospholipid mobility [37]. Ethanol was added to the release medium since cyclosporine is soluble in ethanol but not in water [38]. To further eliminate the risk of possible interferences, a 14 kDa cut-off membrane was used. In fact, the obtained data showed, by comparing release studies carried out using pig skin and cellulose acetate membrane, an absence of significant interferences. Drug release studies were performed on dermatological formulations at different time intervals (1, 4, 8, 12, and 24 h). Drug release profiles were determined by UV-Vis spectrometry and expressed as percentage of the drug released with respect to the total loaded amount as a function of time. Data showed that, with cellulose acetate membrane, cyclosporin A was released within 8 h from the membranes, in quantities ranging from 0.15% (membrane CHIT + prodrug) to 0.9% (membrane CHIT + CsA) of the total loaded amount. After 1 h, release was not observed from membrane containing free CsA. Instead, the release from membrane containing the prodrug stopped after 4 h. Studies conducted by means of pig skin revealed a total CsA percentage of 4.2% for membrane containing the free CsA and of 2.7% for membrane containing the prodrug, within 24 h. The higher percentage of cyclosporine released using pig skin is probably due to the presence of skin components as previously pointed out. After that, to evaluate if CsA had been released from the membrane in the pig skin, given the low percentage present in the acceptor compartment after carrying out the transdermal release, the chitosan membranes were solubilized and subjected to observation on a UV-Vis spectrophotometer in the range of 195–215 nm. The obtained results revealed the presence of percentage of free CsA and prodrug equal to 21% and 18%, respectively. This result suggests that the remaining portions are placed in the pig skin used during transdermal birth. To validate this hypothesis, chitosan membranes were also prepared using coumarin-6 as a model drug, being a particularly lipophilic substance in analogy to CsA. An observational skin study was performed to verify how coumarin arranged itself within the pig's skin after transdermal release. Fluorescence microscopy imaging (CLSM) was used to visualize its distribution and penetration depth through the pig skin. As clearly visible in Figure 7, the coumarin-6 was found to be concentrated into the dermis layer of the pig skin after release from membrane containing free CsA as compared to control chitosan membrane. On the other hand, coumarin-6 released from membrane containing the CsA prodrug was positioned both on the shin surface and in the more internal layer, probably the subcutaneous one. Obtained results represent a starting point. Other studies are required to verify with certainty the

effectiveness of the prepared membranes and the release mechanisms of CsA.

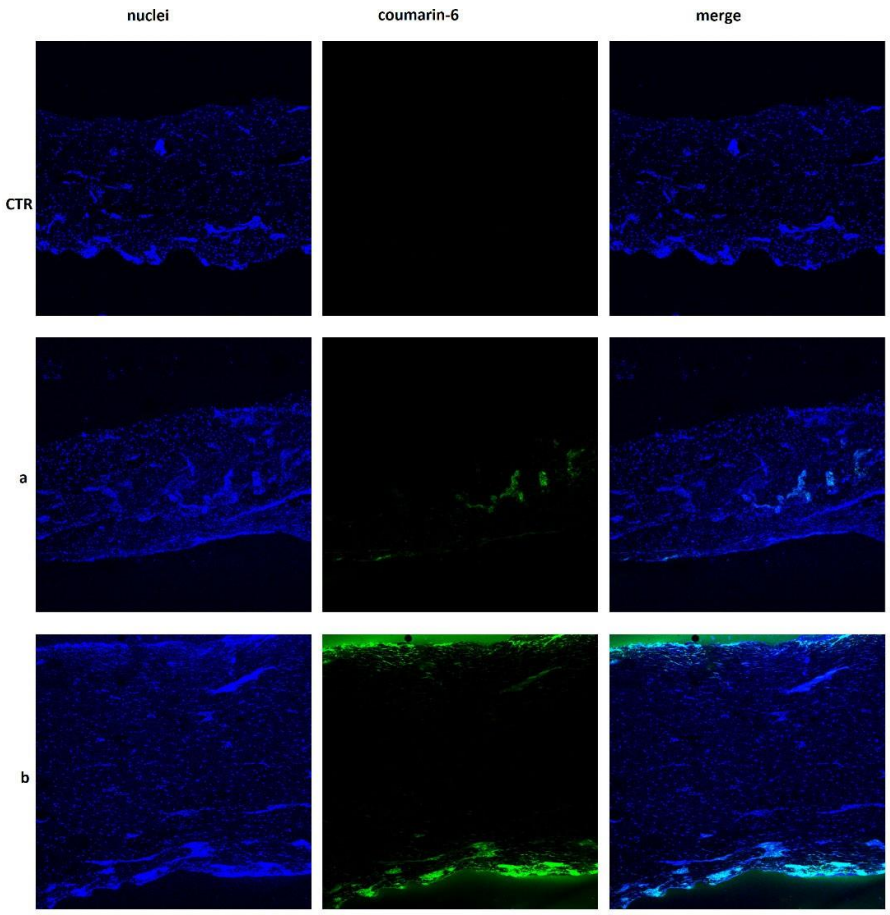

Figure 7. Confocal imagine of chitosan membrane (CTR), membrane based on free CsA containing coumarin-6 (**a**), and membrane based on CsACC containing cumarin-6 (**b**).

3.4 Cell Proliferation Assays

The effects of CsACC membranes and CsA free on the viability processes of cellulose in human breast cancer cells MDA-MB-231, were analyzed by cell proliferation assay. At the concentrations used in the experiment, after 72 h of treatment, significant biological effects were observed in our experimental model. In particular, the results obtained showed a

significant decrease in cell viability especially in cells treated with CsACC and with chitosan mixed with free CsA. This effect is not observed by treating the cells uniquely with CsA at the same concentration with which it is present in the membranes (Figure 8).

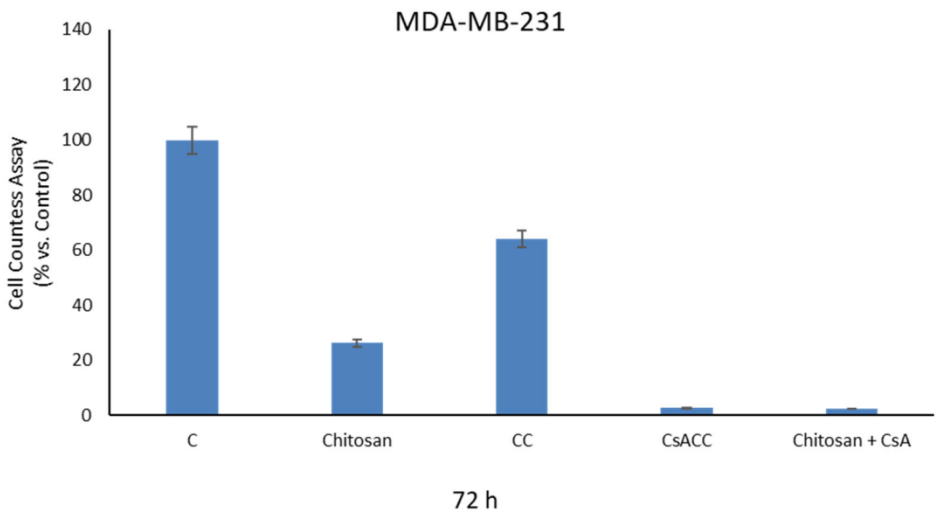

Figure 8. Cell proliferation assay on MDA-MB-231 cell lines of chitosan membranes with and without CsA.

4. Conclusions

The present work aimed to design and realize CsACC-based membranes that were potentially useful in the treatment of breast cancer in the form of subcutaneous implants. The membranes obtained were prepared starting from the polymeric product based on carboxylated chitosan and cyclosporin A. Such precursor was obtained by reaction of amidation of the active principle with the previous carboxylated chitosan and characterized by FT-IR and DSC. In vitro permeation studies showed that membranes could potentially release the cyclosporin-A in the skin internal layers. In addition, membranes containing both CsACC membranes and free CsA showed a significant decrease in human breast cancer MDA-MB-231 cell viability. This effect is not observed by treating the cells uniquely with free CsA at the same concentration with which it is present in the membranes. Therefore, the obtained membranes could be an interesting strategy for the delivery of cyclosporin-A in patients affected by breast cancer to limit its systemic toxicity.

REFERENCES

Sonia Trombino, Federica Curcio, Teresa Poerio, Michele Pellegrino, Rossella Russo, Roberta Cassano. Chitosan membranes filled with Cyclosporine A as possible devices for local administration of drugs in the treatment of breast cancer. *Molecules*, 2021, 26, 1889.

1. Budker, V.G.; Monahan, S.D.; Subbotin, V.M. Loco-regional cancer drug therapy: Present approaches and rapidly reversible hydrophobization (RRH) of therapeutic agents as the future direction. *Drug Discov. Today* 2014, *19*, 1855–1870.
2. Chou, H.S.; Larsson, M.; Hsiao, M.H.; Chen, Y.C.; Röding, M.; Nydén, M.; Liu, D.M. Injectable insulin-lysozyme-loaded nanogels with enzymatically-controlled degradation and release for basal insulin treatment: In vitro characterization and in vivo observation. *J. Control. Release* 2016, *224*, 33–42.
3. Hsiao, M.H.; Chiou, S.H.; Larsson, M.; Hung, K.H.; Wang, Y.L.; Liu, C.J.; Liu, D.M. A temperature-induced and shear-reversible assembly of latanoprost-loaded amphiphilic chitosan colloids: Characterization and in vivo glaucoma treatment. *Acta Biomater.* 2014, *10*, 3188–3196.
4. Mathew, A.P.; Uthaman, S.; Cho, K.H.; Cho, C.S.; Park, I.K. Injectable hydrogels for delivering biotherapeutic molecules. *Int. J. Biol. Macromol*. 2018, *110*, 17–29.
5. Rossi, S.M.; Murray, T.; McDonough, L.; Kelly, H. Loco-regional drug delivery in oncology: Current clinical applications and future translational opportunities. *Expert. Opin. Drug Deliv.* 2020, doi:10.1080/17425247.2021.1856074.
6. Xu, C.; Wang, P.; Zhang, J.; Tian, H.; Park, K.; Chen, X. Pulmonary codelivery of doxorubicin and siRNA by pH-sensitive nanoparticles for therapy of metastatic lung cancer. *Small* 2015, *11*, 4321–4333.
7. Sharma, P.; Mehta, M.; Dhanjal, D.S.; Kaur, S.; Gupta, G.; Singh, H.; Thangavelu, L.; Rajeshkumar, S.; Tambuwala, M.; Bakshi, H.A.; Chellappan, D.K. Emerging trends in the novel drug delivery approaches for the treatment of lung cancer. *Chemico-Biol.Interact.* 2019, *309*, 108720.
8. Lee, H.-Y.; Mohammed, K.A.; Nasreen, N. Nanoparticle-based targeted gene therapy for lung cancer. *Am. J. Cancer Res.* 2016, *6*, 1118–1134.

9. Ruan, R.; Chen, M.; Sun, S.; Wei, P.; Zou, L.; Liu, J.; Gao, D.; Wen, L.; Ding, W. Topical and targeted delivery of siRNAs to melanoma cells using a fusion peptide carrier. *Sci. Rep*. 2016, *6*, 29159.
10. Fahmy, H.M.; Saad, E.A.E.M.S.; Sabra, N.M.; Sabra, N.M.; El-Gohary, A.A.; Mohamed, F.F.; Gaber, M.H. Treatment merits of Latanoprost/Thymoquinone—Encapsulated liposome for glaucomatus rabbits. *Int. J. Pharm.* 2018, *548*, 597–608.
11. Woodrow, K.A.; Cu, Y.; Booth, C.J.; Saucier-Sawyer, J.K.; Wood, M.J.; Saltzman, W.M. Intravaginal gene silencing using biodegradable polymer nanoparticles densely loaded with small-interfering RNA. *Nat. Mater.* 2009, *8*, 526–533.
12. Wang, C.; Ye, Y.; Hochu, G.M.; Sadeghifar, H.; Gu, Z. Enhanced cancer immunotherapy by microneedle patch-assisted delivery of anti-PD1 antibody. *Nano Lett.* 2016, *16*, 2334–2340.
13. Tang, T.; Deng, Y.; Chen, J.; Zhao, Y.; Yue, R.; Choy, K.W.; Wang, C.C.; Du, Q.; Xu, Y.; Han, L.; Chung, T.K. Local administration of siRNA through microneedle: Optimization, bio-distribution, tumor suppression and toxicity. *Sci. Rep.* 2016, *6*, 30430.
14. Depieri, L.V.; Borgheti-Cardoso, L.N.; Campos, P.M.; Otaguiri, K.K.; de Carvalho Vicentini, F.T.; Lopes, L.B.; Fonseca, M.J.; Bentley, M.V. RNAi mediated IL-6 In vitro knockdown in psoriasis skin model with topical siRNA delivery system based on liquid crystalline phase. *Eur. J. Pharm. Biopharm.* 2016, *105*, 50–58.
15. Cullen, J.K.; Simmons, J.L.; Parsons, P.G.; Boyle, G. M. Topical treatments for skin cancer. *Adv. Drug Deliv. Rev.* 2020, *153*, 54– 64.
16. Ritprajak, P.; Hashiguchi, M.; Azuma, M. Topical application of cream-emulsified CD86 siRNA ameliorates allergic skin disease by targeting cutaneous dendritic cells. *Mol. Ther.* 2008, *16*, 1323–1330.
17. Gulati, K.; Aw, M.S.; Losic, D. Nanoengineered drug-releasing Ti wires as an alternative for local delivery of chemotherapeutics in the brain. *Int. J. Nanomed.* 2012, *7*, 2069–2076.
18. Kaur, G.; Willsmore, T.; Gulati, K.; Zinonos, I.; Wang, Y.; Kurian, M.; Hay, S.; Losic, D.; Evdokiou, A. Titanium wire implants with nanotube arrays: A study model for localized cancer treatment. *Biomaterials* 2016, *101*, 176–188.

19. Kumar, A.; Pillai, J. Implantable drug delivery systems: An overview. In *Nanostructures for the Engineering of Cells, Tissues and Organs*, 1st ed.; Grumezescu, A.M., Eds.; Elsevier: Amsterdam, The Netherlands, 2018; chapter 18, pp. 473–511, ISBN:9780128136652.
20. Benchetrit, S. Implantable Device for Injecting Medical Substances. U.S. Patent US 6,878,137, 12 April 2005.
21. Arps, J. Implantable drug delivery devices. *Pro. Med. Pharma*. 2013, *1*.
22. Park, H.; Park, K. Biocompatibility issues of implantable drug delivery systems. *Pharm. Res.* 1996, *13*, 1770–1776.
23. Fournier, E.; Passirani, C.; Montero-Menei, C.N.; Benoi, J.P. Biocompatibility of implantable synthetic polymeric drug carriers: Focus on brain biocompatibility. *Biomaterials* 2003, *24*, 3311–3331.
24. Bhatt, P.; Trehan, S.; Inamdar, N.; Mourya, V.K.; Misra, A. Polymers in Drug Delivery: An Update. In *Applications of Polymers in Drug Delivery*, 2nd ed.; Misra, A., Shahiwala, A., Eds.; Elsevier: Amsterdam, The Netherlands, 2021; Chapter 2, pp. 1–42.ISBN:9780128196595.
25. Caillol, S. Special Issue "Natural Polymers and Biopolymers II". *Molecules* 2021, *26*, 112.
26. Ottenbrite, R.M.; Kim, S.W. *Polymeric Drugs, and Drug Delivery Systems*, 1st ed.; 2019, CRC Press, Taylor & Francis,Boca raton,USA.
27. Amber, T.; Tabassum, S. Cyclosporin in dermatology: A practical compendium. *Dermatol. Ther.* 2020, *33*, e13934.
28. Prodanovic, E.M.; Korman, N.J. Traditional systemic therapy: Metrotexate and cyclosporine. In *Treatment of Psoriasis*; Birkhäuser: Verlag, Switzerland 2008; pp. 108–120.
29. Dittmar, J.; Rothstein, R.J.; Reid, R.J.D.; Parsons, R.; Maurer, M.; Shaw, J.; Du, X. Methods to Treat Cancer Cyclosporine and Cyclosporine Derivates. U.S. Patent WO2012145427A1, 26 October 2012.
30. Jiang, K.; He, B.; Lai, L.; Chen, Q.; Liu, Y.; Guo, Q.; Wang, Q. Cyclosporine a inhibits breast cancer cell growth by downregulating the expression of pyruvate kinase subtype M2. *Int. J. Mol. Med.* 2012, *30*, 302–308.

31. Sun, J.; Jiang, G.; Wang, Y.; Ding, F. Thermosensitive Chitosan Hydrogel for Implantable Drug Delivery: Blending PVA to Mitigate Body Response and Promote Bioavailability. *J. Appl. Polym. Sci.* 2012, *125*, 2092–2101.
32. Islam, M.M.; Shahruzzaman, M.; Biswas, S.; Sakib, M.N.; Rashid, T.U. Chitosan based bioactive materials in tissue engineering applications-A review. *Bioact. Mater.* 2020, *5*, 164–183.
33. Peptu, C.; Humelnicu, A.C.; Rotaru, R.; Fortuna, M.E. Chitosan-based drug delivery systems. In *Chitin and Chitosan: Properties and Applications*, 1st ed.; van den Broek, L.A.M., Boeriu, C.G., Eds.; John Wiley & Sons Ltd.: New York, NY, USA. 2019.
34. Denbanks, E.B.; Ottenbrite, R.M. Perspectives on: Chitosan Drug Delivery Systems Based on their Geometries. *J. Bioact. Compat. Polym.* 2006, *21*, 351–368.
35. Yee, G.C.; Gmur, D.J.; Kennedy, M.S. Liquid-chromatographic determination of cyclosporine in serum with use of a rapid extraction procedure. *Clin. Chem.* 1982, *28*, 2269–2271.
36. Frei, R.W.; Zech, K. *Selective Sample Handling and Detection in High-Performance Liquid Chromatography*; Frel, R.W., Zech, K., Eds.; Elsevier: Amsterdam, The Netherlands, 1988; p. 457.
37. Moore, T.; Croy, S.; Mallapragada, S.; Pandit, N. Experimental investigation and mathematical modeling of Pluronic® F127 gel dissolution: Drug release in stirred systems. *J. Control. Release* 2000, *67*, 191–202.
38. Pose-Vilarnovo, B.; Rodríguez-Tenreiro, C.; dos Santos, J.F.R.; Vázquez-Doval, J.; Concheiro, A.; Alvarez-Lorenzo, C.; Torres- Labandeira, J.J. Modulating drug release with cyclodextrins in hydroxypropyl methylcellulose gels and tablets. *J. Control. Release* 2004, *94*, 351–363.
39. Cassano, R.; Di Gioia, M.L.; Mellace, S.; Picci, N.; Trombino, S. Hemostatic gauzed based on chitosan and hydroquinone: Preparation, characterization and blood coagulation evaluation. *J. Mater. Sci. Mater. Med*. 2017, *28*, 190.
40. Cassano, R.; Trombino, S.; Bloise, E.; Muzzalupo, R.; Iemma, F.; Chidichimo, G.; Picci, N. New broom fiber (*Spartiumjunceum* L.) derivatives: Preparation and characterization. *J. Agric. Food Chem.* 2007, *55*, 9489–9495.
41. Hamel, A.R.; Hubler, F.; Carrupt, A.; Wenger, R.M.; Mutter, M. Cyclosporine A

prodrug: Design, synthesis, and biophysical properties. *J. Pept. Res.* 2004, *63*, 147–154.

42. Foley, D.W.; Bermudez, I.; Baileys, P.D.; Meredith, D. A cyclosporine derivative is a substrate of the oligopeptide transporter PepT1. *Med. Chem. Commun.* 2016, *7*, 999–1002.
43. Clasen, C.; Wilhelms, T.; Kulicke, W.M. Formation and characterization of chitosan membranes. *Biomacromolecules* 2006, *7*, 3210– 3222.
44. Cirillo, F.; Pellegrino, M.; Malivindi, R.; Rago, V.; Avino, S.; Muto, L.; Dolce, V.; Vivacqua, A.; Rigiracciolo, D.C.; De Marco, P.; Sebastiani, A.; et al. GPER is involved in the regulation of the estrogen-metabolizing CYP1B1 enzyme in breast cancer. *Oncotarget* 2017, *8*, 106608–106624.

PART C

Polymersomes as promising vehicle for controlled drug delivery

Abstract:

Polymersomes (Ps) are defined as artificial vesicles, resulting from the assembly of synthetic amphiphilic copolymer blocks, able to carry and release drugs. Compared to other vesicular nanovectors, such as liposomes or nanoparticles, they are very versatile because it is possible to encapsulate within them, drugs of different nature, such as hydrophilic, lipophilic, DNA and RNA molecules and vaccines. It is also possible to functionalize their surface, by increasing their transport across biological membranes and optimizing the pharmacokinetics and biodistribution of drugs conjugated to them at target site. Also polymersomes possess, remarkable colloidal stability, tunable membrane permeability, excellent robustness and relatively long blood circulation times attributable to their high biocompatibility with biological systems.

In recent years, attention to these nanovectors has increased because they could mediate drugs release in response to a series of internal biological stimuli (pH, redox potential, glucose concentration) and external physical ones (temperature, light, ultrasound), which can induce significant changes in the structure of the polymersomes with consequent destruction of the membrane and drug release. The advantages, offered in terms of therapeutic efficacy and reduction of side effects make these carriers excellent delivery systems for drug but also for medical imaging and diagnostics. Therefore, the aim of this chapter is to investigate the strategies, progresses and advantages of using polymersomes as carriers for stimuli-responsive drug delivery**.**

Keywords: polimersomes, drug delivery, diagnostic imaging, biological stimuli, physical stimuli.

1. Introduction

Polymersomes (Ps) are spherical artificial polymer vesicles [1], consisting of a hydrophilic core, capable of encapsulating water-soluble molecules, and surrounded by a hydrophobic membrane suitable to incorporate hydrophobic molecules [2,3]. These products are synthetically derived, obtained by assembling blocks of amphiphilic copolymers (diblock or triblock), and modifying the hydrophobic ratio of the copolymers. In fact it is possible to increase or decrease the thickness of the polymeric membranes enveloping them (bilayer or interdigitalized), thus giving the entire system a high degree of robustness and permeability [4]. The type of copolymer used, influences the characteristics of these carriers. In particular non-degradable polymers such as conjugated/aromatic hydrocarbons, make polymersomes with non-degradable structures, that are poorly biocompatible with biological systems, and therefore cannot be used as drug delivery systems; conversely, the use of water-soluble polymers such as poly(ethylene) glycole make these systems highly biocompatible and biodegradable [5]. Generally, polymersomes are produced by exploiting the action of solvents or the displacement of solvents [6,7]. Specifically, solvent-assisted techniques include film rehydration [8], electroforming [9,10,11] and polymerisation-induced self-assembly [12], while solvent displacement can be achieved by direct injection [13], emulsion phase transfer [14,15] and microfluidics [16]. Generally, an organic solvent is used to dissolve block copolymers, so the addition of a solvent-polymer solution in aqueous solution and the subsequent removal of the organic solvent leads to the production of polymersomes.

The aforementioned techniques are chosen according to the type of amphiphilic copolymer block used, since, for example, hydrophobic blocks with high glass transition temperatures cannot be used for the production of Ps via the polymer rehydration technique [17,18].

A key feature of these carriers is the ability to contain a considerable amount of active ingredient [19]. The drug loading into a polymersome can take place within the aqueous core (hydrophilic drugs), within the lipid bilayer of the membrane (lipophilic drugs) or through functionalisation on the membrane itself (small molecules) [20]. Encapsulation takes place by dissolving or dispersing the substances of different natures with the copolymer blocks used [21]; while the release of the active ingredient takes place by following a concentration gradient (passive diffusion) between the membrane and the external environment [22]. The modulation of this parameter to obtain slow release

kinetics, is closely linked to the composition of the membrane and its constituents. For this reason, controlled drug delivery from polymersomes is only possible following the use of polymeric blocks susceptible to the action of exogenous and endogenous stimuli [23]. These stimuli are present at the target site, and they able to induce a change in the hydrophilic/hydrophobic properties of the copolymers resulting in the disintegration of the polymersome or a cleavage of the covalent bonds in the chains of the polymeric components of the membrane with the formation of pores and release of substance [24]. In addition to being susceptible to stimuli, the amphiphilic copolymer building blocks used must also possess properties of biodegradability, biocompatibility, high permeability, physico-chemical stability and robustness that can then be transferred to the polymersome itself [25] Figure 1.

The aim of the present chapter, is to investigate the use of stimuli-responsive polymersomes as an innovative strategy for drug delivery, gene therapy, bioimaging, biosensing, in vivo diagnosis and regenerative medicine.

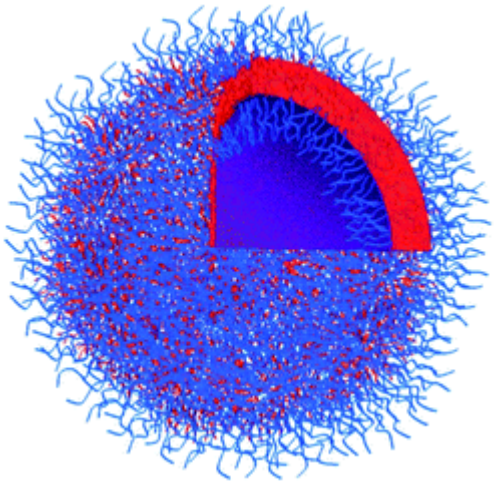

Figure 1. Polimersome structure

2. Polymersomes responsive to physical and chemical stimuli

Drug release from polymersomes into the target site can be influenced by the response of these carriers to endogenous and exogenous stimuli that occur as a result of physiological changes typical in diseased and/or healthy tissues [26]. For example, chemical alterations such as pH, hypoxia, redox and enzymatic reactions, and physical ones such as mechanical triggers, and temperature changes can induce significant changes in the solubility of a polymer block, dissolve or disintegrate polymersomes and create pores in their membrane to the drugs release [27,28].

Exogenous stimuli such as light, ultrasound, magnetic fields and gases can also promote the release of bioactive substances following polymer-some bursting [29] Figure 2.

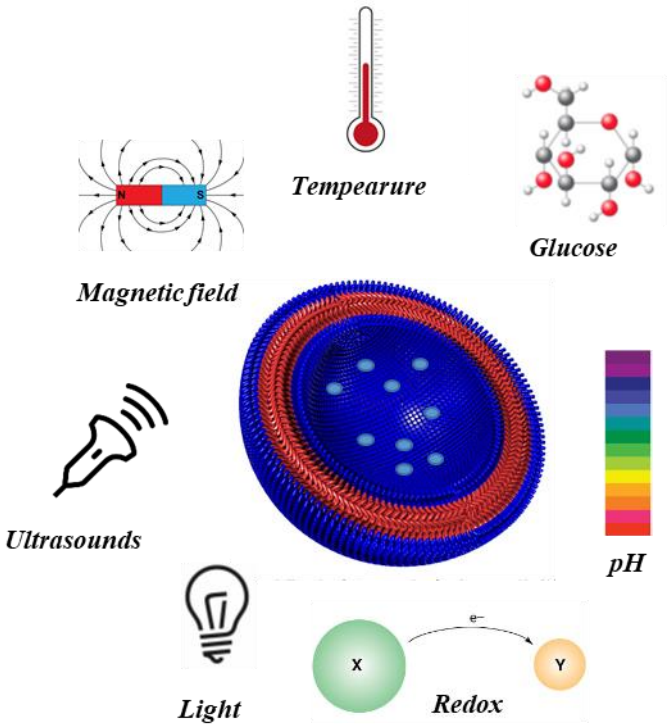

Figure 2. stimuli responsive polimersome

The reason why these nanocarriers are able to respond to such stimuli stems from the use of smart polymers susceptible to the action of chemical or physical factors [30] that are assembled together through techniques of anionic or cationic polymerization, controlled radical, nitroxide-mediated radical and atom transfer radical polymerisation [31].

3. Chemical stimuli responsive polymersome

3.1 pH-responsive polymersome

pH-responsive polymersomes are nanocarriers designed and manufactured to respond to changes in physiological pH gradients in intracellular compartments, specific organs and microenvironments associated with certain pathological conditions such as cancer, inflammation etc. [32]. They are generally made using polymers defined as “pH-reactive”, capable of donating or accepting protons as a result of changes in the surrounding environment [33]. For this reason, ionisable groups are inserted into the amphiphilic block

copolymers, which react inducing hydrolysis of the polymersome and releasing the substance it contains [34]. The most commonly used polymers are aliphatic polyesters such as poly (lactic acid) (PLA) and poly(e-caprolactone) (PCL) [35]. At this regard Puglisi et al., described that incorporating a benzoic imine bond into a poly(ε-caprolactone) copolymer block, the result was the hydrolysis of the imine bond in an acidic environment (pH 5.5), with subsequent degradation of the structural architecture of the polymersome and release of the encapsulated substances. Specifically, stability studies have shown that this nanostructure did not undergo particular changes at physiological pH (7.4), whereas it was hydrolyzed at acid pH (5.5). It could therefore be useful in the delivery of cyclodextrins to endosomes or liposomes in the treatment of cholesterol-related diseases, since these cell organelles are in a purely acidic environment [36]. Most of the responsible pH polymersomes are made with the intention of not being altered during passage through the systemic circulation. According to Albuquerque et al., the biodistribution of these nanostructures in the systemic circulation could be increased by using microfluidic technology as a method of producing polymersomes. This technique would make it possible to create highly uniform polymer assemblies, with associated control over the size, shape and polydispersion of the nanoparticles. To this end, engineered polymersomes were produced with poly([N-(2-hydroxypropyl)]-methacrylamide)-b-poly[2-(diisopropylamino)ethyl methacrylate] and loaded with doxorubicin (DOX). Release studies have shown the ability of the polymersome to support hydrophilic encapsulated molecules (doxorubicin) when placed in contact with a physiological environment (pH 7.4), preventing drug loss during systemic circulation. Furthermore, the use of poly(N-(2-hydroxypropyl) methacrylamide), as the hydrophilic one of proteosomes, increased their durability in the blood circulation [37]. Some pH-sensitive copolymers, such as 2-(diisopropylamino) ethyl methacrylate (DPA), had a hydrophilic segment at pH 6.2 that can change to a hydrophobic segment when the solvent pH rises above 6.4 due to deprotonation. Making polymersomes with DPA minimises the possibility of denaturing and inactivating substances such as proteins, nucleic acids etc., which were sensitive to extremely acidic environments. Wang et al. designed and synthesised a new diblock copolymer, poly (2- (methacryloyloxy) ethylcholine phosphate)-b-poly(2-(diisopropylamino) ethyl methacrylate) (PMCP-b-PDPA) by atomic transfer radical polymerisation (ATRP), to form an amphiphilic and a hydrophobic portion. These nanocarriers would be able to penetrate tumour intracellular compartments showing stability at pH 7.4, and degraded within the endosome (pH 5.0) due to changes in PDPA

segments from hydrophobic to hydrophilic, which contributed to the rapid release of drugs such as doxorubicin. In addition, the sponge effect attributable to the diisopropyl-substituted tertiary amine chains of the PDPA copolymer would increase the release of drug from the polymersome into the cellular endosome, resulting in a cytotoxic effect on the cell itself [38].

Polymersomes could act as vectors for the release of several substances, even of different nature. In this regard, Curcio et al. have developed an amphiphilic PEG-based polymersome for the co-delivery of hydrophilic methotrexate (MTX) and hydrophobic curcumin (CUR) substances. The presence of both substances in the nanoparticles would increase pharmacological efficacy at the target site, especially at acidic pH. Indeed, release studies have shown that pH sensitivity was correlated with changes in the average diameter of the particles, which increase significantly when placed in contact with acidic pH environments [39] Figure 3.

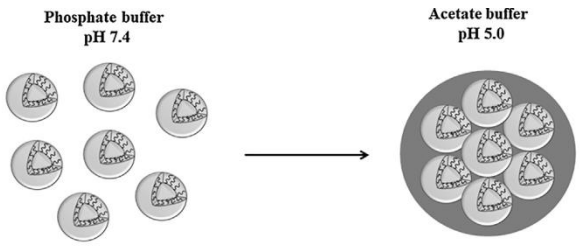

Figure 3. Polimersome aggregation at acidic pH (Adapted from article 39)

Another very promising study in the use of pH-responsive polymersomes was carried out by Oroojalian et al. that synthetized a thermoresponsive hydrogel based on poly(N-isopropylacrylamide)-doxorubicin (PNIPAM-DOX) subsequently loaded into pH-responsive polymersomes based on polyethylene glycol reactive 2,4,6-trimethoxy benzylidene pentaerythritol carbonate (PEG-PTMBPEC) in order to fabricate an intelligent thermo-pH stimulated drug delivery system. In vitro and in vivo release studies showed increased drug stability in these systems when delivered through the bloodstream. In addition, an increment in the residence time of the drug at tumour sites has been observed with an increase in the therapeutic index and a decrease in cytotoxic effects [40].

3.2 Redox responsive polymersome

Changing redox potentials in the extracellular and intracellular compartments of tissues can alter the membrane properties of polymeric nanostructures [41,42]. For example, reducing agents such as glutathione, in high concentrations in the cytosol and nucleus of cells, can lead to the disassembly of polymersomes present in reductive environments with the consequent release of active substances [43,44]. In fact, the disulphide bonds, introduced into the side chain of an amphiphilic polymer, in order to improve its stability, was reduced in the intracellular environment by glutathione, since a thiol-disulphide exchange reaction occurs that damages the outer membrane of the polymersome [45]. In this regard, reduction-sensitive polymersomes have been developed for the delivery of tumour agents into damaged tissues where the presence of glutathione was greater than in healthy tissues [46]. In the work of Nehate et al., polymersomes based on polycaprolactone copolymers modified with polyethylene glycol (PEG) by introducing a disulphide bond between the two were mentioned. *In vitro* studies have shown that loading an anti-tumour agent such as doxycycline into these nanostructures increases their internalisation in tumour cells of the Hela and MDA-MB-231 lines, thus increasing the cytotoxicity of the drug at the site concerned Figure 4.

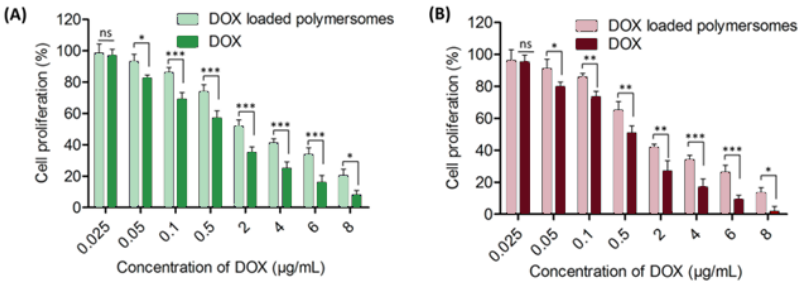

Figure 4. In vitro cytotoxicity study of DOX loaded polymersomes and free DOX on HeLa (a) and MDA-MB-231(b) cells (Adapted from article 54)

In vivo studies in albino mice with Ehrlich ascites tumor (EAT) showed a 7.16-fold reduction in tumor volume compared to tumor inhibition induced by conventional chemotherapy. Thus, the redox potential of tumour cells was used as an activation mechanism to enhance intracellular drug delivery as high concentrations of glutathione would induce disruption of disulfide bonds present in the polymersome matrix [47].

In another study conducted by Nehate et al. on the release of doxycycline in tumour tissues, it could be observed that the creation of polymersomes by means of Free Atomic Transfer Radical Polymerization improves the drug release capacity of the nanostructure. Indeed, by optimising the design phases of the polymersomes, with the relative insertion of the disulfide bond into the starting copolymer matrix, it was possible to develop nanocarriers with an encapsulation and drug release efficiency 20 times higher than other nanocarriers [48]. According to Benito et al., it was also possible to synthesize simple three-block amphiphilic copolymers starting from poly(ethylene glycol) methyl ether (mPEG2000) with a hydrophobic core containing multiple disulfide bonds. Such copolymers could self-assemble into polymersomes that were highly sensitive to reductive conditions and serve as carriers for anticancer agents [49].

The group of Zhong et al. also made dual-responsive polymersomes using three poly (ethylene glycol)-poly(acrylic acid)-poly(2-(amino diethyl)-ethyl methacrylate) (PEG-PAA-PDEAEMA) copolymer blocks modified with cysteamine to produce the thiol-containing PEG-PAA(SH)-PDEAEMA copolymer. This copolymer yielded robust, monodisperse polymersomes with excellent colloidal stability, which underwent rapid dissociation upon contact with glutathione. These polymersomes showed excellent potential for intracellular distribution of proteins [50].

Recently, it was observed that conjugating a ligand to the surface of a redox-sensitive polymersome would increase the specificity of the nanovector towards tumour cells. Kumar et al. developed, manufactured and tested polymersomes based on a multi-block copolymer consisting of poly(ester-urethane,-PLA-PEG-PLA-urethane-ss-) with multiple disulfide bonds to which folic acid and trastuzumab were conjugated and in which doxycycline was encapsulated. Release studies confirmed the redox reactive behaviour of the polymersomes with a percentage of drug released ~72% at pH 5.5 in the presence of 10 mM GSH compared to the percentage released at pH 7.4; while in vitro absorption studies revealed greater absorption of conjugated nanoparticles compared to unconjugated ones. In addition, in vitro and in vivo toxicity studies were also carried out, showing the antiproliferative capacity exerted by the vectors on MCF-7 cell lines and a 91% tumour regression in Ehrlich ascites tumour (EAT) [51].

The same research group had previously developed polymersomes based on multi-block copolymers with E-caprolactone to assess their doxorubicin release profile in the treatment of tumour lesions. Tests showed that there was no difference between the use of lactides and caprolactone in the nanoparticle structure, as the release profile of faramco was

comparable to that previously described [52]. Similar results were also obtained by the group of Lale et al. with the development of poly (ethylene glycol)-polylactic acid-poly(ethylene)glycol) polymersomes also conjugated with folic acid and trastuzumab [53]. Amphiphilic polypropharmaceuticals responsive to the reductive environment have been developed through reversible fragmentation chain transfer (RAFT) polymerisation of a camptothecin-based propharmaceutical monomer (CPT) with a poly (-ethylene oxide)-based agent. Such nanostructures could selectively release drugs into the cytosol of cells responsible for inflammatory processes [54].

Oxidation-responsive polymersomes were structures affected by the action of reactive oxygen species (ROS) such as hydrogen peroxide (H2O2), peroxynitrite (ONOO-), hydroxyl radical (OH), and superoxide (O2-), which play important roles in cell signalling and proliferation, apoptosis, and immune responses [55,56]. However, overproduction of ROS is linked to oxidative stress, cancer, infectious processes, inflammation, cardiovascular disease and diabetes [57]. All these conditions could be exploited to make nanostructures that release pharmacologically active substances in contact with these environments [58].

Zhang et al. designed polymersomes by synthesising the starting copolymer, poly (ethylene oxide)-b-poly(trifluoro-3-oxobutyl phenyl methacrylate, from scratch. The presence of ketone groups in the side chain of the copolymer could make the formed nanoparticles chemoselective to peroxynitrite (ONOO-), thus triggering oxidation-elimination cascade reactions by cleavage of the side groups of the polymer chain, altering the degree of amphiphilicity of the copolymer and decreeing the disassembly of the self-assembled vesicular structures [59]. In a recent study, it was found that even polyprodrugs could be reactive to ROS and thus self-assemble into stable nanoparticles with high drug loading. One example was the polyprodrug developed by Xu et al. which consisted of a ROS-reactive inner core to promote the release of active molecules, a polyethylene glycol (PEG) outer shell to prolong blood circulation, and a conjugated RGD factor to improve targeting and penetration of the tumour parenchyma. *In vivo* and *in vitro* studies have shown that these nanostructures exert an inhibiting action on tumour cell proliferation with more than promising results [60]. The destruction of polymersomes after contact with reactive oxygen species could take place in aqueous solution containing H2O2 or by means of a photo-sensitiser. In vivo, the concentration of H2O2 used was in the millimetre range but if one wanted to reproduce the in vivo conditions, one could exploit the encapsulation of enzymes that generate oxidation to produce a high concentration of H2O2 in situ [61] Figure 5.

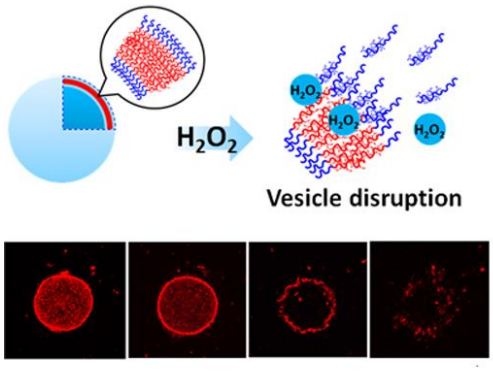

Figure 5. Polymersome destruction afeter contact with H_2O_2 (Adapted from article 68)

3.3 Glucose responsive polymersome

Glucose-responsive polymersomes are intelligent delivery systems for insulin, a well-known drug for treating type 1 and type 2 diabetes. In particular, by incorporating glucose-reactive substances such as glucose oxidase (GOx), glucose-binding proteins and boronic acids, structural transformations in the polymer matrix, such as shrinkage, swelling and dissociation, can be observed after changes in the ambient glucose concentration [62].

Boronic acid-containing materials possess the ability to reversibly form complexes with glucose such as 1,2-cis-diol, whereas glucose oxidase (GOx) systems that are affected by changes in glucose concentration are always integrated with other materials that in turn undergo changes related to pH, hypoxia or oxidation [63].

At this regard, Wang et al. have developed smart polymersomes consisting of glucose-responsive polymers decorated with peptides that easily bind to the ganglioside-monosial (GM1) present in the intestinal epithelium. These nano-structures could accumulate in the liver and release encapsulated insulin under hyperglycaemic conditions as a result of GOx-induced oxidation [64]. Di et al. also made glucose-responsive formulations for self-regulated insulin delivery with injectable hyaluronic acid (HA) microgels supplemented with dextran-based glucose nanoparticles modified with degradable dextran-based acid. Through the introduction of the GOx enzyme into the polymer matrix, the dextran nanoparticles could release insulin in a hyperglycaemic state, following the enzymatic conversion of glucose to gluconic acid [65]. Polyethylene glycol (PEG)-based block copolymers containing boronic acid-functionalized segments showed interesting reactions to changes in glucose concentration. In a study conducted Zhang et al., was shown that vesicles changed their shape from a round to a cylindrical shape at concentrations of 0.1-

0.5% glucose and deteriorated at higher concentrations, indicating that they were responsive to glucose [66].

4. Physycal stimuli responsive polymersome

4.1 Temperature responsive polymersome

Temperature responsive polymersomes are produced using temperature-sensitive polymers with a variable critical solution temperature that depends on the release of water molecules near of the polymer, its dissolution in the aqueous medium, intra- and intermolecular forces and solvation [67]. For example, polymers that are insoluble in an aqueous medium upon heating possess a lower critical solution temperature (LCST) due to hydrogen interactions between the hydrophilic polymer chains and water molecules that will induce increased swelling of the matrix; those that are soluble upon heating possess a higher critical solution temperature (UCST) as there is a prevalence of hydrophobic interactions between the hydrophobic polymer segments that will induce collapse [68].

Polymers considered to be thermally responsive are poly(N-alkylacrylamide) poly(N-isopropylacrylamide) (PNIPAAM), poly(methyl vinyl ether) (PMVE), poly(Nvinyl caprolactam) (PVCa) and poly(N-ethyl oxazoline) (PEtOx) [69]. PNIPAM is a thermally responsive polymer with the ability to transition from a hydrophilic to a hydrophobic nature at temperatures around 32°C. Specifically, the hydrophobic component self-assembles to form vesicles at temperatures of 37°C with substance release at temperatures of 32°C [70]. In the work of Quin et al. was shown that the release of hydrophilic and hydrophobic drugs encapsulated in the aqueous lumen and membrane of polymersomes, respectively, made of diblock copolymer PEO-b-PNIPAM, occurs at a temperature of 32°C. This condition was favourable for the release of antitumour drugs at the site of the malignant lesion [71]. It was important to consider that the permeability of polymersomes, loaded with a deteminated drug can be controlled by the length of the PVCL in the temperature range of 37-42 °C. According to Liu et al., increasing the temperature above the lower critical one of a PVCL solution was favoured the formation of small vesicles or beadlike aggregates without any size change, which induce prolonged drug release. Morphological changes, caused by temperature, were reversible in nature and therefore did not alter vesicle stability [72]. The inability of PVCL to form non-aggregated vesicular

structures permitted Kozlovskaya et al. to create thermoresponsive polymersomes based on poly(3-methyl-N-vinylcaprolactam)-bPVPONn (PMVC-PVPON), a copolymer block capable of self-assembling into stable vesicular structures due to its low LCST ranging from 15 to 19 °C. Tests also reveal optimal encapsulation efficiency with reduced cytotoxic effects [73].

4.2 Light responsive polymersome

Photoresponsive polymersomes are commonly made by incorporating photoresponsive substances into block copolymers, which can induce structural changes in the vesicles [74], changes in the hydrophobic-hydrophilic balance, photo-crosslinking and degradation or cleavage of the junctions constituting the matrices themselves [75,76]. Photosensitive polymersomes can respond reversibly or irreversibly depending on the substances in their structure [77,78].

Azobenzene spiropyran [79], dithienylethene [80] and diazonaphthoquinone [81] are considered reversible photoresponsive substances; whereas irreversible ones include o-nitrobenzyl [82], pyrenylmethyl, and coumarin [83].

With light irradiation, a series of reactions, some of them photocleavage, occur at the expense of the above-mentioned functional groups. In particular, the azobenzene spiropyran group undergoes isomerisation, passing from the trans to the cis form; the o-nitrobenzyl group, on the other hand, was subjected to a change in structure, passing from the cationic amphiphilic form to the hydrophilic zwitterionic form. In this regard, Zhou et al. studied nanostructures loaded with anticancer drugs such as doxorubicin hydrochloride, which underwent controlled drug release due to photo-induced disintegration of the polymersomes [84]. Exposure to light irradiation at 365 nm could trigger a photo-dissolution reaction of o-nitrobenzyl groups, resulting in dissociation of polymersomes with simultaneous release of hydrophilic and hydrophobic drugs on demand. Indeed, the studies conducted by Hou et al. have shown that an o-nitrobenzyl ester group of the hydrophobic block of the synthesized copolymer undergoes, following irradiation, an efficient photocatalytic reaction to generate an o-nitrosobenzaldehyde and a free carboxylic acid, and trigger the dissociation of the polymersomes [85] Figure 6.

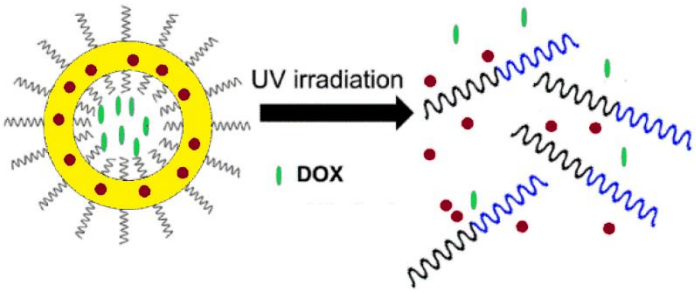

Figure 6. Light-responsive co-release of hydrophobic and hydrophylic drug from polymersome (Adapted from article 85)

The o-nitrobenzyl photoresponsive groups could be located in the side chains of the hydrophobic block of amphiphilic diblock copolymers, or as junctions between the hydrophobic and hydrophilic groups. Yamamoto et al. studied the structure and photorelease characteristics of a series of linker-type photoresponsive polymersomes, with different species of hydrophobic block polymers of varying molecular weight. Studies have shown that substance release from these polymersome types was closely related to the chemical variation of the hydrophobic segments and the nature of the residual functional groups obtained after photolysis [86].

4.3 Magnetic and ultrasound responsive polymersome

Polymersomes responsive to stimuli such as ultrasound and/or magnetic fields are very promising nano-particulate systems due to their non-invasive nature, ease of control and delivery, low cost and deep penetration into the body [87,88].

Magnetic responsive polymersomes are synthesized by incorporating ferromagnetic or paramagnetic materials into the membranes of amphiphilic block copolymers and are useful for magnetically triggered drug delivery systems or MRI [89]. In the absence of external magnetic fields, magnetic nanoparticles in the intramembrane space are in a "gaseous" state or form chain structures due to magnetic dipole-dipole interaction [90]. The presence of a magnetic field straightens the polymer chains of the particles, causing deformation of the membrane which takes on an anisometric shape [91]. This deformation is associated with a change in the volume of the internal cavity of the magnetic polymersomes, resulting in the release of the material it contains or the suction of the fluid in which it is suspended [92].

In this regard, Ryzhkov and Raikher have developed a magnetic polymersome whose magnetoactivity was related to the characteristics of the shell (membrane). The latter has been designed as a pair of two concentric interfaces, between which was a viscous fluid layer in which the magnetic nanoparticles were free within the layer [93].

Polymersomes, which are used to deliver superparamagnetic iron oxide nanoparticles (SPION), were studied by Duan et al. who encapsulated them in mesenchymal stem cells to assess their long-term survival after transplantation in stroke-affected areas. Magnetic resonance imaging made it possible to track the viability of mesenchymal stem cells, thanks to the fluorescence expressed by SPIONs present in the polymersomes encapsulated in the cells themselves [94]. This imaging technique has been labelled as a valuable tool for assessing the clinical course of a disease.

However, in the diagnosis and/or treatment of cerebral ischaemia, it was possible to combine the action of ferromagnetic particles encapsulated in the polymersome and the action of ultrasound. It was interesting to note, the studies carried out by Kan et al. that magnetic targeting decreases the accumulation of the magnetic nanoparticles containing the drug and encapsulated in the polymersome, while the deformation of the membrane and the release of the substances at the site of the ischaemic lesion is attributable to the action of ultrasound [95]. Through ultrasounds, it is possible to derive new insights into easier control of anticancer drug delivery systems and precise tumour therapy through the use of polymersomes. As studied by Wang et al. it is possible to exploit ultrasounds, as a non-invasive stimulus, for the controlled release of doxorubicin from polymersomes thus offering the possibility of targeted anticancer therapy with reduced systemic effects [96].

5. Conclusion

The design and development of polymersomes in the biomedical field has made it possible to expand strategies for drug delivery, the improvement of existing therapies and imaging mechanisms for the diagnosis and treatment of diseases. The introduction of stimuli capable of triggering the reactivity of these nanostructures has made it possible to recognise external or internal chemical, physical or biological variations such as pH, redox reactions, enzymes, temperature, light, magnetic fields and ultrasound as factors capable of disrupting the hydrophobic-hydrophilic balance of polymersomes to destabilise their assemblies. In this regard, conformational changes in the structure of the polymersomes,

induced by the response to a stimulus of a different nature, would cause the collapse of the polymer membrane and consequently the release of useful substance.

In this chapter, a series of stimulus-responsive polymersomes have been described and analysed as possible controlled release or imaging systems in the treatment and diagnosis of pre-existing diseases. In vitro studies have shown that these nanostructures are highly biocompatible with biological systems, have low toxicity and are more effective than conventional therapies. However, there are still no useful informations on the efficacy of these drug delivery systems in vivo. Therefore, despite the fact that in vitro studies show appreciable results in terms of permanence in the bloodstream, site-specific localisation, biocompatibility, low side effects, etc., in vivo studies are needed to confirm the advantage of stimuli-responsive polymersomes as carriers in nano-medicine.

REFERENCES

S. Trombino, F. Curcio, R. Cassano. Polymersomes as promising vehicle for controlled drug delivery. In: Stimuli-Responsive Nanocarriers: Recent Advances in Tailor-Made Therapeutics, Eds. Virendra Gajbhiye. Elsevier. 2021.

[1] J.S. Lee, J. Feijen, Polymersomes for drug delivery: Design, formation and characterization, Journal of Controlled Release 161 (2012) 473–483. doi:10.1016/j.jconrel.2011.10.005

[2] Y. Deng, J. Ling, M.H. Li, Physical stimuli-responsive liposomes and polymersomes as drug delivery vehicles based on phase transitions in the membrane, Nanoscale (2018) 10- 6781. doi: 10.1039/c8nr00923f

[3] F.H. Meng, Z.Y. Zhong, Polymersomes spanning from nano- to microscales: Advanced vehicles for controlled drug delivery and robust vesicles for virus and cell mimicking. Journal of Physical Chemistry Letters 2(13) (2011) 1533–1539. doi.org/10.1021/bm801127d

[4] X.Y. Zhang, P.Y. Zhang, Polymersomes in Nanomedicine - A Review, Current Nanoscience, (2017) 13 124-129. doi: 10.2174/1573413712666161018144519

[5] F. Meng, C. Hiemstra, G.H.M. Engbers, J. Feijen, Biodegradable Polymersomes, Macromolecules (2003)36 9 3004–3006. doi.org/10.1021/ma034040

[6] C. Wong, M.H. Stenzel, P. Thordarson, Non-spherical polymersomes: formation and characterization, Chemical Society Reviews (2019) 48 4019-4035. doi: 10.1039/C8CS00856F

[7] J. Liao, C. Wang, Y. Wang, F. Luo, Z. Qian, Recent advances in formation, properties, and applications of polymersomes. Current Pharmaceutical Design (2012) 18 (23) 3432-41. doi.org/10.2174/138161212801227050

[8] E. Rideau, F. R. Wurm, K. Landfester, Giant polymersomes from non-assisted film hydration of phosphate-based block copolymers, Polymer Chemistry (2018) 9 5385–5394. doi: 10.1039/C8PY00992A

[9] J. E. Bartenstein, J. Robertson, G. Battaglia, W. H. Briscoe, Stability of polymersomes prepared by size exclusion chromatography and extrusion Colloids Surface A (2016) 506 739–746. doi.org/10.1016/j.colsurfa.2016.07.032

[10] E. Ibarboure, M. Fauquignon, J.F. Le Meins, Obtention of Giant Unilamellar Hybrid Vesicles by Electroformation and Measurement of their Mechanical Properties by Micropipette Aspiration, JoVE (2020) 60199. doi: 10.3791/60199

[11] C. Kunzler, S. Handschuh-Wang, M. Roesener, H. Schönherr, Giant Biodegradable Poly(ethylene glycol)-block-Poly(ε-caprolactone) Polymersomes by Electroformation, Macromolecular Bioscience (2020) 20 2000014. doi.org/10.1002/mabi.202000014

[12] B. Charleux, G. Delaittre, J. Rieger and F. D'Agosto, Polymerization-Induced Self-Assembly: From Soluble Macromolecules to Block Copolymer Nano-Objects in One Step, Macromolecules (2012) 45 6753–6765. doi.org/10.1021/ma300713f

[13] A.B. Pijpers, F.H. Meng, J.C.M. van Hest, L. Abdelmohsen, Macromolecular design and preparation of polymersomes, Polymer Chemistry (2020) 11 275–280. doi: 10.1039/D0PY01247E.

[14] M.R. Kim, I.W. Cheong, Stimuli-triggered Formation of Polymersomes from W/O/W Multiple Double Emulsion Droplets Containing Poly(styrene)-block-poly(N-isopropylacrylamide-co-spironaphthoxazine methacryloyl), Langmuir (2016) 32 9223–9228. doi.org/10.1021/acs.langmuir.6b02178

[15] A.A. Asl, S. Rahmani, Synthesis characterization and self-assembly investigation of novel PEG-g-PCL copolymers by combination of ROP and ''click'' chemistry method as a sustained release formulation for hydrophobic drug, Intenational Journal Polymeric Materials and Polymeric Biomaterials (2019) 68 540–550. doi.org/10.1080/00914037.2018.1466140

[16] A.S. Utada, E. Lorenceau, D. R. Link, P. D. Kaplan, H. A. Stone, D. A. Weitz, Monodisperse Double Emulsions Generated from a Microcapillary Device, Science (2005) 308 537–541. doi: 10.1126/science.1109164

[17] B. Zhang, X. Lv, A. Zhu, J. Zheng, Y. Yang, Z. An. Morphological Stabilization of Block Copolymer Worms Using Asymmetric Cross-Linkers during Polymerization-Induced Self-Assembly, Macromolecules (2018) 51 8 2776–2784. doi.org/10.1021/acs.macromol.8b00246

[18] A. Jahn, W.N. Vreeland, M. Gaitan, L.E. Locascio, Controlled Vesicle Self-Assembly in Microfluidic Channels with Hydrodynamic Focusing, Journal of the American Chemical Society (2004) 126 (9) 2674- 2675 doi.org/10.1021/ja0318030

[19] T. Anajaf, S. Mallik, Polymersome-based drug-delivery strategies for cancer therapeutics, Therapeutic Delivery (2015) 6(4) 521–53. doi.org/10.4155/tde.14.125

[20] Y.Q. Zhu, B.Yang, S. Chen, J.Z. Du, Polymer vesicles: Mechanism, preparation, application, and responsive behavior, Progress in Polymer Science (2017) 64-1. doi.org/10.1016/j.progpolymsci.2015.05.001

[21] J. Leong, J.Y. Teo, V.K. Aakalu, Y.Y Yang, H. Kong, Engineering Polymersomes for Diagnostics and Therapy, Advanced Healthcare Material (2018) 7 1701276. doi: 10.1002/adhm.201701276

[22] C.P. O'Neil, T. Suzuki, D. Demurtas, A. Finka, J.A. Hubbell, A novel method for the encapsulation of biomolecules into polymersomes via direct hydration, Langmuir 25 (2009) 9025–9029. doi.org/10.1021/la900779t

[23] M.C. García, Stimuli-responsive polymersomes for drug delivery applications, Advanced Nanocarriers for Therapeutics, (2019) 345-392. doi.org/10.1016/B978-0-08-101995-5.00019-2

[24] U. Kauscher, M.N. Holme, M. Björnmalm, M.M. Stevens, Physical stimuli-responsive vesicles in drug delivery: Beyond liposomes and polymersomes, Advanced Drug Delivery Reviews, 138 (2019) 259–275. doi.org/10.1016/j.addr.2018.10.012

[25] S.J. Rijpkema, B.J. Toebes, M.N. Maas, N.R.M. de Kler, D.A. Wilson, Designing Molecular Building Blocks for Functional Polymersomes, Israel Journal of Chemistry, (2019) 59 928 – 944. doi: 10.1002/ijch.201900039

[26] M. Wei, Y. Gao, X. Li, M. J. Serpe, Stimuli-responsive polymers and their applications, Polymer Chemistry, (2017) 8 127. doi: 10.1039/c6py01585a

[27] P. Schattling, F.D. Jochuma, P. Theato, Multi-stimuli responsive polymers – the all-in-one talents, Polymer Chemistry, (2014) 5 25. doi: 10.1039/c3py00880k

[28] M. Lomora, M. Garni, F. Itel, P. Tanner, M. Spulber, C.G. Palivan, Polymersomes with engineered ion selective permeability as stimuli-responsive nanocompartments with preserved architecture, Biomaterials 53 (2015) 406-414. doi.org/10.1016/j.biomaterials.2015.02.080

[29] S. Chatterjee, P. Chi-leung Hui, Review of Stimuli-Responsive Polymers in Drug Delivery and Textile Application, Molecules (2019) 24 2547. doi:10.3390/molecules24142547

[30] H. Sun, C.P. Kabb, M.B. Sims, B.S. Sumerlin, Architecture-transformable polymers: Reshaping the future of stimuli-responsive polymers, Progress in Polymer Science 89 (2019) 61–75. doi.org/10.1016/j.progpolymsci.2018.09.006

[31] Y. Gao, M. Wei, X. Li, W. Xu, A. Ahiabu, J. Perdiz, Z. Liu, M. J. Serpe, Stimuli-responsive polymers: Fundamental considerations and applications, Macromolecular Research, (2017) 25 513–527. doi:10.1007/s13233-017-5088-7

[32] A.E Felber, M. H. Dufresne, J. C. Leroux, pH-sensitive vesicles, polymeric micelles, and nanospheres prepared with polycarboxylates, Advanced Drug Delivery Review (2012) 64 979. doi.org/10.1016/j.addr.2011.09.006

[33] B. Iyisan, J. Kluge, Petr. Formanek, B. Voit, D. Appelhans, Multifunctional and Dual-Responsive Polymersomes as Robust Nanocontainers: Design, Formation by Sequential Post-Conjugations, and pH-Controlled Drug Release. Chemistry of Materials (2016) 28 5 1513–1525. doi.org/10.1021/acs.chemmater.5b05016

[34] E. Fleige, M.A. Quadir, R. Haag, Stimuli-responsive polymeric nanocarriers for the controlled transport of active compounds: Concepts and applications, Advanced Drug Delivery Reviews, (2012) 64 9 866-884. doi.org/10.1016/j.addr.2012.01.020

[35] S. Bazban-Shotorbani, M. MahdiHasani-Sadrabadi, A. Karkhaneh, V. Serpooshan, K. IJacob, A. Moshaverinia, M. Mahmou, Revisiting structure-property relationship of pH-responsive polymers for drug delivery applications, Journal of Controlled Release, (2017) 253 10 46-63. doi: 10.1016/j.jconrel.2017.02.021

[36] A. Puglisi, E. Bayir, S. Timur, Y. Yagci, pH-Responsive Polymersome Microparticles as Smart CyclodextrinReleasing Agents, Biomacromolecules (2019) 20 4001-4007. doi.org/10.1021/acs.biomac.9b01083

[37] L.J.C. Albuquerque, V. Sincari, A. Jager, R. Konefał, J. Panek,´ P. Černoch, E. Pavlova, P. Štepa˘nek,´ F.C. Giacomelli, E. Ja´ger, Microfluidic-Assisted Engineering of Quasi-Monodisperse pHResponsive Polymersomes toward Advanced Platforms for the Intracellular Delivery of Hydrophilic Therapeutics, Langmuir (2019) 35 8363-8372. doi.org/10.1021/acs.biomac.9b01083

[38] W. Wanga, X. Maa, X. Yua, pH-responsive Polymersome Based on PMCP-b-PDPA as a Drug Delivery System to Enhance Cellular Internalization and Intracellular Drug Release, Chinese Journal of Polymer Science (2017) 35 11 1352-1362. doi: 10.1007/s10118-017-1982-x

[39] M. Curcio, L. Mauro, G.D. Naimo, D. Amantea, G. Cirillo, L. Tavano, I. Casaburi, F.P. Nicoletta, C. Alvarez-Lorenzo, F. Iemma, Facile synthesis of pH-responsive polymersomes based on lipidized PEG for intracellular co-delivery of curcumin and methotrexate Colloids and Surfaces B: Biointerfaces (2018) 167 568–576. doi.org/10.1016/j.colsurfb.2018.04.057

[40] F. Oroojaliana, M. Babaeia, S. Mohammad Taghdisic, K. Abnousa, M. Ramezania, M. Alibolandi, Encapsulation of Thermo-responsive Gel in pH-sensitive Polymersomes as Dual-Responsive Smart carriers for Controlled Release of Doxorubicin Journal of Controlled Release (2018) 288 45–61 doi.org/10.1016/j.jconrel.2018.08.039

[41] F. Meng, W.E. Hennink, Z. Zhong, Reduction-sensitive polymers and bioconjugates for biomedical applications, Biomaterials (2009) 30 (12) 2180–2198. doi: 10.1016/j.biomaterials.2009.01.026

[42] T. Fukino, H. Yamagishi, T. Aida, Redox-Responsive Molecular Systems and Materials, Advanced Materials (2017) 29 1603888. doi: 10.1002/adma.20160388

[43] R. Cheng, F. Feng, F. Meng, C. Deng, J. Feijen, Z. Zhong, Glutathione-responsive nanovehicles as a promising platform for targeted intracellular drug and gene delivery, Journal of Controlled Release (2011) 152 (1) 2–12. doi: 10.1016/j.jconrel.2011.01.030

[44] H. Xiao, H. Song, Q. Yang, H. Cai, R. Qi, L. Yan, S. Liu, Y. Zheng, Y. Huang, T. Liu, X. Jing, A prodrug strategy to deliver cisplatin (IV) and paclitaxel in nanomicelles to improve efficacy and tolerance, Biomaterials (2012) 33 6507. doi.org/10.1016/j.biomaterials.2012.05.049

[45] S.Cerritelli, D. Velluto, J. A. Hubbell, PEG-SS-PPS: Reduction-Sensitive Disulfide Block Copolymer Vesicles for Intracellular Drug Delivery, Biomacromolecules, (2007) 8 1966. doi.org/10.1021/bm070085x

[46] K. M. Park, D. W. Lee, B. Sarkar, H. Jung, J. Kim, Y. H. Ko,
K. E. Lee, H. Jeon, K. Kim, Reduction-Sensitive, Robust Vesicles with a Non-covalently Modifiable Surface as a Multifunctional Drug-Delivery Platform, Small (2010) 6 1430. doi.org/10.1002/smll.201000293

[47] C. Nehate, A. Nayal, V. Koul, Redox Responsive Polymersomes for Enhanced Doxorubicin Delivery, ACS Biomaterial Science Engineering, (2019) 5 70-80. doi: 10.1021/acsbiomaterials.8b00238

[48] C. Nehate, A.A. Moothedathu Raynold, V. Haridas, V. Koul, Comparative Assessment of Active Targeted Redox Sensitive Polymersomes Based on pPEGMA-S-S-PLA Diblock Copolymer with Marketed Nanoformulation
Biomacromolecules, (2018) 19 2549-2566. doi: 10.1021/acs.biomac.8b00178

[49] E. Benito, L. Romero-Azogil, E. Galbis, M.V. de-Paz, M. García-Martín, Structurally simple redox polymersomes for doxorubicin delivery, European Polymer Journal (2020) 137 109952. doi.org/10.1016/j.eurpolymj.2020.109952

[50] Z. Zhong, C. Deng R. Cheng F. Meng H. Sun, Reduction and pH dual-bioresponsive crosslinked polymersomes for efficient intracellular delivery of proteins and potent induction of cancer cell apoptosis, Acta Biomater. (2014) 10 (5) 2159–2168. doi.org/10.1016/j.actbio.2014.01.010

[51] A. Kumara, S. V. Lalea, M.R. Aji Alexa, V. Choudharyc, V. Koula, Folic acid and trastuzumab conjugated redox responsive randommultiblock copolymeric nanocarriers for breast cancer therapy: In-vitro and in-vivo studies, Colloids Surf B Biointerfaces, (2017) 149:369-378. doi: 10.1016/j.colsurfb.2016.10.044.

[52] A. Kumar, S.V. Lale, F. Naz, V. Choudhary, V. Koul, Synthesis and biological evaluation of dual functionalized glutathione sensitive poly(ester-urethane) multiblock polymeric nanoparticles for cancer targeted drug delivery, Polymer Chemistry, (2015) 6 7603–7617. doi: 10.1039/c5py00898k

[53] S. V. Lale, A. Kumar, S. Prasad, A.C. Bharti, V. Koul, Folic Acid and Trastuzumab Functionalized Redox ResponsivePolymersomes for Intracellular Doxorubicin Delivery in Breast Cancer, Biomacromolecules (2015) 16 1736−1752. doi: 10.1021/acs.biomac.5b00244

[54] J. Tan, Z. Deng, G. Liu, J. Hu, S, Liu, Anti-inflammatory polymersomes of redox-responsive polyprodrug amphiphiles with inflammation-triggered indomethacin release characteristics, Biomaterials (2018) 178 608-619. doi.org/10.1016/j.biomaterials.2018.03.035

[55] H. Ye, Y. Zhou, X. Liu, Y. Chen, S. Duan, R. Zhu, Y. Liu, L. Yin, Recent Advances on Reactive Oxygen Species-Responsive Delivery and Diagnosis System, Biomacromolecules (2019) 20 2441−2463. doi: 10.1021/acs.biomac.9b00628

[56] G. Saravanakumar, J. Kim, W. J. Kim, Reactive-Oxygen-Species-Responsive Drug Delivery Systems: Promises and Challenges. Advanced Science (2017) 4 (1) 1600124. doi: 10.1002/advs.201600124

[57] Z. Deng, J. Hu, S. Liu, Reactive Oxygen, Nitrogen, and Sulfur Species (RONSS)-Responsive Polymersomes for Triggered Drug Release, Macromolecular Rapid Communnications, (2017) 38 1600685. doi.org/10.1002/marc.201600685

[58] C. Tapeinos, A. Pandit, Physical, Chemical, and Biological Structures Based on ROS-Sensitive Moieties That Are Able to Respond to Oxidative Microenvironments, Advaced Materials (2016) 28 5553−5585. doi.org/10.1002/adma.201505376

[59] J. Zhang, J. Hu, W. Sang, J. Wang, Q. Yan, Peroxynitrite (ONOO-) Redox Signaling Molecule-Responsive Polymersomes, ACS Macro Letters, (2016) 5 919-924. doi: 10.1021/acsmacrolett.6b00474.

[60] X. Xu, P. Er Saw, W. Tao, Y. Li, X. Ji, S. Bhasin, Y. Liu, D. Ayyash, J. Rasmussen, M. Huo, J. Shi, O. C. Farokhzad, ROS-Responsive Polyprodrug Nanoparticles for Triggered Drug Delivery and Effective Cancer Therapy
Advnced Materials, (2017) 29 1700141. doi: 10.1002/adma.201700141

[61] Y. Deng, H. Chen, X. Tao, F. Cao, S. Trepout, J. Ling, M.L. Li, Oxidation-Sensitive Polymersomes Based on Amphiphilic Diblock Copolypeptoids Biomacromolecules (2019) 20 3435-3444. doi: 10.1021/acs.biomac.9b00713

[62] R. M. Di Santo, V. Subramanian, Z. Gu, Advances in nanotechnology for diabetes treatment, Wiley Interdisciplinary Reviews-Nanomedicine and Nanobiotechnology (2015) 7 548. doi.org/10.1002/wnan.132

[63] V.K. Rai, N. Mishra, A.K. Agrawal, S. Jain, N.P. Yadav, Novel drug delivery system: an immense hope for diabetics, Drug Deliv (2016) 23(7): 2371–2390. DOI: 10.3109/10717544.2014.991001

[64] A. Wang, W. Fan, T. Yang, S. He, Y. Yang, M. Yu, L. Fan, Q. Zhu, S. Guo, C. Zhu, Y. Gan, Liver-Target and Glucose-Responsive Polymersomes toward Mimicking Endogenous Insulin Secretion with Improved Hepatic Glucose Utilization, Advance Functional Material, (2020) 30 1910168. doi: 10.1002/adfm.201910168,

[65] J. Di, J. Yu, Y. Ye, D. Ranson, A. Jindal, Z. Gu, Engineering Synthetic Insulin-Secreting Cells Using Hyaluronic Acid Microgels Integrated with Glucose-Responsive Nanoparticles, Cellular and Molecular Bioengineering, (2015) 8 3 445–454. doi: 10.1007/s12195-015-0390-y

[66] Y. Zhang, W. Zhao, J. Yang, B. Hammouda, J. Yang, G. Cheng, SANS study on self-assembled structures of glucose-responsive phenylboronate ester-containing diblock copolymer, European Polymer Journal (2016) 83 173–180. doi.org/10.1016/j.eurpolymj.2016.08.019

[67] F. Meng, Z. Zhong, J. Feijen, Stimuli-Responsive Polymersomes for Programmed Drug Delivery Biomacromolecules, (2009) 10 2 197-209. doi.org/10.1021/bm801127d

[68] C. Sanson, J.-F. Le Meins, C. Schatz, A. Soum, S. Lecommandoux, Temperature responsive poly(trimethylene carbonate)-block-poly(L-glutamic acid) copolymer: polymersomes fusion and fission, Soft Matter, (2010) 6 1722-1730. doi: 10.1039/B924617G

[69] X. Liu, D. Zhou, Y. Feng, J. Gou, C. Li, C. He, W. Zhao, S. Sun, C. Zhao, D. Appelhans, B. Voit, Quantitative Synthesis of Temperature-responsive Polymersomes by Multiblock Polymerization, Angewandte Chemie International Edition, doi:10.1002/anie.201910138

[70] X.R. Chen, X. B Ding, Z. H. Zheng, Y. X. Peng, Thermosensitive cross-linked polymer vesicles for controlled release system, New Journal of Chemistry (2006) 30 577–582. doi: 10.1039/b516053g

[71] S. Qin, Y. Geng, D. E. Discher, S. Yang, Temperature-Controlled Assembly and Release from Polymer Vesicles of Poly(ethylene oxide)-block-poly(N-isopropylacrylamide), Advanced Materials, (2006) 18 2905–2909. doi.org/10.1002/adma.200601019

[72] F. Liu, V. Kozlovskaya, S. Medipelli, B. Xue, F. Ahmad, M. Saeed, D. Cropek, E. Kharlampieva, Temperature-Sensitive Polymersomes for Controlled Delivery of Anticancer Drugs, Chemistry of Materials, (2015) 27 23 7945–7956. doi.org/10.1021/acs.chemmater.5b03048

[73] V. Kozlovskaya, F. Liu, Y. Yang, K. Ingle, S. Qian, G. V. Halade, V. S. Urban, E. Kharlampieva, Temperature-Responsive Polymersomes of Poly(3-methyl-N-vinylcaprolactam)-block-poly(N-vinylpyrrolidone) To Decrease Doxorubicin-Induced Cardiotoxicity, Biomacromolecules (2019) 20 3989-4000. doi: 10.1021/acs.biomac.9b01026

[74] Y. Zhou, R. Chen, H. Yang, C. Bao, J. Fan, C. Wang, Q. Lin, L. Zhu, Light-responsive polymersomes with a charge-switch for targeted drug delivery. Jourbal Material Chemistry B (2020) 8 727–735. doi: 10.1039/C9TB02411E

[75] F. Zhu, S. Tan, M.K. Dhinakaran, J. Cheng, H. Li, The light-driven macroscopic directional motion of a water droplet on an azobenzene-calix [4] arene modified surface. Chemical Communication (2020) 56 10922–10925. doi: 10.1039/D0CC00519C

[76] S.K. Choi, M. Verma, J. Silpe, R.E. Moody, K. Tang, J.J. Hanson, J.R.Jr., Baker, A photochemical approach for controlled drug release in targeted drug delivery. Bioorganic Medical Chemistry (2012) 20 1281–1290. doi.org/10.1016/j.bmc.2011.12.020

[77] Y. Kim, D. Jeong, V.V. Shinde, Y. Hu, C. Kim, S. Jung, Azobenzene-grafted carboxymethyl cellulose hydrogels with photo-switchable, reduction-responsive and self-healing properties for a controlled drug release system, International Journal of Biological Macromoecules, (2020) 163 824–832. doi.org/10.1016/j.bmc.2011.12.020

[78] J. Zhang, N. Shi, J. Zhang, Y. Guan, W. Qiao, X. Wan, Light Triggered Co-Assembly of Photocleavable Copolymers and Polyoxometalates with Enhanced Photoluminescence. Macromol. Rapid Commun, (2017) 38 1600550. doi.org/10.1002/marc.201600550

[79] Zhang, D.; Shah, P.K.; Culver, H.R.; David, S.N.; Stansbury, J.W.; Yin, X.; Bowman, C.N.
Photo-responsive liposomes composed of spiropyran-containing triazole-phosphatidylcholine: Investigation of
merocyanine-stacking effects on liposome-fiber assembly-transition. Soft Matter 2019, 15, 3740–3750.

[80] H. Xi, Z. Zhang, W. Zhang, M. Li, C. Lian, Q. Luo, H. Tian, W.H. Zhu, All-Visible-Light-Activated Dithienylethenes Induced by Intramolecular Proton Transfer, Journal of the American Chemical Society, (2019) 141 18467–18474. doi.org/10.1021/jacs.9b07357

[81] Q. Li, Z. Cao, G. Wang, Diazonaphthoquinone-based amphiphilic polymer assemblies for NIR/UV lightand pH-responsive controlled release, Polymer Chemistry (2018) 9 463–471. doi: 10.1039/C7PY01822C

[82] Y.C. Chung, C.H. Yang, R.H. Lee, T.L. Wang, Dual Stimuli-Responsive Block Copolymers for Controlled Release Triggered by Upconversion Luminescence or Temperature Variation, ACS Omega (2019) 4 3322–3328. doi.org/10.1021/acsomega.8b03414

[83] W. Shen, J. Zheng, Z. Zhou, D. Zhang, Approaches for the synthesis of o-nitrobenzyl and coumarin linkers for use in photocleavable biomaterials and bioconjugates and their biomedical applications. Acta Biomaterials (2020) 115 75–91. doi.org/10.1016/j.actbio.2020.08.024

[84] Y. Zhou, R. Chen, H. Yang, C. Bao, J. Fan, C. Wang, Q. Lin, L. Zhu, Light-responsive polymersomes with a charge-switch for targeted drug delivery.
Journal Material Chemistry B. (2019) doi: 10.1039/c9tb02411e

[85] W. Hou, R. Liu, S. Bi, Q. He, H. Wang, J. Gu, Photo-Responsive Polymersomes as Drug Delivery System for Potential Medical Applications, Molecules (2020) 25 542–552. doi:10.3390/molecules25215147

[86] S. Yamamoto, T. Yamada, G. Kubo, K. Sakurai, K. Yamaguchi, J. Nakanishi, Preparation of a Series of Photoresponsive Polymersomes Bearing Photocleavable a 2-

nitrobenzyl Group at the Hydrophobic/Hydrophilic Interfaces and Their Payload Releasing Behaviors, Polymers (2019) 11 1254. doi:10.3390/polym11081254.

[87] Y. Zhang, J. Yu, H.N. Bomba, Y. Zhu, Z. Gu, Mechanical Force-Triggered Drug Delivery, Chemical Reviews (2016) 116 19 12536–12563. doi.org/10.1021/acs.chemrev.6b00369

[88] R. S. Rikken, H. H. Kerkenaar, R. J. Nolte, J. C. Maan, J. C. van Hest, P. C. Christianen, D. A. Wilson, Chemical Communications (2014) 50 5394.

[89] A.V. Ryzhkov, Y.L. Raikher, Field-Induced Deformation and Structure Changes in a Magnetic Polymersome: Many-Particle Simulation, IOP Conference Series: Materials Science and Engineering (2019) 581 012020, doi:10.1088/1757-899X/581/1/012020

[90] R.J. Hickey, A.S. Haynes, J.M. Kikkawa, S.J. Park, Controlling the Self-Assembly Structure of Magnetic Nanoparticles and Amphiphilic Block-Copolymers: From Micelles to Vesicles, Journal of American Chemical Society (2011) 133 1517–1525. doi.org/10.1021/ja1090113

[91] S. Lecommandoux, O. Sandre, F. Chécot, J. Rodriguez-Hernandez, R. Perzynski, Magnetic Nanocomposite Micelles and Vesicles, Advanced Materials (2005) 17 712–718. doi: 10.1002/adma.200400599

[92] C. Sanson, O. Diou, J. Thévenot, E. Ibarboure, A. Soum, A. Brûlet, S. Miraux, E. Thiaudière, S. Tan, A. Brisson, V. Dupuis, O. Sandre, S .Lecommandoux, Doxorubicin Loaded Magnetic Polymersomes: Theranostic Nanocarriers for MR Imaging and Magneto-Chemotherapy ACS Nano 5, (2011) 5 (2) 1122–1140. doi 10.1021/nn102762f

[93] A. Ryzhkov, Y. Raikher, Coarse-Grained Molecular Dynamics Modelling of a Magnetic Polymersome, Nanomaterials (2018) 8 763. doi:10.3390/nano8100763.

[94] X. Duan, L. Lu, Y. Wang, F. Zhang, J. Mao, M. Cao, B. Lin, X. Zhang, X. Shuai, J. Shen, The long-term fate of mesenchymal stem cells labeled with magnetic resonance imaging-visible polymersomes in cerebral ischemia, International Journal of Nanomedicine (2017) 12 6705–6719. doi:10.2147/IJN.S146742.

[95] C.D. Kan, J.N. Wang, W.P. Li, S.H. Lin, W.L. Chen, Y.P. Hsu, C.S. Yeh, Clinical ultrasound stimulating angiogenesis following drug-release from polymersomes on the ischemic zone for peripheral arterial occlusive disease, Nanomedicine: Nanotechnology, Biology, and Medicine (2018) 14 2205–2213. doi:10.1016/j.nano.2018.07.010

[96] P. Weia, M. Suna, B. Yanga, J. Xiaoa, J. Dua, Ultrasound-responsive polymersomes capable of endosomal escape for efficient cancer therapy, Journal of Controlled Release (2020) 322 81–94. Doi:10.1016/j.jconrel.2020.03.013

Acknowledgements

I would like to thank my supervisor and guide, Prof. Sonia Trombino, for having first of all given me the opportunity to have this experience and also for having welcomed me warmly into her research group, teaching me the passion for this work. I want to thank also, Prof. Roberta Cassano for the example she gave me, which I consider unforgettable, of how it is possible to love studying and learning about a job that is not always easy, through our always constructive dialogues and comparisons.

I would like to thank Prof. Francesca Iemma, for allowing me to work and deepen my research in the lab of "Pharmaceutical and Cosmetological technologies".

A special thank goes to my colleagues in the lab, with whom I shared intense days of work, laughter and discussion. More than a research group, we have become one big family. I would like to thank all the people I met during this wonderful experience, but above all I would like to thank my family, a milestone in every stage of my life.